FROM THE: MAX PLANCK INSTITUTE OF PSYCHIATRY


# Decoding the Brain Mosaic: Region and Cell Type-Specific Dysregulation Patterns in Stress and Psychiatric Disorders

Dissertation zum Erwerb des
Doctor rerum naturalium (Dr. rer. nat.)
an der Fakultät für Biologie der
Ludwig-Maximilians-Universität München

vorgelegt von
**Nathalie Gerstner**

am
27.03.2024

Mit Genehmigung der Fakultät für Biologie
Ludwig-Maximilians-Universität München

**Supervisor:** Dr. Janine Knauer-Arloth
Research Group Medical Genomics in Psychiatry
Department of Genes and Environment
Max Planck Institute of Psychiatry

**Erstgutachter:** PD Dr. Mathias Schmidt
**Zweitgutachter:** Prof. Dr. Korbinian Schneeberger

Tag der Abgabe: 27.03.2024
Tag der mündlichen Prüfung: 11.10.2024

# Eidesstattliche Erklärung

Ich versichere hiermit an Eides statt, dass die vorgelegte Dissertation von mir selbständig und ohne unerlaubte Hilfe angefertigt ist.

München, den 13.11.2024 Nathalie Gerstner
(Unterschrift)

# Erklärung

Hiermit erkläre ich, *

☒ dass die Dissertation nicht ganz oder in wesentlichen Teilen einer anderen Prüfungskommission vorgelegt worden ist.

☒ dass ich mich anderweitig einer Doktorprüfung ohne Erfolg **nicht** unterzogen habe.

☐ ~~dass ich mich mit Erfolg der Doktorprüfung im Hauptfach .....~~

~~und in den Nebenfächern .....~~

~~bei der Fakultät für ..... der .....~~
(Hochschule/Universität)

~~unterzogen habe.~~

☐ ~~dass ich ohne Erfolg versucht habe, eine Dissertation einzureichen oder mich der Doktorprüfung zu unterziehen.~~

München, den 13.11.2024 Nathalie Gerstner
(Unterschrift)

*) Nichtzutreffendes streichen

# Publication Statement

The work presented in this doctoral thesis is part of a published scientific article "DiffBrainNet: Differential analyses add new insights into the response to glucocorticoids at the level of genes, networks and brain regions" (Gerstner N. & Krontira A. *et al.*, 2022, Neurobiology of Stress) and a manuscript submitted to a peer-reviewed journal "Contrasting genetic predisposition and diagnosis in psychiatric disorders: a multi-omic single-nucleus analysis of the human orbitofrontal cortex" (Gerstner N. *et al.*, 2024, submitted).
The Materials and Methods, Results, and significant portions of the Discussion sections have been adapted from these manuscripts, including the content and figures.

# Publications

### Peer-reviewed publications

- Matosin N, Arloth J, Czamara D, Edmond KZ, Maitra M, Fröhlich AS, Martinelli S, Kaul D, Bartlett R, Curry AR, Gassen NC, Hafner K, Müller NS, Worf K, Rehawi G, Nagy C, Halldorsdottir T, Cruceanu C, Gagliardi M, **Gerstner N**, Ködel M, Murek V, Ziller MJ, Scarr E, Tao R, Jaffe AE, Arzberger T, Falkai P, Kleinmann JE, Weinberger DR, Mechawar N, Schmitt A, Dean B, Turecki G, Hyde TM, Binder EB. *Associations of psychiatric disease and ageing with FKBP5 expression converge on superficial layer neurons of the neocortex.* Acta Neuropathol. 2023 Apr;145(4):439-459. doi: 10.1007/s00401-023-02541-9. Epub 2023 Feb 2. PMID: 36729133; PMCID: PMC10020280.

- **Gerstner N**, Krontira AC, Cruceanu C, Roeh S, Pütz B, Sauer S, Rex-Haffner M, Schmidt MV, Binder EB, Knauer-Arloth J. *DiffBrainNet: Differential analyses add new insights into the response to glucocorticoids at the level of genes, networks and brain regions.* Neurobiol Stress. 2022 Oct 14;21:100496. doi: 10.1016/j.ynstr.2022.100496. PMID: 36532379; PMCID: PMC9755029.

- Hu Y, Rehawi G, Moyon L, **Gerstner N**, Ogris C, Knauer-Arloth J, Bittner F, Marsico A, Mueller NS. *Network Embedding Across Multiple Tissues and Data Modalities Elucidates the Context of Host Factors Important for COVID-19 Infection.* Front Genet. 2022 Jul 8;13:909714. doi: 10.3389/fgene.2022.909714. PMID: 35903362; PMCID: PMC9315940.

- Cruceanu C, Dony L, Krontira AC, Fischer DS, Roeh S, Di Giaimo R, Kyrousi C, Kaspar L, Arloth J, Czamara D, **Gerstner N**, Martinelli S, Wehner S, Breen MS, Koedel M, Sauer S, Sportelli V, Rex-Haffner M, Cappello S, Theis FJ, Binder EB. *Cell-Type-Specific Impact of Glucocorticoid Receptor Activation on the Developing Brain: A Cerebral Organoid Study. Am J Psychiatry.* 2022 May;179(5):375-387. doi:

10.1176/appi.ajp.2021.21010095. Epub 2021 Oct 26. Erratum in: Am J Psychiatry. 2022 Feb;179(2):169. PMID: 34698522.

- Benedetti E, Pučić-Baković M, Keser T, **Gerstner N**, Büyüközkan M, Štambuk T, Selman MHJ, Rudan I, Polašek O, Hayward C, Al-Amin H, Suhre K, Kastenmüller G, Lauc G, Krumsiek J. *A strategy to incorporate prior knowledge into correlation network cutoff selection.* Nat Commun. 2020 Oct 14;11(1):5153. doi: 10.1038/s41467-020-18675-3. PMID: 33056991; PMCID: PMC7560866.

- Benedetti E, **Gerstner N**, Pučić-Baković M, Keser T, Reiding KR, Ruhaak LR, Štambuk T, Selman MHJ, Rudan I, Polašek O, Hayward C, Beekman M, Slagboom E, Wuhrer M, Dunlop MG, Lauc G, Krumsiek J. *Systematic Evaluation of Normalization Methods for Glycomics Data Based on Performance of Network Inference.* Metabolites. 2020 Jul 2;10(7):271. doi: 10.3390/metabo10070271. PMID: 32630764; PMCID: PMC7408386.

## Preprints and Submitted Manuscripts

- **Gerstner N**, Fröhlich AS, Matosin N, Gagliardi M, Cruceanu C, Ködel M, Rex-Haffner M, Xu T, Mostafavi S, Ziller MJ, Binder EB, Knauer-Arloth J. *Contrasting genetic predisposition and diagnosis in psychiatric disorders: a multi-omic single-nucleus analysis of the human orbitofrontal cortex*. Submitted

- Fröhlich AS, **Gerstner N**, Gagliardi M, Ködel M, Yusupov N, Matosin N, Czamara D, Sauer S, Roeh S, Murek V, Chatzinakos C, Daskalakis NP, Knauer-Arloth J, Ziller MJ, Binder EB. *Cell-type-specific aging effects in the human OFC and implications for psychiatric disease.* Submitted

- Worf K, Matosin N, **Gerstner N**, Fröhlich AS, Koller AC, Degenhardt F, Thiele H, Rietschel M, Udawela M, Scarr E, Dean B, Theis FJ, Knauer-Arloth J, Mueller NS. *Variant-risk-exon interplay impacts circadian rhythm and dopamine signaling pathway in severe psychiatric disorders.* medRxiv 2022.08.09.22278128; doi: https://doi.org/10.1101/2022.08.09.22278128

# Declaration of Contributions

The following tables declare my respective contributions and those of my colleagues and collaborators within the respective research projects.

**Transcriptomic analysis of stress response in 8 mouse brain regions**

| | |
|---|---|
| Design and conduction of experiments | Anthi Krontira, Mathias Schmidt |
| Conceptualization of research | Nathalie Gerstner, Anthi Krontira, Janine Knauer-Arloth, Elisabeth Binder |
| Sequencing alignment and preprocessing | Simone Roeh |
| Differential gene expression and network analysis | Nathalie Gerstner |
| Enrichment analyses | Anthi Krontira |
| Implementation of R Shiny App | Nathalie Gerstner |
| Deployment and hosting of R Shiny App | Benno Puetz |
| Graphs and figures (except Figure 2.1, Figure 3.8, and Supplementary Figure 3) | Nathalie Gerstner, exceptions by Anthi Krontira |
| Writing of respective manuscript draft | Nathalie Gerstner, Anthi Krontira |

**Multi-omics analysis of psychiatric disorders in the OFC of postmortem human brain**

| | |
|---|---|
| Brain tissue acquisition | Elisabeth Binder, Natalie Matosin |
| Conceptualization of research | Nathalie Gerstner, Janine Knauer-Arloth |
| Randomization | Nathalie Gerstner, Anna Fröhlich |
| Nuclei extraction of postmortem brains | Anna Fröhlich, Miriam Gagliardi |
| Loading of 10x Genomics Chromium Controller | Anna Fröhlich, Miriam Gagliardi |
| 10x library preparation | Anna Fröhlich, Maik Ködel |
| Sequencing alignment | Nathalie Gerstner |
| Downsampling of reads | Nathalie Gerstner |
| Quality control and processing of single-nucleus sequencing data | Nathalie Gerstner |
| Label transfer for cell type assignment | Nathalie Gerstner |
| Manual curation of cell type labels | Anna Fröhlich (RNA), Nathalie Gerstner (ATAC) |
| Correlation analysis of gene expression and chromatin accessibility | Nathalie Gerstner |
| Differential gene expression and chromatin accessibility analysis | Nathalie Gerstner |
| Functional annotations | Nathalie Gerstner |
| Network inference | Nathalie Gerstner |
| Randomization and DNA extraction for genotyping | Anna Fröhlich |
| Prepping of DNA for genotyping | Maik Ködel, Susann Sauer |
| Processing and imputation of genotype data | Darina Czamara, Jade Martins |
| Calculation of polygenic risk scores | Nathalie Gerstner |
| Graphs and figures | Nathalie Gerstner |
| Writing of respective manuscript draft | Nathalie Gerstner |

# Abstract

*Background*
Psychiatric disorders rank among the top causes of global disability, leading to a substantial decrease in quality of life and imposing significant challenges on society. Their development involves a complex interplay of genetic and environmental factors that initiate molecular, cellular, and structural changes in the human body, specifically in the brain. Yet, the molecular architecture of psychiatric disorders remains elusive, largely due to their polygenic nature and the complex interplay among a mosaic of diverse cell types and various brain regions. The prefrontal cortex, a brain region orchestrating higher cognitive function, has shown structural and functional abnormalities in psychiatric disorders, such as schizophrenia, major depressive disorder (MDD), and bipolar disorder. This group of mood and psychotic disorders does not only display overlapping symptoms but also shares a common genetic architecture. While moderate stress can foster resilience and prevent psychiatric conditions, chronic stress can disrupt the body's stress response systems like the hypothalamic-pituitary-adrenal (HPA) axis, posing a major risk factor for the development of such disorders. This thesis aims to delineate the transcriptomic response to stress across various brain regions and the shared molecular architecture of schizophrenia, MDD, and bipolar disorder in the prefrontal cortex on a cell type level.

*Methodology*
To decipher the brain's stress response via the HPA axis, this work utilized RNA-sequencing to analyze the transcriptional response to the glucocorticoid receptor agonist dexamethasone across eight brain regions implicated in stress within a mouse model (n=30). With a combination of differential expression and network analyses, we sought to unravel complex gene networks that evade detection at the single-gene level. For insights into the molecular basis of psychiatric disorders within the orbitofrontal cortex – a subregion of the prefrontal cortex and focal point in psychiatric research – single-nucleus RNA-sequencing and ATAC-sequencing, a technique assessing chromatin accessibility, were conducted. These methods were applied to 92 postmortem human brain samples from a transdiagnostic cohort that included healthy controls and psychiatric cases with a diagnosis for schizophrenia, schizoaffective disorder, MDD, or bipolar disorder. Profiles of gene expression and chromatin accessibility, for 800,000 and 400,000 nuclei respectively, were generated and subsequently integrated with genetic risk and clinical profiles. Differential expression and chromatin accessibility analyses between cases and controls were complemented by differential analyses contrasting groups of high and low genetic risk.

*Results*
The findings uncover a brain region-specific response to glucocorticoid stimulation in mice (5-27% of differentially expressed genes per brain region), yet a large number of genes ($n_{genes}$=172) demonstrates a consistent response throughout various regions. Network analyses enhance the understanding gained from differential expression, such as for genes like *Abcd1*, involved in the active transport of glucocorticoids, and part of a

differential network highlighting the role of ABC transporters in glucocorticoid response. Additionally, the gene *Tcf4*, which is implicated in psychiatric disorders, may modulate the Wnt pathway in a subregion-specific manner within the dentate gyrus. Furthermore, cell type-specific alterations in gene expression and chromatin accessibility within the human orbitofrontal cortex reveal a pronounced impact in excitatory neurons associated with psychiatric diagnoses and additionally in glial and endothelial cells influenced by genetic risk. Notably, there is minimal overlap between genes affected by psychiatric diagnosis and those influenced by genetic risk, yet the affected biological pathways often converge. The genes *INO80E* and *HCN2* stand out due to their dysregulation on the level of both gene expression and chromatin accessibility in excitatory neurons of layers 2/3 influenced by genetic risk for schizophrenia.

*Conclusion*

In conclusion, this thesis significantly enriches our understanding of the stress response via the activation of the glucocorticoid receptor across multiple brain regions. Additionally, it sheds light on the complex genetic, transcriptomic, and epigenetic landscape of psychiatric disorders in a multitude of cell types. By contrasting genetic predisposition with clinical diagnoses, this research underscores the complexities inherent in integrating genetic risk factors with clinical phenotypes and highlights the necessity for a deeper understanding of the underlying biology. This thesis contributes to addressing these complexities, paving the way for advancements in personalized mental health care and the development of more targeted diagnostic and therapeutic strategies. The DiffBrainNet Shiny app as well as data and code repositories provide a wealth of materials and results, opening avenues for further exploration.

# Zusammenfassung

*Hintergrund*
Psychische Störungen gehören weltweit zu den häufigsten Erkrankungen, beeinträchtigen die Lebensqualität von Betroffenen erheblich und stellen eine große gesellschaftliche Herausforderung dar. Ihre Entstehung ist von einem komplexen Zusammenspiel genetischer und umweltbedingter Faktoren geprägt, die molekulare, zelluläre und strukturelle Veränderungen im menschlichen Körper, insbesondere im Gehirn, auslösen. Dennoch bleibt die molekulare Basis psychischer Störungen weitgehend unergründet, was vor allem durch ihre polygene Beschaffenheit und die komplexen Interaktionen zwischen einer Vielfalt von Zelltypen und verschiedenen Gehirnregionen bedingt ist. Der präfrontale Kortex ist eine Gehirnregion, die höhere kognitive Prozesse koordiniert und bei psychischen Störungen wie Schizophrenie, Depression und bipolarer Störung strukturelle und funktionelle Anomalien zeigt. Diese Gruppe von affektiven und psychotischen Störungen zeigt nicht nur überlappende Symptome, sondern teilt auch eine gemeinsame genetische Basis. Während moderater Stress die Resilienz fördern und psychischen Erkrankungen vorbeugen kann, kann chronischer Stress die körpereigenen Stressreaktionssysteme, wie die Hypothalamus-Hypophysen-Nebennierenrinden-Achse (HPA-Achse), stören und stellt somit einen erheblichen Risikofaktor für die Entwicklung solcher Erkrankungen dar. Diese Doktorarbeit zielt darauf ab, die transkriptomische Reaktion auf Stress über verschiedene Gehirnregionen hinweg sowie die gemeinsame molekulare Basis von Schizophrenie, Depression und bipolarer Störung im präfrontalen Kortex auf der Zellebene zu ergründen.

*Methodik*
In dieser Arbeit wurde die RNA-Sequenzierung genutzt, um die transkriptomische Reaktion auf den Glukokortikoidrezeptor-Agonisten Dexamethason in acht für die Stressreaktion relevanten Gehirnregionen anhand eines Mausmodells (n=30) zu analysieren. Die Intention dabei war, die Stressreaktion des Gehirns über die HPA-Achse zu entschlüsseln und komplexe Gen-Netzwerke aufzudecken, die auf der Einzelgen-Ebene nicht erkennbar sind. Hierfür wurde eine Kombination aus differentieller Expressions- und Netzwerkanalyse verwendet. Um Einblicke in die molekulare Basis psychischer Störungen innerhalb des orbitofrontalen Kortex, einer Unterregion des präfrontalen Kortex und Schwerpunkt der psychiatrischen Forschung, zu gewinnen, wurde neben Einzelkern-RNA-Sequenzierung auch Einzelkern-ATAC-Sequenzierung durchgeführt – ein Verfahren zur Analyse der genomweiten Chromatin-Zugänglichkeit. Diese Methoden wurden an 92 postmortalen humanen Gehirnproben aus einer transdiagnostischen Kohorte angewandt, welche gesunde Kontrollen und psychiatrische Fälle mit Diagnosen für Schizophrenie, schizoaffektive Störung, Depression oder bipolare Störung umfasst. Genexpression und Chromatin-Zugänglichkeit für 800.000 bzw. 400.000 Zellkerne wurden mit genetischem Risiko für psychische Störungen und klinischen Daten integriert. Neben der Analyse von differentieller Expression und Chromatin-Zugänglichkeit zwischen Erkrankten und

Kontrollen, wurden Gruppen mit hohem und niedrigem genetischem Risiko in differentiellen Analysen verglichen.

*Ergebnisse*
Die Ergebnisse zeigen eine regionsspezifische Reaktion auf Glukokortikoid-Stimulation im Maushirn (5-27% der differentiell exprimierten Gene pro Gehirnregion), wobei eine hohe Anzahl an Genen ($n_{Gene}$=172) in verschiedenen Regionen konsistent reagiert. Netzwerkanalysen erweitern das Verständnis, das aus der differentiellen Expressionsanalyse gewonnen wurde. Ein Beispiel hierfür ist das Gen *Abcd1*, das am aktiven Transport von Glukokortikoiden beteiligt und Teil eines differentiellen Netzwerks ist, welches die Rolle der ABC-Transporter in der Glukokortikoidreaktion hervorhebt. Ein weiteres Gen ist *Tcf4*, das mit psychischen Störungen in Verbindung gebracht wird und möglicherweise den Wnt-Signalweg in einer subregionsspezifischen Weise innerhalb des Gyrus dentatus moduliert.
Darüber hinaus wurden zelltypspezifische Veränderungen der Genexpression und der Chromatin-Zugänglichkeit im humanen orbitofrontalen Kortex beobachtet, die einen ausgeprägten Einfluss auf erregende Neuronen in Assoziation mit psychiatrischen Diagnosen, sowie zusätzlich auf Glia- und Endothelzellen im Zusammenhang mit genetischem Risiko aufzeigen. Obwohl es zwischen Genen, die durch die den Krankheitsverlauf und solchen, die durch genetisches Risiko beeinflusst sind, nur eine minimale Überschneidung gibt, stimmen die betroffenen biologischen Prozesse oft überein. Die Gene *INO80E* und *HCN2* heben sich hervor, da sie sowohl auf Ebene der Genexpression als auch der Chromatin-Zugänglichkeit in erregenden Neuronen der Schichten 2/3 durch das genetische Risiko für Schizophrenie beeinflusst werden.

*Schlussfolgerung*
Die Ergebnisse dieser Doktorarbeit tragen maßgeblich zu einem verbesserten Verständnis der Stressreaktion über die Aktivierung des Glukokortikoidrezeptors in verschiedenen Gehirnregionen bei. Außerdem geben Sie Aufschluss über die komplexe genetische, transkriptomische und epigenetische Landschaft psychischer Störungen in einer Vielzahl von Zelltypen. Durch die Gegenüberstellung von genetischem Risiko und klinischer Diagnose ebnet diese Doktorarbeit den Weg für Fortschritte in der personalisierten Gesundheitsversorgung und der Entwicklung gezielterer diagnostischer und therapeutischer Strategien. Die DiffBrainNet Shiny-App sowie Daten- und Quellcode-Repositorien stellen eine Fülle von Materialien und Ergebnissen bereit, die Wege für daran anknüpfende Forschung eröffnen.

# Table of Contents

# 1 Introduction

Psychiatric disorders are highly prevalent and complex diseases that not only impair the lives of millions but also pose a substantial challenge in diagnosis procedures and finding effective treatments (Arias, Saxena, & Verguet, 2022; Vos et al., 2020). It is well known that psychiatric disorders arise from a complex interplay of genetic and environmental factors (Caspi & Moffitt, 2006; Uher, 2014). However, our understanding of their molecular and cellular architecture within the intricate landscape of the brain remains notably incomplete. This deficiency in understanding includes the interactions of genes, regulatory elements, pathways, and the variety of cell types involved in the manifestation and progression of psychiatric disorders. This thesis aims to uncover molecular alterations within the brain, specifically focusing on transcriptomic and epigenomic changes associated with psychiatric disorders and glucocorticoid exposure, a prominent factor linked to stress and implicated in psychiatric disorders.

I study the transcriptomic response to glucocorticoid exposure across different brain regions using data from a mouse model treated with dexamethasone, a synthetic glucocorticoid. Within this framework, differential expression and differential network analyses are employed to delineate the unique molecular responses across key brain regions, previously linked to psychiatric disorders and stress response. This approach not only contributes to our understanding of distinct transcriptomic signatures associated with glucocorticoid exposure but also unravels the complexity of brain region-specific responses.

In addition, I investigate the molecular alterations in human postmortem brain tissue obtained from a cohort of psychiatric patients and healthy controls. Here, the focus lies on the orbitofrontal cortex and the power of single-cell sequencing is leveraged to decipher transcriptomic and epigenomic alterations at the level of individual cell types. Besides the investigation of molecular signatures differentiating psychiatric cases from controls, my research delves into examining the influence of genetic risk for psychiatric disorders on both gene expression and chromatin accessibility. With this approach, I seek to dissect the molecular architecture of psychiatric disorders and the genetic risk for these at a cellular resolution, offering a unique perspective on the role of specific cell populations within the orbitofrontal cortex.

This thesis aspires to enhance the understanding of the molecular architecture of glucocorticoid exposure and psychiatric disorders through the integration of an animal model and a human postmortem study. By dissecting the molecular details across various brain regions and cell types, my research aims to illustrate how genomic and genetic risk factors translate to clinical manifestations, potentially informing more precise diagnostics and therapeutic interventions.

The subsequent sections provide an overview of stress and psychiatric disorders, delving into the current understanding of molecular dysregulation within these conditions. Furthermore, I introduce various techniques and methodologies used for collecting and analyzing molecular data in the study of stress and psychiatric research.

## 1.1 Global Impact and Challenges of Psychiatric Disorders

Psychiatric disorders represent a significant global health challenge, leading to a substantial decrease in an individual's quality of life and imposing a significant economic burden on society (Arias et al., 2022; Vos et al., 2020). The impact of severe psychiatric disorders extends beyond the impairment in daily functioning and often culminates in severe consequences such as job loss, or in most tragic cases, suicide. In 2019, mental disorders accounted for 16% of global disability-adjusted life years (DALYs), composed of the years lived with a disability and the years lost due to early death. The associated economic cost was estimated at approximately 5 trillion US dollars (Arias et al., 2022; Institute for Health Metrics and Evaluation, 2020). The prevalence and burden of psychiatric disorders, particularly depressive disorders, are highlighted by their status as leading causes of global DALYs across all age groups (Institute for Health Metrics and Evaluation, 2020; Vos et al., 2020). Epidemiological data indicates a rising prevalence of psychiatric disorders worldwide (Figure 1.1) with almost 280, 39, and 24 million people affected by depressive disorders, bipolar disorder, and schizophrenia respectively in 2019 (Institute for Health Metrics and Evaluation, 2020; Vigo, Thornicroft, & Atun, 2016). Between 1990 and 2019, the number of DALYs and the prevalence of schizophrenia, depressive, and bipolar disorders have increased by approximately 60%, imposing an increasing challenge to global health systems.

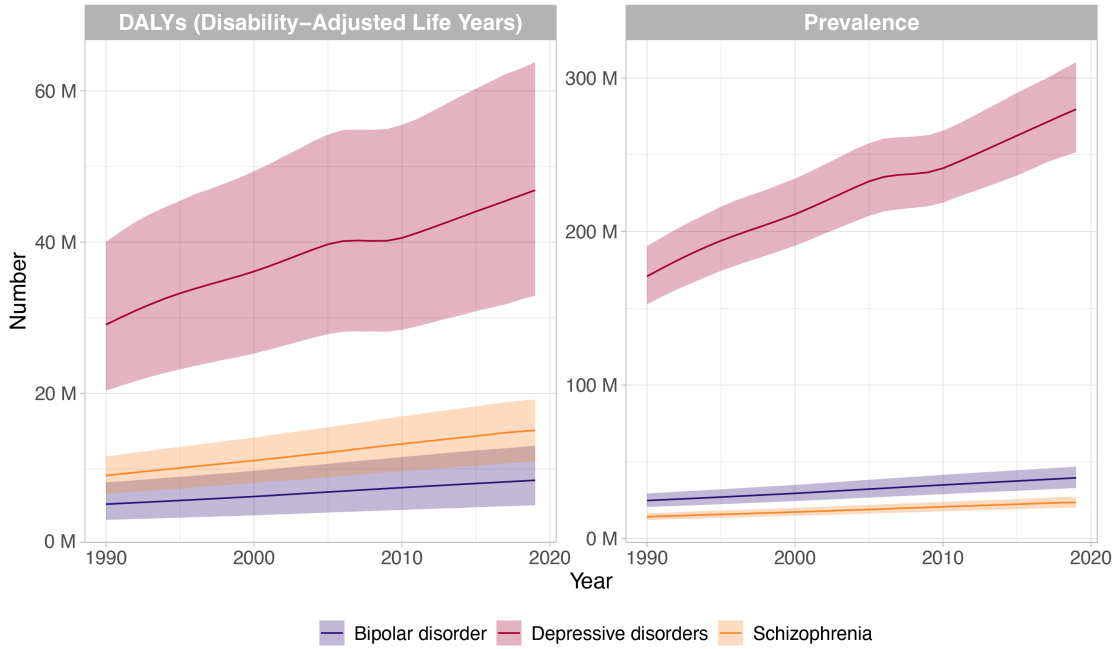


**Figure 1.1. Global burden of severe psychiatric disorders over time.** Disability-adjusted life years (DALYs, left) and prevalence (right) of schizophrenia, bipolar, and depressive disorders from 1990 to 2019 in millions. Dark lines represent the mean estimates. Ribbons represent 95% uncertainty intervals. Data was obtained from (Institute for Health Metrics and Evaluation, 2020; Vigo et al., 2016).

The contemporary relevance of understanding the molecular basis of mental disorders becomes evident in the context of recent global events, including the COVID-19 pandemic, war, and natural disasters. Different studies highlighted a general decline in overall societal well-being during the COVID-19 pandemic and an increase in symptom

severity experienced by patients diagnosed with a psychiatric disorder already before the pandemic started (Leung et al., 2022; Vindegaard & Benros, 2020). Social and economic loss due to war and natural disasters lead to mental instability which can culminate in post-traumatic stress disorder, anxiety, and depression (Makwana, 2019). Psychiatric drug development has seen minimal progress over the last decades, with current medications offering limited efficacy beyond those first introduced in the mid-20th century (Paul & Potter, 2024; "The right treatment for each patient," 2023). Better insights into the underlying molecular mechanisms are crucial for developing effective treatments and supporting resilience in the face of adversities.

The multifactorial nature of psychiatric disorders involves a complex interplay of genetic and environmental risk factors (Caspi & Moffitt, 2006; Uher, 2014). Epigenetic mechanisms act as mediators between environmental stressors – like trauma, extreme stress, or substance abuse – and gene expression (Keverne & Binder, 2020). This thesis centers its investigation on the molecular foundations of mood and psychotic disorders, specifically directing attention to schizophrenia and schizoaffective disorder, bipolar disorder, and major depressive disorder (MDD). This cluster of disorders has a substantial impact on global mental health, marked by a high overall prevalence and a pronounced intersection of genetic and environmental risk factors (Consortium., 2019). Furthermore, the presence of shared symptoms and treatment options across these severe psychiatric disorders (Newson, Pastukh, & Thiagarajan, 2021) adds to the reasoning of their unified exploration to shed light on commonalities and contribute to a more comprehensive understanding of their pathophysiology, a refinement of their diagnostic architecture and the development of more effective therapeutic strategies (Patrick F. Sullivan & Geschwind, 2019). In the following sections, I will delineate the specific symptoms and current treatment options for each of these disorders, further contextualizing their interconnectedness.

**Schizophrenia** is a complex mental disorder characterized by a spectrum of symptoms that can be broadly categorized into positive, negative, and cognitive symptoms. Positive symptoms manifest as hallucinations, delusions, or suspiciousness, while negative symptoms include anhedonia, volitional impairment, and social withdrawal (*Diagnostic and statistical manual of mental disorders*, 2013; *The ICD-10 classification of mental and behavioural disorders*, 1992). Cognitive symptoms involve deficits in working memory, executive function, or attention (McCutcheon, Reis Marques, & Howes, 2020; Patel, Cherian, Gohil, & Atkinson, 2014).
The heterogeneity of symptoms observed in schizophrenia has led to a lack of consensus regarding etiology and pathophysiology, complicating the optimization of effective treatment (Patel et al., 2014). The pathophysiology of schizophrenia involves abnormalities in neurotransmission, with an imbalance in neurotransmitters such as serotonin, dopamine, glutamate, aspartate, glycine, and gamma-aminobutyric acid (GABA) (Patel et al., 2014). Above all, the abnormal activity of dopamine receptors, specifically dopamine D2 receptors, is associated with symptoms of schizophrenia (Abi-Dargham et al., 2000; Patel et al., 2014).
The disorder, with a typical onset in early adulthood, is marked by a cortical excitatory-inhibitory imbalance leading to disrupted synchronization of gamma-oscillations

(McCutcheon et al., 2020). Treatment options for schizophrenia include pharmacological interventions with antipsychotics, such as D2-receptor blockers, which primarily help with positive symptoms but show limited efficacy for negative and cognitive symptoms (McCutcheon et al., 2020). Psychotherapeutic interventions, cognitive-behavioral therapy, and in rare cases also electroconvulsive therapy, can be part of schizophrenia treatment (Dickerson & Lehman, 2011; Grover, Sahoo, Rabha, & Koirala, 2019; Patel et al., 2014).

**Bipolar disorder** is an affective disorder characterized by episodes of mania (or hypomania), depression, or both, involving recurrent changes in energy levels and behavior (Vieta et al., 2018). In addition, the disorder is associated with cognitive symptoms such as alterations in verbal and visual memory, executive function, and reaction time (Vieta et al., 2018). During manic episodes, affected individuals experience hyperactivity, inflated self-esteem, decreased need for sleep, expansive mood, and potentially psychotic symptoms. In contrast, during depressive episodes, symptoms include depressed mood, low self-esteem, social withdrawal, sleep disturbances, and a loss of energy (*Diagnostic and statistical manual of mental disorders*, 2013; *The ICD-10 classification of mental and behavioural disorders*, 1992). The pathophysiology of bipolar disorder, which typically also has an onset in early adulthood, involves disruptions in monoaminergic signaling, neuronal-glial plasticity, inflammatory homeostasis, cellular metabolic pathways, and mitochondrial activity (McIntyre et al., 2020).
In the pharmacological management of bipolar disorder, mood stabilizers like lithium and antipsychotics are commonly used, while antidepressants are prescribed cautiously, given their risk of precipitating mood instability during maintenance treatment (Müller-Oerlinghausen, Berghöfer, & Bauer, 2002). Lithium stands out as the gold standard for mood stabilization, demonstrating antimanic, antidepressant, and anti-suicidal efficacy (McIntyre et al., 2020). Non-pharmacological treatment options include psychotherapy, electroconvulsive therapy, deep brain stimulation, vagus nerve stimulation, and lifestyle interventions (Perugi et al., 2017; Vieta et al., 2018).

**Major depressive disorder** (MDD) is characterized by symptoms such as depressed mood, anhedonia, and a loss of energy (Fava & Kendler, 2000). Additional symptoms can include decreased or increased appetite, sleep disturbances, feelings of guilt and worthlessness, abnormalities of psychomotor activity, and suicidal ideation (*Diagnostic and statistical manual of mental disorders*, 2013; *The ICD-10 classification of mental and behavioural disorders*, 1992). The course of MDD follows an episodic pattern, though in some instances it becomes even chronic (Fava & Kendler, 2000). The etiology of MDD is associated with complex neuroregulatory systems and neural circuits, leading to secondary disturbances of monoamine neurotransmitter systems, such as the serotonergic, noradrenergic, and dopaminergic systems (Saveanu & Nemeroff, 2012). Glutamatergic and GABAergic neurotransmitter systems, as well as abnormalities in neuroendocrine systems, especially the hypothalamic-pituitary-adrenal (HPA) axis, further contribute to the pathophysiology of MDD (Saveanu & Nemeroff, 2012).
Pharmacological treatment options for MDD include antidepressants, such as selective serotonin reuptake inhibitors (SSRIs) and serotonin-norepinephrine reuptake inhibitors (SNRIs), and can be augmented with mood stabilizers (Fava & Kendler, 2000). Non-

pharmacological interventions encompass psychotherapy (e.g. interpersonal psychotherapy, behavioral therapy, or cognitive-behavioral therapy), electroconvulsive therapy, light therapy, physical activity, and lifestyle changes (Campbell, Miller, & Woesner, 2017; Fava & Kendler, 2000; Singh et al., 2023).

**Schizoaffective disorder** is characterized by a combination of affective and psychotic symptoms that do not fully align with the diagnostic criteria for schizophrenia, nor do they correspond precisely with those of depressive or manic episodes (*Diagnostic and statistical manual of mental disorders*, 2013; *The ICD-10 classification of mental and behavioural disorders*, 1992). The diagnosis of schizoaffective disorders remains controversial in the psychiatric research community, with debates surrounding its reliability and practicability (Malaspina et al., 2013). Nevertheless, it is currently maintained as an independent diagnosis in the latest diagnostic manuals (*Diagnostic and statistical manual of mental disorders*, 2013; *The ICD-10 classification of mental and behavioural disorders*, 1992).

Besides a high prevalence of comorbidities with other psychiatric disorders (McGrath et al., 2020), patients are also at high risk for non-psychiatric comorbidities, such as cardiovascular diseases (e.g. heart attacks, hypertension) or metabolic disease (e.g. diabetes, metabolic syndrome) (Correll et al., 2017; Vieta et al., 2018). Major risk factors contributing to these comorbidities are the use of antipsychotics, an unhealthy lifestyle, or an elevated body mass index (Correll et al., 2017; Vancampfort et al., 2016). In addition to suicide, the presence of comorbid disorders contributes to premature mortality in psychiatric patients compared to the general population (Roshanaei-Moghaddam & Katon, 2009).

In conclusion, the diagnostic processes of psychiatric disorders present intricate and systemic challenges, marked by overlapping symptoms and shared genetic foundations. The current clinical framework, based on the ICD-10 (*The ICD-10 classification of mental and behavioural disorders*, 1992) and DSM-5 (*Diagnostic and statistical manual of mental disorders*, 2013) classification system, tends to neglect biological variables and frequently encounters challenges in distinguishing between symptom profiles, leading to difficulties in diagnosis and a lack of effective treatment options for certain patients (Brückl et al., 2020; Newson et al., 2021). Acknowledging these challenges underscores the urgent need for personalized medicine in psychiatry, making use of genomic advances to inform tailored treatment plans (Paul & Potter, 2024; "The right treatment for each patient," 2023). A more nuanced understanding of the transdiagnostic molecular foundations is essential to refine diagnostic precision, customize existing treatments, and develop new therapeutic strategies, ultimately improving the quality and effectiveness of mental health care.

## 1.2 Stress Response and its Role in Psychiatric Disorders

Stress is commonly defined as the response to a difficult situation where the demands surpass an individual's resources, posing a threat to homeostasis and requiring adaptive measures (Lazarus & Folkman, 1984; Schneiderman, Ironson, & Siegel, 2005). Stressors play a significant role in influencing mood, behavior, and mental health, with acute stress responses in young, healthy individuals usually being adaptive (Schneiderman et al., 2005). However, in older or less healthy individuals, persistent or intense stress can lead to long-term health damage (Schneiderman et al., 2005).

The multisystemic stress response in the human body, including neuroinflammatory, neuroendocrine, epigenetic, and metabolic responses, is essential not only for initiating an effective stress response but also related to resilience and vulnerability to stress (Atrooz, Liu, & Salim, 2019). Resilience to stress involves the ability to adapt and recover from stressors, maintaining or quickly regaining psychological and physiological homeostasis (Bush & Roubinov, 2021). This capacity for resilience is influenced by a complex interplay of genetic predispositions, environmental exposures, and lifestyle factors (Bush & Roubinov, 2021; McEwen, Nasca, & Gray, 2016). Understanding the mechanisms underlying stress response and resilience can inform interventions aimed at enhancing an individual's ability to cope with stress, potentially mitigating the development of stress-related psychiatric disorders.

A central part of the endocrine stress response is the activation of the **hypothalamic-pituitary-adrenal (HPA) axis** (de Kloet, Joëls, & Holsboer, 2005). As described by Smith and Vale (2006) as well as Griffiths and Hunter (2014), the corticotropin-releasing hormone (CRH) is released by the paraventricular nucleus of the hypothalamus and stimulates the anterior lobe of the pituitary gland. This induces the secretion of adrenocorticotropic hormone (ACTH) into the systemic blood circulation. Circulating ACTH targets the adrenal gland which synthesizes and secretes glucocorticoids in response to stimulation. This stress hormone exerts negative feedback on the hypothalamus and pituitary gland while also binding to **glucocorticoid receptors (GR)** and mineralocorticoid receptors (MR, Figure 1.2). These nuclear hormone receptors, which function as transcription factors, are central to the stress response and translocate from the cytoplasm to the nucleus upon activation by glucocorticoids (cortisol in humans and corticosterone in rodents) (Griffiths & Hunter, 2014; S. M. Smith & Vale, 2006). The GR has a lower affinity to glucocorticoids compared to the MR, meaning that under baseline conditions, glucocorticoids predominantly bind to MR. However, during periods of stress, when glucocorticoid levels are elevated, they bind to GR (McEwen & Akil, 2020). Once bound to glucocorticoids, the GR interacts with glucocorticoid response elements (GRE) in the DNA, intricately modulating gene expression and eliciting a strong transcriptomic response (McKay & Cidlowski, 1999; Phuc Le et al., 2005; Weikum, Knuesel, Ortlund, & Yamamoto, 2017).

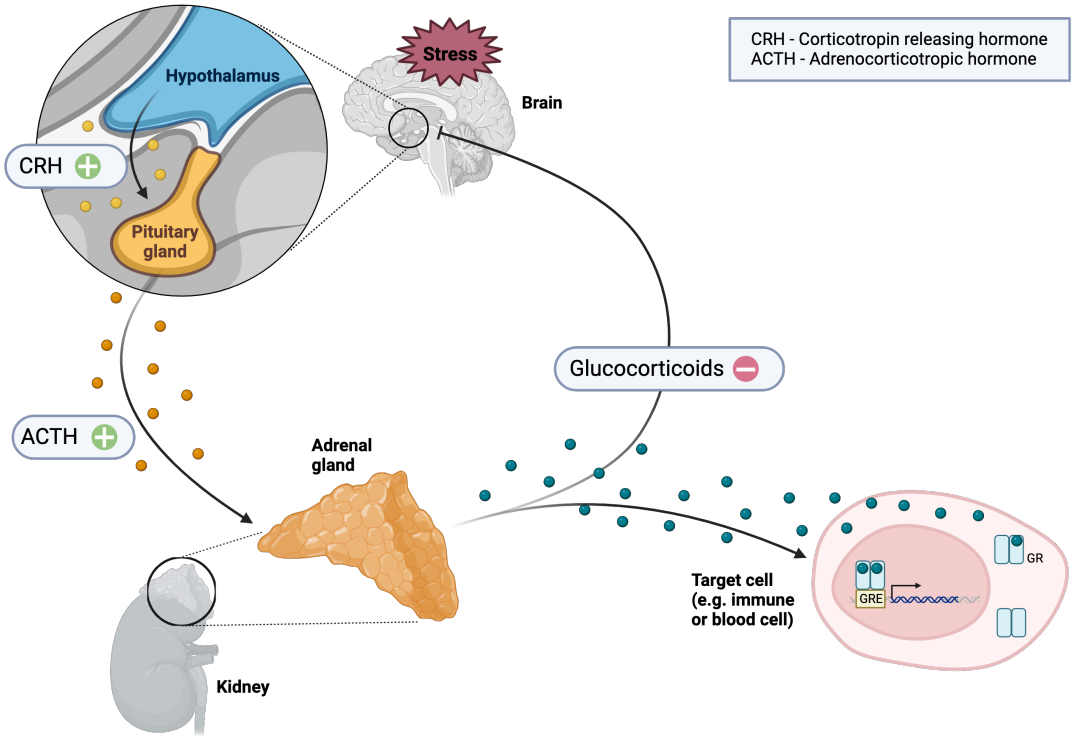


**Figure 1.2. The HPA axis and activation of the glucocorticoid receptor.** The hypothalamus releases corticotropin-releasing hormone (CRH) during stress. CRH triggers the secretion of adrenocorticotropic hormone (ACTH) from the pituitary gland, which in turn stimulates the adrenal glands to produce glucocorticoids, a key stress hormone. Glucocorticoids exert a negative feedback effect on both the hypothalamus and the pituitary gland, but also bind to the glucocorticoid receptor (GR), triggering its translocation into the nucleus and binding to glucocorticoid response elements (GREs). Based on (Griffiths & Hunter, 2014; S. M. Smith & Vale, 2006). Created with Biorender.com

The molecular response elicited by GR activation plays a pivotal role in the **physiological adaptations** initiated by stress (Sapolsky, Romero, & Munck, 2000). Energy-consuming and less important functions, such as digestion, growth, reproduction, and immunity are getting suppressed, while the vascular tone, respiratory rate, and intermediary metabolism are increased and energy stores are getting mobilized (Herman et al., 2016; Majer et al., 2023; S. M. Smith & Vale, 2006).

The regulation of glucocorticoid levels involves a feedback inhibition mechanism that controls both the extent and duration of their release (Majer et al., 2023). This mechanism attempts to reestablish homeostasis and bring glucocorticoid levels back to baseline levels after the termination of the stressor (Majer et al., 2023). The speed at which this return to baseline occurs, governed by the strength of the individual's HPA axis **negative feedback** systems (Romero, 2004), plays a crucial role in minimizing the duration of glucocorticoid exposure which is known to be associated with various health risks, such as oxidative stress, cardiovascular issues, and increased mortality (Majer et al., 2023; Sapolsky et al., 2000). The dysfunction of this stress response system has been also implicated in psychiatric disorders (de Kloet et al., 2005; McEwen & Akil, 2020) and is closely linked to early-life stress and a lack of resilience – a major risk factor for these disorders (Heim & Binder, 2012; McEwen et al., 2015; Wilkinson & Goodyer, 2011).

To explore the molecular alterations induced by stress, this thesis employs a mouse model treated with dexamethasone, a synthetic glucocorticoid preferentially activating the GR. This model, consistent with the conserved nature of stress response across mammals (M. Joëls, Karst, & Sarabdjitsingh, 2018; Lin, Sawa, & Jaaro-Peled, 2012; McEwen et al., 2016), aims to provide valuable insights into the molecular mechanisms affected in stress-related disorders, such as MDD, bipolar disorder, and schizophrenia. By exploring the impact of glucocorticoid exposure on transcriptomic alterations within different brain regions, the goal is to clarify the intricate relationship between stress, molecular changes, and the onset of psychiatric disorders.

## 1.3 Animal Models and Human Postmortem Tissue Studies in Psychiatric Research

Psychiatric research employs a wide range of biological platforms, spanning from animal models to human postmortem tissues (Figure 1.5 left). These platforms provide varied insights into the underlying mechanisms of psychiatric disorders, each with its own set of strengths and challenges.

The lack of definitive biomarkers for psychiatric disorders underscores the essential role of robust **animal models** in their research (Richtand, Harvey, & Hoffman, 2022). These models are invaluable investigative tools, yet their design and purpose must be clearly defined (Nestler & Hyman, 2010). Their effectiveness depends on their ability to demonstrate face validity through symptom homology, construct validity by replicating the disorder's pathology, and predictive validity by forecasting the response to treatment (Malik et al., 2023). Behavioral measures in animal models are crucial for formulating hypotheses on the origins of disorders, pinpointing diagnostic markers, exploring treatment options, and predicting outcomes (Richtand et al., 2022).

Despite the considerable advantages of models that closely reflect human biology, such as primates, numerous challenges hinder their widespread use in research. These include primarily ethical considerations and practical constraints (Schmidt, Wang, & Meijer, 2011). Rodent models, particularly for depression, capture core symptomatic parallels such as anhedonia and anxiety but cannot replicate uniquely human experiences like self-esteem issues or suicidality (Schmidt et al., 2011). The intricate etiology of schizophrenia presents a similarly challenging task of developing models that fully capture the disorder's comprehensive symptomatology (Malik et al., 2023). Although animal models provide invaluable insights, they often cannot fully represent the complexities of human psychological states or precisely mirror the individual nuances of behavioral symptoms (Nestler & Hyman, 2010).

Acknowledging these limitations, animal models retain their critical role in research, specifically to explore the interaction of genetic predispositions and environmental challenges. Genetic mouse models are particularly useful for dissecting molecular alterations observed in patient brains and how these may influence neuronal circuitries

and behavior (Lin et al., 2012). In this thesis, a mouse model is employed to investigate the transcriptomic alterations following GR activation, a crucial component of the highly conserved HPA axis (M. Joëls et al., 2018; Lin et al., 2012; McEwen et al., 2016), thereby establishing the mouse a highly appropriate model organism for this study.

While animal models provide controlled environments for dissecting potential pathophysiological mechanisms, they are complemented by cell lines, human-induced pluripotent stem cell (iPSC)-derived models, and brain organoids. These cell-based models offer a platform to study the human-specific genetic contributions to psychiatric disorders (Soliman, Aboharb, Zeltner, & Studer, 2017). However, only **postmortem tissue studies** can directly investigate human brain tissue to discern disease-related cellular, synaptic, and molecular alterations, and capture the full spectrum of psychiatric disorders as categorized in clinical diagnostic manuals (D. A. Lewis, 2002; Soliman et al., 2017).

Although postmortem tissue provides an irreplaceable resource for research, it comes with its own set of challenges. These include the availability of tissue, which can be impeded by the circumstances of death, and the consent from next of kin for brain donation (Padoan et al., 2022). The integrity of the tissue is vulnerable to a variety of confounders, including the postmortem interval and agonal factors, both of which can significantly affect study outcomes (Harrison, 2011; Stan et al., 2006). Additionally, postmortem research typically captures the advanced stages of disease and offers minimal insight into the early development of disorders (D. A. Lewis, 2002; Soliman et al., 2017). The nature of these studies is largely descriptive and correlational. Thus, the establishment of causality is not feasible, as it is not possible to perturb variables and measure the response within this context (Harrison, 2011).

Despite these challenges, postmortem studies are essential in understanding how genetic predispositions translate into altered gene expression (D. A. Lewis, 2002). Integrating these studies with large-scale genomic analysis can delineate pathophysiological pathways and identify novel therapeutic targets, thus furthering the molecular phenotyping of psychiatric disorders (D. A. Lewis, 2002). Furthermore, postmortem studies include the ability to directly observe disease etiology and patient genetics, an aspect that often cannot be replicated in cell lines or iPSC-derived models which are limited by factors like cellular diversity or low reproducibility (Soliman et al., 2017). Access to premortem human brain tissue is challenging, with biopsies being highly invasive and limited in availability (Krassner et al., 2023; Soliman et al., 2017).

By carefully considering potential confounders and methodological limitations, postmortem studies remain a cornerstone in psychiatric research, offering invaluable insights into the molecular basis of psychiatric disorders and complementing findings from animal models. Here, I examine molecular changes in the orbitofrontal cortex that underpin severe psychiatric disorders using postmortem brain tissue. This method offers unparalleled access to a broad scope of investigational paths and the genomic signatures inherent to these disorders, paths that remain elusive through other research platforms.

## 1.4 Correlates of Stress Across Brain Regions

The brain's response to stress is a complex, multi-faceted process that engages various regions and functions. Stress triggers molecular changes like epigenetic modifications and transcriptional regulation, mediated by epigenetic changes or transcription factors like GR and MR (Griffiths & Hunter, 2014; Keverne & Binder, 2020). Additionally, stress exerts structural changes within the brain, notably affecting neurogenesis and neuronal morphology in regions such as the hippocampus, amygdala, and prefrontal cortex (Marian Joëls, Krugers, & Karst, 2007; McEwen et al., 2016; Sapolsky et al., 2000). Functionally, stress can alter brain activity, with acute stress sometimes enhancing functions like memory, and chronic stress leading to adaptive or maladaptive plasticity, influencing cognition and emotional regulation (McEwen et al., 2016). Various brain regions play a significant role in the cognitive and emotional aspects of the stress response, including limbic structures and the cerebellum (Harlé et al., 2017). Here, I will introduce the various brain regions under investigation in this thesis (Figure 1.3) and discuss current knowledge on how they are affected by stress.

The **prefrontal cortex** (PFC) is considered the most advanced brain region, playing a critical role in executing high-level cognitive processes (Funahashi, 2001; Gao et al., 2012). It is highly interconnected, coordinating complex decision-making (Arnsten, 2009). Stress can impair PFC functions, such as working memory and attention, and under stress, brain activity may shift from the PFC's deliberate control to more automatic, emotional responses driven by the amygdala (Arnsten, 2009). The PFC also has extensive connections with the limbic system, influencing emotion, motivation, and memory (Fuster, 1988). Chronic exposure to glucocorticoids during stress can lead to structural changes within the PFC, such as dendritic retraction and synaptic loss in the medial PFC as well as dendritic growth and new synapse formation in the OFC (McEwen & Akil, 2020). Over time, some of these alterations may be partly reversible (Romeo, 2010). A detailed description of the cortical layer structure and the various cell types in the prefrontal cortex can be found in Section 1.5.

The **hippocampus** is crucial for memory, neurogenesis, and brain plasticity. It expresses receptors for stress hormones that mediate learning and memory (J. J. Kim & Diamond, 2002; McEwen & Akil, 2020). Stress affects its neurogenesis, influencing emotional and cognitive functions and potentially contributing to psychiatric disorders (Levone, Cryan, & O'Leary, 2014). The hippocampus is divided into regions with distinct roles: the dorsal/posterior for spatial memory and the ventral/anterior (rodents/primates respectively) for stress and anxiety regulation (Levone et al., 2014).

The **amygdala** is central to forming emotional responses, such as fear and anxiety, and connecting emotions to memories (Gallagher & Chiba, 1996). It undergoes unique stress-induced changes that can result in its overactivity and enlargement, which are linked to mood disorders (McEwen et al., 2016). Stress alters the amygdala's structure, modulating the dendritic structure (McEwen et al., 2016). Glucocorticoids impact the lateral amygdala directly, with receptors located at postsynaptic sites (McEwen et al., 2016).

Endocannabinoids in the amygdala help regulate stress responses and the HPA axis activity (Hill & McEwen, 2010).

The **hypothalamus** manages the HPA axis activation and its inhibition, releasing CRH in response to stress and controlling ACTH release through feedback mechanisms involving glucocorticoid receptors (Herman et al., 2016). Endocannabinoid signaling in the paraventricular nucleus (PVN) of the hypothalamus can also suppress HPA axis activity (Hill & McEwen, 2010). Overexpression of *Fkbp5*, a key regulator of glucocorticoid receptors in the PVN, has been linked to chronic over-activation of the HPA axis (Häusl et al., 2021).

The **cerebellum**, traditionally associated with motor functions, is increasingly recognized for its involvement in nonmotor functions, including stress responses (Moreno-Rius, 2019). It exhibits high densities of GR and may influence stress-induced motor alterations (Harlé et al., 2017). Adaptations in the cerebellar CRH (receptor) system may affect the cerebellum's response to stress, especially impacting motor learning and possibly causing motor changes (Ezra-Nevo et al., 2018; Harlé et al., 2017). Moreover, the cerebellum's connections to other stress-related brain areas underscore its role in stress-induced behavioral anomalies (Moreno-Rius, 2019).

The goal of studying these brain regions and their transcriptional response to stress is to uncover the cellular and molecular mechanisms that underlie the onset and progression of stress-related disorders. By mapping the specific transcriptional changes within these structures, I aim to improve the understanding of how stress can precipitate or exacerbate psychiatric conditions.

## 1.5 Cellular Heterogeneity in the Prefrontal Cortex

The prefrontal cortex (PFC) is part of the frontal lobe of the neocortex, a highly organized and complex structure, characterized by its laminar formation. The laminar layers 1 to 6 contain a structurally and functionally diverse range of glial and neuronal cell types (Molyneaux, Arlotta, Menezes, & Macklis, 2007). The PFC plays a crucial role in higher cognitive functions, including executive control, decision-making, social and emotional control (Funahashi, 2001). However, it is also susceptible to environmental risk factors and is implicated in the development of psychiatric disorders (Funahashi, 2001; Gao et al., 2012). Given the strong associations of MDD, bipolar disorder and schizophrenia with this structure (Howard et al., 2019; Mullins et al., 2021; Trubetskoy et al., 2022), it has received substantial attention in the study of these disorders (Bristot, De Bastiani, Pfaffenseller, Kapczinski, & Kauer-Sant'Anna, 2020; Fromer et al., 2016; Nagy et al., 2020; Ruzicka et al., 2022; Worf et al., 2022). Specifically, structural and functional abnormalities of the orbitofrontal cortex (OFC), a key component of the ventral prefrontal cortex, have been widely reported in many psychiatric disorders (Frisoni et al., 2009; Jackowski et al., 2012; Opel et al., 2020; Zhou, Xiong, Chen, & Wang, 2023). Brodmann area 11 (Brodmann, 1909), a subregion of the OFC, has shown reduced gray matter volume in elderly schizophrenia patients compared to healthy elders (Frisoni et

al., 2009) and dysregulation of gene expression and DNA methylation in depressed and suicidal patients (Zhou et al., 2023).

Understanding the mechanisms of psychiatric disorders in the OFC is exacerbated by the complex interplay between its diverse cell types. While the ratio of glia to neurons across the entire human brain has been estimated to be around 10 for a long time, more recent studies indicate the ratio to be closer to 1-1.5 (von Bartheld, Bahney, & Herculano-Houzel, 2016). However, the proportion of non-neuronal (mostly glial) cells to neurons varies significantly across brain regions, with estimates between 1.3 and 2.7 across cortical subregions (2.3 in PFC) (Ribeiro et al., 2013). Although diverse in function, glial cells are universally characterized by their non-excitable nature, which distinguishes them from neurons. Unlike neurons, which are responsible for creating and transmitting electrical and chemical signals, glial cells primarily regulate neuronal activity and communication (Rasband, 2016). All neurons and glial cells originate from a common progenitor – the neuroepithelial cell (Kintner, 2002). Here, I give an overview of the diverse cortical cell types, and their morphological and functional characteristics (Figure 1.3).

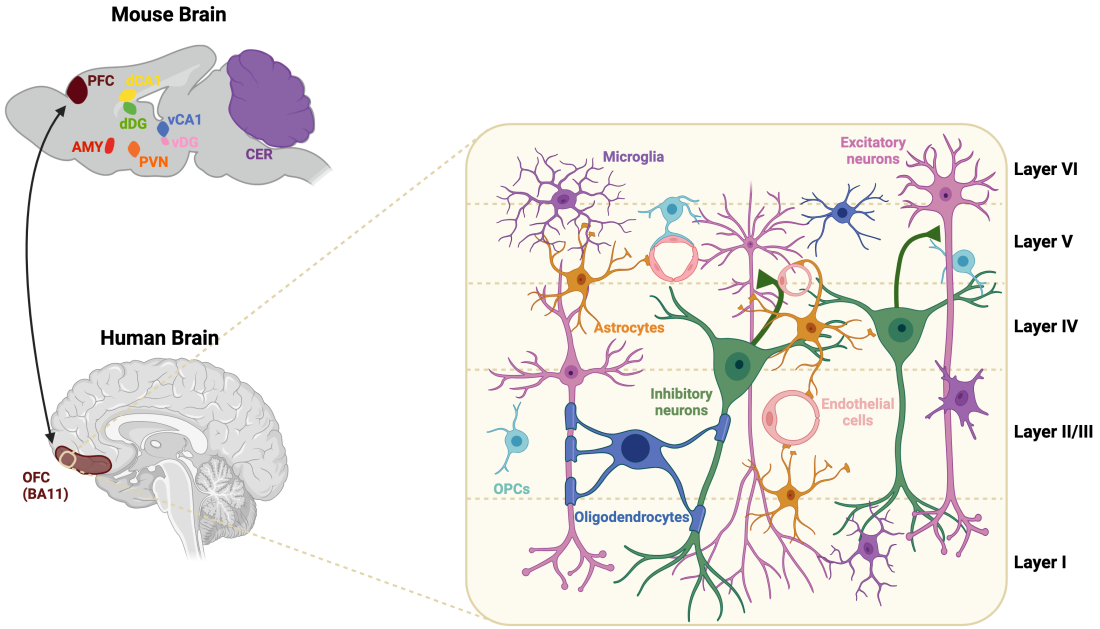


**Figure 1.3. Dissected brain regions and cortical cell types for stress response and psychiatric disorder studies.** This schematic representation outlines the 8 brain regions analyzed (amygdala – AMY, prefrontal cortex – PFC, dorsal and ventral *cornu ammonis* 1 – dCA1 and vCA1, dorsal and ventral dentate gyrus – dDG and vDG, paraventricular nucleus of the hypothalamus – PVN, cerebellum – CER) for examining the transcriptomic response to glucocorticoid receptor activation in stress response in the mouse brain (upper left) and the subregion of the orbitofrontal cortex (OFC – BA11) dissected to study the molecular basis of psychiatric disorders on a cell type level (lower left). On the right, the diverse cell types present in the OFC's cortical layers are depicted which are the focus of the psychiatric disorder study. Based on (R. Fang et al., 2022; Fuster, 1988). Created with Biorender.com

**Glutamatergic projection neurons**, shortly also referred to as **excitatory neurons**, account for 70-80% of neocortical neurons and are primarily responsible for neural activation in the brain (Markram et al., 2004). Their role is to release neurotransmitters like glutamate, which elicit postsynaptic action potentials, essential for neural communication (Nieuwenhuys, 1994). Originating from progenitors in the dorsolateral wall of the telencephalon (Molyneaux et al., 2007), these neurons are characterized by their pyramidal-shaped cell bodies, an axon, and extensive dendritic trees, which are essential for receiving a wide range of synaptic inputs (Spruston, 2008). Excitatory neurons are distributed across different cortical layers, each with unique connections and functions (Douglas & Martin, 2004; Molyneaux et al., 2007), as well as layer and subtype-specific patterns of gene expression (Tasic et al., 2018). As described by Nieuwenhuys (1994) and Molyneaux et al. (2007), callosal neurons, a subset of associative projection neurons, are predominantly situated in layers II/III, V, and VI of the cortex. These neurons are characterized by their long axons, projecting to different cortical regions that traverse the corpus callosum. Meanwhile, corticothalamic neurons, which fall under the category of corticofugal projection neurons, are mainly found in cortical layer VI. These neurons project their axons subcortically to various nuclei within the thalamus. In addition, subcerebral projection neurons, also a class of corticofugal projection neurons, reside in the deeper regions of layer V. These neurons extend their projections down to the brainstem and spinal cord, playing a crucial role in the communication between the cortex and subcortical structures (Molyneaux et al., 2007; Nieuwenhuys, 1994).

In contrast to their excitatory counterparts, **GABAergic interneurons**, also referred to as **inhibitory neurons**, comprise 20-30% of the neocortical neuronal population and serve as essential regulators of excitatory signaling (Markram et al., 2004). Interneurons are essential for maintaining the balance of neural activity within the brain (Markram et al., 2004). Inhibitory neurons release neurotransmitters like GABA, which hyperpolarize the postsynaptic membrane, reducing the likelihood of an action potential (Fritschy & Brünig, 2003). These neurons arise from progenitors in the ventral telencephalon and display a rich morphological and functional diversity (Molyneaux et al., 2007). Most interneurons, including basket cells and chandelier cells, have aspiny dendrites and exhibit extensive dendritic trees, allowing them to receive input from multiple sources (Markram et al., 2004). They play a crucial role in suppressing neural activity, targeting the somata and axons of pyramidal neurons, and are critical for the timing and synchronization of action potentials (Markram et al., 2004). According to Fishell and Kepecs (2020), interneurons come in various subtypes, each with a specific role in the neural network. Parvalbumin-expressing (PVALB) interneurons are known for synchronizing neural activity and contributing to the generation of gamma oscillations. Somatostatin (SST) interneurons, found in layers 2-5, target the dendrites of excitatory neurons across multiple layers and are involved in dendritic inhibition. Other subtypes, such as those expressing vasoactive intestinal polypeptide (VIP), often disinhibit other interneurons, adding another layer of complexity to the regulation of neural circuits. Additional subtypes like RELN (reelin) and LAMP5 (lysosomal-associated membrane protein family member 5) interneurons further diversify the inhibitory landscape of the neocortex (Fishell & Kepecs, 2020).

**Astrocytes** are the most abundant type of glial cells, comprising approximately 25% of the brain's volume (Guillamón-Vivancos, Gómez-Pinedo, & Matías-Guiu, 2015). As described by Guillamón-Vivancos et al. (2015), astrocytes, traditionally viewed as support cells, play a crucial role in maintaining the brain's microenvironment. Morphologically, they are divided into two major groups: protoplasmic and fibrous. Protoplasmic astrocytes, primarily located in gray matter, have a rounded shape and highly branched, uniformly distributed processes, making contact with both synapses and blood vessels. Fibrous astrocytes, usually located in white matter, are characterized by their less branched, longer, and more fiber-like processes that often extend endfeet wrapping around blood vessels. Although they do not generate action potentials, astrocytes are excitable cells that play a role in communication. They can be activated by various signals and engage in gliotransmission, sending specific messages to adjacent cells. Functionally, astrocytes are involved in the development of the nervous system and synaptic plasticity, guiding growing axons with astrocyte-derived molecules and actively participating in synaptogenesis (Guillamón-Vivancos et al., 2015). They provide metabolic support to neurons, maintaining stable concentrations of glutathione (Sidoryk-Wegrzynowicz, Wegrzynowicz, Lee, Bowman, & Aschner, 2011). Additionally, astrocytes regulate neurotransmitter levels by taking up and releasing glutamate and GABA, with high levels of glutamine synthetase facilitating the conversion of glutamate to glutamine, thus maintaining optimal synaptic glutamate concentrations (Kimelberg & Nedergaard, 2010). They also regulate the extracellular environment, including ion homeostasis, and produce and release growth factors, further underscoring their supportive role for neurons (Sidoryk-Wegrzynowicz et al., 2011).

**Microglia** are specialized glial cells of immune origin that play a pivotal role as the central nervous system's (CNS) primary defense mechanism (Guillamón-Vivancos et al., 2015). These cells migrate into the brain from the bloodstream during early development (Guillamón-Vivancos et al., 2015). They comprise roughly 10% of the cells in the CNS and function similarly to macrophages, though with a homeostatic phenotype (Colonna & Butovsky, 2017). Morphologically, microglia are highly dynamic, characterized by their highly branched structure. Their processes are in constant motion, allowing microglia to make contact with neurons, astrocytes, and blood vessels (Colonna & Butovsky, 2017). Upon encountering injuries or inflammatory stimuli, microglia can transform from their ramified state into an amoeboid form, a change that facilitates their defensive functions (Colonna & Butovsky, 2017). Functionally, microglia are responsible for phagocytosis, clearing the CNS of harmful entities such as microbes, dead cells, and other potentially dangerous substances (Colonna & Butovsky, 2017; Nayak, Roth, & McGavern, 2014). They are also the primary source of proinflammatory cytokines, making them key players in neuroinflammation (Colonna & Butovsky, 2017). Beyond their role in defense, microglia contribute to neuronal survival by releasing growth factors that aid in the formation and maintenance of neuronal circuits (Nayak et al., 2014). Additionally, microglia express immune receptors and neurotransmitter receptors, which facilitate glia-neuron communication and allow them to monitor neuronal and synaptic activity (Colonna & Butovsky, 2017).

**Oligodendrocyte precursor cells (OPCs)**, constituting approximately 5% of cells in the CNS, maintain a state of constant homeostasis and are permanently present throughout the CNS (Xiao & Czopka, 2023). Also referred to as synantocytes, polydendrocytes, or NG2 glia, these cells exhibit a distinct morphology that varies by brain region (Nishiyama, 2007; Xiao & Czopka, 2023). Their processes are radially oriented in gray matter and more elongated in white matter (L.-P. Fang & Bai, 2023). OPCs differentiate into myelinating oligodendrocytes, a process essential for forming new myelin, as existing oligodendrocytes do not generate it (Nishiyama, 2007; Xiao & Czopka, 2023). Beyond myelination, OPCs regulate neural circuits by controlling neuronal density, synaptic activity, and action potential conduction velocity (L.-P. Fang & Bai, 2023). They integrate into local neural circuits, receiving glutamatergic signals through AMPA and NMDA receptors, and sense neuronal activity via the potassium channel Kir4.1 (L.-P. Fang & Bai, 2023). OPCs also engage in synaptic neurotransmission, in immunomodulation by influencing microglia and T cells, and contribute to axonal remodeling and synapse pruning, impacting neural network activity and function (L.-P. Fang & Bai, 2023).

**Oligodendrocytes** are pivotal in forming myelin sheaths around axons in the CNS, with myelination being their primary function (Guillamón-Vivancos et al., 2015). They originate from OPCs and progress through stages of maturation, from immature to mature myelinating oligodendrocytes (Simons & Nave, 2016). Their morphology is characterized by two major cytoskeletal components: microtubules and F-actin (Michalski & Kothary, 2015). The life cycle of an oligodendrocyte encompasses four phases: birth, migration, and proliferation of OPCs; morphological differentiation with process expansion; axonal contact leading to myelin sheath formation; and long-term metabolic support of axons (Michalski & Kothary, 2015). Oligodendrocytes synthesize various myelin components and transport them to the myelin sheath during development (Simons & Nave, 2016). They also provide metabolic support to axons, transferring energy metabolites like lactate, which axons utilize for ATP production (Simons & Nave, 2016). This metabolic exchange is facilitated by cytoplasmic channels and monocarboxylate transporters in the myelin sheath, underscoring the critical role oligodendrocytes play in neuronal function and health (Philips & Rothstein, 2017).

**Endothelial cells** constitute the inner lining of blood vessels in the human cortex and are a critical component of the blood-brain barrier (BBB) (Zlokovic, 2008). This selective interface is responsible for regulating the passage of substances between the bloodstream and the brain (Zlokovic, 2008). Morphologically, endothelial cells are elongated and thin, creating a continuous single layer that lines the interior surface of blood vessels (Nag, 2011). These cells are interconnected by tight junctions, which contribute to the BBB's selective permeability properties and are crucial for preventing neurotoxic substances from entering the brain while allowing essential nutrients and gases to pass through (Abbott, Patabendige, Dolman, Yusof, & Begley, 2010). Endothelial cells play a key role in physiological functions including angiogenesis, which is the formation of new blood vessels from existing ones (Carmeliet & Jain, 2011). In addition to their structural role, cortical endothelial cells secrete factors that influence the function and maintenance of other BBB components, including pericytes and astrocytic end-feet

(Abbott et al., 2010). Furthermore, endothelial cells contribute to immune surveillance by regulating immune cell migration into the CNS, thereby participating in neuroprotective and neuroinflammatory processes (B. Engelhardt & Ransohoff, 2005).

Within the scope of this thesis, I examine the molecular architecture of psychiatric disorders across the described cortical cell types, aiming to characterize their distinct pathological signatures.

## 1.6 Genetic Architecture of Psychiatric Disorders

Psychiatric disorders exhibit a substantial genetic component which has been the focus of many studies aiming to unravel their complex etiology. Twin studies have been instrumental in determining the **heritability** of psychiatric disorders, with early twin studies emphasizing strong heritable effects for schizophrenia and bipolar disorder (Smoller et al., 2019). More recent twin studies, including those focused on MDD and anxiety disorders, have confirmed a substantial genetic component in these conditions. Twin studies suggest a heritability of 77% for schizophrenia, 68% for bipolar disorder, and 45% for MDD (Polderman et al., 2015; Smoller et al., 2019). In contrast, Single Nucleotide Polymorphism (SNP)-based heritability is significantly lower, ranging from 8% to 24% for the three disorders (Consortium., 2019; Howard et al., 2019; Mullins et al., 2021; Smoller et al., 2019; Trubetskoy et al., 2022). SNP arrays are commonly used to detect polymorphisms, covering a curated set of biallelic genetic markers optimized for robust measurements and genomic coverage (Patrick F. Sullivan & Geschwind, 2019). Possible explanations of the missing heritability include rare *de novo* variants which are not covered by current genotyping arrays, undiscovered common and structural variants, epigenetic factors, a lack of power to identify gene-gene interactions, and the failure to adequately account for shared environmental effect among relatives (Geschwind & Flint, 2015; Manolio et al., 2009; Yang, Zeng, Goddard, Wray, & Visscher, 2017).

Epidemiological studies implicate a high **comorbidity** between psychiatric disorders, as individuals diagnosed with one disorder exhibit an increased likelihood of developing other psychiatric conditions (McGrath et al., 2020). This, besides their overlapping symptoms, emphasizes the common genetic architecture of psychiatric disorders, a phenomenon referred to as pleiotropy (Consortium., 2019; Sivakumaran et al., 2011; Smoller et al., 2019). Genetic correlation analyses have revealed distinct clusters of interconnected disorders, with one highly genetically correlated group comprising mood and psychotic disorders such as MDD, bipolar disorder, and schizophrenia (SNP-based correlations: schizophrenia-bipolar 0.7, schizophrenia-MDD 0.34, and MDD-bipolar 0.36) (Consortium., 2019). This group of disorders with shared genetic architecture has been the focus of extensive research (Blokland et al., 2022; Cardno & Owen, 2014; Consortium., 2019; Docherty, Moscati, & Fanous, 2016; Opel et al., 2020; Worf et al., 2022).

**Genome-wide association studies (GWASs)**, characterized by the need for large sample sizes, have significantly advanced our understanding of the genetic architecture of psychiatric disorders, with substantial numbers of significant variants associated with MDD ($n_{sig.\ loci}$=102, $n_{MDD\ cases}$=246K) (Howard et al., 2019), bipolar disorder ($n_{sig.\ loci}$=64, $n_{bipolar\ cases}$=42K) (Mullins et al., 2021) and schizophrenia ($n_{sig.\ loci}$=287, $n_{schizophrenia\ cases}$=77K) (Trubetskoy et al., 2022), as of March 2024. Genes implicated by schizophrenia GWAS variants are predominantly expressed in excitatory and inhibitory neurons, and enriched in pathways of synaptic organization and neuronal function (Trubetskoy et al., 2022). Similarly, bipolar disorder GWAS variants are fine-mapped to genes with a particularly high expression in cortical and hippocampal neurons and part of synaptic signaling pathways (Mullins et al., 2021). MDD GWAS variants are also mapped to genes active in the nervous system and involved in synapse function and neurotransmission (Howard et al., 2019), suggesting shared molecular underpinnings in neuronal processes across these psychiatric disorders.

Despite the massive scale of these GWAS and the high number of identified SNPs, it is crucial to recognize that many more variants, including rare variants and copy number variations (Kirov et al., 2012), are expected to be associated with the genetic architecture of these highly polygenic disorders. Even larger sample sizes and different approaches will hopefully lead to a more comprehensive detection of causal variants in the future. Efforts such as the GWAS catalog, a standardized and interoperable collection of GWASs, or the Psychiatric Genomics Consortium, performing GWAS meta- and mega-analyses on psychiatric disorders, are pivotal in advancing towards this objective (Buniello et al., 2019; Sollis et al., 2022; P. F. Sullivan, 2010).

**Polygenic risk scores (PRS)** have emerged as a valuable tool to capture the cumulative genetic risk for a particular disease or trait and may be instrumental in the development of tailored treatment strategies in personalized medicine (C. M. Lewis & Vassos, 2020; S. M. Purcell et al., 2009; Patrick F. Sullivan & Geschwind, 2019). The application of PRS has enabled a deeper exploration of the relationship between genetic risk and various genomic layers (Võsa et al., 2021), such as gene expression and chromatin accessibility, to understand the full spectrum of psychiatric disorders.

In the subsequent sections of this thesis, I link the genetic risk for psychiatric disorders with cell type-specific changes in gene expression and chromatin accessibility in the human brain. Recognizing the research community's agreement that reliable risk predictions are most feasible at the tails of the PRS distributions (Andlauer & Nöthen, 2020; Patrick F. Sullivan & Geschwind, 2019), my thesis focuses on these high and low risk groups rather than treating PRS on a continuous scale.

## 1.7 Transcriptomics in Psychiatric Research

Transcriptomics, particularly **RNA-sequencing (RNA-seq)**, has emerged as a pivotal tool in psychiatric research, offering unprecedented insights into the molecular correlates of stress and psychiatric disorders. By quantifying RNA in biological samples, this method enables the identification of gene expression changes or splice variants, providing a dynamic view of the transcriptome in various conditions (Wang, Gerstein, & Snyder, 2009).

RNA-seq involves the reverse transcription of RNA into cDNA fragments, which are then sequenced and aligned to a reference genome to quantify transcriptome-wide gene expression levels (Wang et al., 2009). Differential expression analysis is widely used to study gene-level associations with phenotypes like psychiatric conditions (Fromer et al., 2016; Merikangas et al., 2022; Ramaker et al., 2017). Complementary to this, gene set enrichment (Subramanian et al., 2005) and network analyses (de la Fuente, 2010; Langfelder & Horvath, 2008; Ogris, Hu, Arloth, & Müller, 2021) allow for the exploration of complex interactions among genes, tissues, and outcomes (Bagot et al., 2016; Bowen, Burgess, Granger, Kleinman, & Rhodes, 2019; Geng et al., 2020; Huggett & Stallings, 2020; Kapoor et al., 2019; Kwon, Kim, Choi, Seol, & Kang, 2019; Labonté et al., 2017; X. Li et al., 2019; J. Liu, Jing, & Tu, 2016; Parikshak, Gandal, & Geschwind, 2015; Pierson, Koller, Battle, & Mostafavi, 2015; Sato et al., 2019; Zimmermann et al., 2019). Regulatory transcriptional networks have been constructed to identify master regulators in disorders like MDD, bipolar disorder, and schizophrenia (Funahashi, 2001), highlighting the power of transcriptomics in discerning key molecular players. More information on molecular network analysis can be found in Section 1.10.

The **intersection of genetics and the transcriptome** is an important field in psychiatric research trying to shed light on the complex interplay between inherited genetic variations and associated expression patterns. For instance, approximately 20% of GWAS variants associated with schizophrenia have been found to potentially influence gene expression (Fromer et al., 2016). Expression quantitative trait loci (eQTL) studies have been instrumental in pinpointing genetic variants associated with disease that influence gene expression, frequently manifesting in *trans*-regulatory effects, as indicated by research in various tissues including blood (Porcu et al., 2021; Võsa et al., 2021) and brain (Bryois et al., 2022; Dobbyn et al., 2018). Recognizing the high tissue specificity of gene expression and correspondingly eQTLs, the Genotype-Tissue Expression (GTEx) project has developed an extensive resource facilitating the examination of eQTLs across different tissues (Lonsdale et al., 2013). Additionally, the CommonMind Consortium has assembled a large collection of brain samples, which enables the investigation of eQTLs associated with psychiatric disorders (Hoffman et al., 2019). Transcriptome-wide association studies (TWAS) for MDD and schizophrenia, integrating GWAS with gene expression levels, identified 94 and 157 genes respectively with significant association, thereby offering insights into causal genes and the nature of their impact on these diseases (Dall'Aglio, Lewis, & Pain, 2021; Gusev et al., 2018). However, the vast number of risk variants identified by GWAS, along with their often non-coding nature, and the complex phenomena of pleiotropy and incomplete

penetrance make the translation of these findings into mechanistic insights challenging (Hernandez et al., 2021). There is a notable correlation between PRS for psychiatric disorders and variations in gene expression, underscoring the significant impact of cumulative small genetic effects on the regulation of gene activity (Võsa et al., 2021; Worf et al., 2022).

Transcriptomics serve as a bridge connecting genetic predisposition to molecular function in psychiatric research. The subsequent chapters will delve deeper into how these molecular insights translate into psychiatric conditions and genetic risk factors.

## 1.8 Epigenomics in Psychiatric Research

The exploration of epigenomics in psychiatric disorders has become an important aspect of understanding the molecular basis that underlies these complex conditions. Epigenetic modifications are known to be tissue- and cell-specific, and act as major risk factors for psychiatric disorders, **integrating the influence of genetic and environmental factors** on cellular function (Keverne & Binder, 2020).

Epigenetic processes are of particular importance in the brain, as they need to ensure optimal functioning and interactions in an assembly of primarily postmitotic cells (Cholewa-Waclaw et al., 2016). They contribute to cell differentiation and developmental processes in the brain, but their modifications can be triggered by environmental factors and mediate the relationship between environment and gene regulatory mechanisms (Egervari, 2021; Griffiths & Hunter, 2014). Negative life events, especially during childhood, have been linked to an increased risk for psychiatric disorders mediated by epigenetic mechanisms (Griffiths & Hunter, 2014; Weaver et al., 2004; Weaver, Meaney, & Szyf, 2006).

Keverne and Binder (2020) review the epigenetic layers associated with psychiatric disorders. Some of the major carriers of epigenetic information in psychiatric disorders are **DNA methylation**, **chromatin modifications**, **non-coding RNAs**, and **RNA modifications**. The accessibility of specific DNA sequences to transcription regulators – and RNA sequences to translational regulators in the case of RNA modifications – is collectively shaped by these epigenetic layers. DNA methylation represents the most studied layer of epigenetic regulation in MDD. Nonetheless, findings consistent in position and directionality are still to be reported (Keverne & Binder, 2020).

The primary positions for regulatory elements in the genome, including promoters, enhancers, silencers, or transcription factor binding sites, are thought to be open chromatin regions (Tsompana & Buck, 2014). Using the **assay for transposase-accessible chromatin sequencing (ATAC-seq)**, these accessible chromatin regions can be easily detected by high-throughput sequencing after sequencing adaptors are transposed into the DNA backbone by the Tn5 transposase (Buenrostro, Giresi, Zaba, Chang, & Greenleaf, 2013). ATAC-seq requires low amounts of starting material which makes it a

practical choice for large-scale sequencing experiments, even at the single-cell level (Buenrostro et al., 2013; Buenrostro et al., 2015).

While several studies reported a positive correlation between gene expression and chromatin accessibility in the respective gene's promoter region (Reske, Wilson, & Chandler, 2020; Wong et al., 2023), other studies reported that changes in gene expression often occur independently of alterations in chromatin accessibility in the respective genomic region (de la Torre-Ubieta et al., 2018). Different factors such as transcription factor binding, DNA methylation, or histone modifications might primarily regulate gene expression in these cases (de la Torre-Ubieta et al., 2018; Natarajan, Yardımcı, Sheffield, Crawford, & Ohler, 2012). This complexity was further elucidated by Starks et al., who identified distinct groups with varying gene expression and accessibility patterns, each associated with different cellular functions, such as housekeeping genes, or tissue-specific genes (Starks, Biswas, Jain, & Tuteja, 2019).

The focus of psychiatric research has shifted in many cases towards epigenetic studies, which have the potential to clarify the complex interplay between genetics, gene regulation, and environmental variables since the majority of GWAS variants linked to psychiatric diseases are found in non-coding regulatory elements (Bryois et al., 2018; Consortium., 2019). A study by Bryois et al. (2018) evaluated the relationship between schizophrenia and chromatin accessibility in the human prefrontal cortex, and observed an enrichment of accessible regions for psychiatric risk variants but identified only a small number of differentially accessible regions between schizophrenia patients and controls. This discrepancy was attributed to a significant limitation in bulk studies - the potential masking of cell type-specific effects (Bryois et al., 2018). A high variability of chromatin accessibility between cell types in different cortical regions in human postmortem brain samples was actually detected using fluorescence-activate nuclear sorting (Hauberg et al., 2020). Additionally, a single-cell study of MDD revealed accessibility alterations predominantly in deep-layer excitatory neurons of the prefrontal cortex (Chawla et al., 2023).

By studying epigenetic mechanisms in the brain, including chromatin accessibility, I aim to reach a better understanding of the gene regulatory processes and their impairments contributing to the development and manifestation of psychiatric disorders.

## 1.9 Single-Cell Molecular Profiling in Psychiatric Research

Recent advances of single-cell sequencing technologies have significantly enhanced our capability to perform high-resolution studies of different tissues at the level of individual cell types (Buenrostro et al., 2015; Kulkarni, Anderson, Merullo, & Konopka, 2019; Wagner, Regev, & Yosef, 2016). These technologies have facilitated the development of single-cell transcriptomic and epigenomic atlases for the human brain, revealing hundreds of unique cell types and even thousands of cellular subtypes among millions of cells from various brain regions (Y. E. Li et al., 2023; Siletti et al., 2023).

It is of major importance to address cellular heterogeneity in postmortem human brain studies for psychiatric disorders (Price, Jaffe, & Weinberger, 2021). Techniques such as computational deconvolution of bulk tissue signals, based on known cell type-specific profiles, offer a rapid and cost-effective approach, yet they provide only estimates of cell type proportions (Newman et al., 2015). Historically, methods like laser capture microdissection and fluorescence-activated nuclear sorting have enabled the study of individual cells or nuclei, yet they come with limitations in throughput and other technical constraints (Matevossian & Akbarian, 2008; Price et al., 2021; Rossner et al., 2006).

Nowadays, single-cell sequencing technologies enable transcriptomic and epigenomic profiling of single cells (Figure 1.4). While plate-based methods allow for the isolation and analysis of individual cells or nuclei within PCR plates (Picelli et al., 2014), droplet-based methods offer the capacity to sequence thousands of cells in isolation within nanoliter droplets (Macosko et al., 2015). Droplet-based strategies like the 10x Genomics Chromium platform, which was utilized to generate the single-cell sequencing data parts of this thesis rely on, provide much sparser RNA coverage, but offer higher throughput than plate-based strategies (Price et al., 2021).

The choice between single-cell and single-nuclei sequencing depends on the availability of intact cells, a condition frequently unmet in postmortem brain samples, which are commonly fresh-frozen and sourced from brain banks. Research indicates that nuclear RNA can serve as a proxy for the whole transcriptome, thereby justifying the use of single-nuclei sequencing in scenarios where intact cells cannot be obtained (Trygve E. Bakken et al., 2018; Price et al., 2021).

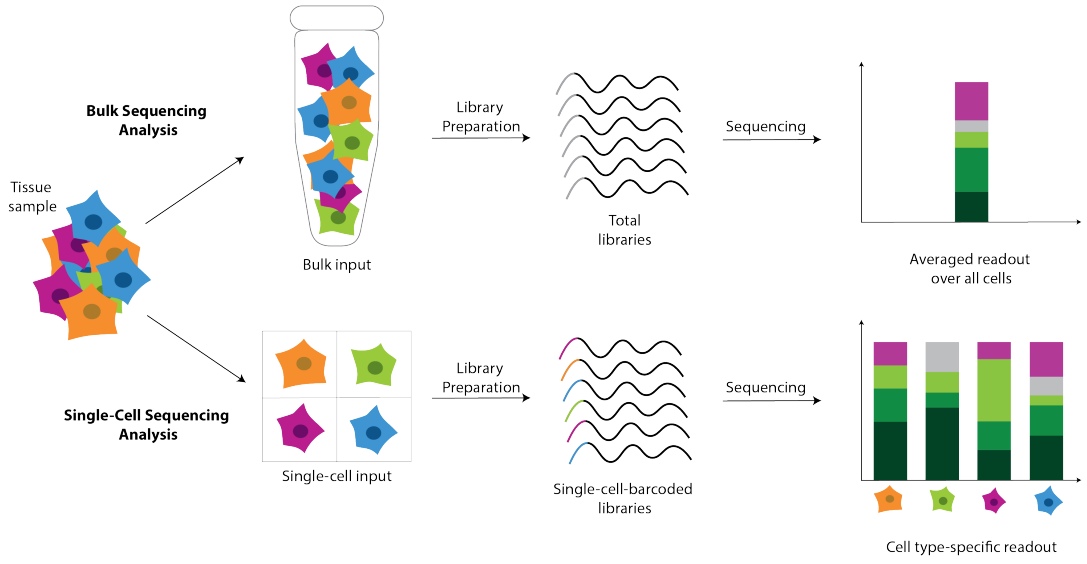


**Figure 1.4. Bulk and single-cell sequencing analysis.** During single-cell sequencing reads are getting barcoded on the single-cell level which provides molecular profiles for individual cells that can be mapped to cell types, while bulk sequencing provides molecular profiles averaged across all cells of a tissue sample. Based on (Clark)

Single-cell molecular profiling significantly advances our understanding of the complex etiology of psychiatric disorders. Comparative studies between diseased and healthy donors are increasingly transitioning from broad bulk analyses to more granular single-cell resolution (Chawla et al., 2023; Nagy et al., 2020; Ruzicka et al., 2022). Psychiatric studies focusing on cellular populations within the prefrontal cortex related to MDD highlighted the crucial role of excitatory neurons in modulating both gene expression and chromatin accessibility (Chawla et al., 2023; Nagy et al., 2020). Another investigation, employing single-nucleus transcriptomics to explore molecular alterations associated with schizophrenia, revealed that a significant proportion of differentially expressed genes identified within specific cell types were also detected in bulk data analyses. However, inhibitory neurons and non-neuronal cell types exhibited a substantial number of cell type-specific hits, thereby underscoring how findings derived from bulk and cell type-specific approaches complement each other (Ruzicka et al., 2022).

Here, I explore the transcriptomic and epigenomic profiles of the orbitofrontal cortex in psychiatric disorders, using single-nuclei sequencing data from postmortem brain samples from patients and controls. The dissection on the level of single cells provides a detailed map of cell type-specific alterations in psychiatric disorders.

## 1.10 Multi-Omics and Network-Based Analyses of Psychiatric Disorders

Multi-omics studies in psychiatric research are enabling an integrated analysis of diverse data types, including molecular data, such as genomics, transcriptomics, epigenomics, and proteomics, but also phenotypic data (Figure 1.5). These studies are based on the understanding that psychiatric disorders arise from complex interactions within biological pathways, rather than from changes in single biomolecules (Sathyanarayanan et al., 2023). Multi-omics approaches enable the identification of biomarkers and unravel disease mechanisms that are consistently associated with a condition. A better understanding of these pathomechanisms is essential for the development of personalized medicine, whereby treatments can be tailored towards the unique molecular profiles of individual patients (Joyce et al., 2021; Sathyanarayanan et al., 2023).

The integration of different data modalities is accomplished through bioinformatics tools, which employ statistical methods such as enrichment-based methods for overlap and association analysis (Sey et al., 2020; Watanabe, Taskesen, Van Bochoven, & Posthuma, 2017; Wu et al., 2021), statistical fine-mapping for establishing causality (Giambartolomei et al., 2014), and imputation-based methods like TWAS for predicting gene expression from genotypic data (Dall'Aglio et al., 2021). Machine learning further enhances multi-omics by applying for example linear and logistic regression, clustering, graph neural networks, and random forests (Sathyanarayanan et al., 2023). These techniques are instrumental for diagnostic classification and for predicting risk and treatment responses (Joyce et al., 2021).

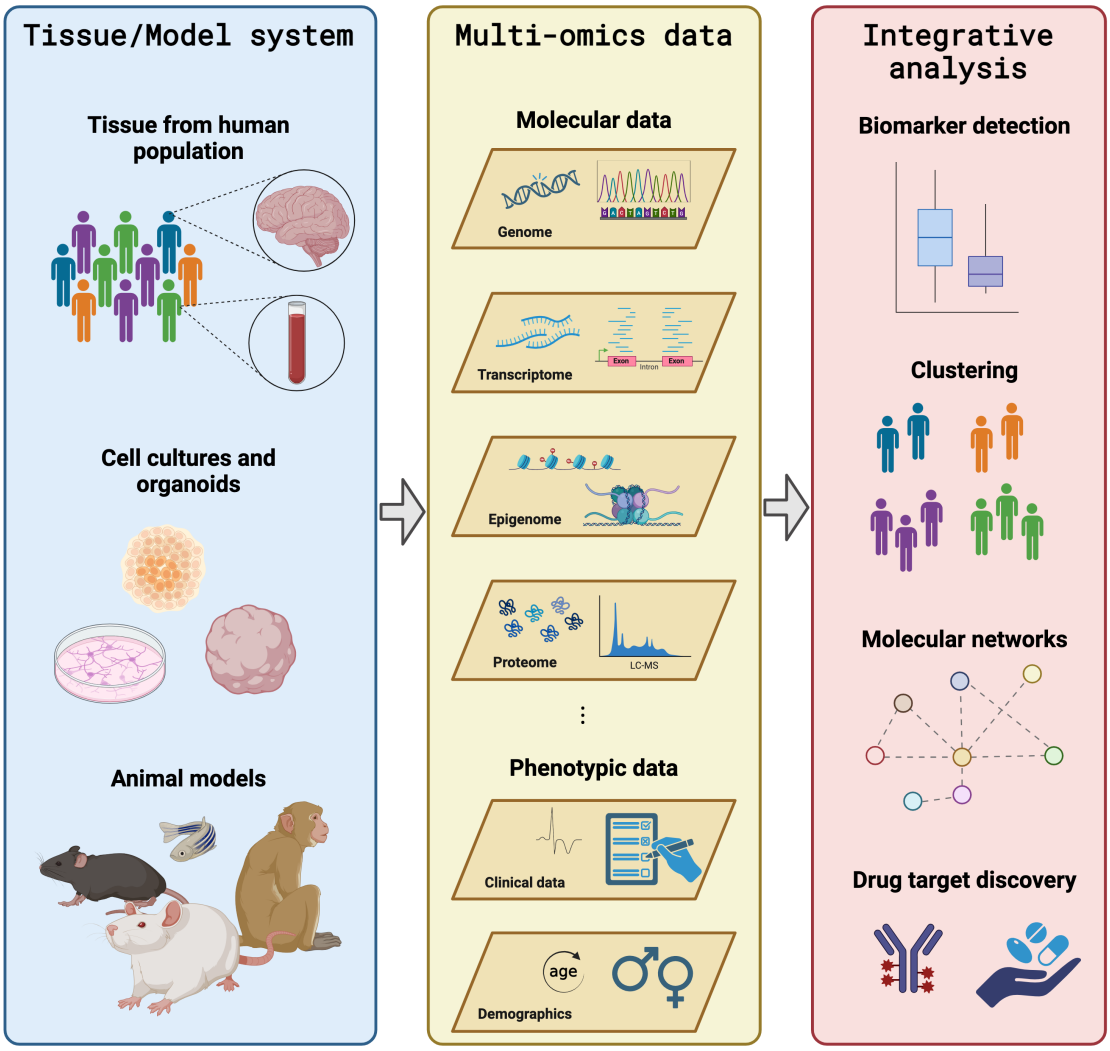


**Figure 1.5. Multi-omics analyses in psychiatric research.** Data is obtained from tissue of human populations, animal models, or cell cultures and organoids. The data modalities may include various molecular measurements, such as genomics, transcriptomics, epigenomics, or proteomics, as well as phenotypic data, including clinical data or demographics. Integrative statistical and machine learning methods are used for biomarker detection, clustering (e.g., patient stratification), inference of molecular networks, drug target discovery, and more. Created with BioRender.com

Graph- and network-based modeling are vital for the exploration of the interactions among multiple genes, tissues, and clinical outcomes in complex disorders. While strong differential expression is evident when major genetic or environmental factors are at play, as seen in conditions like cancer (Perduca, Omichessan, Baglietto, & Severi, 2018; Sondka et al., 2018), psychiatric disorders are highly polygenic, whereby many genetic variants with small effect sizes cumulatively contribute to the overall risk (Akbarian et al., 2015; M. Li et al., 2018).

Combining differential expression analysis with network analysis has proven to be particularly effective in dissecting the pathomechanisms of complex disorders (Parikshak et al., 2015). Gene co-expression networks, constructed using Pearson's correlation, alongside differential expression analysis, have been employed to examine the shared and distinct transcriptomic profiles of various psychiatric disorders, leading

to the identification of gene modules associated with specific cell types and disorders (Gandal, Zhang, et al., 2018).
However, correlation-based network inference can result in over-connectivity and low specificity (Saint-Antoine & Singh, 2020). To combat this, alternative methods like regression-based and Bayesian techniques are employed. Bayesian methods, although less suited for large datasets, are advantageous for smaller networks. Conversely, regression and other machine learning algorithms require large sample sizes to infer connections confidently (Bersanelli et al., 2016; Saint-Antoine & Singh, 2020). To optimize performance on datasets with limited samples, reduction of the input space through prior knowledge is often required (Linde, Schulze, Henkel, & Guthke, 2015).

KiMONo exemplifies this approach by utilizing prior knowledge of functional relationships sourced from public databases, to infer integrated multi-level networks (Ogris et al., 2021). Differential network analysis further extends the capability to represent differential co-expression and regulatory interactions within a single network, enabling the study of directed multivariate effects of treatments or disease states on gene neighborhoods (Kim Youngsoon, 2018). The advantage of combining differential network analysis with prior knowledge-based network inference is the resulting topological coherence. This is reflected in network metric such as node degree, which measures the number of edges a particular node has, or node-betweenness, measuring the degree to which a node is located on the shortest path between other nodes (Freeman, 1977), thereby increasing the robustness of differential connection calculations.

In this thesis, I aim to harness the power of multi-omics to uncover the molecular intricacies of psychiatric disorders and the biological effects of glucocorticoid exposure. I infer differential transcriptomic networks that are guided by prior knowledge to observe the intricate changes in gene expression patterns resulting from glucocorticoid exposure. By integrating genetic, transcriptomic, and epigenomic data, I aim to map the complex landscape of molecular alterations that underpin psychiatric disorders.

## 1.11 Aims of the Thesis

The overall aim of my thesis is to enhance our understanding of molecular alterations underlying stress and psychiatric disorders, with a particular emphasis on the specificity of these dysregulations to brain regions and cell types. My focus lies on transcriptomic and epigenomic changes in response to stress, and in relation to psychiatric disorders and the genetic predisposition for such disorders.

The project detailed in Chapter 3.1 of my thesis focuses on understanding the brain region-specific responses to glucocorticoid receptor activation at a transcriptome-wide level using a mouse model. The study explores whether genes that are differentially expressed upon glucocorticoid exposure also exhibit changes in co-expression patterns. Additionally, the project seeks to determine whether differential network analysis can provide further insights beyond differential expression analysis.

The second project within my thesis (Chapter 3.2) is designed to discern cell type-specific dysregulations related to psychiatric disorders and the genetic predisposition for those in the orbitofrontal cortex. By using single-nuclei RNA-seq and ATAC-seq data, I aim to determine if gene expression correlates with chromatin accessibility both across and within cell types. The research focuses on the comparison of gene expression between trans-diagnostic psychiatric cases and controls across distinct cell types, investigating the biological processes affected at the gene expression level in these psychiatric disorders. Another crucial aspect is to examine how chromatin accessibility patterns vary between cases and controls and whether changes in accessibility occur nearby regions of differentially expressed genes, emphasizing the importance of multi-modal integration. Further, the study assesses dysregulations in gene expression and chromatin accessibility between donors with high and low genetic risk for psychiatric phenotypes within different cell types. It investigates whether the dysregulated patterns differ from those observed between cases and controls, thereby contributing to a better understanding of the molecular architecture of psychiatric disorders.

In addition, my doctoral thesis aims to unravel the complex interplay between stress, glucocorticoid receptor activation, and dysregulations in psychiatric disorders in the prefrontal cortex, examining the extent to which glucocorticoid receptor activation disrupts the same genes and pathways implicated in stress-related disorders. This will elucidate whether the genetic and molecular disruptions observed in stress-related disorders align with those induced by glucocorticoid receptor activation.

Overall, my doctoral thesis strives to dissect the molecular mechanisms underlying stress-related and psychiatric dysregulations in different regions and cell types of the brain. Through this integrated approach, the research anticipates providing novel insights into the pathophysiology of psychiatric disorders, which could ultimately lead to more targeted therapeutic strategies.

# 2 Materials and Methods

## 2.1 Methodological Approaches to Analyzing Transcriptomic Response to Glucocorticoid Treatment in Mouse Brain Tissue

### 2.1.1 Experimental Animals

As previously reported (Gerstner et al., 2022), all experiments and protocols were performed in accordance with the European Communities' Council Directive 2010/63/EU and were approved by the committee for the Care and Use of Laboratory animals of the Government of Upper Bavaria. All mice were obtained from the Max Planck Institute of Psychiatry's in-house breeding facility and maintained in group-housed conditions in individually ventilated cages (IVC; 30 cm 16 cm x 16 cm; 501 cm2) with central airflow (Tecniplast, IVC Green Line – GM500). The animals were kept under constant environmental conditions (12:12 h light/dark cycle, 23 ± 2 °C and 55% humidity) and had unlimited access to water and standard chow. Every IVC had a sufficient amount of bedding and nesting materials, along with a wooden tunnel to enhance the environment. A semi-randomized method was used to assign animals to experimental groups. Data analysis and execution of experiments were performed blinded to group allocation.

Male C57Bl/6n mice, aged 3 months (n=15 per condition), were given intraperitoneal injections of either 0.9% saline as control (vehicle) or 10 mg/kg body weight of dexamethasone (treatment). The mice were sacrificed four hours later, and the brains were perfused with a solution of Heparin in 0.9% saline, extracted and snap-frozen in butanol on dry ice, and preserved at 80 °C until needed. After slicing the brains into 250 µm coronal slices, 8 different brain regions were isolated utilizing the mouse brain atlas's stereotaxic coordinates (Paxinos & Franklin, 2008). Specifically, the isolated brain regions included: cingulate cortex 1 and 2 (bregma 2.34 to -0.22), from now on referred to as prefrontal cortex (PFC); paraventricular nucleus of the hypothalamus (PVN; bregma -0.58 to -1.22); amygdala (AMY; bregma 0.02 to -0.94); dorsal *cornu ammonis* 1 (dCA1; bregma -1.22 to -2.80); ventral *cornu ammonis* 1 (vCA1; bregma -2.92 to -3.88); dorsal dentate gyrus (dDG; bregma -0.94 to -2.80), ventral dentate gyrus (vDG; bregma -2.92 to -3.88) and cerebellar cortex (CER; bregma -5.80 to -6.24), see Figure 2.1. Brain punches were kept in dry ice while cutting and at -80°C until RNA extraction was carried out.

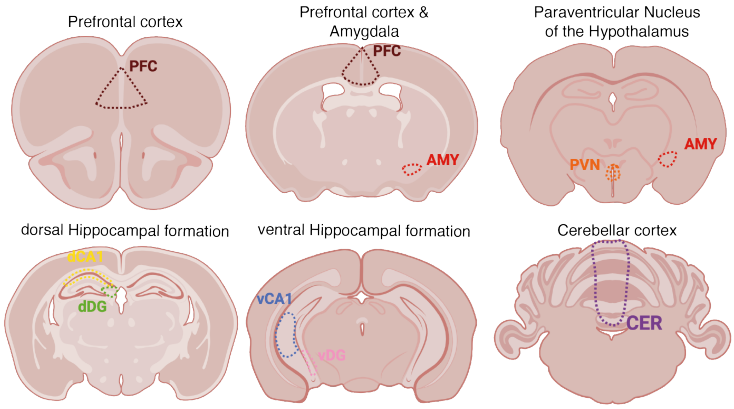


**Figure 2.1. Mouse brain regions isolated from experimental animals.** Prefrontal cortex (PFC), amygdala (AMY), paraventricular nucleus of the hypothalamus (PVN), dorsal and ventral *cornu ammonis* (dCA1 and vCA1), dorsal and ventral dentate gyrus (dDG and vDG) and the cerebellar cortex (CER) were isolated from coronal slices. Figure created with BioRender.com.

### 2.1.2 RNA Extraction

Following the manufacturer's instructions, RNA was extracted using an automated Chemagic 360° device with an integrated dispenser and the Chemagic RNA Tissue Kit (CMG-1212). Briefly said, magnetic beads are employed during Chemagic 360° RNA extraction to bind the nucleic acids, which are subsequently isolated using magnetized metal rods. Rotating zirconium beads were used to homogenize the tissue. Turning off the magnet while the rods were still rotating in a buffer of preference, allowed for the washing steps and the following elution of the RNA. DNase I was used to digest DNA, whereas Proteinase K was used to break down proteins. A Nanodrop was used to assess the concentration of RNA, and Tapestation RNA ScreenTapes (High Sensitivity RNA ScreenTapes, Cat No. 5067–5579) were used to measure the quality of the RNA.

### 2.1.3 RNA Sequencing

The QuantSeq 3′ mRNA Fwd kit (Lexogen) was utilised to prepare 3′ tag RNA sequencing libraries in accordance with the manufacturer's instructions. Additionally, individual transcripts were tagged with unique molecular IDs (UMIs – UMI Second Strand Synthesis Module for QuantSeq FWD). Using 75 bp long reads, libraries were single-end sequenced using an Illumina HiSeq 4000 sequencer, aiming for a total coverage of 10 million reads per library. Due to technical problems with the library preparation, two dexamethasone-treated dCA1 samples, one dexamethasone-treated PFC sample, one vehicle PVN sample, and one vehicle vCA1 sample were eliminated from sequencing and/or further analysis.

### 2.1.4 RNA Sequencing Analysis

FastQC v0.11.4 was used to assess the quality of the sequencing data (Andrews Simon, 2019), and cutadapt v1.11 was used to trim the adapters (M. Martin). Following the extraction of unique molecular identities using UMI-tools v.0.5.4 (T. Smith, Heger, & Sudbery, 2017), the reads were aligned to the mouse reference genome (mm10, Ensembl

release 84) using STAR v2.6.0a (Dobin et al., 2013). Additionally, UMI-tools were applied to deduplicate the reads, and gene expression was quantified with featureCounts v1.6.4 (Liao, Smyth, & Shi, 2014). R version 4.0.5 ("R: A language and environment for statistical computing. R Foundation for Statistical Computing, Vienna, Austria.," 2021) was used to carry out downstream analyses. 12,976 genes remained in the dataset after all genes not detected in at least one complete treatment group were filtered out. Genes with less than 10 counts across all samples within each brain region were then removed (Supplementary Table 1 provides the number of genes per brain region). Principal component analysis (PCA) was performed on the samples from each treatment group and brain area separately to detect outliers. The first principal component was used to exclude samples that deviated from the mean by more than 2.5 standard deviations (Supplementary Table 1 lists the number of outliers by treatment group and brain area). To account for unwanted variation in the data, surrogate variable analysis (SVA) was applied (Leek, 2014).

### 2.1.5 Differential Expression Analysis

The model fitted for differential expression (DE) analysis included significant surrogate variables as covariates; the precise amounts are shown in Supplementary Table 1. Using DESeq2's (v1.30.1) variance stabilizing transformation (Love, Huber, & Anders, 2014), the expression data was transformed and normalized before SVA and network analysis. DE analysis was carried out for each brain region separately between the two treatment groups. The Wald test in DESeq2 was applied to test for DE. Genes with a false discovery rate (FDR) $\leq 10\%$ were considered to be significant. The less stringent threshold of 10% for the DE analysis was used to allow for a more systemic comparison between brain regions on the gene and network level.

### 2.1.6 Network Analysis

#### 2.1.6.1 Network Inference

In the study, separate networks were constructed for vehicle- (hereafter referred to as "vehicle") and dexamethasone-treated (hereafter referred to as "treatment") samples for each brain region. This was achieved using the KiMONo network inference method (Ogris et al., 2021). KiMONo leverages prior knowledge from biological databases to provide the foundational network layout, which includes the connections among the transcripts. The method then makes use of different omic layers (in this case, only transcriptomic data) on top of this basic network layout to adjust the edge weights in the network. If an edge weight falls below a certain threshold, it is removed from the network (Figure 3.1). More specifically, KiMONo employs a multivariate regression approach with sparse group LASSO penalization to model the transcripts' expression levels. The potential predictors in the regression model are derived from the gene's connections in a prior network. In the resulting directed gene expression networks, the nodes represent transcripts from the input data, and the edge weights are the beta coefficients ($\beta$ value) determined by the regression approach. A $\beta$ value > 0 indicates a positive correlation between the expression levels of two genes, while a $\beta$ value < 0

indicates a negative correlation. Significant surrogate variables identified during the DE analysis were used as covariates for network inference and were treated as a separate group in the regression penalization (Supplementary Table 1). The $R^2$ value assigned to each regression model serves as a confidence score, indicating the model's goodness of fit. In both the vehicle and treatment networks, all interactions with an absolute $\beta$ value < 0.01 or an $R^2$ value < 0.1, as well as the connections to the surrogate variables, were removed.

As a prior network, we utilized FunCoup 5 (Persson, Castresana-Aguirre, Buzzao, Guala, & Sonnhammer, 2021), a database containing approximately 6.7 million interactions among 19,771 genes in the mouse organism. This database serves as a framework for inferring genome-wide functional couplings based on data from 10 different evidence types: physical protein interactions, mRNA co-expression, protein co-expression (based on the human protein atlas), genetic interaction profile similarities, shared regulation by transcription factor binding, shared regulation by miRNA targeting, subcellular colocalization, domain interactions, phylogenetic profile similarity, quantitative mass spectrometry data and gene regulatory data inferred from transcription factor bindings. FunCoup provides the edges for the basic network layout, and KiMONo calculates the weights of these edges, which are fitted from the expression of the transcripts in each brain region and treatment paradigm.

### 2.1.6.2 Differential Network Analysis

For each brain region, a differential network (DN) was computed by merging the vehicle and treatment networks. This was done using the DiffGRN method (Kim Youngsoon, 2018), which outlines the differential relationships between two genes. Consequently, differential gene interactions were derived from the regression's $\beta$ values and their standard errors via a $z$ test:

$$z_{XY} = \frac{\beta_{XY}^{T} - \beta_{XY}^{V}}{\sqrt{SE(\beta_{XY}^{T})^2 + SE(\beta_{XY}^{V})^2}}$$

Here, $\beta^{T}{}_{XY}$ and $\beta^{V}{}_{XY}$ represent the $\beta$ values of genes $X$ and $Y$ in the treatment and vehicle networks, respectively. A $z$ value > 0 signifies either a stronger positive correlation ($0 < \beta^{V}{}_{XY} < \beta^{T}{}_{XY}$), a weaker negative correlation ($\beta^{V}{}_{XY} < \beta^{T}{}_{XY} < 0$), or a transition from negative to positive correlation ($\beta^{V}{}_{XY} < 0 < \beta^{T}{}_{XY}$) between genes $X$ and $Y$ from the vehicle to the treatment network. Conversely, a $z$ value < 0 indicates a stronger negative correlation ($\beta^{T}{}_{XY} < \beta^{V}{}_{XY} < 0$), a weaker positive correlation ($0 < \beta^{T}{}_{XY} < \beta^{V}{}_{XY}$), or a switch from positive to negative correlation ($\beta^{T}{}_{XY} < 0 < \beta^{V}{}_{XY}$) between genes $X$ and $Y$ from the vehicle to the treatment network. $Z$ values > 0 can be interpreted as relative changes in gene expression resulting in a more positive correlation (referred to as positive regulatory effect), while $z$ values < 0 can be interpreted as relative changes in gene expression resulting in a more negative correlation (referred to as negative regulatory effect) (Figure 2.2). Differential interactions with an FDR adjusted $p$ value ≥ 0.01 linked to the $z$ score were omitted.

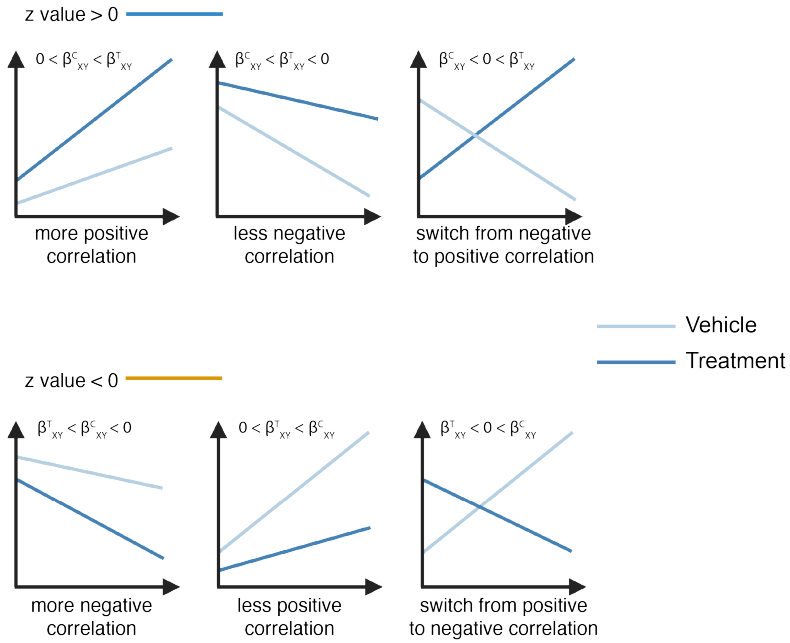


**Figure 2.2. Differential networks metrics explained.** $Z$ values > 0 indicate relative changes in gene expression leading to a more positive correlation, so an overall positive regulatory effect, while $z$ values < 0 indicate relative changes in gene expression leading to a more negative correlation, so an overall negative regulatory effect.

#### 2.1.6.3 Hub Gene Analysis

Key regulators in the vehicle, treatment, and differential networks were identified; respectively referred to as vehicle-, treatment-, and differential-hub genes. We used the node-betweenness, which is defined as the number of shortest pathways passing through a node and is implemented in the igraph package (Csardi, 2014; Csárdi, 2023), as a metric to identify the key genes. The node-betweenness in the networks (vehicle, treatment, differential) is determined by the prior network as they were created on top of it. As a result, we normalized the node-betweenness as follows:

$$\text{node-betweennessNorm}_{\text{network } A}(\text{gene } X) = \frac{\text{node-betweenness}_{\text{network } A}(\text{gene } X)}{\text{node-betweenness}_{\text{network } Prior}(\text{gene } X)}$$

where $\text{node-betweenness}_{\text{network } A}(\text{gene } X)$ is the node-betweenness of gene $X$ in network $A$ (e.g. DN of one brain region) and $\text{node-betweenness}_{\text{network } Prior}(\text{gene } X)$ is the node-betweenness of the same gene $X$ in the prior network. Genes that had a node-betweenness > 10,000 and a normalized node-betweenness > 1.0 were classified as hub genes. These genes were then compared with the DE genes identified in the DE analysis and with each other across different brain regions.

### 2.1.7 Enrichment Analysis

The enrichment of differentially expressed (DE) genes or differential hub genes for biological processes and pathways was carried out using the FUMA GENE2FUNC analysis (Watanabe et al., 2017). This analysis is based on the Gene Ontology (GO (Ashburner et al., 2000; Carbon et al., 2021)), KEGG (Kanehisa, 2019; Kanehisa, Furumichi, Sato, Ishiguro-Watanabe, & Tanabe, 2021; Kanehisa & Goto, 2000), Reactome (Jassal et al., 2020), and genes that single nucleotide polymorphisms (SNPs) with

genome-wide association to various traits are mapped to (analysis references the NHGRI-EBI GWAS Catalog (Buniello et al., 2019), accessed in September 2021). All genes expressed above the threshold in all brain areas ($n_{genes}$=12,830 genes) served as the background list when FUMA's default parameters were used. Only terms with at least 10% (unless otherwise stated) of the input genes overlapping with the term genes were taken into consideration in order to account for differently sized input gene lists. To allow for multiple comparisons, *p* values were adjusted using the Benjamini-Hochberg (FDR) method (Benjamini & Hochberg, 1995). A 5% FDR cutoff was applied to assess statistical significance. Enrichment results are visualized with their FDR, gene ratio (genes associated with GR activation in the gene set/total genes in the gene set) and $log_2$-transformed odds ratio (proportion of genes associated with GR activation in gene set to the other genes in the gene set/proportion of genes associated with GR activation not in the gene set to the genes in background set that are neither associated nor in the gene set).

We also tested for overrepresentation of DE and differential hub genes within network modules of a postmortem human brain study (autism spectrum disorder (n=51), schizophrenia (n=559), bipolar disorder (n=222), and controls (n=936)) (Gandal, Zhang, et al., 2018). This was done using a one-sided Fisher's exact test implemented in R ("R: A language and environment for statistical computing. R Foundation for Statistical Computing, Vienna, Austria.," 2021). *P* values were FDR corrected (Benjamini & Hochberg, 1995), and a cutoff of 5% was applied to determine statistical significance.

### 2.1.8 Shiny App

We developed DiffBrainNet, which is available online at http://diffbrainnet.psych.mpg.de, to enable all interested scientists to search these data and analyses. The application was generated in R v4.0.5 ("R: A language and environment for statistical computing. R Foundation for Statistical Computing, Vienna, Austria.," 2021). It makes use of the shiny package v1.7.1 and a variety of other publicly available packages, including org.Mm.eg.db v3.14.0, shinythemes v1.2.0, ggplot 2 v3.3.5, plotly v4.10.0, visNetwork v2.1.0, data.table v1.14.2, dplyr v1.0.7, and stringer 1.4.0. The app is hosted using ShinyProxy, and its source code can be found on github (see Data and Code Availability).

## 2.2 Methods for the Analysis of Cell Type-Specific Molecular Signatures in Postmortem Brain Tissue in a Cross-Disorder Psychiatric Cohort

### 2.2.1 Postmortem Brain Tissue

As reported previously (Fröhlich et al.; Gerstner et al.; Matosin et al., 2023), the work was approved by the University of Wollongong's Human Research Ethics Committee (HE2018/351) and Ludwig Maximilians-Universität (22-0523). Informed permission for a brain autopsy was given by donors or their next of kin. We performed single-nucleus RNA-sequencing (snRNA-seq) and single-nucleus ATAC-sequencing (snATAC-seq) using freshly-frozen postmortem tissues of the orbitofrontal cortex (Brodmann area 11 cut from the 3rd 8-10mm coronal slice), obtained from the NSW Brain Tissue Resource Centre in Sydney, Australia. The cohort comprised 92 donors, including 35 psychologically healthy controls and 57 cases with a diagnosis of bipolar disorder, major depressive disorder (MDD), schizoaffective disorder (SCA), or schizophrenia (n=5,7,7,38, respectively). The case and control groups were matched according to brain pH (mean ± s.d. = 6.60 ± 0.24), postmortem interval (mean ± s.d. = 33.90 ± 14.82), age (mean ± s.d. = 54.27 ± 13.64), and sex (38% female representation), see Table 2.1. Structured information of comorbid diseases was not available. However, there is a notably high rate of natural deaths (94.3% in controls, 63.2% in cases), predominantly from cardiac and respiratory causes, among the cohort at a relatively young age of death. This fact, combined with a high mean body mass index (mean ± s.d. = 32.73 ± 7.68), indicates decreased physical health in the cohort compared with the general population.

**Table 2.1. Postmortem brain cohort characteristics.** Data is presented as the mean ± standard deviation. F (female), M (male), PMI (postmortem interval), RIN (RNA integrity number), BMI (body mass index), BIP (bipolar disorder), MDD (major depressive disorder), SCA (schizoaffective disorder), SCZ (schizophrenia).

| | *Controls (n=35)* | *Cases (n=57)* | *Overall (n=92)* |
|---|---|---|---|
| *Age [years]* | 55.83 ± 13.56 | 53.32 ± 13.73 | 54.27 ± 13.64 |
| *Sex* | 13 F \| 22 M | 22 F \| 35 M | 35 F \| 57 M |
| *Psychiatric diagnosis* | 0 | BIP (5), MDD (7), SCA (7), SCZ (38) | No diagnosis (35), BIP (5), MDD (7), SCA (7), SCZ (38) |
| *PMI [h]* | 31.80 ± 11.30 | 35.18 ± 16.58 | 33.90 ± 14.82 |
| *pH* | 6.66 ± 0.24 | 6.57 ± 0.23 | 6.60 ± 0.24 |
| *RIN* | 7.17 ± 1.34 | 7.25 ± 1.21 | 7.22 ± 1.25 |
| *BMI* | 34.43 ± 9.50 | 31.46 ± 6.00 | 32.73 ± 7.68 |
| *Manner of Death* | Accident (1), Natural (33), Unknown (1) | Accident (3), Natural (36), Suicide (16), Unknown (2) | Accident (4), Natural (69), Suicide (16), Unknown (3) |

### 2.2.2 Nuclei Isolation and Single-Nucleus RNA and ATAC Sequencing

Nuclei were isolated from approximately 50 mg of frozen postmortem brain tissue (Brodmann area 11). The tissue was homogenised by dounce-homogenization in a 1 ml nuclei extraction buffer, which had the following ingredients: 10 mM Tris-HCl pH 8.1, 0.1 mM EDTA, 0.32 M Sucrose, 3 mM Mg(Ac)2, 5 mM CaCl2, 0.1% IGEPAL CA-630, and 40 U/ml RiboLock RNase-Inhibitor (ThermoScientific). Next, using a Thermo ScientificTM SorvallTM WX+ 471 ultracentrifuge, the homogenate was placed onto 1.8 ml of sucrose cushion (10 mM Tris-HCl pH 8.1, 1.8 M Sucrose, 3 mM Mg(Ac)2) and ultracentrifuged for 2.5 hours at 28,100 rpm at 4°C. The nuclei pellet was gently resuspended in 80 µl of resuspension buffer (1X PBS, 3 mM Mg(Ac)2, 5 mM CaCl2, 1% BSA, and 40 U/ml RiboLock RNase-Inhibitor) after the supernatant was removed using vacuum suction. Chromium Next GEM Single Cell ATAC Kit v1.1 and Chromium Next GEM Single Cell 3' Kit v3.1, respectively, were used to prepare sn-ATAC libraries and sn-RNA libraries from the identical nuclei suspension, in accordance with the manufacturer's instructions. For both the sn-ATAC and sn-RNA libraries, the targeted recovery was 10,000 nuclei per sample. Libraries of the different donors were pooled equimolarly (separately for snATAC and snRNA libraries). As directed by the manufacturer, Illumina Free Adaptor blocking Reagent was administered. The NovaSeq 6000 System (Illumina, San Diego, California, USA) was used to sequence libraries.

### 2.2.3 Processing of Single-Nucleus Data

#### 2.2.3.1 Randomization of Samples

To ensure an experimental design that was not biased by variables of interest, samples were distributed into 16 batches, utilizing OSAT (Yan et al., 2012) for randomization based on age, sex, and disease status. Nuclei were extracted and libraries for snRNA-seq and snATAC-seq were prepared following this randomization of samples.

#### 2.2.3.2 snRNA-seq Data Workflow

Using Cell Ranger (cellranger count v6.0.1) (Zheng et al., 2017), the preliminary processing of the snRNA-seq data was carried out, including read alignment to a pre-mRNA reference (genome build GRCh38, Ensembl 98), cell barcoding, and UMI counting. We downsampled reads to the 75% quantile, which equates to 14,786 reads per cell, in order to account for the notable variations in sequencing depth between cells and samples. The downsampleReads function from the DropletUtils package v1.12.2 (Lun et al., 2019) was used to carry out this downsampling process. In order to reduce bias in the analysis, we were able to achieve a more comparable degree of sequencing depth for cells across samples by downsampling the reads.

The count matrices of all donors were concatenated and subjected to additional processing using Scanpy v1.7.1 (Wolf, Angerer, & Theis, 2018) in Python (Python Software Foundation, https://www.python.org/). The minimum number of genes expressed, counts, and percentage of mitochondrial genes (counts <500, genes <300, Mito% ≥ 15) were used to filter the nuclei. Genes expressed in less than 500 nuclei were eliminated. Due to generally poor data quality, which corresponded with a low RIN

score, one donor was filtered out. We used the DoubletDetection software v3.0 (Gayoso, Shor, Carr, Sharma, & Pe'er, 2020) to perform doublet removal in order to guarantee data integrity and the accuracy of our research. Sctranform v0.3.2 (Hafemeister & Satija, 2019) was used to transform and normalise the data. Scanpy (Wolf et al., 2018) was utilised to identify highly variable genes and to perform dimensionality reduction, principal component analysis (PCA), and uniform manifold approximation and projection (UMAP). The leiden clustering algorithm (resolution 1.0) was used to cluster nuclei according to highly variable genes (Traag, Waltman, & van Eck, 2019). Four donors were removed because one cluster included more than half of their nuclei (Online Table 31).

#### 2.2.3.3 snATAC-seq Data Workflow

Cell Ranger ATAC (cellranger-atac count v2.0.0) (Satpathy et al., 2019) was used for the initial processing of the snATAC-seq data. This included aligning the reads to a reference (genome build GRCh38, Ensembl 98), calling cells, and creating a count matrix.
R v4.0.5 ("R: A language and environment for statistical computing. R Foundation for Statistical Computing, Vienna, Austria.," 2021) was used to process the data further using the ArchR package v1.0.2 (Granja et al., 2021). Nuclei exhibiting a low signal-to-noise ratio were removed throughout the per-cell quality control process based on their transcription start site (TSS) enrichment score (< 4). Moreover, nuclei with 100,000 or fewer distinct nuclear fragments were excluded. ArchR was used to infer doublet scores, and a filter ratio of 2.5 was used to eliminate the corresponding doublet. A low RIN value and general poor data quality led to the filtering out of one donor. To deal with the high sparsity of snATAC-seq data, dimensionality reduction was performed using iterative latent semantic indexing (LSI). To facilitate visualisation, a UMAP embedding was obtained from this lower dimensional space. Using an interface to the FindClusters method from Seurat v4.0.4 (Hao et al., 2021), which is based on the Louvain clustering algorithm (Waltman & van Eck, 2013), nuclei were clustered with resolution 1.0. Another donor with most of its nuclei grouping together and six clusters with low data quality in terms of doublet scores and number of fragments were eliminated during a final filtering step (Online Table 31).
In order to evaluate chromatin accessibility at the gene level, ArchR (Granja et al., 2021) was used to compute gene scores. Gene scores are predictions of gene expression based on the accessibility of regulatory elements surrounding a gene (100 kb up- and downstream). The signal gets weighted based on the distance between a regulatory element and the gene.

#### 2.2.3.4 Cell Type Assignment of snRNA-seq and snATAC-seq Data

Using a label transfer approach (scArches v0.4.0 (Lotfollahi et al., 2022)/scANVI (Xu et al., 2021)), an initial cell type assignment to nuclei clusters in the snRNA-seq data was performed. Using this variational inference model, cell type labels were transferred from a cortical dataset of the Allen Brain Map (Human Multiple Cortical Areas (Map., 2019)) to our snRNA-seq dataset. The cell type that accounted for the majority of the cluster's nuclei was labelled on each cluster. The cell type assignments were then manually refined based on the curation of known marker genes. Marker genes included:

Astrocytes: *AQP4*, *CLU*, *GFAP*, *GJA1*; Endothelial: *CLDN5*, *COBLL1*, *FLT1*, *SYNE2*; Excitatory neurons: *SATB2*, *SLC17A6*, *SLC17A7*; Inhibitory neurons: *GAD1*, *GAD2*, *NXPH1*, *SLC32A1*; Microglia: *APBB1IP*, *C3*, *P2RY12*; Oligodendrocytes: *MPB*, *MOBP*, *PLP1*, *RNF220*; Oligodendrocyte Precursors (OPC): *OLIG1*, *OLIG2*, *PDGFRA*, *VCAN*. Astrocyte subtypes: higher *GFAP* and *ARHGEF4* expression (fibrous astrocytes (Astro_FB)) vs. higher expression of *ATP1A2*, *GJA1* and *SGCD* (protoplasmic astrocytes (Astro_PP)) (Velmeshev et al., 2019). Excitatory neuron subtypes were labeled based on the expression of cortical-layer specific marker genes: layers 2-3: *CUX2*, *RFX3*; layer 4: *IL1RAPL2*, *CRIM1*, *RORB*; layers 5-6: *RXFP1*, *TOX*, *DLC1*, *TLE4* (Nagy et al., 2020; Velmeshev et al., 2019). Inhibitory neuron subtypes were labeled based on the expression of interneuron markers *LAMP5*, *PVALB*, *RELN*, *SST*, and *VIP*. PVALB inhibitory neurons consisted of two subtypes: basket cells (In_PVALB_Ba) and chandelier cells (In_PVALB_Ch; identified based on the high expression of *RORA*, *TRPS1*, *NFIB*, and *UNC5B*) (T. E. Bakken et al., 2021).
A parallelized interface to the FindTransferAnchors function in Seurat (Hao et al., 2021) was used to integrate the snATAC-seq data with the snRNA-seq data in ArchR (Granja et al., 2021) for the initial assignment of cluster identities. By comparing the gene score matrix with the gene expression matrix, nuclei from snATAC-seq and scRNA-seq are being aligned. The cell type of the most comparable scRNA-seq nucleus gets transferred to each snATAC-seq nucleus. Subsequently, gene scores of the aforementioned marker genes were used to manually refine cluster identities. Endothelial cells were confidently identified as such despite known marker genes of endothelial cells not exhibiting distinct gene scores in the respective cluster. Its clear separation from other clusters, the unambiguous assignment as endothelial cells via label transfer, and imputed gene scores (Dijk et al., 2018) all contributed to this conclusion.

#### 2.2.3.5 Pseudobulk Replicates of snRNA-seq and snATAC-seq Data

Pseudobulk replicates were created to facilitate downstream studies that call for replicates with statistically significant observations, including peak calling on ATAC-seq data or differential testing. Thus, for each cell type-donor combination, gene expression and chromatin accessibility count matrices were aggregated, resulting in pseudobulk replicates resembling bulk RNA-seq and ATAC-seq data per cell type.
To avoid sparsity, an ArchR method (Granja et al., 2021) summarizes several sufficiently comparable donors within a cell type to create pseudobulk duplicates that are employed for cell type-specific peak calling. These ArchR-generated replicates were solely used for peak calling since such multi-individual pseudobulk replicates are not appropriate for our downstream analyses.

#### 2.2.3.6 Peak Calling on snATAC-seq Data

Using an interface to MACS2 in ArchR (Granja et al., 2021; Yong Zhang et al., 2008), peak calling was carried out for each cell type based on the aforementioned multi-sample pseudobulk replicates. Peaks have a fixed width of 501 bp to ease downstream calculations. They are merged across cell types and pseudobulk replicates via a ranking

of normalized significance and the iterative elimination by overlap. There is one merged peak set of fixed-width peaks in the resulting matrix.

### 2.2.4 Genotype Data

#### 2.2.4.1 DNA Extraction, SNP Genotyping and Imputation

Using the QIAamp DNA mini kit (Qiagen) and following the manufacturer's instructions, genomic DNA was recovered from 10 mg of brain tissue. DNA samples were extracted and then concentrated using the DNA Clean & Concentrator-5 (Zymo Research). Illumina GSA-24v2-0_A1 arrays were used to genotype the samples in accordance with the manufacturer's protocols (Illumina Inc., San Diego, CA, USA). A quality control (QC) run on PLINK v1.90b3.30 (S. Purcell et al., 2007) was conducted. Donors with a missing rate > 2% or cryptic relatives (PI-HAT > 0.125) were excluded during sample QC. Additionally, genetic outliers (distance in ancestry components from the mean > 4 SD) and donors with autosomal heterozygosity deviation (|Fhet| > 4 SD) were removed. During variant QC, variants with a call rate < 98%, minor allele frequencies (MAF) < 1%, and $p$ values equal to ≤ 10-6 from the Hardy-Weinberg equilibrium (HWE) test were filtered out. Imputation was performed with shapeit2 (Delaneau, Marchini, & Zagury, 2011) and impute2 (Marchini, Howie, Myers, McVean, & Donnelly, 2007), leveraging the 1000 Genomes Phase III reference sample. A final collection of 9,652,209 SNPs in 92 donors was obtained by discarding imputed SNPs with an INFO score below 0.6, MAF < 1%, or deviation from Hardy-Weinberg equilibrium ($p$ value < 1 × 10-5).

#### 2.2.4.2 Calculation of Polygenic Risk Scores

Polygenic risk scores (PRS) were computed based on summary statistics of GWAS studies for a cross-disorder phenotype (Consortium., 2019), schizophrenia (Trubetskoy et al., 2022), MDD (Howard et al., 2019), bipolar disorder (Mullins et al., 2021), and height (Yengo et al., 2022) (as a non-psychiatric control). PRS-CS v1.0.0 (Ge, Chen, Ni, Feng, & Smoller, 2019) was used to infer posterior effect sizes from the GWAS summary statistics. The 1000 Genomes Project phase 3 European samples, available on the PRS-CS GitHub page, served as linkage disequilibrium (LD) reference panel for the calculations. The global shrinkage parameter (phi) of PRS-CS was set to 0.01 for schizophrenia, a highly polygenic trait. For the other traits, with larger sample sizes in the respective GWAS studies, phi could be derived from the data and no specific parameter was specified. Using the score parameter in PLINK v2.00a2.3LM (S. Purcell et al., 2007), the previously inferred posterior effect sizes were used to calculate the polygenic risk scores for each donor (Online Table 32).

## 2.2.5 Differential Analysis

### 2.2.5.1 Definition of Disease Status for Differential Testing

Tests for differential expression (DE) and accessibility (DA) were performed on all donors who had been diagnosed with bipolar disorder, schizophrenia, schizoaffective disorder (SCA), or major depressive disorder (MDD) in comparison to all donors in the control group. Because psychiatric disorders share a genetic risk and have overlapping symptomatology (Consortium., 2019; Newson et al., 2021; Smoller et al., 2019), they were analysed as a cross-disorder phenotype. This increased the statistical power of the analyses and made it possible to find shared molecular dysregulations and underlying pathways.

### 2.2.5.2 Definition of Groups for Testing Between High and Low Genetic Risk

To evaluate DE and DA with regard to overall genetic predisposition, we conducted differential testing between individuals at opposite ends of the genetic risk spectrum for specific traits or diseases. In line with the established consensus in the research community that the most accurate risk predictions occur at the extreme quantiles of PRS distributions (Andlauer & Nöthen, 2020; C. M. Lewis & Vassos, 2020), genetic risk was classified into two distinct categories representing these extremes, as opposed to viewing it on a continuous scale. For each trait or disease, we identified the top and bottom 20 PRS scorers within our cohort.

Subsequently, propensity score matching was applied to align the extreme groups on covariates like age, sex, brain pH, PMI, and RIN (Figure 2.3a), ensuring an exact match for sex (Figure 2.3b-f). This was achieved using the 'matchit' function from MatchIt v4.5.5 (Ho, Imai, King, & Stuart, 2011). The matched groups varied in size from 11 to 17 donors, specifically: 17 in both high and low PRS extremes for cross-disorder, 13 for schizophrenia, 14 for bipolar disorder, 11 for MDD, and 14 for height in both extremes (Online Table 31).

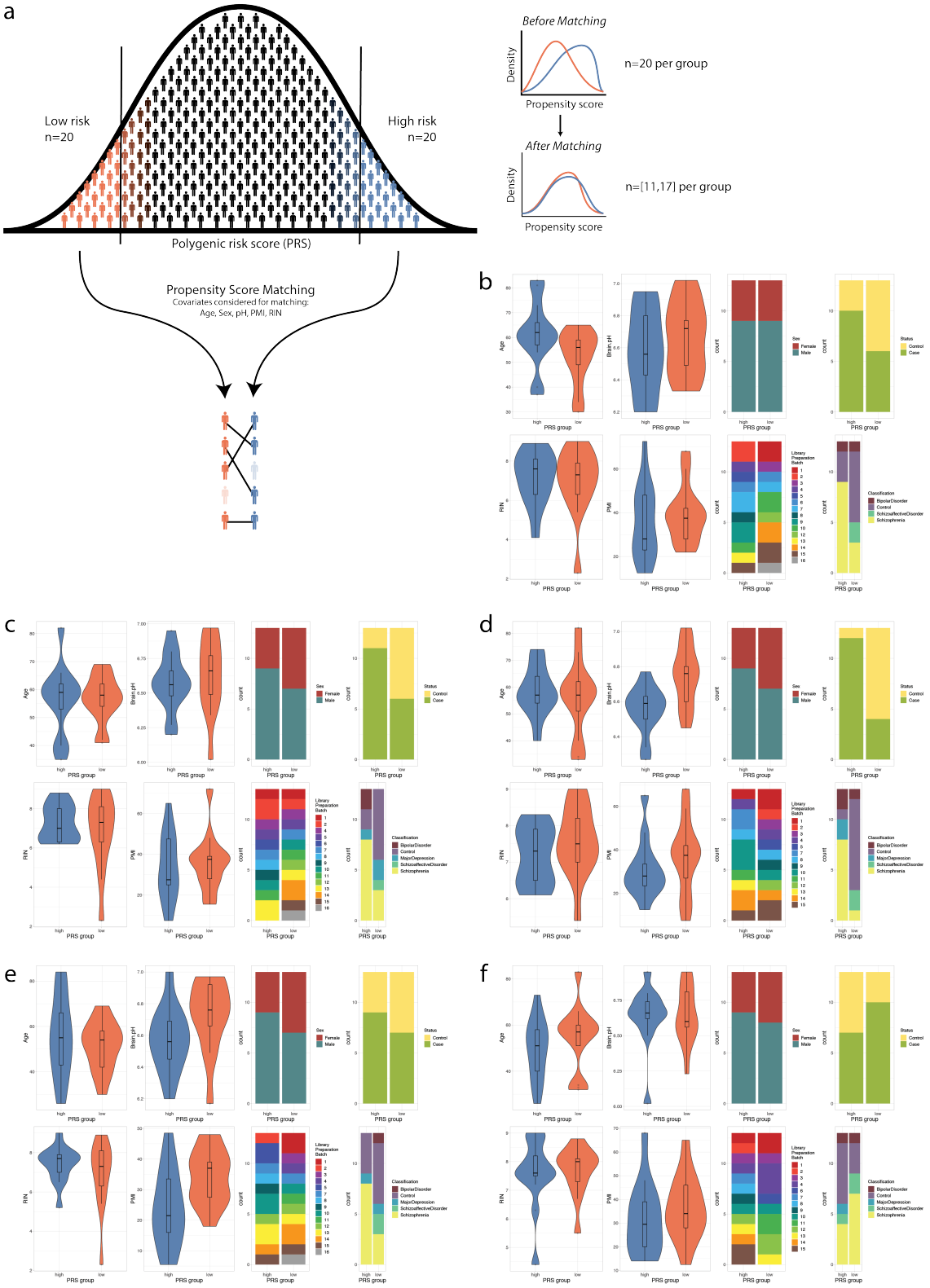


**Figure 2.3. Definition of extreme groups for genetic risk.** (a) Schematic overview of the definition of high and low genetic risk groups. 20 donors with the highest PRS and 20 donors with the lowest PRS were selected from both tails of the PRS distribution for each trait or disease. These groups were matched based on age, sex (exact), brain pH, PMI and RIN using propensity score matching. (b-f) Matched covariates and distribution of disease status and diagnoses for high and low risk groups for cross-disorder phenotype (b), bipolar disorder (c), major depressive disorder (d), schizophrenia (e) and height (f).

#### 2.2.5.3 Selection of Covariates for Differential Testing Between Disease Status and Genetic Risk Groups

The effect of potential confounders on the RNA-seq data was evaluated in order to carefully analyze the effects of biological variables and batch effects on the data and to identify relevant covariates for differential testing. Anticipating that technical variables are consistent across cell types, a full pseudobulk count matrix was generated by aggregating the gene-wise counts across all cell types. To be used in the covariate selection procedure, genes had to have at least 10 counts in at least 90% of the samples. After normalizing the data using DESeq2's variance stabilizing procedure (Love et al., 2014), principal component analysis (PCA) was performed. Continuous variables such as RNA integrity number (RIN), postmortem interval (PMI), pH and age showed a significant correlation with one of the first ten principal components (PCs). "Library preparation batch" (lib_batch) was discovered as a covariate after additional investigation using canonical correlation analysis (CCA). However, because of the minimal number of observations per library preparation batch in the genetic risk model, this covariate was only included in the model for disease status. Sex, a well-known confounder, was also added to our model as a covariate.

After normalizing, transforming, and regressing out the effects of all covariates and our variable of interest (disease status or genetic risk group, respectively) using voom and removeBatchEffect from the limma package v3.56 (Ritchie et al., 2015), PCA was conducted to capture hidden noise. We added the first PC (PC_noise) as another covariate to our final differential testing model, which read as follows: (~Disease_Status/Genetic_Risk + Sex + Age + pH + RIN + PMI + lib_batch + PC_noise). RIN was imputed to the cohort's median value as it was lacking for one donor.

The model of differential chromatin accessibility analysis included the same covariates, except RIN, in order to maintain consistency across analyses. This was motivated by the fact that library preparation for both modalities – snRNA-seq and snATAC-seq – was carried out in the same batches and that the data were generated from the same tissue.

#### 2.2.5.4 Differential Expression Analysis

DE was assessed using DESeq2 v1.40.2 (Love et al., 2014) at the pseudobulk level for each cell type individually. Genes were filtered for a minimum of 10 counts in 75% of the pseudobulk samples within each cell type-specific count matrix. Outlier samples were eliminated after data normalization using the variance stabilizing transformation in DESeq2 via iterative PCA and the removal of samples with a distance from the mean on the first PC of more than 3 standard deviations. The Wald test in DESeq2 was used to test for DE. Considering that the pseudobulk approach is thought to be more conservative than single-cell DE methods (Squair et al., 2021; Zimmerman, Espeland, & Langefeld, 2021), genes with an FDR ≤ 10% were reported as significant.

To enable a comparison of cell type-specific DE genes and those detected on the bulk level within the same cohort, we extended our analysis to include the full pseudobulk level. This involved aggregating the count data for each gene across all cell types, followed by conducting the DE analysis using the same methodology applied at the cell type level.

#### 2.2.5.5 Differential Chromatin Accessibility Analysis

Gene scores were used to assess DA for each cell type at the pseudobulk level. DESeq2 was not used for differential testing since gene scores do not conform to the usual characteristics of count data. The number of cells aggregated per pseudobulk sample was used to normalize pseudobulk gene scores, and outliers were filtered in the same manner as during DE analysis. Genes that showed scores higher than 0.1 in fewer than 75% of the samples were eliminated and filtered out before being subjected to additional analysis. Following the fitting of a linear model incorporating the covariates previously mentioned, a Wald test was run and log2-fold changes were computed. Significant genes were defined as those having an FDR ≤ 10%.

#### 2.2.5.6 Differential Risk Analysis

According to differential testing between cases and controls, differential risk studies were carried out on the level of gene expression (DE risk analysis) and chromatin accessibility (DA risk analysis) between donors with high and low genetic risk for a trait. The same rules applied to gene filtering, normalization, and outlier elimination. Genes with an FDR ≤ 10% were considered significant.

### 2.2.6 Functional Annotation

#### 2.2.6.1 Pathway Enrichment Analysis

The analysis of pathway enrichment was performed with the enrichKEGG function of the clusterProfiler package v4.8.1 (Wu et al., 2021). To ensure that this study is comparable across cell types, the 250 genes that showed the most significant up- and down-regulation for each cell type based on FDR values were evaluated for over-representation of KEGG pathways (Kanehisa, 2019; Kanehisa et al., 2021; Kanehisa & Goto, 2000). We decided to extend this analysis beyond just the significant DE and DA genes to facilitate a consistent comparison across different cell types. Selecting 250 genes for each direction of regulation accounts for roughly half of the DE genes found in Exc_L2-3, which is the cell type exhibiting the greatest number of DE genes when comparing cases to controls. The corresponding heatmap displays any KEGG pathway that is significantly over-represented in at least one cell type (FDR ≤ 0.05). The enrichment heatmap was annotated with a hierarchy of KEGG pathways that was retrieved from the KEGG Pathway Database (https://www.genome.jp/kegg/pathway.html, accessed: June 2023) in order to summarize individual KEGG pathways in categories.

#### 2.2.6.2 GWAS Enrichment Analysis

The GWAS enrichment analysis was carried out using H-MAGMA v1.10 (Sey et al., 2020). SNPs were mapped to genes using the European 1,000 genomes reference panel, which was obtained from the H-MAGMA github website (https://github.com/thewonlab/H-MAGMA), and the GWAS summary statistics for schizophrenia (Trubetskoy et al., 2022), bipolar disorder (Mullins et al., 2021), and MDD (Howard et al., 2019). The respective results were used in the subsequent gene property

analysis with the "--gene-covar" argument in MAGMA. With this approach, the gene-level regression framework may be used to examine if DE related to disease status/genetic risk is associated with GWAS results. Here, DE (risk) results are entered as a continuous variable, represented as -log10(*p* value)*log2(fold change)).

#### 2.2.6.3 Transcription Factor Motif Enrichment Analysis

An analysis of transcription factor (TF) motif enrichment was carried out within the ArchR framework (Granja et al., 2021) to determine whether peaks in the promoter regions of a particular gene are enriched for binding sites of particular TFs. Using the addMotifAnnotation function, binary information was first obtained for each peak-TF pair indicating whether or not the corresponding motif is present in the peak. TF motif data was taken from the JASPAR 2020 database (Fornes et al., 2020). The peaks in a specific gene's promoter region were then tested for enriched presence of TF motifs relative to the presence in all peaks using a hypergeometric test, utilising an adapted version of the peakAnnoEnrichment function. TF motifs were considered significantly enriched when their adjusted $p$ value ≤ 0.05.

### 2.2.7 Correlation Analysis Between Gene Expression and Chromatin Accessibility

Every cell type was evaluated independently at the pseudobulk level for the number of peaks in proximity to each gene and the quantity of correlated peaks nearby each gene. Genes with less than 5 counts in more than 75% of the samples were eliminated from the gene expression count matrix, while peaks with less than 5 counts in more than 50% of the samples were eliminated from the peak matrix. Because of the even sparser signal in the ATAC-seq data, a less stringent filtering was applied in the peak matrix. DESeq2's variance stabilising transformation (Love et al., 2014) was used to normalise the peak matrix and gene expression. Peaks were considered to be close to a gene and subjected to a correlation analysis if they fell within a 100 kb window from the gene, which is also the default distance utilised by ArchR (Granja et al., 2021) to determine gene scores. The association between chromatin accessibility and gene expression was measured using Pearson's correlation coefficient.

Expression levels were correlated with chromatin accessibility on the level of gene scores in addition to the correlation analysis at the peak level. All cell types were analyzed individually as well as collectively. At the pseudobulk level, Spearman correlation coefficients were computed between expression and gene scores averaged across all samples. Furthermore, the distribution of Spearman correlation coefficients, which were computed for each gene between gene expression and gene scores across all pseudobulk samples, was compared to a random distribution that was produced by correlating gene expression with a random permutation of gene scores.

A GO enrichment analysis was conducted across all cell types collectively to determine if groups of genes, characterized by distinct gene expression and chromatin accessibility patterns, are associated with different biological processes. Genes exhibiting expression levels above the 70$^{th}$ percentile were assigned to the high expression (HE) group, while those below the 50$^{th}$ percentile were assigned to the low expression (LE) group.

Equivalently, genes with gene scores above the 70th percentile were classified as highly accessible (HA), and those below the 50th percentile as lowly accessible (LA), following the methodology outlined by Starks et al. (Starks et al., 2019). The enrichGO method from the clusterProfiler package v3.18.1 (Yu, Wang, Han, & He, 2012) was used to test for significant enrichment (FDR ≤ 0.05) of GO terms related to biological processes. Genes with measurements of both gene expression and chromatin accessibility levels above the previously described cutoffs were used as a background. Lists of significant GO terms were reduced and grouped based on semantic similarity, and visualized in treemaps with the rrvgo package v1.2.0 (Sayols, 2023).

### 2.2.8 Contrasting Findings with Previous Studies

In assessing our DE results for disease status, we compared them with cell type-specific transcriptomic alterations in the prefrontal cortex of individuals with schizophrenia from prior research. Our objective was to determine the consistency of our results with those from earlier work. We aligned our effect sizes with those from a meta-analysis of single-cell RNA-seq by Ruzicka et al., which included 140 samples and over 469K cell counts (Ruzicka et al., 2022). We employed Pearson's correlation coefficient for each corresponding cell type to quantify the association between effect sizes across genes investigated in both studies.

### 2.2.9 Network Inference

The inference of correlation-based networks for given genes that exhibited differential expression and chromatin accessibility between schizophrenia risk groups was performed to integrate different data modalities. Besides gene expression and chromatin accessibility across various cell types, disease status and PRS for the aforementioned disorders and traits were included in the network analysis. Only donors who fall into the high and low genetic risk categories for schizophrenia were included in the network analysis. The levels of gene expression and gene scores were adjusted for age, sex, RIN, PMI, pH, and library preparation batch. Spearman correlation coefficients were computed for each pair of features. In each network, correlations with a nominal $p$ value ≤ 0.05 are displayed, while edge strength and weight correspond to the absolute correlation coefficient. The R packages igraph (Csardi, 2014; Csárdi, 2023) and ggnetwork (Tyner, Briatte, & Hofmann, 2017) were used to visualize networks.

### 2.2.10 Comparison of Differentially Expressed Genes Between Results in Mouse and Human Studies

To determine the overlap of DE genes between the mouse PFC after glucocorticoid receptor stimulation and various cell types within the human OFC in psychiatric disorders, we matched the Ensembl IDs of mouse genes to those of their human orthologs using the Biomart database (Durinck et al., 2005).

# 3 Results

The results section of this thesis presents a dual-faceted exploration, addressing two distinct yet interconnected research questions. The first question delves into the brain region-specific transcriptomic response to glucocorticoid stimulation in a mouse model, highlighting the activation of the hypothalamic-pituitary-adrenal (HPA) axis – a critical component of the stress response mechanism – and its significance in stress-related disorders. The study probes the connection between glucocorticoid-induced gene expression alterations and variations in gene co-expression networks. The findings are showcased through the DiffBrainNet Shiny App, an interactive online resource created within the scope of this project.

The second question investigates the molecular alterations characteristic of psychiatric disorders, with a particular focus on the genetic susceptibility associated with these conditions. This is examined in the human orbitofrontal cortex of postmortem brain tissue, through the genome-wide quantification of gene expression and chromatin accessibility at the single-cell level. Cell type-specific alterations in gene expression associated with psychiatric diagnoses were evaluated and compared to corresponding changes in chromatin accessibility. Additionally, molecular variations related to the genetic risk for psychiatric disorders were explored and contrasted with the molecular changes associated with clinical diagnoses.

A comparative analysis bridges the findings from both research questions, offering insights into the affected genes and the intricate relationship between stress responses and psychiatric disorders.

## 3.1 Transcriptomic Response to Glucocorticoid Activation in Different Brain Regions

The objective of this study was to develop a resource of region-specific transcriptomic alterations in the brain, analyzing the impacts of a 4-hour, 10 mg/kg dexamethasone treatment across eight distinct mouse brain regions (Figure 3.1 top and Figure 2.1). Utilizing RNA sequencing, we profiled the whole transcriptome, identifying 12,976 genes expressed across these brain regions (detailed numbers for each region are presented in Supplementary Table 1), with a set of 12,830 genes shared across all regions examined. Network analysis revealed the relative changes in gene expression that might elude detection at the level of differential expression (DE) analysis. Consequently, we computed gene expression networks for each condition within each brain region using regression analysis, informed by prior knowledge, with KiMONo (Ogris et al., 2021). The prior network was derived from FunCoup 5 (Persson et al., 2021), comprising experimental data encompassing approximately 6.7 million interactions among 19,771 mouse genes, with our dataset reflecting 11,083 of these genes (5.4 million interactions). Differential networks (DNs) for each brain region were inferred by contrasting the regression analysis's $\beta$ values between control and treated networks, applying a z-test, following the DiffGRN methodology (Kim Youngsoon, 2018). Additionally, DE analysis was conducted to discern gene-level reactions to glucocorticoid receptor (GR) stimulation, contrasting vehicle and dexamethasone treatment (Figure 3.1 middle).

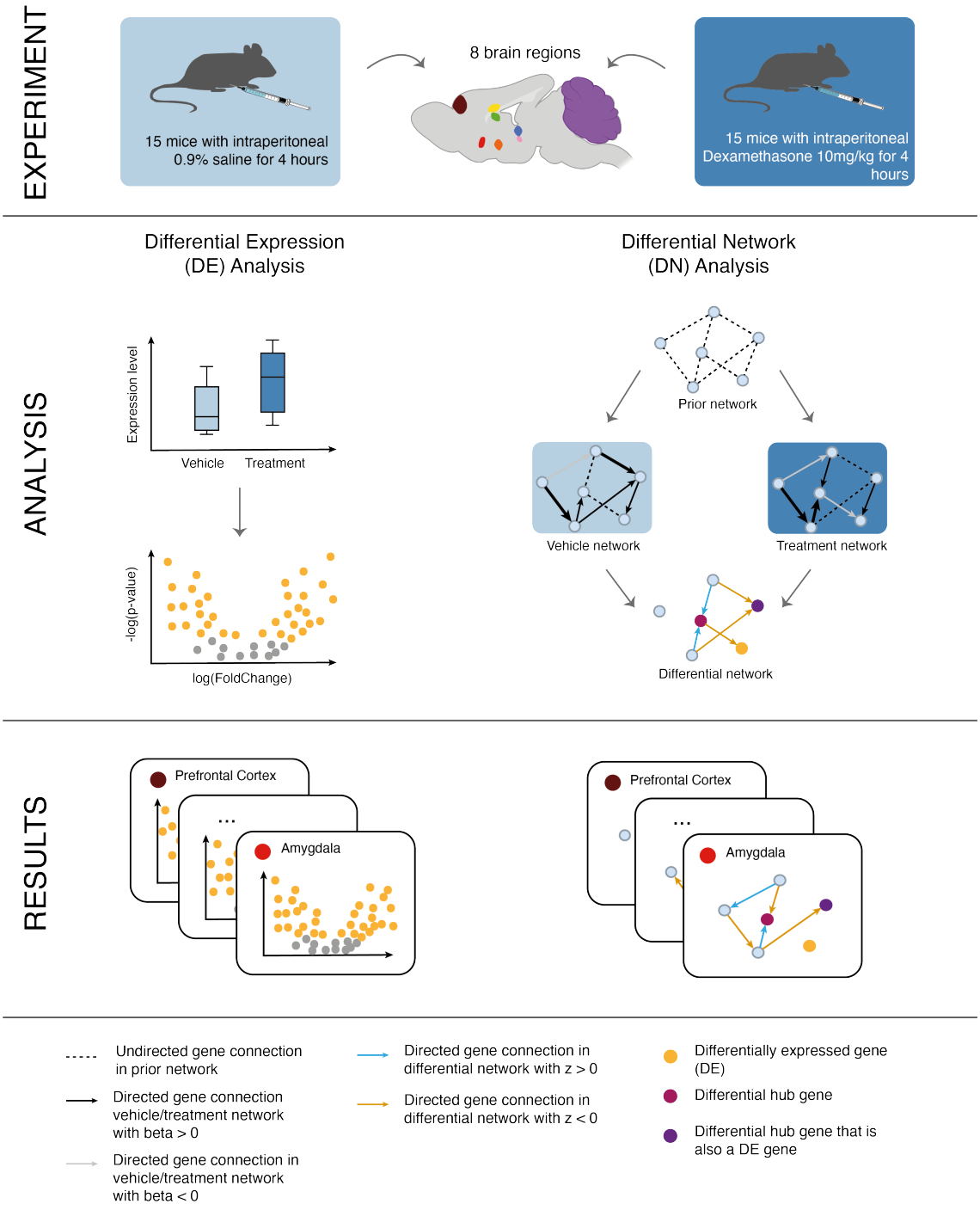


**Figure 3.1. Schematic representation of experimental and analytical procedures used for differential expression and network analysis across 8 mouse brain regions.** (Experiment) C57Bl/6 mice were administered an intraperitoneal injection of either 10mg/kg dexamethasone or 0.9% saline solution as a vehicle for 4h. Brain region isolated include the amygdala (AMY), cerebellar cortex (CER), prefrontal cortex (PFC), paraventricular nucleus of the hypothalamus (PVN), dorsal *cornu ammonis* 1 (dCA1), ventral *cornu ammonis* 1 (vCA1), dorsal dentate gyrus (dDG), ventral dentate gyrus (vDG). (Analysis) Subsequent RNA sequencing of these brain regions informed both differential expression and network analysis, leveraging prior-knowledge. (Results) The interactive DiffBrainNet online resource compiles comprehensive differential expression and network results for the 8 brain regions.

To determine whether DE genes also exhibit prominent co-regulatory changes within the DNs, we pinpointed differential hub genes, characterized by a normalized node-betweenness above 1 (Figure 3.1 bottom). Moreover, to identify pathways influenced by DE genes and/or differential hub genes, we performed enrichment analyses involving GO terms, KEGG and Reactome pathways, and GWAS genes. We were able to compare the transcriptomic responses across eight different brain regions on multiple complementary levels by using this analysis framework. All findings are accessible in an interactive online resource (DiffBrainNet, http://diffbrainnet.psych.mpg.de/), with subsequent sections presenting detailed results of our analyses.

### 3.1.1 Differential Expression and Networks in Response to Glucocorticoid Activation in 8 Different Brain Regions

By integrating DE and DN analysis, we studied the region-specific transcriptomic alterations following glucocorticoid exposure in mice. Analysis of gene expression variance through principal component analysis revealed that the first two principal components accounted for 62% of the variance and distinguished the different brain regions (Figure 3.2a). When assessing all regions collectively, the fourth and fifth principal components separated the treatment groups (Figure 3.2b). Across all eight regions, 2092 genes were differentially expressed following dexamethasone treatment (FDR ≤ 0.1), with 172 genes consistently altered across all regions (Figure 3.2c, Online Table 1). Most DE genes were dysregulated in multiple regions, with a minority (5.4–26.6%) unique to a single region (Figure 3.2d, Supplementary Table 2-10, Online Table 2-9). The upregulated genes common to all regions ($n_{genes}$=129) significantly correlated with processes like cell death and signal transduction, while downregulated genes ($n_{genes}$=43) were associated with development, including neurogenesis (Supplementary Figure 1a, and Online Table 19). Intriguingly, even though GR (gene name *Nr3c1*), the primary receptor activated by dexamethasone and hence initiating the transcriptional response, is differentially downregulated in every region, its normalized expression does not correlate with the number of DE genes across regions at vehicle condition (Supplementary Figure 1c). This observation also applied to MR (gene name *Nr3c2*), a glucocorticoid receptor with a higher affinity for cortisol and less for dexamethasone (Supplementary Figure 1d), as well as to the expression ratio of GR to MR (Supplementary Figure 1e). Although GR and MR vehicle expression levels vary across regions, the differences are small, potentially explaining the absence of correlation with DE gene counts in each region.

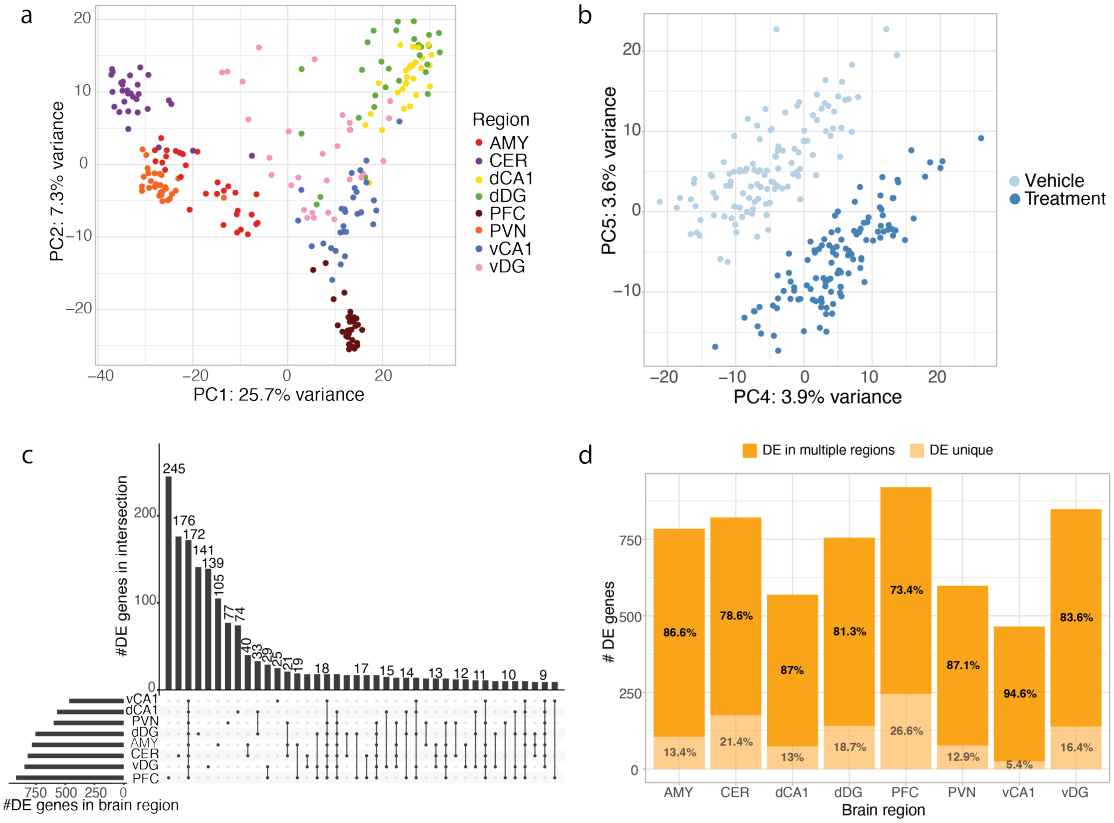


**Figure 3.2. Differential gene expression across 8 mouse brain regions.** (a) Principal component (PC) analysis plot visualizes the variance related to brain region along PCs 1 and 2. (b) PC analysis plot detailing variance in gene expression related to treatment groups along PCs 4 and 5. (c) UpSet plot revealing the overlap of DE genes (FDR ≤ 0.1) across the 8 brain regions. (d) Barplot representing the proportions of unique and shared DE genes within each brain region.

### 3.1.2 Enhanced Biological Insights Through Differential Network Analysis

Beyond DE analysis, we performed DN analysis within each of the eight brain regions. A comparison of the number and enrichment patterns of differential hub gene enrichment revealed 755 differential hub genes, with the majority (>73%) being common to at least two brain regions (Figure 3.3a-b, Supplementary Table 2,11-18, and Online Table 11-18). Notably, seven hub genes were consistently identified across all regions included in the study (*Sox5, Lpar1, Thy1, Mcam, Nell2, Rab3c, Zic1*) (Figure 3.3a, Supplementary Figure 1b, Online Table 10+20). Out of the 755 differential hub genes, only 174 were also identified as DE genes in any of the brain regions (Figure 3.3a).

We delved deeper into the PFC, which had the highest number of unique DE genes (920 in total, with 245 unique to the PFC, Figure 3.2c). The PFC, along with the AMY, also displayed the most unique differential hub genes (293 in total, with 29 unique to the PFC, Figure 3.3a, Supplementary Table 2). Intriguingly, none of the PFC's 29 unique differential hub genes overlapped with DE genes. GO enrichment analysis among the PFC's unique DE and differential hub genes revealed distinct biological functions for each gene set. The highly enriched biological processes for unique DE genes primarily related to development and signaling (Figure 3.3c, and Online Table 21), while the unique differential hub genes correlated with broader terms related to stress or stimuli

responses (Figure 3.3d, and Online Table 22). This pattern implies that DE and DN analyses, while different, provide complementary insights into the brain's transcriptional responses to stimuli.

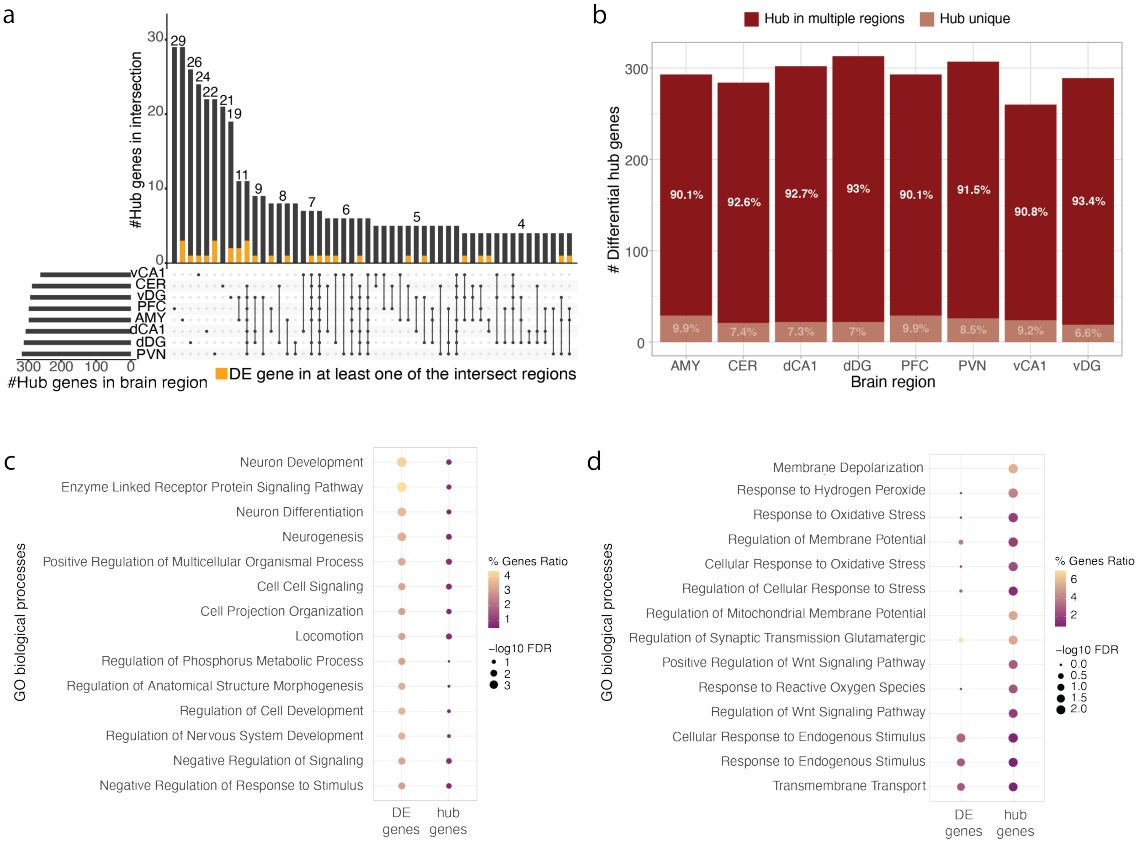


**Figure 3.3. Differential network analysis in the PFC provides unique biological insights not captured by differential expression alone.** (a) UpSet plot visualizing the overlap of differential hub genes with a normalized node-betweenness > 1.0 across 8 brain regions. Yellow parts of the intersection size bars represent genes concurrently identified as significant DE genes in at least one brain region within the intersection. (b) Barplot representing the proportions of unique and shared differential hub genes within each brain region. (c-d) Dot plots displaying the top 14 GO terms that are most significantly enriched among the PFC's unique DE genes (c) and unique differential hub genes (d).

To demonstrate the added value of DN analysis, we highlight *Abcd1*, a gene involved in the active transport of glucocorticoids and part of the ABC protein family (Müller et al., 2003; Uhr et al., 2002). Although not classified as a DE gene in the PFC (FDR = 0.935; Figure 3.4a), *Abcd1* emerged as a prominent differential hub gene with the highest normalized node-betweenness in the PFC network (Supplementary Table 15) and numerous differential correlations. Within its DN, we found four PFC DE genes (FDR ≤ 0.1) and seven genes with a nominal DE *p* value ≤ 0.05 (Figure 3.4b). Pathway enrichment analysis of *Abcd1*'s DN highlighted a broader role for ABC transporters in the response to glucocorticoids (Figure 3.4c-d, and Online Table O23). Furthermore, it can be inferred that *Abcd1* is associated with extensive interconnected DNs based on its direct or indirect connections to *Tm7sf2* and *Pex5l*, two additional differential hub genes (Figure 3.4b). The small expression changes in genes linked to *Abcd1* add up, elevating its status as a differential hub gene, indicative of its pivotal role despite the modest individual

expression change. These insights underscore the ability of network analyses to dissect subtle transcriptomic responses, uncovering molecular pathways in a way that single-gene analysis cannot, thus underlining the integral nature of gene networks in cellular function and the discovery of pathway-specific molecular mechanisms.

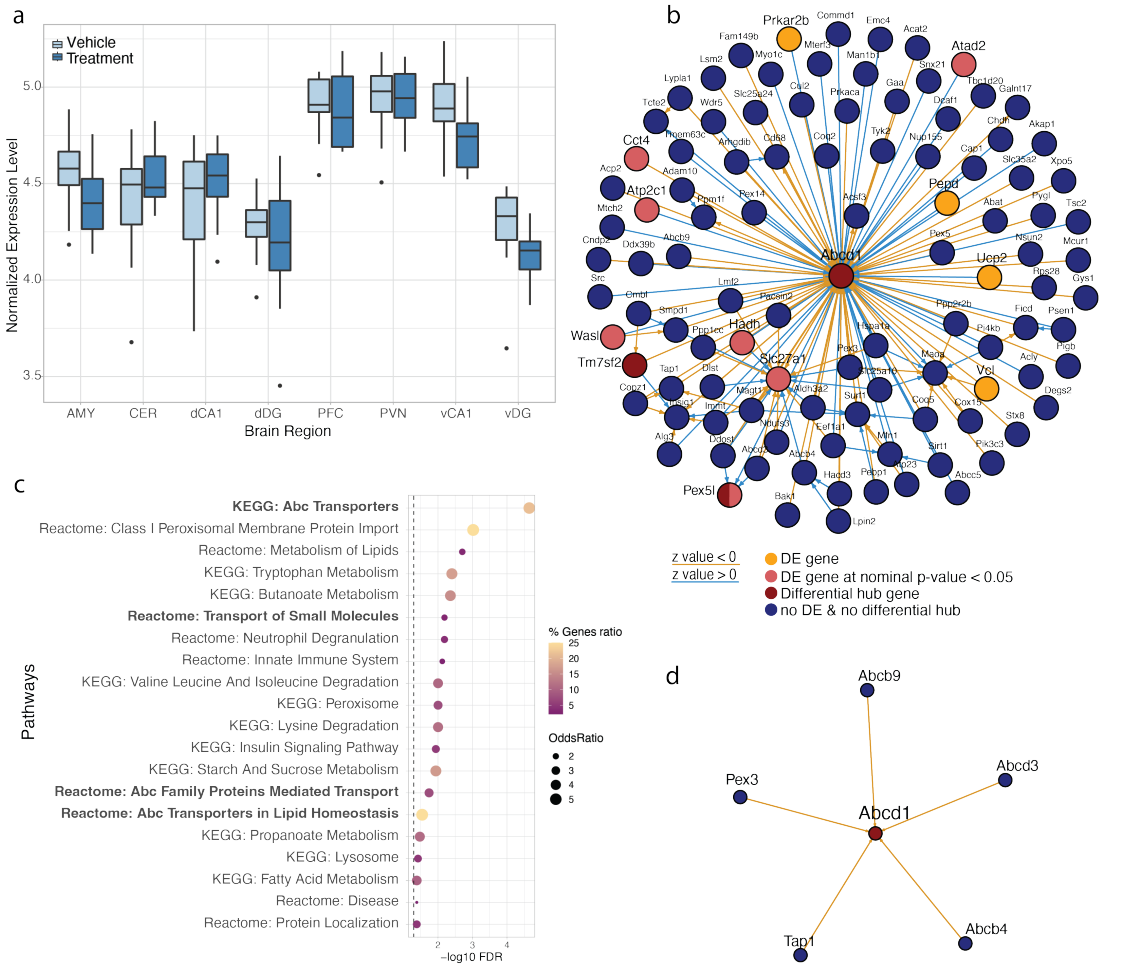


**Figure 3.4. ABC transporters and their role in dexamethasone responses in the PFC at the network level.** (a) Boxplot visualizing the normalized expression of *Abcd1* across all brain regions at vehicle and treatment level. *Abcd1* is not differentially expressed in any of the 8 regions. (b) Differential network of *Abcd1* and its neighbors in the PFC. (c) Pathway enrichment analysis for *Abcd1* and its differentially connected neighbors in the PFC, based on KEGG and Reactome, with bold terms highlighting the broader involvement of the ABC transporters pathway in the PFC's response to glucocorticoids. (d) Differential network of the ABC transporters pathway in the PFC.

### 3.1.3 Disease relevance of genes associated with stress response on single-gene and network level

To assess the translatability of transcriptomic responses to dexamethasone in mice to human conditions, we examined the consensus between dexamethasone-responsive genes in the mouse PFC and genes implicated in autism spectrum disorder, bipolar disorder, and schizophrenia in the human cortex from a postmortem study (Gandal, Zhang, et al., 2018). Our analysis revealed that 41.3% of the mouse DE genes ($n_{genes}$=380 out of 920) were also associated with human psychiatric disorders (Figure 3.5a), emphasizing the importance of glucocorticoid-mediated transcriptional alterations in these conditions. This correlation was also evident when aligning our findings with network modules derived from human postmortem brain analyses (Gandal, Zhang, et al., 2018), showing that stress-related DE genes and differential hub genes were significantly enriched in modules linked to autism spectrum disorder, bipolar disorder, and schizophrenia (Figure 3.5b).

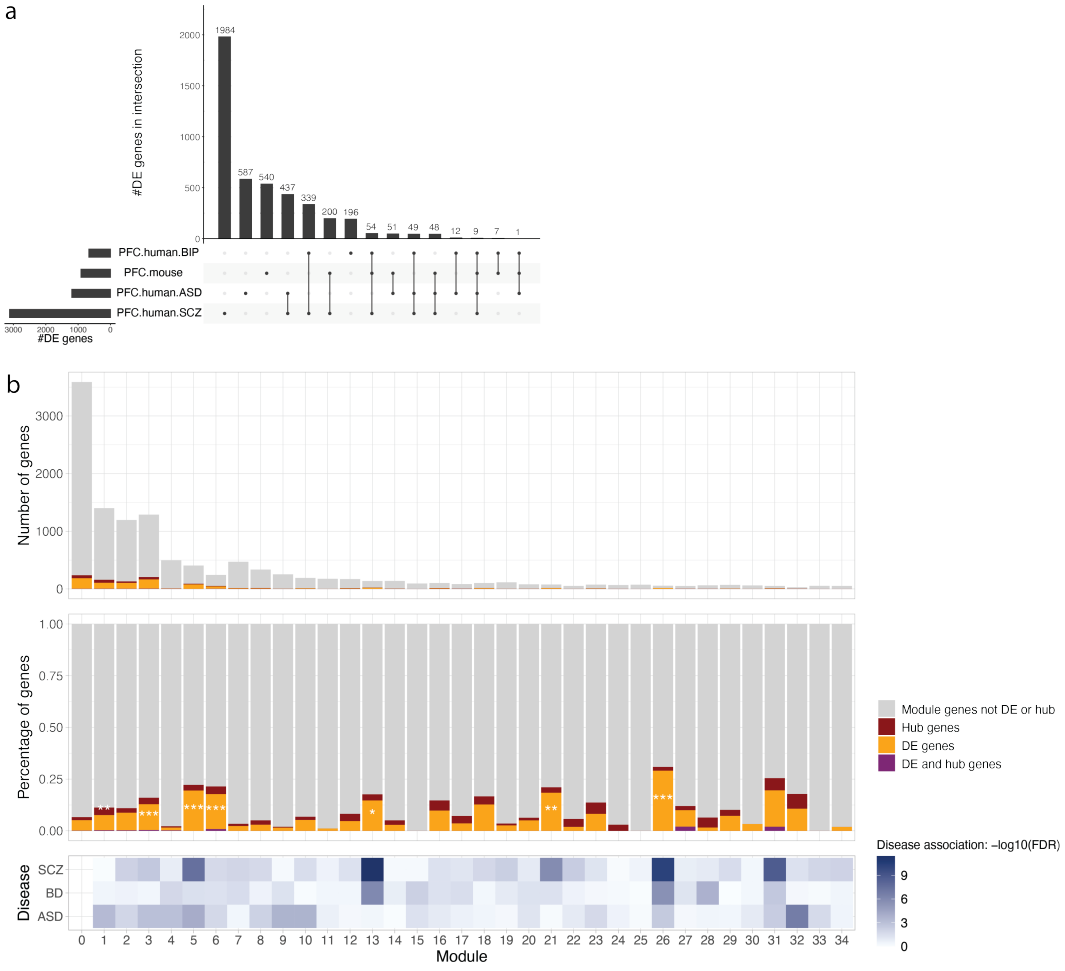


**Figure 3.5. Aligning DiffBrainNet discoveries with human studies.** (a) UpSet plot comparing the DE genes identified in the mouse PFC with DE genes from the postmortem human cortex of individuals with bipolar disorder (BIP, n=222), autism spectrum disorder (ASD, n=51), and schizophrenia (SCZ, n=559) as reported by (Gandal, Zhang, et al., 2018). (b) Enrichment analysis of DE genes and differential hub genes from our PFC analysis in modules associated with SCZ, ASD, and BIP as identified by (Gandal, Zhang, et al., 2018). The significance of enrichment within each module, determined via a one-sided Fisher's exact test, is denoted by asterisks: * FDR ≤ 0.05, ** FDR ≤ 0.01, *** FDR ≤ 0.001.

### 3.1.4 Differential Network Analysis Augments the Biological Understanding of Differentially Expressed Genes

We aimed to enhance the interpretative power of DE results by integrating them with DN results, which is particularly useful when DE gene numbers are too low to imply clear pathway involvement, suggesting minimal gene-level effects. In the vCA1 region of the hippocampus, only 5.4% of the DE genes ($n_{genes}$=25 out of 466) were unique to this area (Figure 3.2c, Figure 3.6a, Supplementary Table 9, and Online Table 8), and GO enrichment analysis did not reveal any significant terms (Supplementary Figure 2, and Online Table 24). We used the 25 unique DE genes from the vCA1 as seed nodes in our network analysis, identifying their differential neighbors, which culminated in a DN comprising 745 nodes, incorporating both the 25 unique vCA1 DE genes and an additional 720 differential neighbors. This network was enriched for genes linked to general cognitive ability, schizophrenia, and autism spectrum disorder through GWAS (Figure 3.6b, and Online Table 25). Furthermore, the network displayed significant enrichment for GO terms related to nervous system processes, cell morphogenesis, ion transport, and synaptic signaling (Figure 3.6c, and Online Table 26), indicating subtle but widespread molecular connectivity alterations in vCA1 not apparent in DE analysis alone.

Focusing on the enriched GO term based on the gene ratio, "regulation of trans-synaptic signaling" (FDR=$8.71 \times 10^{-22}$), we investigated the differential network of the genes both related to this term and part of the vCA1 DE gene network (Figure 3.6d). *Grm4*, coding for a metabotropic glutamate receptor, was central in this network, exhibiting numerous differential associations with other hub and DE genes, including *Cacna1a*, which is crucial for neuronal communication and synaptic signaling (Luo et al., 2017). This network demonstrated shifts in connectivity among various differential hub genes. These changes extended beyond *Grm4* and *Cacna1a*, including alterations between *Brsk1*, *Nlgn3*, *Cspg5*, *Rab3a*, and *Grin2b*. Thus, the combined DE and DN analysis was key to unveiling complex biological responses to dexamethasone in vCA1 that DE analysis alone could not discern.

### 3.1.5 Network Analysis Facilitates Hypothesis Generation for Candidate Genes

Next, we looked into biological pathways and processes regulated by genes previously linked to psychiatric disorder risk using our resource and analytical framework. This allowed us to examine co-regulatory patterns of specific genes under normal conditions and following stimuli, such as glucocorticoid exposure. Our focus centered on *Tcf4* (Transcription factor 4) which is associated with various psychiatric disorders including schizophrenia, major depressive disorder, and autism spectrum disorders (Teixeira, Szeto, Carvalho, Muotri, & Papes, 2021), and implicated in neurodevelopmental disorders like Pitt-Hopkins syndrome (Sirp et al., 2021). Therefore, we investigated the biological pathways that *Tcf4* modulates in DNs reflecting GR activation responses.

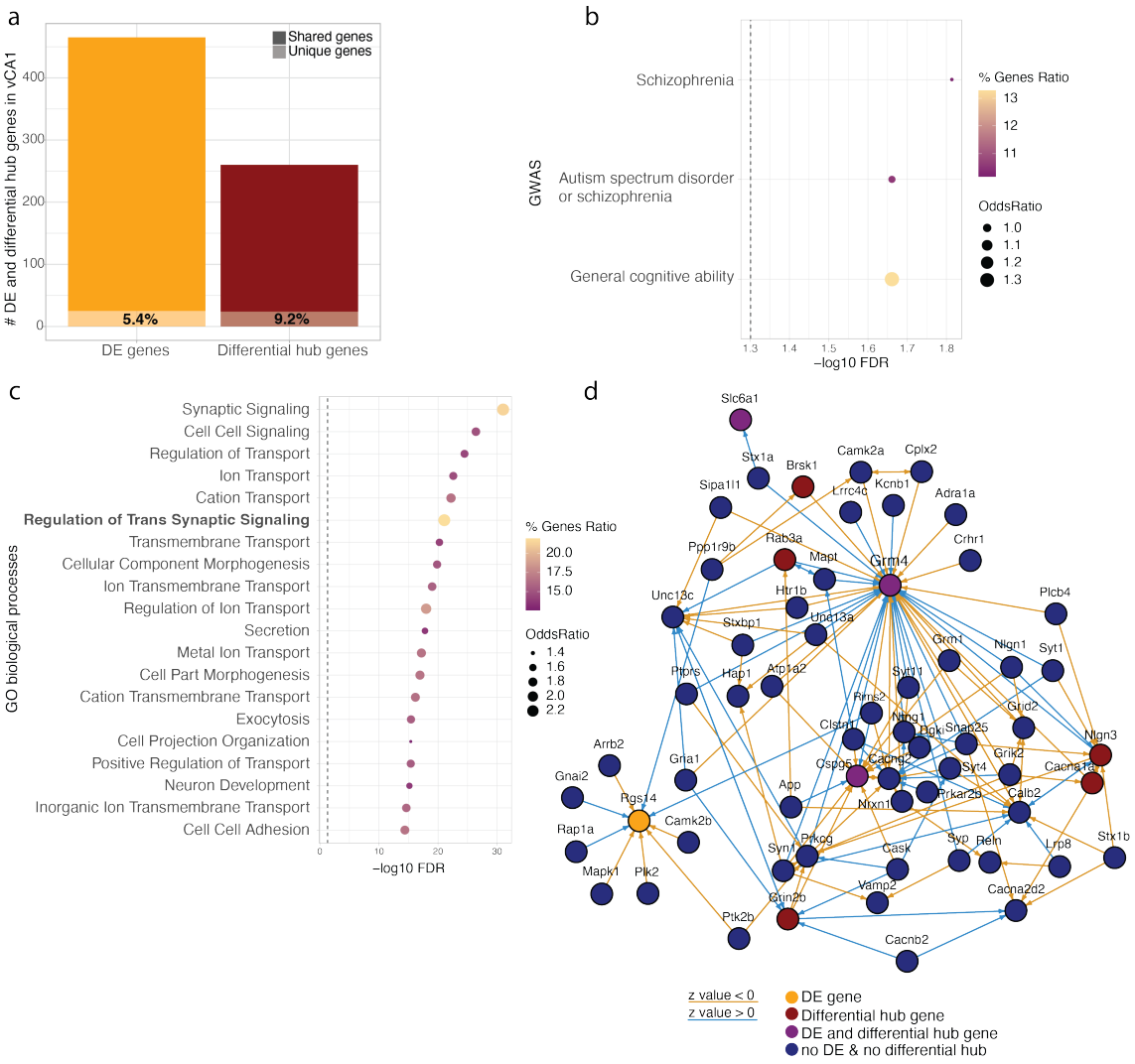


**Figure 3.6. Network-based differential analysis enhances the biological interpretation of differential expression: the case of vCA1.** (a) Barplot depicting the number of unique and shared DE and hub genes in the vCA1. The vCA1 shows the smallest proportion of unique DE genes but the highest rate of unique differential hub genes compared to other brain regions. (b) GWAS enrichment analysis of the unique vCA1 DE genes and their differential neighbors shows enrichment for genes linked to SNPs associated with schizophrenia, autism spectrum disorder or schizophrenia, and general cognitive ability. (c) GO enrichment analysis of biological processes in the unique vCA1 DE genes and their neighbors shows enrichment of ion transport, and synaptic signaling. (d) Differential network of the genes linked to the GO term "regulation of trans-synaptic signaling" and connected with vCA1's unique DE genes.

*Tcf4* exhibited significant differential expression with dexamethasone treatment in the amygdala, vDG, and dDG, all showing a consistent downregulation (Figure 3.7a). While *Tcf4*'s expression change was not statistically significant in the PFC, previous human postmortem brain network analyses have identified it as a schizophrenia master regulator (Torshizi et al., 2019). In the PFC DN centered around *Tcf4*, we pinpointed 26 genes with differential connectivity to both DE genes and differential hub genes (Figure 3.7b). This network, associated with various neurobehavioral traits in GWAS, underscores *Tcf4*'s relevance to schizophrenia and the impact of stress on *Tcf4* networks (Figure 3.7c, and Online Table 27). Notably, the differential *Tcf4* network showed enrichment for development-related GO terms, as well as autophagy and chromatin organization (Figure 3.7d, and Online Table 28).

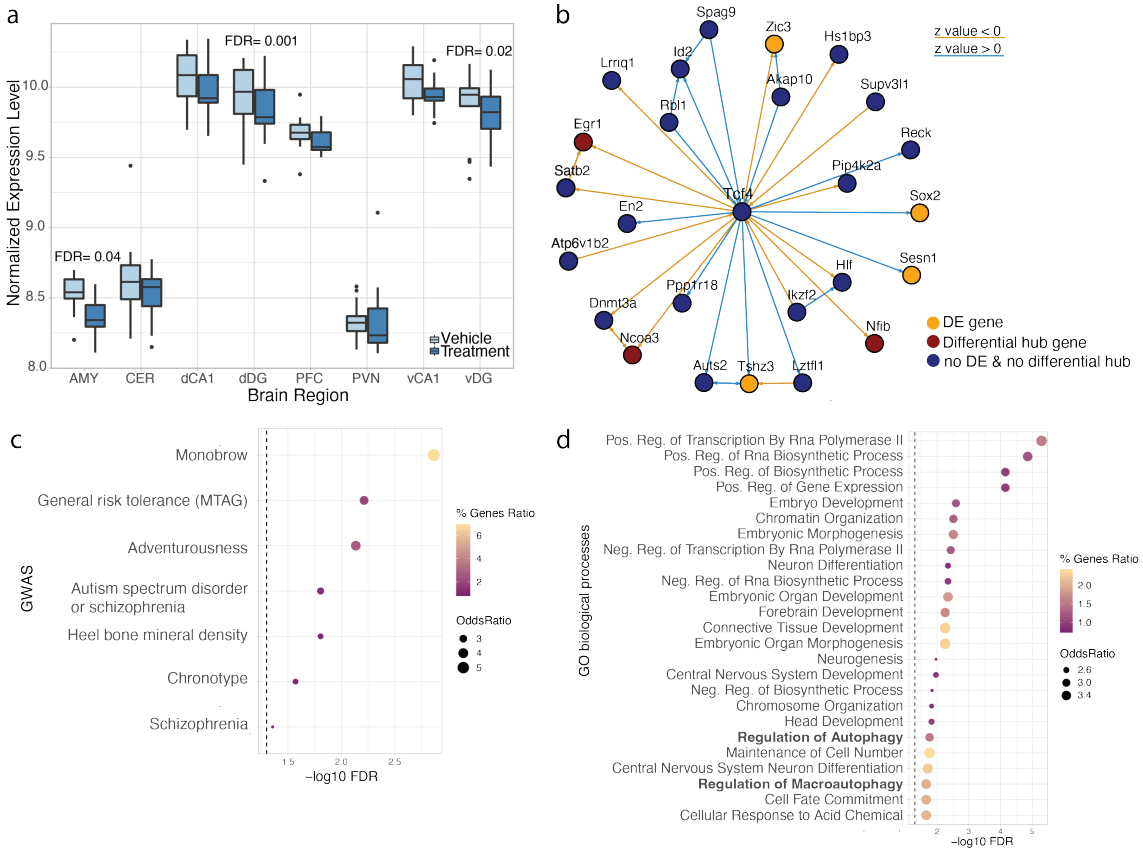


**Figure 3.7. Network dynamics linked to candidate genes: the case of *Tcf4*.** (a) Differential expression of *Tcf4* is observed in the ventral and dorsal dentate gyrus (v/dDG) and in the AMY following the administration of dexamethasone. (b) Differential network of *Tcf4* in the PFC. (c) GWAS enrichment analysis for *Tcf4* and its differential neighbors shows significant enrichment (FDR ≤ 0.05) for genes linked to SNPs associated with the GWAS traits schizophrenia, autism spectrum disorder or schizophrenia, adventureness and general risk tolerance, among others. (d) GO biological processes enrichment analysis for *Tcf4* PFC differential network members shows significant enrichment for development, neuronal differentiation, RNA biosynthetic processes, and gene expression, as well as the regulation of autophagy (bold).

In the hippocampal formation, known for high *Tcf4* expression from prenatal stages to adulthood (Teixeira et al., 2021), *Tcf4* is significantly downregulated in both vDG and dDG regions (Figure 3.8a). Here, we explored how *Tcf4*'s differential expression might affect molecular connectivity within these subregions. The CHEA and TRANSFAC transcription factor targets databases (Lachmann et al., 2010; Wingender, Dietze, Karas, & Knüppel, 1996) and the Pathway commons protein-protein interactions datasets (Cerami et al., 2010) identify 20 of the 55 members of the *Tcf4* vDG and dDG DNs (Figure 3.8a) as known *Tcf4* targets and/or protein interactors. Based on MotifMap (Y. Liu et al., 2017) and TRANSFAC (Wingender et al., 1996), an additional 11 genes are predicted *Tcf4* targets (Supplementary Figure 3, and Online Table 29). While most connections in these networks were similarly regulated in both vDG and dDG, 24 showed opposite regulatory patterns between the regions (Online Table 30, and selected genes in Figure 3.8b) (data obtained from the Harmonizome database (Rouillard et al., 2016)). The connections between *Tcf4* and the Zic gene group, which includes *Zic1*, *Zic2*, and *Zic3*, indicated a negative regulatory effect in dDG and a positive regulatory effect in vDG (see Methods 2.1.6.2 for explanation of term). Zic genes are important in the formation

of body pattern formation through the Wnt pathway (Nagai et al., 1997), which has been closely linked to *Tcf4* (Bem et al., 2019; Petherick et al., 2013). Moreover, *Tcf4*'s interactions with *Runx2*, a Wnt pathway participant (McCarthy & Centrella, 2010), suggested dexamethasone may modulate *Tcf4*'s impact on the Wnt pathway in a subregion-specific manner within the DG.

These findings present a comprehensive approach to generating hypotheses for subsequent experimental validation of these observed effects, underscoring the nuanced role of *Tcf4* and its networks in response to glucocorticoid treatment across different brain regions.

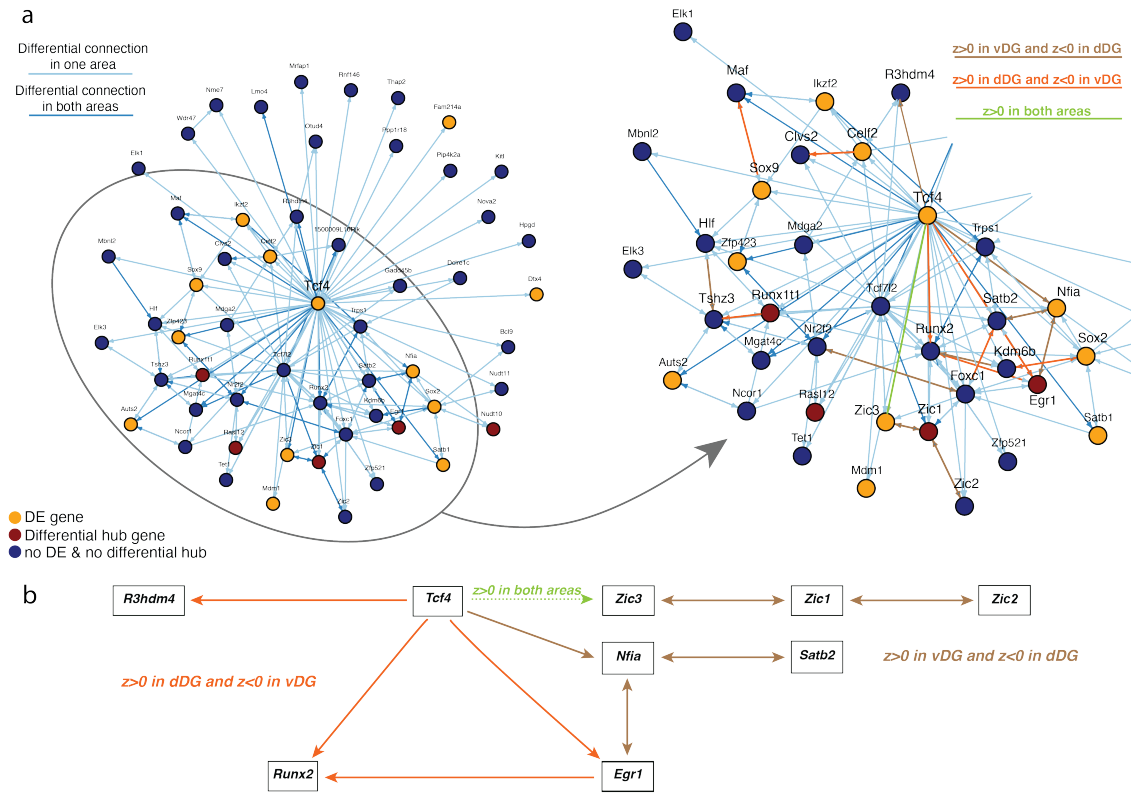


**Figure 3.8. Differential regulations of *Tcf4* in vDG and dDG.** (a) Differential network of *Tcf4* in both the vDG and dDG (left). Close-up view of a highly interconnected segment of the DG *Tcf4* DN (right). Edges are highlighted in orange to indicate a positive regulatory effect in the dDG in contrast to a negative regulatory effect in the vDG. Edges in brown indicate a positive regulatory effect in the vDG and a negative one in the dDG, while the edges colored in green represent a positive regulatory effect in both areas. (b) *Tcf4* molecular pathways that display divergent co-regulation in vDG and in dDG. The interactions between *Tcf4* and the Zic transcripts, along with *Satb2* and *Nfia*, exhibit a positive regulatory effect in vDG but a negative one in the dDG. Conversely, the interactions of *Tcf4* with *Runx2*, *Egr1* and *R3hdm4* show a negative regulatory effect in the vDG and a positive one in the dDG.

## 3.2 Molecular Alterations in Psychiatric Disorders in the Orbitofrontal Cortex on a Cell Type Level

In this chapter, we transition from a bulk transcriptomic study on the response to glucocorticoid receptor (GR) activation in mouse brain tissue to a multi-omics study focusing on mood and psychotic disorders with cell type resolution. This study is conducted in the human orbitofrontal cortex (OFC) – a subregion of the prefrontal cortex (PFC) – using postmortem brain samples. This shift was motivated by several key factors. The PFC was identified as the brain region with the highest number of transcriptional alterations upon GR activation, and is a focal point of psychiatric research, largely due to consistent evidence that dysfunctions in this brain region are fundamental to the cognitive and behavioral symptoms observed in psychiatric disorders (Gao et al., 2012). The heterogeneity of cell types within the PFC necessitates a cell type-specific investigation of the respective molecular alterations.
In addition to a more detailed understanding of transcriptomic alterations, we aimed to explore the epigenomic landscape related to psychiatric disorders within the PFC's cell types. Epigenomic mechanisms are of particular interest in psychiatric research as they are thought to mediate the interaction between environmental influences and molecular processes (Cho, Elizondo, & Boerkoel, 2004; Keverne & Binder, 2020).
Utilizing postmortem brain tissue from a transdiagnostic psychiatric cohort, this study integrates cell type-specific transcriptomic and epigenomic alteration with genetic predisposition for psychiatric disorders. While it is crucial to get a better understanding of the alterations in gene expression among GR activation to dissect the molecular response to stress, primarily via the HPA axis, the postmortem study enables a direct examination of the regulatory interactions within the human prefrontal cortex, offering a unique window into the etiology of mood and psychotic disorders.

### 3.2.1 Study Design and Cohort Characteristics

To decipher cell type-specific molecular changes linked to psychiatric disorders within the OFC, a detailed examination of nuclei from postmortem brain tissue (Brodmann area 11) was performed. This work included the integration of single-nucleus (sn) RNA-seq and ATAC-seq data with genetic profiles, along with demographic and clinical information (Figure 3.9). The analysis was based on a cohort encompassing 92 donors, including 35 controls without psychiatric diagnoses and 57 cases diagnosed with schizophrenia, schizoaffective disorder (SCA), major depressive disorder (MDD), or bipolar disorder (n=38,7,7,5, respectively). Matching for sex (38% female representation), age (mean ± s.d. = 54.27 ± 13.64), postmortem interval (mean ± s.d. = 33.90 ± 14.82), and brain pH (mean ± s.d. = 6.60 ± 0.24), ensured comparability between the case and control groups, as detailed in Table 2.1 (p. 33).
Following stringent quality control measures, we successfully retained a set of high-quality transcriptomic data, representing a total of 787,046 nuclei from 87 donors. The data were characterized by an average number of 9,046 nuclei per donor (range 3,895-15,693 nuclei). The median count of unique molecular identifiers (UMIs) per nucleus was 3,887, allowing the detection of a median of 2,205 genes per nucleus. In addition to the

transcriptomic profiles, we also acquired chromatin accessibility data for 399,439 nuclei from 90 donors after quality control. These profiles were characterized by an average number of 4,438 nuclei per donor (range 982-8,707 nuclei) and a median number of 7,071 ATAC-seq fragments per nucleus.

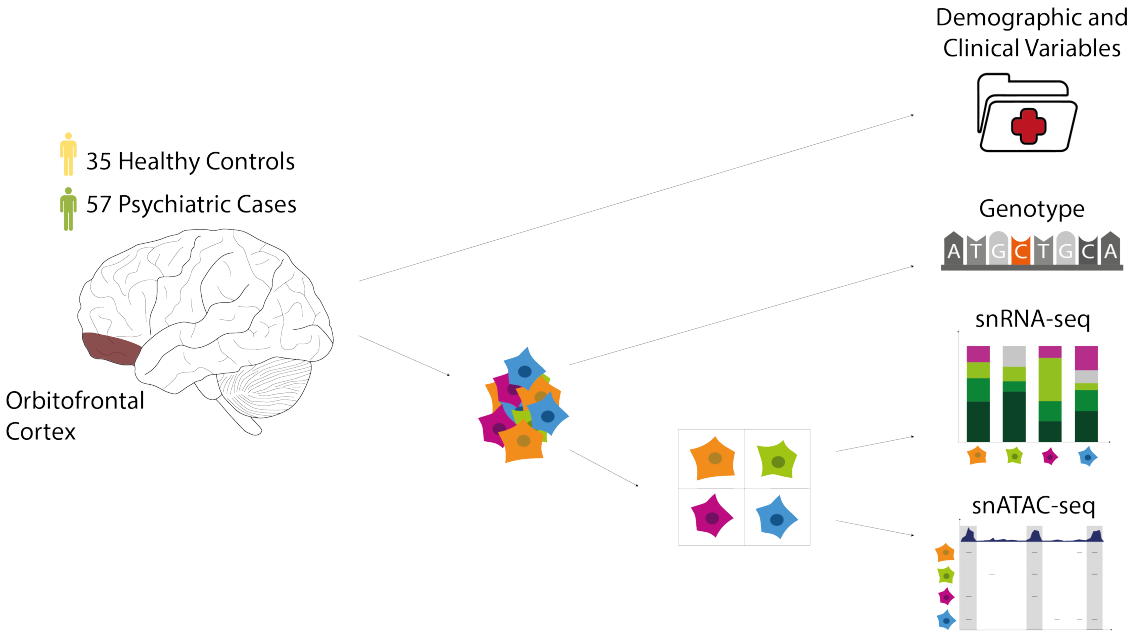


**Figure 3.9. Schematic representation of single-nucleus sequencing study in postmortem human brain samples of the orbitofrontal cortex.** Data is based on a cohort of 92 donors, including 35 healthy controls and 57 psychiatric cases with a diagnosis for either schizophrenia, schizoaffective disorder, MDD, or bipolar disorder (n=38,7,7,5 respectively). Demographic and clinical variables were available for each donor. Genotyping, as well as single-nucleus profiling of gene expression (RNA-seq) and chromatin accessibility were performed on tissue samples of the orbitofrontal cortex (Brodmann Area 11) of the cohort.

### 3.2.2 Identification and Assignment of Cell Types in Single-Nucleus Sequencing Data

The preprocessing of both snRNA-seq and snATAC-seq data was followed by the assignment of cell type labels to the identified cellular clusters. To label the snRNA-seq data, we initially leveraged a cortical dataset from the Allen Brain Atlas (Human Multiple Cortical Areas (Map., 2019)), using a variational inference model (Lotfollahi et al., 2022). Subsequently, we fine-tuned these labels through manual curation based on the expression of marker genes (see Methods 2.2.3.4). Similarly, we defined cluster identity in the snATAC-seq data by integrating it with the previously labeled snRNA-seq data (Granja et al., 2021) and a subsequent refinement based on the chromatin accessibility of known marker genes (Figure 3.10).

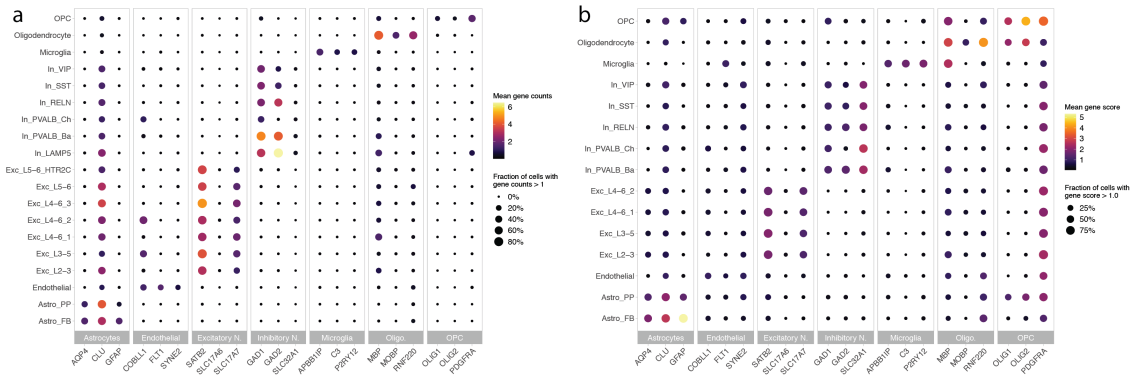


**Figure 3.10. Gene expression and gene scores of established cell type-specific markers**. (a-b) Dotplots illustrating levels of gene expression in snRNA-seq data (a) and gene scores in snATAC-seq data (b) for selected marker genes, categorized by major cell types. Color reflects the mean gene expression or score, while the size of each dot denotes the proportion of nuclei with a gene counts or scores > 1.

Both data modalities facilitated detailed profiling of all major cortical cell types, including multiple subtypes of excitatory and inhibitory neurons from different cortical layers, endothelial cells, and various glial subtypes such as astrocytes, microglia, oligodendrocytes, and oligodendrocyte precursor cells (OPCs). Within the snRNA-seq data, a total of 19 distinct cell types were discerned, and of these, 15 were also identified in the snATAC-seq data (Figure 3.11).

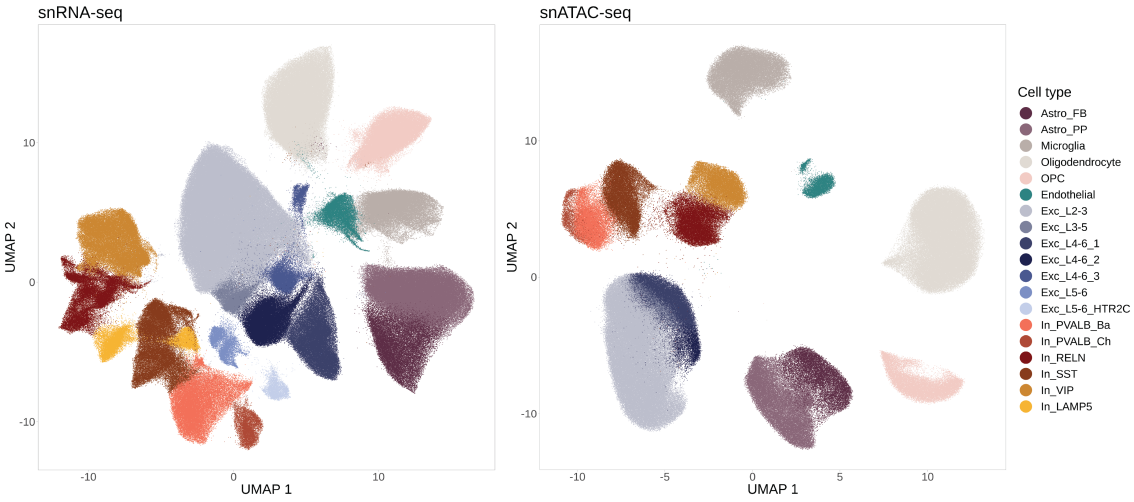


**Figure 3.11. Low-dimensional representation of snRNA-seq and snATAC-seq data.** UMAP visualizations for snRNA-seq (787,046 nuclei) and snATAC-seq (399,439 nuclei) data, colored by the corresponding cell type classification. 19 cell types were identified in the snRNA-seq data, while 15 cell types were discerned in the snATAC-seq data, encompassing the full spectrum of major cortical cell types.

The distribution of library preparation batches, disease status, and sex does not show major differences between the cell types in both snRNA-seq and snATAC-seq data (Figure 3.12), indicating that cell clustering was not influenced by these potential confounding variables. However, the number of nuclei associated with each cell type exhibited considerable heterogeneity, both among different cell types and between snRNA-seq and snATAC-seq (Figure 3.13a). A median Pearson correlation coefficient of 0.86 was observed between the cell type proportions of RNA-seq and ATAC-seq data across donors (Figure 3.13b). There were significant differences (FDR ≤ 0.05) in cell type

proportions when comparing them between the data from RNA-seq and ATAC-seq for all cell types (Figure 3.13c, Supplementary Table 19). Conversely, within each data modality, the cell type proportions did not significantly differ between case and control groups (Figure 3.13d-e). The glia-to-neuron ratio (RNA: 0.47, ATAC: 0.92, Supplementary Table 20) diverges from the numbers reported in histologically-based studies (see Introduction 1.5), a discrepancy that has been previously observed in droplet-based single-cell sequencing studies (Lake et al., 2018; Nagy et al., 2020).

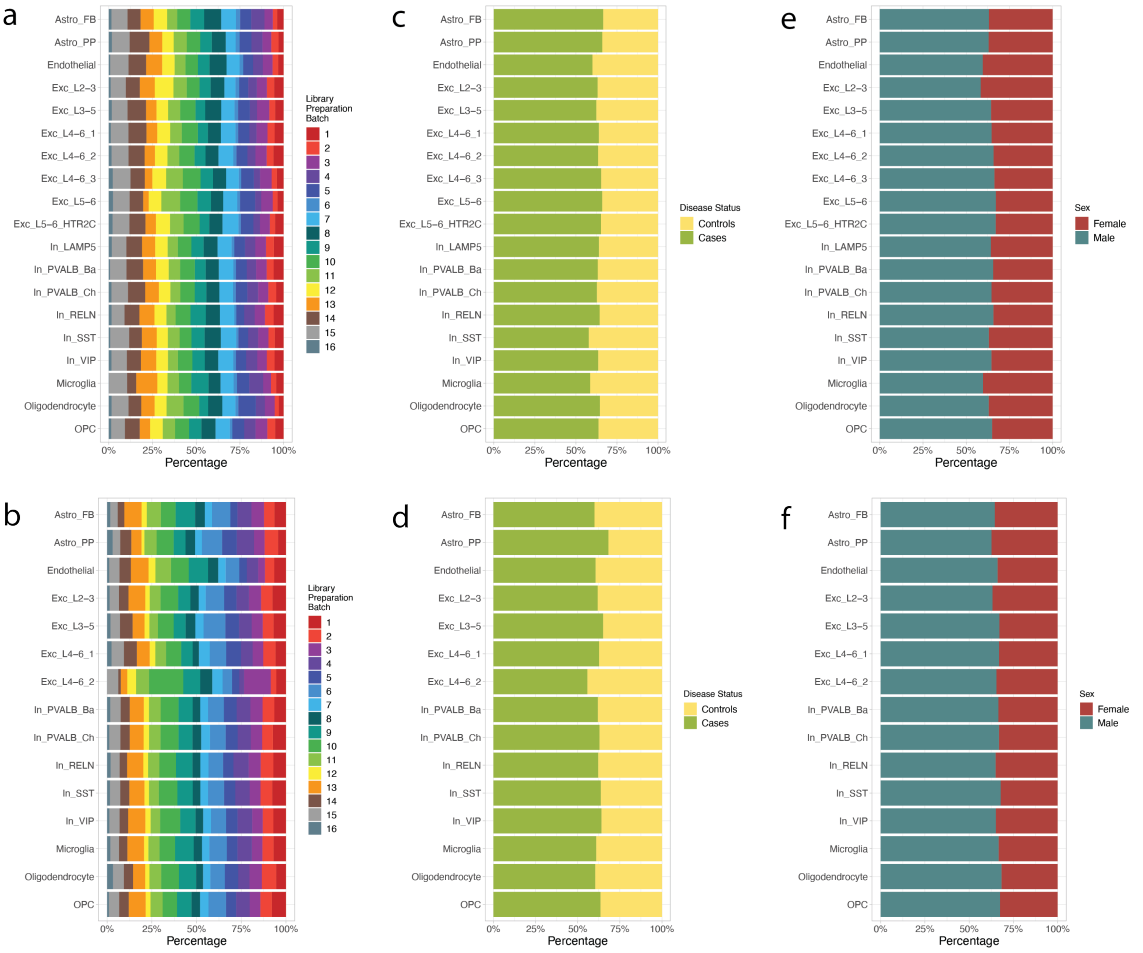


**Figure 3.12. Distribution of library preparation batches, disease status and sex per cell type.** (a-b) Stacked barplots representing the percentage distribution of library preparation batches in snRNA-seq (a) and snATAC-seq (b) data. (c-d) Stacked barplots representing the percentage distribution of cells originating from healthy controls and psychiatric cases in snRNA-seq (c) and snATAC-seq (d) data. (e-f) Stacked barplots representing the percentage distribution of cells originating from female and male donors in snRNA-seq data (e) and snATAC-seq (f) data.

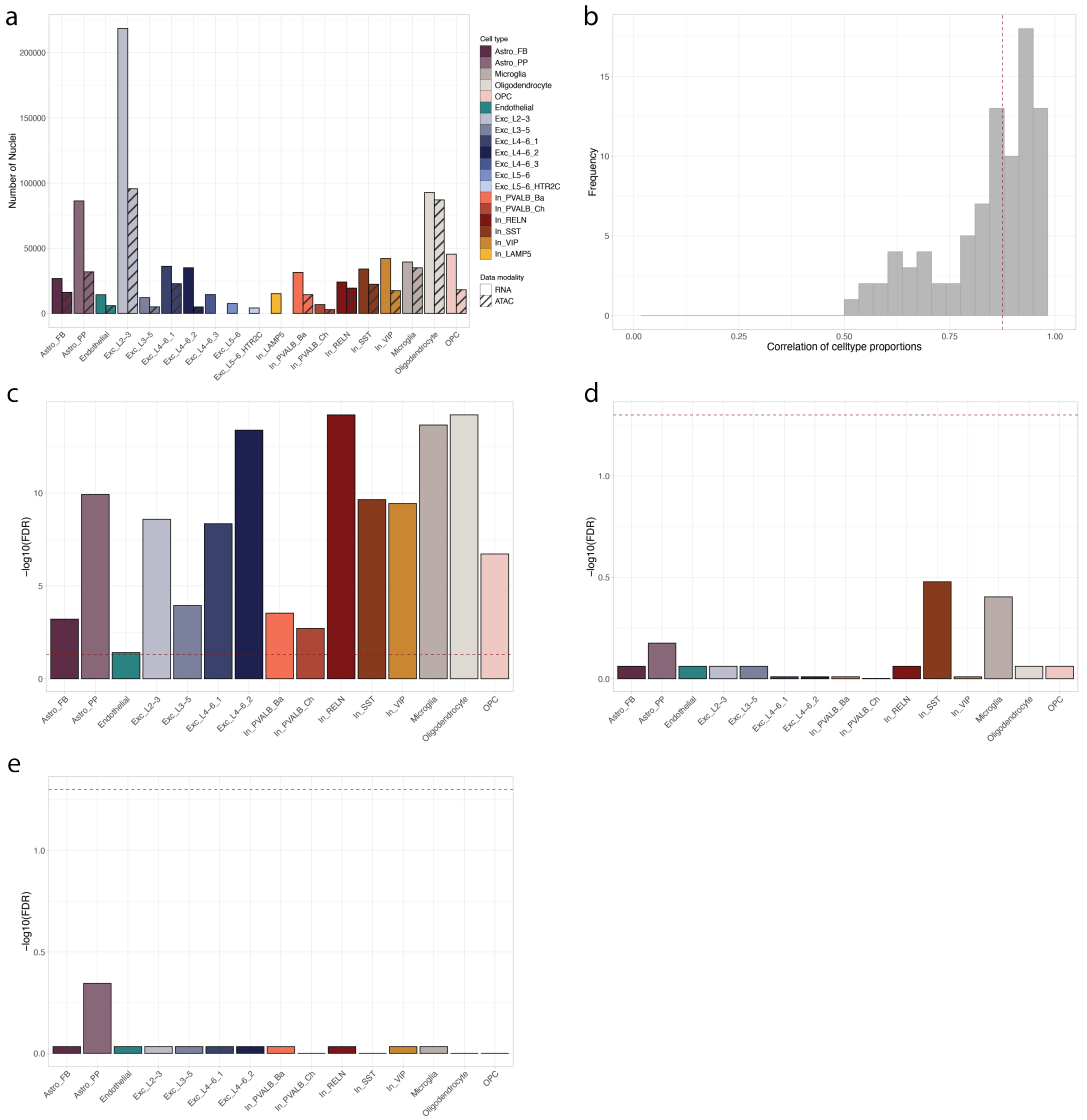


**Figure 3.13. Cell Type Distribution and differences between data modalities and disease status.** (a) Nuclei count retained for each cell type after quality control. Color differentiates cell types hatching indicated the data modality. (b) Histogram depicting the distribution of Pearson correlation coefficients between the cell type proportions in snRNA-seq and snATAC-seq data across donors. (c) Significance levels of the disparities in cell type proportions between snRNA-seq and snATAC-seq data, with bar height indicating the -$\log_{10}$-transformed FDR values from a two-sided Wilcoxon signed-rank test. (d-e) Significance levels of the disparities in cell type proportions between cases and controls in snRNA-seq data (d) and snATAC-seq data (e) with bar height indicating the -$\log_{10}$-transformed FDR values from a two-sided Wilcoxon rank sum test.

### 3.2.3 Correlation of Gene Expression with Chromatin Accessibility Within and Across Cell Types

To clarify the *cis*-regulatory links between chromatin accessibility and gene expression within various cell types, independent of the influence of psychiatric disorders on gene regulation, we performed a detailed investigation. This included the quantification of the number of peaks located nearby (up to 100 kb from the gene body) each gene. We then assessed the correlation between chromatin accessibility and gene expression, applying cell type-specific filtering and normalization methods to the data.
For example in oligodendrocyte precursor cells (OPCs), the distribution of adjacent peaks around the gene body within the 100 kb region varied, ranging from 0 to 112, with the median being 6. It was observed that more than 1,500 genes had no neighboring peaks in their close vicinity (Figure 3.14a). While similar trends were noted in other cell types, they each had their maximum values, generally low median peak counts, and a substantial proportion of genes did not have any proximate peaks within the 100 kb window from their gene body. Furthermore, among the peaks located in the vicinity of a gene, even fewer exhibited a significant correlation with the gene's expression levels. The highest number of peaks achieving nominal significance ($p$ value ≤ 0.05) was 18, while almost 8,000 genes had no peaks correlated with their expression (Figure 3.14b).

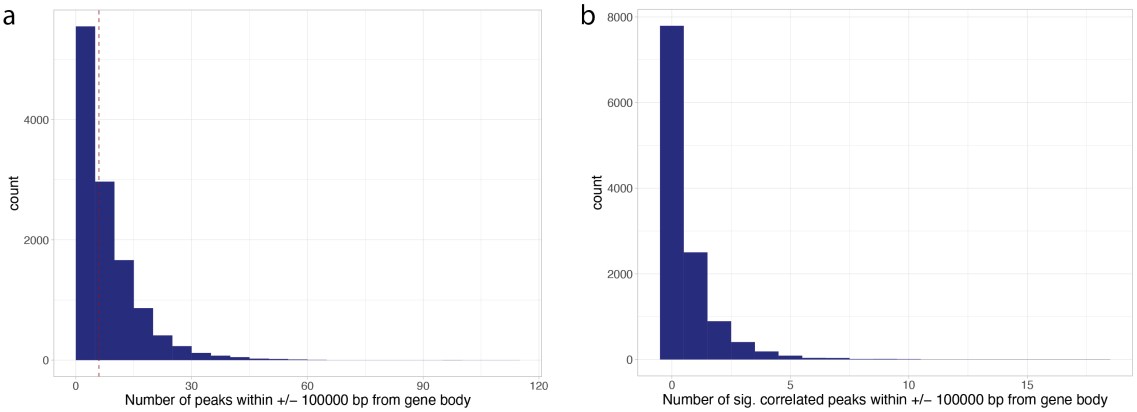


**Figure 3.14. Number of peaks nearby genes.** (a) Histogram of the peak count within a 100kb window from the gene body across all genes tested for differential expression in OPCs. Dashed red line denotes the median peak count. (B) Histogram of the number of nominally significantly correlated peaks ($p$ value ≤ 0.05) within a 100kb distance from the gene body in OPCs.

Given the low density of peaks, we shifted our focus to assess the association between gene expression and chromatin accessibility on the gene level. For this, we utilized gene scores that estimate the gene expression based on the accessibility of nearby regulatory elements, circumventing the need for peak calling (see Methods 2.2.3.3). The Spearman correlation indicates a significant, though modest, relationship between the mean normalized gene expression values and gene scores across (R = 0.35, Figure 3.15a) and within cell types (R = [0.37, 0.46] in all cell types, Figure 3.15b). The modest nature of this correlation might stem from the complexity of open chromatin's role, which is not solely associated with gene activation but may also signify gene repression or genes that are primed for future activation (Daugherty et al., 2017; Shlyueva, Stampfel, & Stark, 2014).

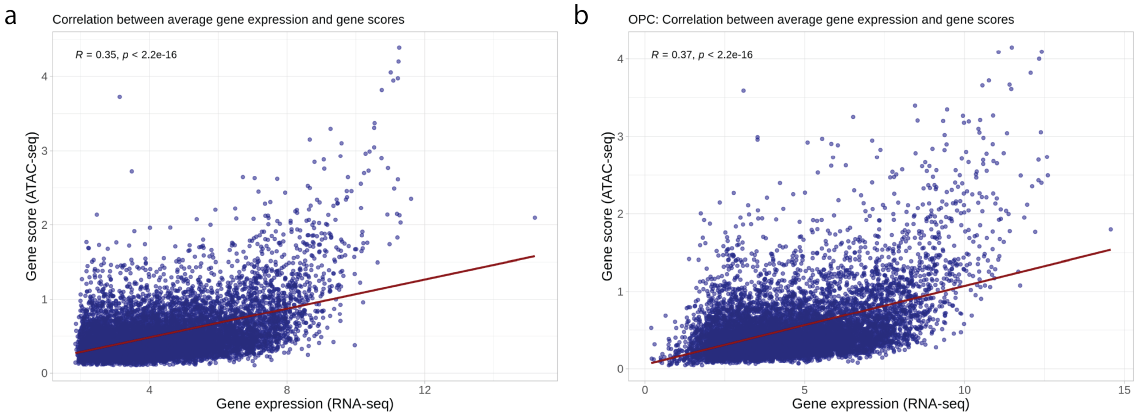


**Figure 3.15. Relationship between mean gene expression and chromatin accessibility.** (a-b) Dotplot depicting the mean gene expression levels plotted against mean gene score levels across all cell types (a) and in OPCs (b). Red line indicates a linear model fitted on the data. Spearman correlation coefficient is displayed in the upper left corner.

To evaluate if groups of genes with different expression and chromatin accessibility patterns are enriched for different functionalities, we grouped genes based on their gene expression (HE: high expression, LE: low expression) and chromatin accessibility levels (HA: high accessibility, LA: low accessibility). We performed a GO enrichment analysis for biological processes to determine the associated functions of genes that are simultaneously highly/lowly expressed and accessible (HE-HA and LE-LA), but also the genes that are highly/lowly expressed while being lowly/highly accessible (HE-LA, LE-HA), as described in the Methods section 2.2.7. We observed a significant enrichment (FDR ≤ 0.05) of biological processes primarily related to the neurons and synapses for the genes that are highly expressed and accessible (HE-HA: 1331 genes, Figure 3.16a), while genes with high expression and low accessibility are more likely to be involved in general cell functionality, such as RNA transport and processing (HE-LA: 795 genes, Figure 3.16b). Genes with high accessibility, though a low expression level, were not enriched for any biological processes (LE-HA: 891 genes), while genes with both a low expression and accessibility seem to be involved in metabolic, catabolic, or mitochondrial processes (LE-LA: 2660 genes, Figure 3.16c). We can therefore conclude that these groups of genes are indeed involved in different biological processes.

The relationship between normalized gene expression and gene scores is notably robust when correlating pseudobulk samples across all cell types, retaining cell type and sample-specific variation within the data (Figure 3.17a). However, when the correlation analysis is limited to pseudobulk samples from the same cell type, thus only accounting for sample-specific variations, the correlations are generally lower and partly even negative (Figure 3.17b). Nonetheless, these correlation distributions remain significantly different from what would be expected by chance ($p$ value < 2.2e-16), as evidenced by comparing it to a random distribution created by permuting gene scores among pseudobulk samples (see Methods 2.2.7).
In light of these findings, our downstream analyses were performed at the level of gene scores. This method effectively circumvents the issue of missing peaks that affect numerous genes, offering a broader perspective of the regulatory landscape surrounding a gene.


**Figure 3.16. Functionalities of groups of genes with different patterns of gene expression and chromatin accessibility levels.** (a-d) Treemaps summarizing significantly enriched biological processes (FDR ≤ 0.05), based on GO terms, for genes with high expression and high accessibility (a), high expression and low accessibility (b), and low expression and low accessibility (c). No enrichments were identified for genes with low expression and high accessibility. GO terms are grouped based on semantic similarity. The size of each rectangle corresponds to the significance of the GO term.

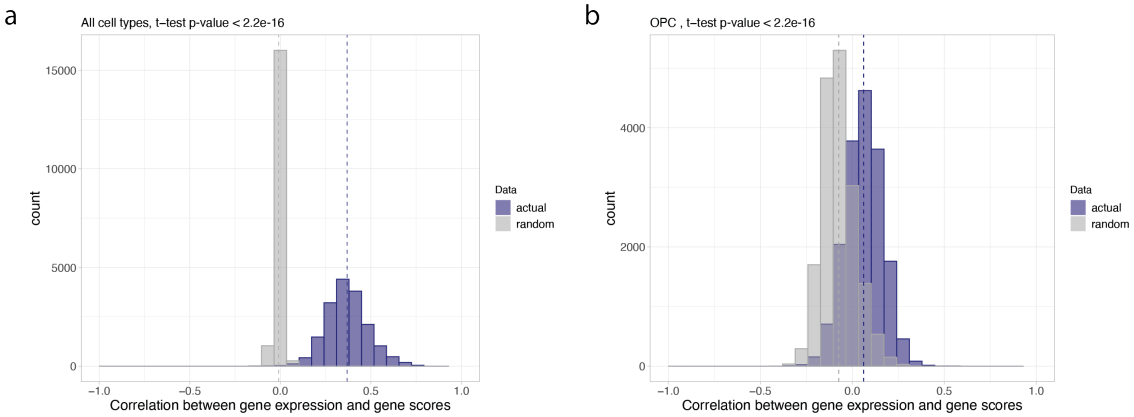


**Figure 3.17. Relationship between gene expression and chromatin accessibility at the cell type-level.** (a-b) Histogram displaying Spearman correlations between gene expression and gene score levels on the donor level across all cell types (a) and in OPCs (b). The observed correlation coefficients (blue) are shown alongside the distribution generated from randomly permuting donor levels (gray). Dashed lines mark the mean values of each distribution.

### 3.2.4 Identification of Cell Type-Specific Changes in Psychiatric Disorders through Differential Gene Expression Analysis

Exploring transcriptional alterations related to psychiatric disorders, this study applied differential expression analysis, comparing cases with controls for each cell type. The number of genes showing significant differential expression (DE, FDR ≤ 0.1) displayed a substantial variation, ranging from 0 to 481 (Figure 3.18a, Supplementary Table 21, Online Table 33). Notably, excitatory neurons stood out for their high counts of DE genes and most substantial $\log_2$-transformed fold changes (FC, ranging from -0.35 to 0.38, see Figure 3.18b). In cell types with at least two hits ($n_{\text{cell types}}$=12 cell types), at least 50% of the identified DE genes were unique (Figure 3.18a), highlighting their distinct transcriptional signatures. For instance, the gene *Slit Guidance Ligand 2* (*SLIT2)* on chromosome 4, which displayed the highest absolute FC of 0.38 and the lowest FDR value (FDR=$1.38 \times 10^{-6}$), manifested a unique and significant upregulation specifically in excitatory neurons of layers 4 to 6, cluster 1 (Exc_L4-6_1, Figure 3.18c-d), despite not presenting the highest expression in that particular cell type (mean exp=0.32 vs. mean exp of 1.66 in basket cells [In_PVALB_Ba], Figure 3.18e). While prior research has implicated *SLIT2*, a glycoprotein in the Slit family known for its conserved role in axon guidance and neuronal migration in depression- and anxiety-like behavior in adult mice (Huang et al., 2020), its cell type-specific dysregulation in the human cortex has not been previously reported. Furthermore, *Potassium Voltage-Gated Channel Subfamily Q Member 3* (*KCNQ3*) on chromosome 8 stands out due to its unique significant downregulation in microglia (FDR=0.02), showing a FC of -0.25. This contrasts with its FCs in all other cell types, ranging between -0.05 and 0.15 (Figure 3.18f-g). *KCNQ3* also exhibits the highest expression specifically in microglia (mean exp=1.75, Figure 3.18h). While *KCNQ3* has been previously linked to the etiology of bipolar disorder in postmortem prefrontal cortex (Kaminsky et al., 2015), the specificity of its downregulation in microglia offers a novel insight.

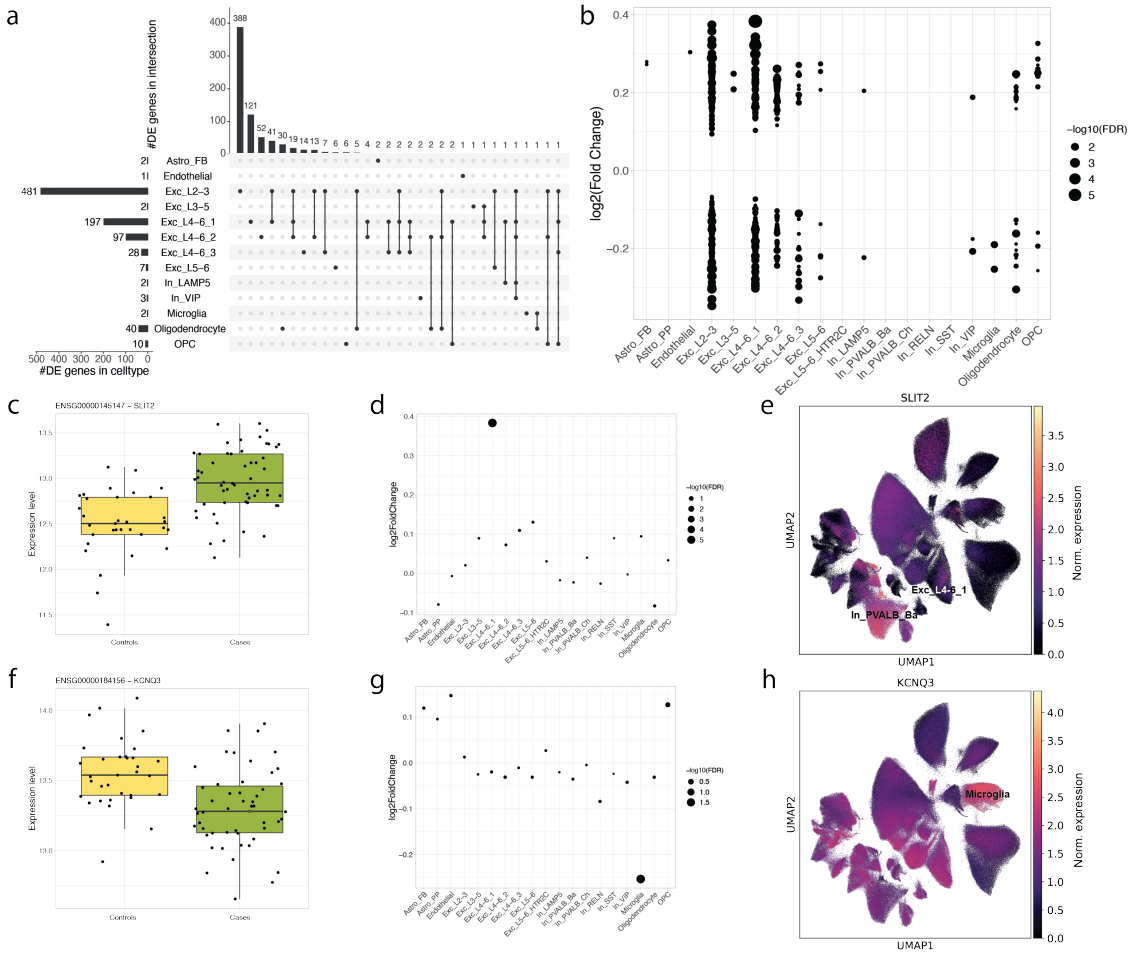


**Figure 3.18. Gene expression changes between psychiatric cases and controls.** (a) UpSet plot displaying the number of DE genes (FDR ≤ 0.1) for each cell type (left), as well as their overlap across cell types (right). (b) Dotplot illustrating the DE genes, with $\log_2$-fold change on the y-axis and dot size corresponding to -$\log_{10}$-transformed FDR values. (c) Boxplot of normalized gene expression levels of *SLIT2* in both controls and cases. (d) Dotplot representing the $\log_2$-fold changes of *SLIT2* across cell types, with dot size reflecting the -$\log_{10}$-transformed FDR values. (e) UMAP plot of snRNA-seq data colored according to the normalized expression levels of *SLIT2*. (f) Boxplot of normalized gene expression levels of *KCNQ3* in both controls and cases. (g) Dotplot representing the $\log_2$-fold changes of *KCNQ3* across cell types, with dot size reflecting the -$\log_{10}$-transformed FDR values. (h) UMAP plot of snRNA-seq data colored according to the normalized expression levels of *KCNQ3*.

The observed disparities in the count of DE genes per cell type motivated an assessment of whether the detection power varied due to the number of nuclei per cell type. Our observations confirmed that the quantity of DE genes for each cell type was indeed driven by the number of nuclei and the number of unique molecular identifier (UMI) counts (Figure 3.19a-b), which ultimately influences the number of genes tested for DE. When the nuclei per cell type were downsampled to the 75%, 50%, and 25% percentiles ($n_{nuclei}$=40,793, 31,504, 14,416, respectively), the disparity in the number of tested genes and DE genes between excitatory neurons and other cell types narrowed. Despite this, excitatory neurons consistently displayed the most DE genes (Figure 3.19c-d). Therefore, it is essential to consider that the extent of dysregulation in a cell type cannot be solely judged by the count of DE genes.

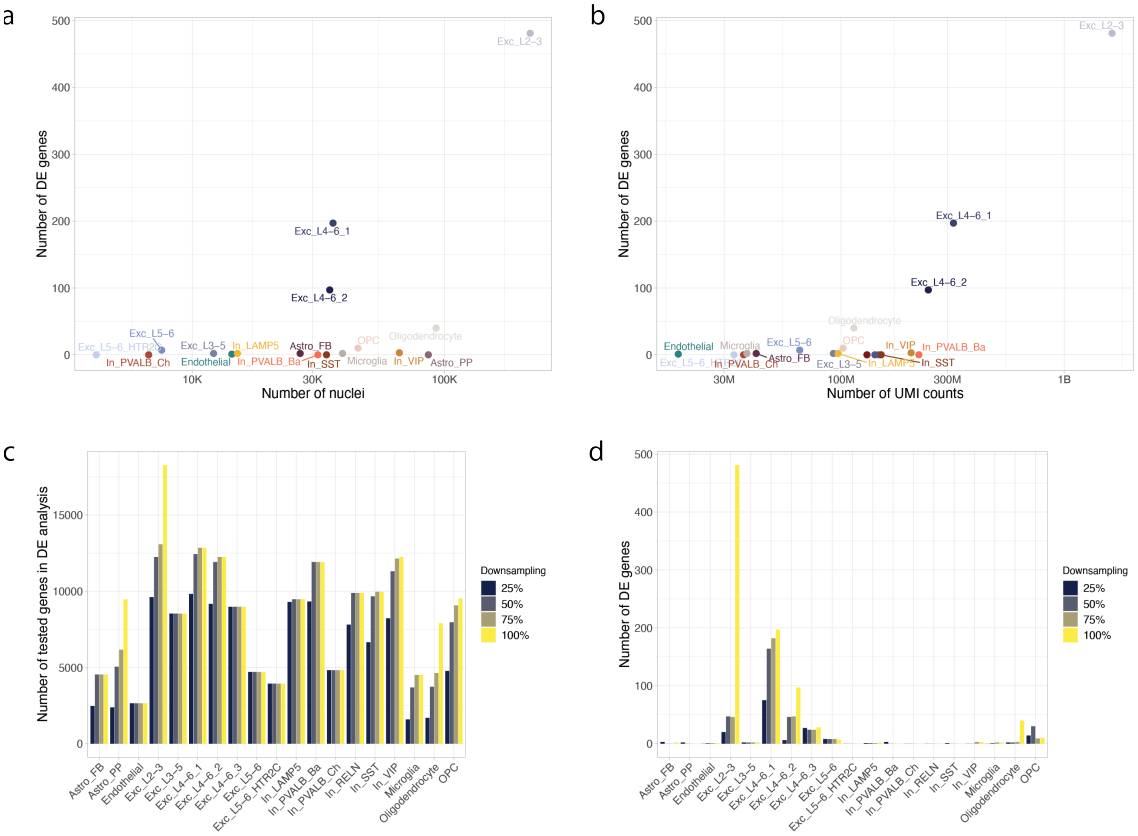


**Figure 3.19. Influence of nuclei count on detection power.** (a-b) Nuclei count (a) and the number of UMI counts (b) plotted against the number of DE genes (FDR ≤ 0.1) per cell type. Dot color indicates the cell type as coded above. (c-d) Barplot representing the number of genes tested for differential expression (c) and the number of significant DE genes (d) using the full dataset and datasets downsampled to the 75%, 50% and 25% percentile of nuclei per cell type which is indicated by color.

### 3.2.5 Transcriptomic Profiling Reveals Enrichment of Disease-Associated Pathways in Microglia

To gain insights into the underlying biological processes and functions perturbed by these DE genes within different cell types, we conducted an enrichment analysis of KEGG pathways in up- and downregulated genes within each cell type (Figure 3.20, see Methods 2.2.6.1). The notable presence of pathways such as long-term depression (FDR=0.04) and mechanisms of cellular interaction, including focal adhesion (FDR=0.04), among the downregulated genes in microglia was uniquely distinctive when compared to other cell types. Additionally, the analysis highlighted certain pathways involved in the nervous and endocrine systems (e.g., various synapses or endocannabinoid signaling) enriched among downregulated genes in specific cell types, including fibrous astrocytes (Astro_FB), chandelier cells (In_PVALB_Ch), and microglia. Various pathways related to neurodegenerative diseases, as well as oxidative phosphorylation, were found to be significantly enriched among both up- and downregulated genes in different cell types. The Ribosome pathway showed significant enrichment, particularly in upregulated genes in oligodendrocytes (FDR=$5.18 \times 10^{-29}$), alongside moderate enrichment in OPCs (FDR=$7.20 \times 10^{-7}$) and endothelial cells (FDR=$6.54 \times 10^{-11}$).

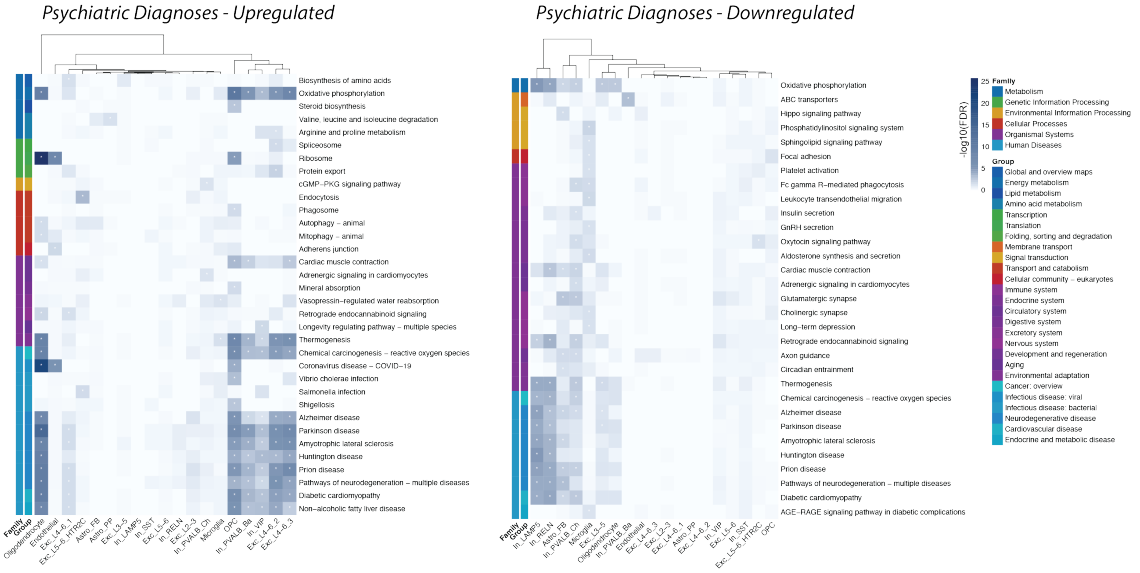


**Figure 3.20. Pathway enrichments among disease-related genes.** Heatmaps displaying the findings from KEGG pathway enrichment analysis conducted on the 250 most up- and downregulated genes for each cell type. The heatmap displays all pathways that have shown significant enrichment in at least one cell type. The intensity of color correlates with the -$\log_{10}$-transformed FDR values, with asterisks indicating significance (FDR ≤ 0.05). Pathway classifications are color-coded on the left of each heatmap to indicate the specific pathway group and family. K-means clustering dendrograms are provided to show how cell types group together based on their pathway enrichment profiles.

### 3.2.6 Comparison to Prior Research and Pseudobulk Analysis Endorses Disease-Related Findings

To evaluate the consistency of our results with previous studies, a correlation analysis was performed to compare effect sizes observed in our study against those reported by Ruzicka et al. (2022). We observed that the highest correlation in effect sizes typically occurred between matching cell types. For instance, the effect sizes of astrocytes in our analysis exhibited the strongest correlation with those of the astrocyte population in the Ruzicka et al. study (Figure 3.21a), suggesting a general alignment of our findings with those in previous studies.

From all DE genes identified across cell types in our study ($n_{genes}$=732 non-redundant), less than half (40%, $n_{genes}$=291) reached significance when assessed at the full pseudobulk level, aggregating the data across all cell types (see Methods 2.2.5.4). Of the DE genes identified from the full pseudobulk analysis ($n_{genes}$=511), 57% ($n_{genes}$=291) were also significant in at least one specific cell type (Figure 3.21b-c), underscoring the value of single-cell investigations.

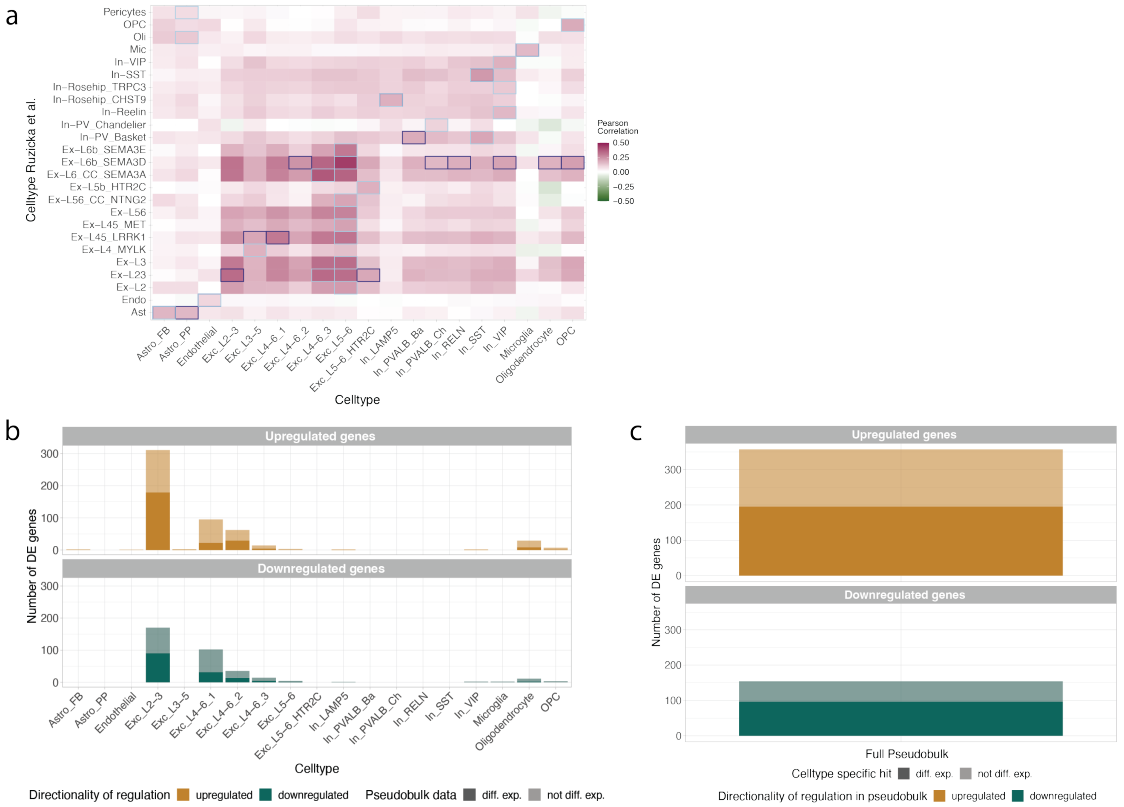


**Figure 3.21. Comparison of DE results with single-cell data on schizophrenia and full pseudobulk analysis.** (a) Heatmap displaying correlations between effect sizes from our study and those published in Ruzicka et al. (2022) for each cell type pair. Color gradient represents the Pearson correlation coefficient based on the effect sizes for genes tested in both studies in the respective cell types. Dark blue borders mark the highest correlation per column, while light blue borders mark the highest correlation per row. (b) Barplot visualizing the number of DE genes in each cell type, categorizing upregulation and downregulation, with the darker sections indicating the subset also found as DE in the full pseudobulk analysis. (c) Barplot visualizing the number of DE genes from the full pseudobulk analysis, categorized by upregulation and downregulation, with the darker sections indicating the subset of genes also found as DE in at least one specific cell type.

### 3.2.7 Signatures of Disease-Related Chromatin Accessibility Alterations Divergent from Gene Expression Patterns

Augmenting our DE results, we performed differential chromatin accessibility (DA) analysis between cases and controls at the gene score level across the different cell types ($n_{\text{cell types}}$=15). We discovered significant alterations in chromatin accessibility (FDR ≤ 0.1) in two subtypes of excitatory neurons (excitatory neurons layers 2 to 3 [Exc_L2-3], $n_{\text{genes}}$=46 and excitatory neurons layers 3 to 5 [Exc_L3-5], $n_{\text{genes}}$=1), as well as in protoplasmic (Astro_PP, $n_{\text{genes}}$=4) and fibrous astrocytes (Astro_FB, $n_{\text{genes}}$=5), as detailed in Figure 3.22a, Supplementary Table 22, and Online Table 34.

Focusing on genes that showed differential expression in the snRNA-seq data within specific cell types, a subset of these genes also exhibited significant changes in chromatin accessibility. The largest group was observed in excitatory neurons of layers 2 to 3 with 13 DE+DA genes (Figure 3.22b, and Online Table 35). For 8% of these genes ($n_{\text{genes}}$=2 out of 24), the analysis revealed contrasting patterns of regulation between the transcriptomic and epigenomic data (Supplementary Figure 4a). However, certain genes

displayed congruent regulatory patterns across both data sets. For instance, *Hes Family BHLH Transcription Factor 4* (*HES4)* in excitatory neuron layers 4 to 6, cluster 1 (Exc_L4-6_1), had FDR values of 0.04 (RNA) and 2.21x10$^{-3}$(ATAC) with FCs of -0.28 (RNA) and -0.43 (ATAC). Similarly, *Insulin-like growth factor-binding protein 5* (*IGFBP5)* in oligodendrocyte precursor cells (OPCs) showed FDR values of 1.70x10$^{-5}$ (RNA) and 0.08 (ATAC) with FCs of 0.33 (RNA) and 0.21 (ATAC). Figure 3.22c-d shows the genome tracks displaying the normalized ATAC signal for cases and controls near these genes. There was no observed overlap of DA genes across different cell types. Moreover, pathway enrichment analysis among the most up- and downregulated genes in each cell type indicated no significant enrichments for the majority of the cell types (Supplementary Figure 4b).

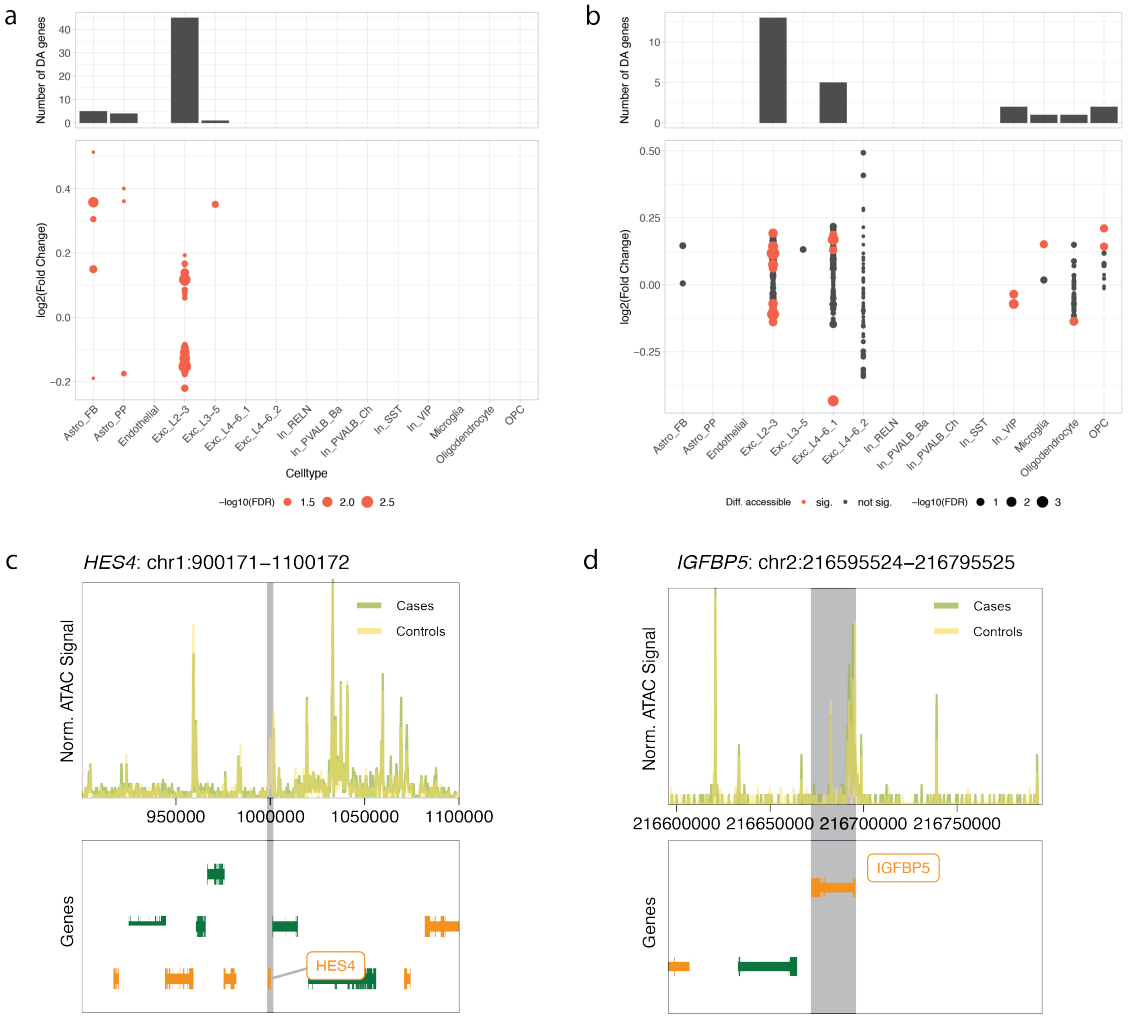


**Figure 3.22. Chromatin accessibility changes between psychiatric cases and controls.** (a-b) Findings from the differential accessibility analysis considering all genes passing filtering step (a) alongside those genes also DE (b). Barplot on top illustrates the count of significant DA genes (FDR ≤ 0.1) per cell type. Dotplot depicts the $\log_2$-transformed fold changes (FCs) for all tested, with color denoting DA significance and dot size corresponding to the -log10-transformed FDR value. (c-d) Genome tracks presenting the normalized ATAC signal in a 100kb around the gene body of *HES4* (c) and *IGFBP5* (d). *HES4* within excitatory neuron layers 4 to 6, cluster 1 (Exc_L4-6_1), observed FDR values were 0.04 (RNA) and 2.21x10$^{-3}$ (ATAC), with FCs of -0.28 (RNA) and -0.43 (ATAC). Likewise, *IGFBP5* in oligodendrocyte precursor cells (OPCs) exhibited FDR values of 1.70x10$^{-5}$ (RNA) and 0.08 (ATAC), with FCs of 0.33 (RNA) and 0.21 (ATAC).

### 3.2.8 Differential Transcriptomic and Epigenomic Patterns Related to Genetic Risk Highlight Variations in Chromatin Accessibility

To unravel the impact of genetic risk on gene expression and chromatin accessibility, independent of the clinical diagnosis, differences between donors at high and low genetic risk were examined. Polygenic risk scores (PRS), derived from summary statistics of several psychiatric GWAS studies (Cross-disorder phenotype (Consortium., 2019), schizophrenia (Trubetskoy et al., 2022), MDD (Howard et al., 2019), and bipolar disorder (Mullins et al., 2021)) and height (Yengo et al., 2022) as a non-psychiatric trait, were employed to capture each donor's overall genetic risk for these conditions (Online Table 32). Notably, even though cases displayed a significantly higher mean PRS compared to controls based on the cross-disorder, the MDD and the bipolar disorder GWAS ($p$ value ≤ 0.05 respectively, one-sided T-test), the score distributions are highly overlapping between controls and cases (Figure 3.23), highlighting that PRS can not pinpoint psychiatric diagnoses, but capture only the genetic predisposition for the actual disease. Instead of treating PRS as a continuum, we adopted an approach comparing extreme groups of the distribution, matched for covariates with propensity score matching (see Methods 2.2.5.2). Focusing on the extreme groups is an approach that has been demonstrated as reliable in previous studies (Andlauer & Nöthen, 2020; C. M. Lewis & Vassos, 2020).

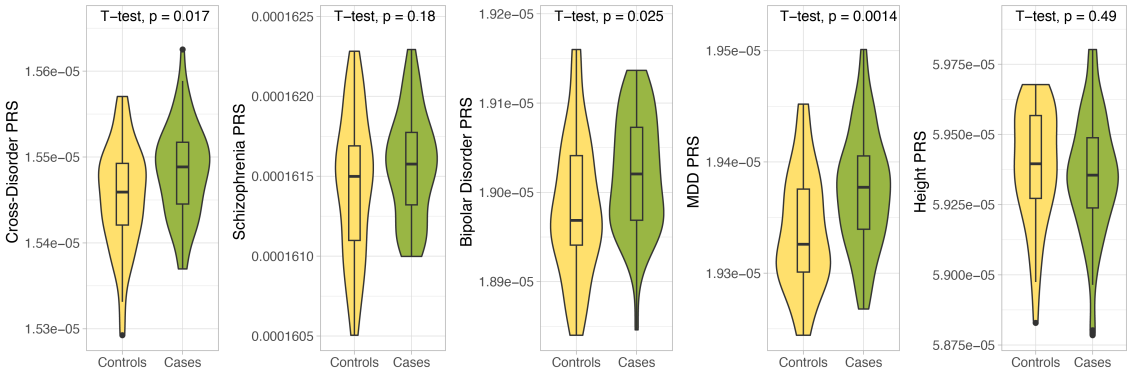


**Figure 3.23. Overlapping PRS distributions for psychiatric cases and controls.** Distribution of cross-disorder, schizophrenia, MDD, bipolar disorder, and height PRS for psychiatric controls and cases. *P* values derived from t-test to test for differences between cases and controls shown on top. A one-sided t-test was utilized for psychiatric PRS to test if the mean PRS of cases was significantly higher than the mean PRS of controls, while a two-sided t-test was utilized for height, as we did not assume a difference in the mean PRS between cases and controls.

Recognizing the need to assess genetic influences independent of clinical diagnosis, we analyzed the alterations in gene expression between high vs. low risk groups (DE risk genes). We detected significant DE risk genes in 3 to 10 of the 19 cell types for each GWAS trait studied (Figure 3.24a, and Online Table 36). In the fibrous astrocytes (Astro_FB), 54 DE risk genes were linked to the cross-disorder phenotype, with some additional hits across other cell types ($n_{genes}$=18 hits in 5 cell types). The majority of DE risk genes for bipolar disorder were prevalent in excitatory neurons ($n_{genes}$=32 out of 35 hits) and displayed some overlap with DE genes differentiating cases from controls ($n_{genes}$=3 out

of 35 hits, gray dots in Figure 3.24a). While genetic risk for schizophrenia was linked to alterations in various cell types ($n_{genes}$=17 hits in 7 cell types), genetic risk for MDD was associated with a lower count of DE risk genes ($n_{genes}$=7 hits in 3 cell types). The effect sizes of DE risk genes were more pronounced than those observed for genes associated with clinical diagnoses (median absolute $FC_{PRS}$=[0.29,0.55] vs. median absolute $FC_{diagnosis}$=[0.18,0.30] per cell type, see Supplementary Figure 5a). Notably, 3 DE risk genes associated with the genetic predisposition for height were identified in 3 distinct cell types, differing from those linked with psychiatric traits.

In an analysis focused on chromatin accessibility differences between extreme PRS groups, a substantial number of genes demonstrated differential accessibility (DA risk genes) across various cell types and GWAS traits (Figure 3.24b, and Online Table 37) with a total of 6,418 DA risk genes compared to 141 DE risk genes. These genes were predominantly identified in excitatory neurons of layers 2 to 3 (Exc_L2-3, $n_{genes}$=5,645 DA risk genes). Moreover, DA risk genes showed larger effect sizes than those DA genes associated with clinical diagnoses (median absolute $FC_{PRS}$=[0.15,0.74] vs. median absolute $FC_{diagnosis}$=[0.12,0.35] per cell type, see Supplementary Figure 5b). Although DA risk genes for height were found, only a single gene overlapped a DA risk gene for bipolar disorder. Despite the substantial number, the overlap between DA risk genes and DE risk genes was minimal (Figure 3.24b, gray dots). Only two genes, the hyperpolarization-activated cyclic nucleotide-channel (*HCN2)* and *IN080 complex subunit E (INO80E*), were identified as both DE risk gene (FCs=0.36 and 0.26, FDR=0.06 and 0.09 respectively) and DA risk gene (FCs=0.14 and 0.16, FDR=0.05 and 0.03 respectively) for the same GWAS trait (schizophrenia) and in the same cell type (Exc_L2-3). Genomic tracks of *HCN2* and *INO80E* depict different ATAC coverage contrasting the high and low schizophrenia risk groups (Figure 3.24c-d). *HCN2* is predominantly expressed in the heart and the nervous system, according to bulk GTEx data (Lonsdale et al., 2013) (Figure 3.24e), and contributes to pacemaker currents (Santoro et al., 1998). *INO80E* shows expression across all tissues in the GTEx data (Lonsdale et al., 2013) (Figure 3.24e), and is involved in ATP-dependent chromatin remodeling as well as DNA replication and repair processes (Conaway & Conaway, 2009).

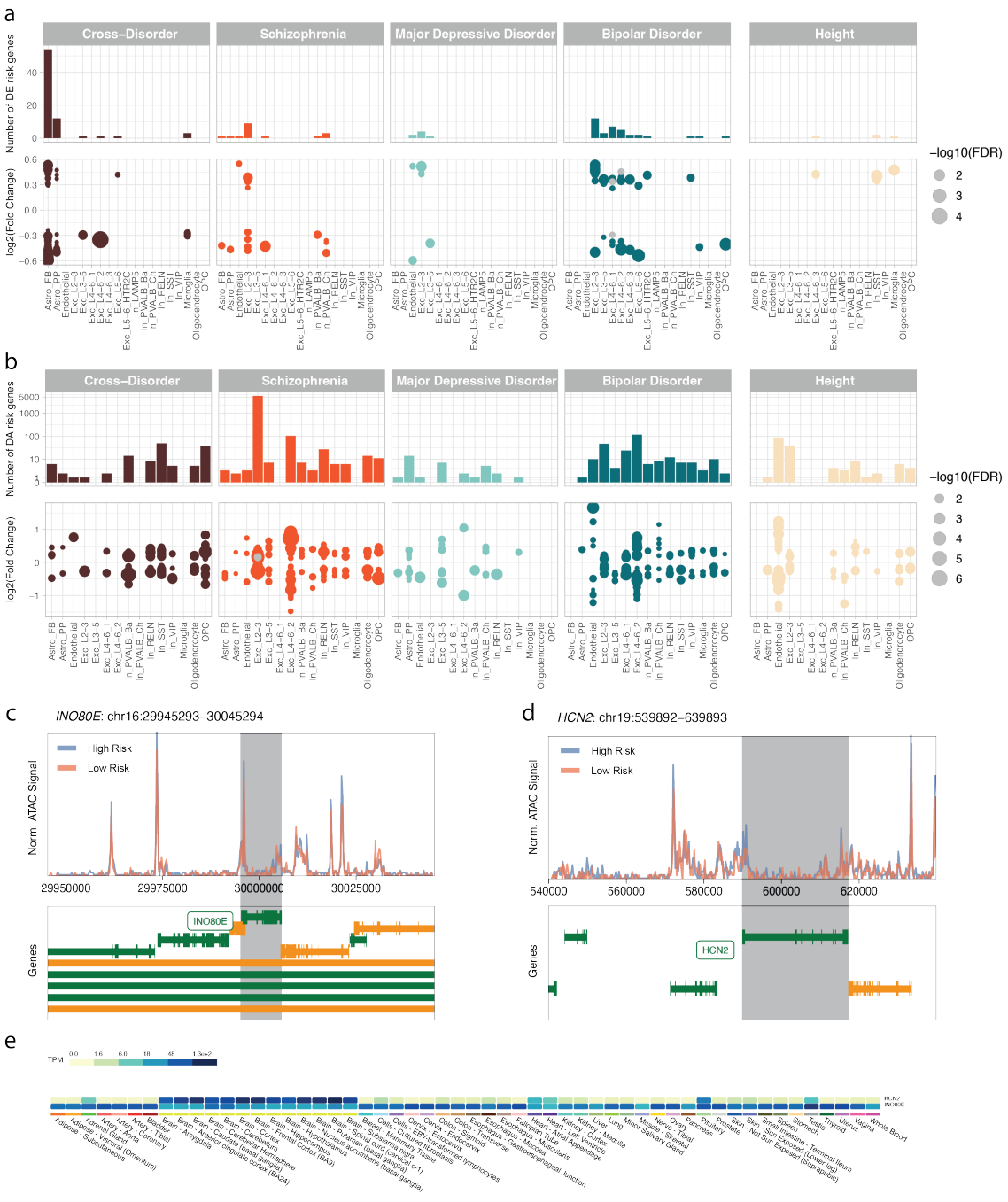


**Figure 3.24. Transcriptomic and epigenomic alterations linked to genetic risk.** (a-b) Findings from DE risk (a) and DA risk (b) analyses between donors with high and low genetic predisposition, as quantified by PRS informed by 5 different GWAS studies (cross-disorder, schizophrenia, MDD, bipolar disorder, and height). Barplots depict the number of significant DE and DA risk genes. Dotplots detail the significant DE/DA risk genes (FDR <= 0.1), with the color denoting the GWAS study and dot size corresponding to the -$\log_{10}$-transformed FDR values. In panel (a), gray dots represent DE risk genes were also identified as DE genes between cases and controls within the same cell type. In panel (b), gray dots represent DA risk genes that were also identified as DE risk genes within the same cell type. (c-d) Genome tracks illustrating normalized ATAC signal in a 100kb window around the gene body of *INO80E* (c) and *HCN2* (d). (e) Heatmap showing gene expression levels (i.e., transcript per million, TPM) for *HCN2* and *INO80E* across various human tissues, sourced from the GTEx database (Lonsdale et al., 2013).

### 3.2.9 Common Pathways Affected by Diagnosis and Genetic Risk

Despite the limited overlap of DE genes associated with psychiatric diagnoses and those associated with genetic risk for psychiatric conditions (DE risk genes), we observed a consensus of commonly affected pathways (Supplementary Figure 6). Across the different GWAS traits, including psychiatric phenotypes, and interestingly also height (included as a non-psychiatric reference), most pathways enriched in at least one cell type are related to human diseases or integral to organismal systems. The pathways influenced by genetic risk factors for psychiatric disorders often involve mechanisms within the endocrine and nervous systems. Across all examined traits, there was a predominant enrichment within endothelial cells and excitatory neurons. However, a distinct pattern emerges in microglia with upregulated genes linked to cross-disorder genetic risk (Supplementary Figure 6a), mirroring the pattern observed for psychiatric diagnoses. In particular, genes affected by genetic risk for schizophrenia, bipolar disorder, and MDD showed significant enrichment for signal transduction pathways (Supplementary Figure 6b-d).
When examining alterations in chromatin accessibility between groups of high and low genetic risk, only a few significant pathways emerged (Supplementary Figure 7). This suggests that the DA genes may participate in distinct biological processes rather than common pathways, but is most likely also influenced by the varying sizes of the gene sets used as backgrounds in our analyses.

### 3.2.10 Genetic Risk Impacts Gene Expression of GWAS Loci

To investigate if DE risk genes for certain traits and cell types show an association with genes implicated in psychiatric disorders via GWAS, specifically bipolar disorder (Mullins et al., 2021), MDD (Howard et al., 2019), and schizophrenia (Trubetskoy et al., 2022), we performed a GWAS enrichment analysis using H-MAGMA (Sey et al., 2020). The results revealed no notable enrichment of GWAS-associated genes within the DE genes for psychiatric diagnoses and the DE genes linked to genetic risk for cross-disorder phenotype, bipolar disorder, MDD, and height (Figure 3.25a-b,d-f). Yet, significant enrichment was observed for schizophrenia GWAS-associated genes in the DE risk genes specifically for schizophrenia among basket cells (In_PVALB_Ba), excitatory neurons layers 2 to 3 (Exc_L2-3), and endothelial cells (Figure 3.25c). Endothelial cells also displayed a marked enrichment for MDD GWAS-associated genes within their DE risk genes for schizophrenia. This observation indicates that genes associated with significant genetic variants identified in GWAS are also affected in their expression levels in certain cell types by the overall genetic predisposition.

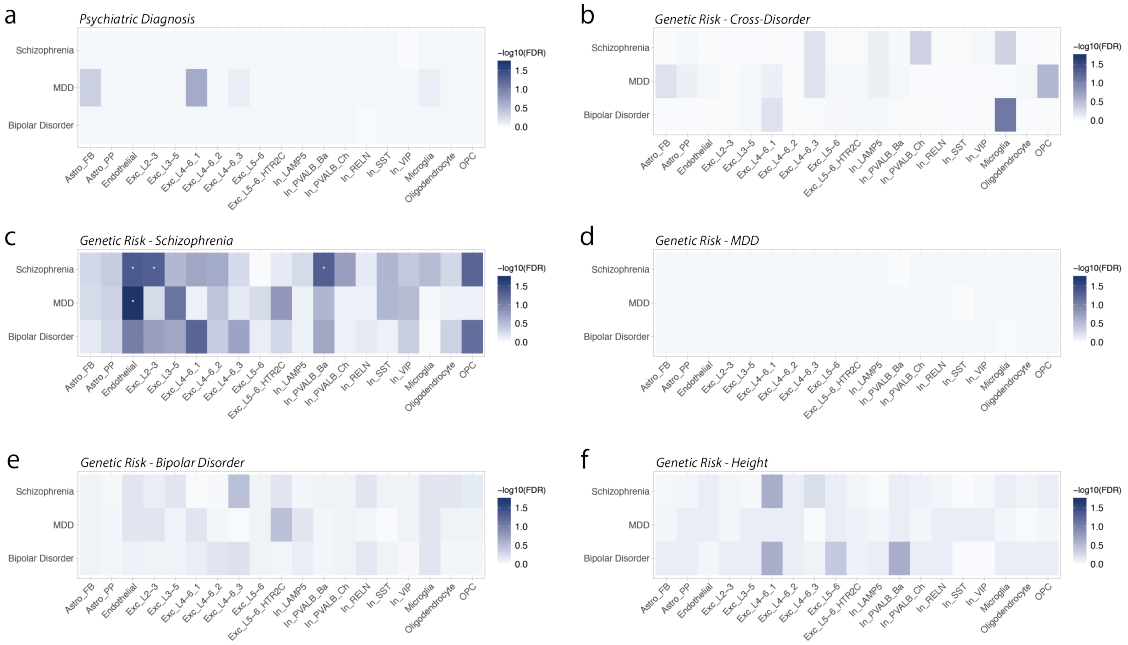


**Figure 3.25. GWAS enrichment in DE genes and DE risk genes.** (a-f) Results of GWAS enrichment analysis in DE genes for psychiatric diagnosis (a), cross-disorder DE risk genes (b), schizophrenia DE risk genes (c), MDD DE risk genes (d), bipolar disorder DE risk genes (e) and height DE risk genes (f) using H-MAGMA for GWAS hits of bipolar disorder, major depressive disorder and schizophrenia. Color indicates -$\log_{10}$-transformed FDR values and asterisks indicate significance (FDR ≤ 0.05).

### 3.2.11 Genetic Risk for Schizophrenia Modulates *INO80E* and *HCN2* Regulation in Excitatory Neurons in Cortical Layers 2/3

*INO80E*, a gene with known association to schizophrenia from prior genomic studies including GWAS, transcriptome-wide association analysis (TWAS), and copy number variation (CNV) analyses (Gusev et al., 2018; Lago & Bahn, 2022; Z. Li et al., 2017; Marshall et al., 2017; Ripke et al., 2014), has emerged as significant in our differential analyses between schizophrenia risk groups (DE and DA risk gene, Figure 3.24b and Figure 3.26a-b) in excitatory neuron of layers 2 to 3 (Exc_L2-3). As one of only two such genes, *INO80E* demonstrated differential expression and accessibility specifically in this cell type but was not differentially regulated in any other cell type (Figure 3.26c).

To gain a deeper understanding of the regulatory mechanisms of *INO80E* across various cortical cell types, we conducted a comprehensive analysis that integrated gene expression, chromatin accessibility, and dysregulation between schizophrenia risk groups. We inferred a correlation-based network, incorporating gene expression and chromatin accessibility across various cell types, PRS for cross-disorder phenotypes, bipolar disorder, MDD, schizophrenia, and height, as well as the disease status (Figure 3.26d). The network reveals that nodes within the same node family (like PRS for various disorders or gene expression across cell types) tend to exhibit positive correlations. However, correlations between different node families are predominantly negative. Of particular note, *INO80E*'s gene score in excitatory neurons of layers 2 to 3 (Exc_L2-3)

correlates with both cross-disorder and schizophrenia PRS, while its gene expression in this cell type exhibits correlation below nominal significance, despite being identified as a significant DE risk gene.

To understand the key transcriptional drivers influencing *INO80E* and identify the regulatory elements governing the observed expression and accessibility changes, we performed a transcription factor motif enrichment analysis within its promoter region. We observed a significant enrichment of the *KLF4* transcription factor motif (Supplementary Table 23, Figure 3.26e), which has a prior association with downregulation in schizophrenia. Interestingly, *KLF4* neither shows expression nor accessibility levels above the set threshold in excitatory neurons of layers 2 to 3 (Exc_L2-3).

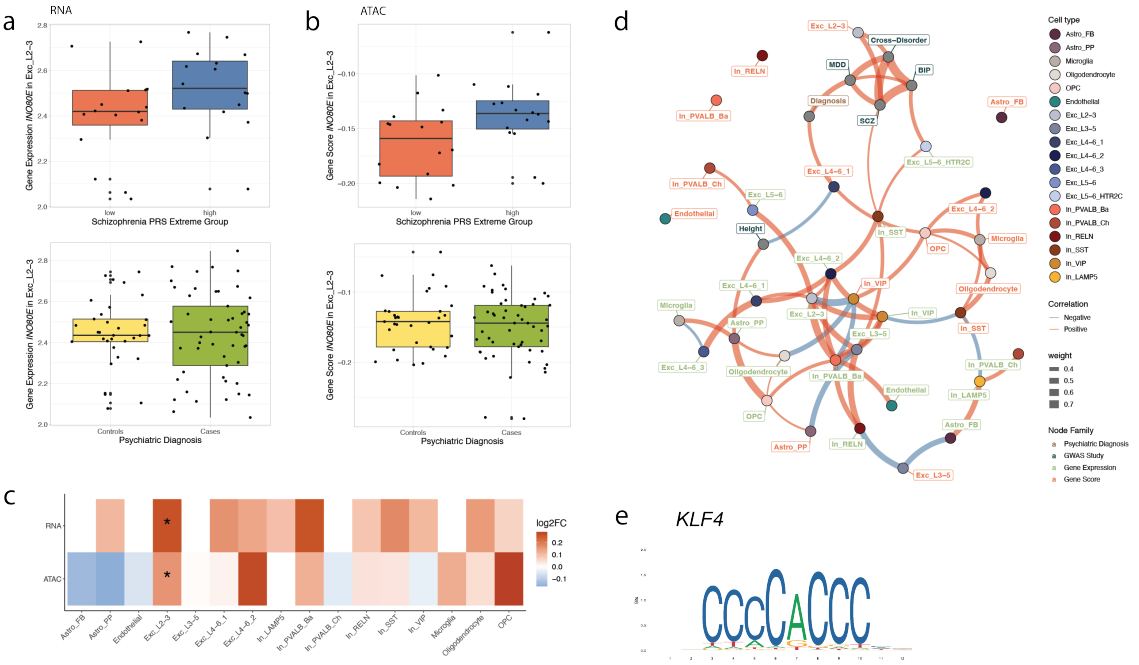


**Figure 3.26. Cell type-specific patterns of gene regulation of *INO80E* in relation to schizophrenia genetic risk.** (a-b) Boxplots depicting gene expression (a) and chromatin accessibility (b) levels of *INO80E* for high and low genetic risk groups for schizophrenia and according to psychiatric diagnosis. (c) Heatmap illustrating $\log_2$-fold changes of *INO80E* from both DE and DA risk analyses related to schizophrenia, with asterisks denoting significance (FDR ≤ 0.1). (d) Correlation-based network inferred from PRS for cross-disorder phenotypes, bipolar disorder, MDD, schizophrenia and height, alongside psychiatric diagnosis, gene expression, and gene scores across different cell types. Edges represent all nominally significant correlations ($p$ value ≤ 0.05). Nodes are colored according to their cell type, with node label colors indicating the node family/data modality, edge width relating to the correlation strength, and edge color reflecting whether the correlation is positive or negative. This network is characterized by predominantly positive correlations within the same data modality (e.g., PRS across various disorders or gene expression levels across cell types), but primarily negative correlations occur between different data modalities. (e) Transcription factor binding motif for *KLF4*, obtained from the JASPAR database (Fornes et al., 2020).

*HCN2*, a gene encoding a hyperpolarization-activated cation channel plays an important role in the generation of native pacemaker activity in the heart and the brain, exhibited differential expression and accessibility (DE and DA risk gene) in excitatory neurons layers of 2 to 3 between low and high risk groups for schizophrenia as well (Figure 3.24b and Figure 3.27a-b). No significant dysregulation of gene expression or chromatin

accessibility was observed within any other cell type (Figure 3.27c). The correlation-based network for *HCN2*, integrating levels of gene expression and chromatin accessibility across various cell types, PRS for cross-disorder phenotypes, bipolar disorder, MDD, schizophrenia, and height, as well as disease status (Figure 3.27d), shows more positive correlations between node families than the *INO80E* integration. Gene scores of *HCN2* in excitatory neurons of layers 2 to 3 (Exc_L2-3) are positively correlated with PRS for bipolar disorder, while gene expression of *HCN2* in Exc_L2-3 are positively correlated with gene expression in other populations of excitatory neurons and negatively correlated with gene score in VIP and SST interneurons (In_VIP and In_SST). Transcription factor motif analysis within the *HCN2* promoter region revealed significant enrichment of numerous transcription factor motifs (Supplementary Table 23), with the most significant ones for *MAZ* (Figure 3.27e) and *ZNF148* (Figure 3.27f). The two respective genes are expressed and accessible in excitatory neurons of layers 2 to 3, as they are in the majority of cell types.

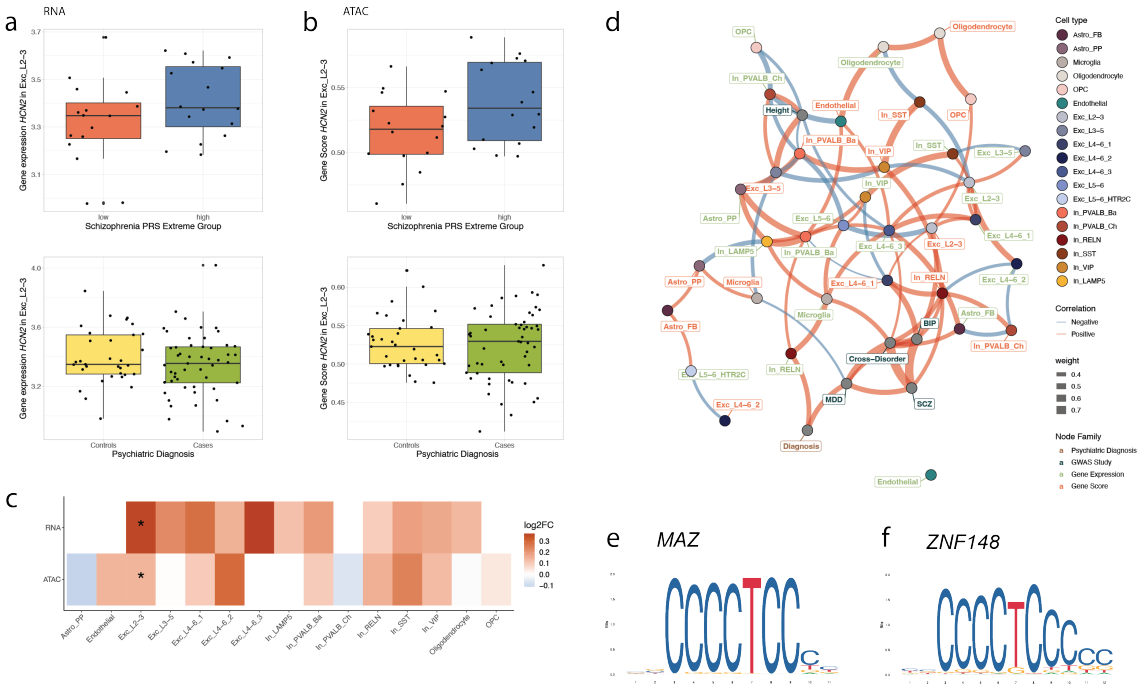


**Figure 3.27. Cell type-specific patterns of gene regulation of *HCN2* in relation to schizophrenia genetic risk.** (a-b) Boxplots depicting gene expression (a) and chromatin accessibility (b) levels of *HCN2* for high and low genetic risk groups for schizophrenia and according to psychiatric diagnosis. (c) Heatmap illustrating $\log_2$-fold changes of *HCN2* from both DE and DA risk analyses related to schizophrenia, with asterisks denoting significance (FDR ≤ 0.1). (d) Correlation-based network inferred from PRS for cross-disorder phenotypes, bipolar disorder, MDD, schizophrenia and height, alongside psychiatric diagnosis, gene expression, and gene scores across different cell types. Edges represent all nominally significant correlations ($p$ value ≤ 0.05). Nodes are colored according to their cell type, with node label colors indicating the node family/data modality, edge width relating to the correlation strength, and edge color reflecting whether the correlation is positive or negative. (e-f) Transcription factor binding motif for *MAZ* (e) and *ZNF148* (f), obtained from the JASPAR database (Fornes et al., 2020).

## 3.3 Cross-Species Transcriptional Dysregulation: Distinct Patterns in Mouse PFC Stress Response and Cell Types of Human PFC in Psychiatric Disorders

We performed a comparative analysis aiming to understand the relationship between gene expression alterations in the mouse PFC following glucocorticoid treatment and the cell type-specific gene expression changes observed in the human postmortem OFC associated with psychiatric diagnoses. Our goal was to discern whether the same genes dysregulated by GR activation in the mouse PFC also show dysregulation in the human postmortem OFC within psychiatric contexts.

Upon mapping mouse genes to their human orthologs and analyzing the overlap of DE genes, we discovered that only a minority of cell type-specific DE genes for psychiatric diagnoses were also DE following GR activation in the mouse model (Figure 3.28). Specifically, out of the cell type-specific DE genes ($n_{genes}$=732 non-redundant DE genes), only 47 were DE in the mouse ($n_{genes}$=920 DE genes in total in mouse PFC), with 30 of these exhibiting regulation in the same direction (Supplementary Table 24). Notably, a substantial number of the cell type-specific psychiatric DE genes ($n_{genes}$=287 genes) were not assessed in the mouse PFC, predominantly due to either very low expression levels or because the human DE genes lacked mouse orthologs (using Biomart (Durinck et al., 2005), December 2021). Out of the 920 DE genes identified in the mouse PFC, 102 were not even tested for differential expression in the human OFC, due to low expression levels.

This modest overlap was not entirely unexpected, given that even within our broader pseudobulk analysis, we observed a limited concurrence between full pseudobulk DE genes and cell type-specific DE genes, despite being derived from the same dataset. The bulk RNA-seq data from our mouse study potentially masks cell type-specific signals, and single-nucleus sequencing data might lack the power to detect many dysregulated genes due to its sparsity.

Among the shared genes, notable examples include *FKBP5*, which was upregulated in both the mouse PFC and the excitatory neurons in layers 2/3 (Exc_L2-3) of the human OFC. *FKBP5*, coding for the protein FKBP51, is a co-chaperone of heat shock protein 90 (Hsp90) and can modulate GR, affecting the HPA axis regulation (Binder, 2009). Elevated *FKBP5* expression levels can reduce GR sensitivity and might impair the HPA axis's negative feedback efficiency (Pariante & Miller, 2001). The pathogenic role of *FKBP5* in psychiatric disorders has been shown consistently in prior research, with increased expression levels across different subregions of the PFC (Matosin et al., 2023; Seifuddin et al., 2013; Sinclair, Fillman, Webster, & Weickert, 2013) and an association of such increased expression levels with psychiatric-like phenotypes in mouse models (C. Engelhardt et al., 2021; Hartmann et al., 2015).

Additionally, *RASD1*, coding for the "Dexamethasone inducible Ras-related protein 1", was upregulated across both excitatory neurons of layers 2/3 and layers 4 to 6, cluster 1 (Exc_L2-3 and Exc_L4-6_1), as well as in the mouse PFC. Glucocorticoids are known to increase expression levels of *RASD1* in the hypothalamus (Greenwood et al., 2016), while our findings implicate the same for the PFC. The gene is also implicated in the negative

feedback loop controlling ACTH secretion (Brogan, Behrend, & Kemppainen, 2001) as part of the HPA axis.

In contrast, *SLIT2*, the gene with the highest absolute fold change in gene expression between psychiatric cases and controls across all cell types (see Results 3.2.4), displayed opposite regulation trends. It exhibits downregulation in the mouse while being upregulated in human excitatory neurons of layers 4 to 6, cluster 1 (Exc_L4-6_1). Interestingly, a divergent expression pattern of *SLIT2* has been observed in a study of prion disease in mice, with upregulation observed in a neuronal cluster and downregulation in astrocytes (Slota, Sajesh, Frost, Medina, & Booth, 2022). An ovarian cancer study showed that gene expression levels of *SLIT* and *ROBO* genes, including *SLIT2*, can be elevated by a reduction of GR expression (Dickinson, Fegan, Ren, Hillier, & Duncan, 2011).

These findings emphasize the intricate nature of gene regulation under psychiatric conditions and GR activation, highlighting both congruent and divergent patterns across species and the potential for distinct regulatory mechanisms at play during acute stress and in the etiology of psychiatric disorders.

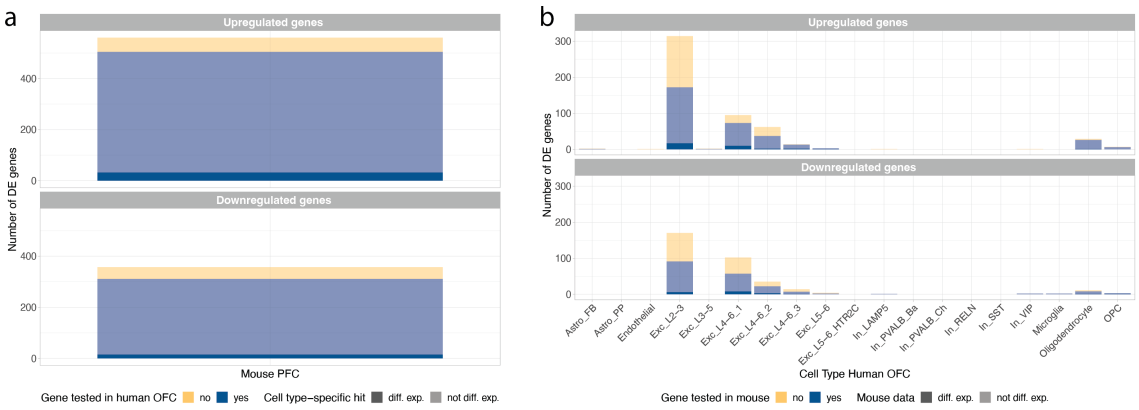


**Figure 3.28. Overlap of dysregulated genes following GR stimulation in mouse PFC and dysregulated genes in psychiatric disorders in cell types of human OFC.** (a) Barplot visualizing the number of up- and downregulated genes following GR stimulation in mouse PFC. Blue portions of the bars represent genes that were also tested for DE in at least one cell type of human OFC. Dark blue portions represent genes identified as DE in at least one cell type of human OFC. (b) Barplot visualizing the number of up- and downregulated genes in psychiatric disorders in cell types of human OFC. Blue portions of the bars represent genes that were also tested for DE in mouse PFC. Dark blue portions represent genes identified as DE in mouse PFC.

# 4 Discussion

In this thesis, I have endeavored to elucidate the intricate molecular mechanisms and alterations that orchestrate the stress response and the etiology of stress-related disorders by employing a diverse array of methodologies and data derived from different biological platforms. Specifically, the outlined research includes a brain region-specific transcriptomic analysis of the stress response utilizing a mouse model. This project has demonstrated the utility of differential network analysis, beyond the gene-level analysis, in uncovering biological processes involved in the response to glucocorticoid receptor activation. The culmination of this research project is the establishment of a publicly available resource, offering an accessible and user-friendly platform for the exploration of differential expression and networks of interest. Further, I have investigated the cell type-specific molecular alterations in the orbitofrontal cortex associated with psychiatric disorders, using postmortem brain tissue, where molecular profiling was conducted on approximately 800,000 cells with single-nucleus RNA-seq and 400,000 cells with single-nucleus ATAC-seq from a cohort of 92 donors. This substantial dataset enabled a comprehensive analysis of the deviations in gene expression and chromatin accessibility between psychiatric cases and controls within 19 and 15 distinct cell types, respectively. The comparative analysis highlighted more pronounced transcriptomic alterations in psychiatric cases versus controls when contrasted with variations in chromatin accessibility, as well as more substantial changes in chromatin accessibility distinguishing individuals with high versus low genetic risk for psychiatric disorders than the differences observed in gene expression.
Here, I discuss the concordance of our findings with previous research and elucidate their contribution to the expansion of current knowledge, and acknowledge their limitations.

## 4.1 Transcriptional Response to Glucocorticoid Exposure in the Brain

A major part of this thesis presents the results of a study in which we used a mouse model for glucocorticoid receptor stimulation to provide a detailed transcriptomic profiling across 8 brain regions, including the prefrontal cortex, amygdala, paraventricular nucleus of the hypothalamus, cerebellum, and four hippocampal subregions (ventral and dorsal *cornu ammonis* 1, ventral and dorsal dentate gyrus). The extensive dataset derived from these brain regions has revealed differential network analysis to be an indispensable tool that, when combined with differential expression analysis, offers a more comprehensive understanding of the transcriptomic intricacies elicited by glucocorticoid receptor activation. This approach enables the exploration of the complex biological processes at play during stress response, both across and within each brain region. The creation of the resource DiffBrainNet enables researchers to delve into molecular pathways crucial to basal functionality and glucocorticoid responses in a brain region-specific manner.

The complementation of differential expression with differential network analyses has augmented our understanding of the transcriptomic response to glucocorticoid stimulation, revealing complementary insights that neither approach could provide alone. For instance, in the prefrontal cortex, differentially expressed genes were primarily associated with signaling and development, whereas hub genes and their neighboring nodes in the differential network were linked to cellular responses to stimuli.

Notably, *Abcd1* emerged as a top differential hub gene within the prefrontal cortex network, despite not being listed among the differentially expressed genes of this brain region. *Abcd1* is part of the ATP-binding cassette (ABC) proteins, which have been recognized for their role in facilitating the transport of dexamethasone across the blood-brain barrier and placenta (Müller et al., 2003; Uhr, Holsboer, & Müller, 2002) and in synaptic function and psychiatric conditions (Gong et al., 2017; Lopez et al., 2021). A deficiency in *Abcd1* within microglia has been correlated with synaptic and axonal degradation, highlighting the importance of the gene in synaptic signaling (Gong et al., 2017). Another transporter in the ABC family, *Abcb1*, is associated with stress response and could potentially influence stress-related psychiatric disorders (Lopez et al., 2021). These findings highlight that the differential network analysis can identify additional, complementary molecular pathways beyond the aspects captured by gene-level analyses.

Additionally, network analysis serves as a powerful tool for generating and testing hypotheses regarding specific genes when an appropriate prior network is selected. In the case of *Tcf4*, a gene implicated in psychiatric risk, we utilized DiffBrainNet to assess the impacts of dexamethasone on *Tcf4* coexpression networks across different brain regions. *Tcf4*'s expression in the cortex, the hippocampus, and the hypothalamic and amygdaloid nuclei is pronounced at the end of prenatal development and decreases to moderate levels during adult life (Teixeira et al., 2021). It plays a crucial role in the maintenance and proliferation of neural progenitor cells (Mesman, Bakker, & Smidt, 2020). Functional modifications in *Tcf4* through animal model studies have underscored its role in cognitive processes, sensorimotor gating, and neuroplasticity (Badowska et al., 2020). Although interactions between *Tcf4* and psychosocial stress have been observed (Volkmann, Stephan, Krackow, Jensen, & Rossner, 2021), there is limited understanding of the specific molecular pathways and brain regions involved. Our analysis has determined that *Tcf4* is involved in the modulation of glucocorticoid effects within two hippocampal subregions, the ventral and dorsal dentate gyrus, evident both in gene expression and network dynamics. However, in the prefrontal cortex, *Tcf4*'s role emerges only within network-level differences, not on the single-gene level. The *Tcf4* network in the prefrontal cortex shows enrichment for autophagy-related functions, aligning with past literature connections between *Tcf4* and autophagic processes (Petherick et al., 2013). However, to the best of our knowledge, this novel link to stress-related autophagy regulation has not been reported before.

The prefrontal cortex stands out in our study as the brain region with the highest number of differentially expressed genes (920 genes) and a high percentage of unique

differentially expressed genes (26.6%), which is consistent with its advanced complexity and extensive study in psychiatric research. Even so, the dorsal dentate gyrus showed the highest number of hub genes (313 genes) and the prefrontal cortex exhibits the highest percentage of unique hub genes together with the amygdala (9.9% each), even though these proportions did not differ too much between all brain regions. This finding suggests a comparable degree of interconnected changes across the different brain regions.

Our methodological approach in this study presents several strengths along with inherent limitations. A primary strength lies in our ability to overcome the challenge of comparing networks across conditions, which is typically constrained by node degree and heavily influenced by the chosen threshold for network analysis. Here, we inferred a differential network by utilizing a two-step method: initially, we inferred prior knowledge-based treatment and control networks using KiMONo (Ogris et al., 2021), followed by the computation of a differential network with DiffGRN (Kim Youngsoon, 2018). This strategy enabled us to focus on differential interactions rather than mere gene comparisons.
One of the key strengths of our method is the alignment of treatment and control networks in terms of their topological layout, achieved by leveraging prior information about potential gene connections. This approach enables a robust and reliable calculation of z-values within the differential network. The method we employ for network inference is informed by prior knowledge rather than correlations, enabling a focused identification of gene interactions through the integration of established functional associations, including transcription factor binding sites, subcellular colocalization, and protein-protein interactions. We utilized the repository of functional associations provided by FunCoup 5 (Persson et al., 2021) to build upon these established connections, thereby substantially reducing the likelihood of false positive findings. Nevertheless, our methodology remains versatile, allowing researchers to source prior knowledge from an array of databases, which can be precisely tailored to address specific research questions.
However, one limitation of our methodology is the inherent bias that network metrics such as node degree, betweenness, and modularity can exhibit due to the influence of the prior network. To address this, we normalized the node-betweenness by dividing the betweenness in the differential network by the betweenness in the prior network, thus attempting to mitigate bias and improve the interpretability of our network metrics.

The ShinyApp resource (http://diffbrainnet.psych.mpg.de/) allows for an in-depth exploration of the transcriptional landscape across these brain regions under various conditions (Figure 4.1). This platform is designed to facilitate the research community's access to these findings, offering functionalities for searching differentially expressed genes, visualizing networks, and comparing hub genes across different treatment levels. Additionally, it provides options for users to download both the data and the corresponding visualizations. This accessible and comprehensive database is an invitation for researchers to extend and apply our findings to novel experimental designs targeting the molecular mechanisms underlying stress response and associated disorders.

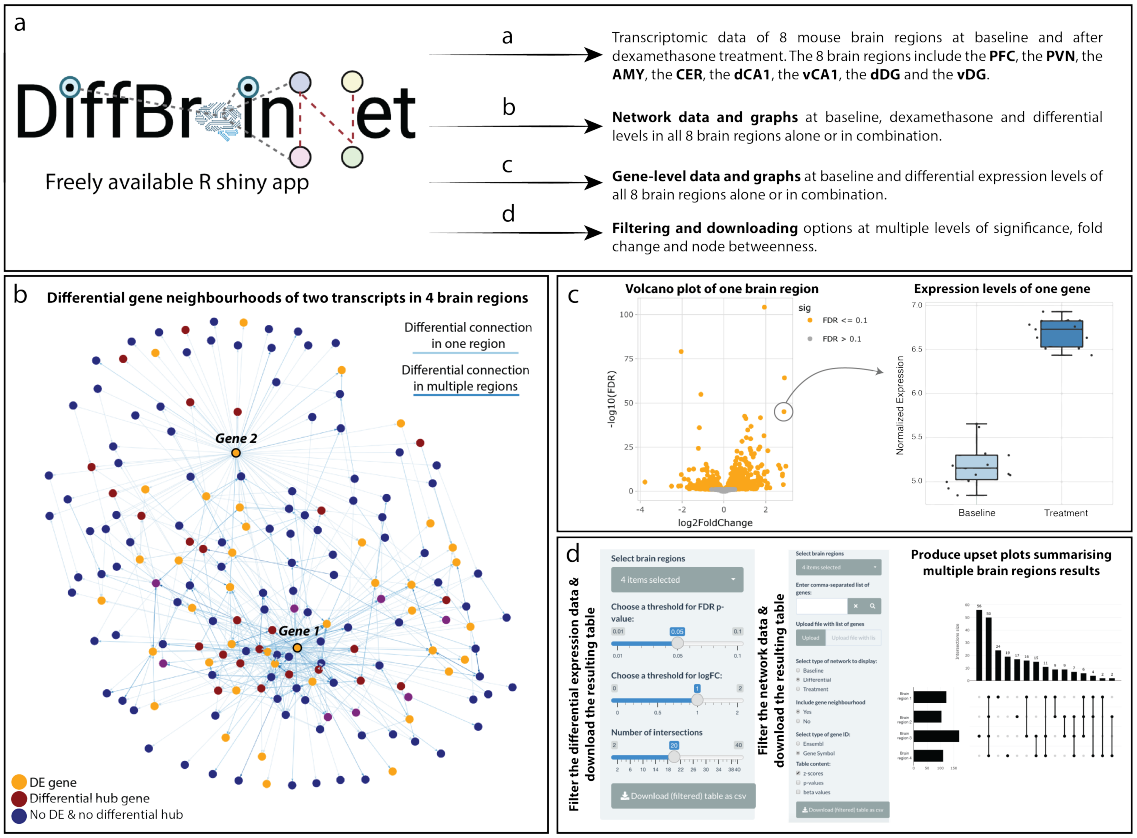


**Figure 4.1. DiffBrainNet: a resource of gene expression and network data for 8 mouse brain regions.** (a) DiffBrainNet compiles gene expression and network data across 8 mouse brain regions at vehicle, dexamethasone and differential levels. (b) The resource offers network data for all brain regions, both individually and collectively, under vehicle, treatment, and differential conditions, with the option to download and visualize the data interactively in the application. (c) It also catalogues gene expression data for all brain regions, with features to download and visualize the data within the application. (d) The tool allows users to tailor downloads to their research needs, providing customizable filters for significance, fold change, and node-betweenness in both network and gene expression data.

## 4.2 Multi-modal Analysis of Psychiatric Disorders and Genetic Risk in Cortical Cell Types

In another major part of this thesis, I present the results of single-nucleus postmortem analyses, specifically within the orbitofrontal cortex of a transdiagnostic psychiatric cohort. An extensive collection of roughly 800,000 and 400,000 nuclei has been analyzed, via single-nucleus RNA-seq and ATAC-seq respectively, involving detailed molecular profiling at the level of gene expression and chromatin accessibility in 19 and 15 distinct cell types. Beyond differential analyses between cases and controls, I studied the molecular alterations between high and low genetic risk groups. Although there was minimal overlap in terms of differentially expressed and accessible genes in diagnostic and genetic risk analyses, a consensus of commonly disrupted biological pathways was observed. Notably, differences in gene expression were predominantly linked to psychiatric diagnoses and alterations in chromatin accessibility were linked to genetic risk rather than diagnosis.

In this study, we followed a **transdiagnostic approach**, thereby building upon previous research that identified shared disease-related signatures between major psychiatric disorders and how these signatures reflect genetic risk (Gandal, Haney, et al., 2018; Lynall et al., 2022; Patrick F. Sullivan & Geschwind, 2019). We studied psychiatric disorders as a cross-disorder phenotype, including donors diagnosed with schizophrenia, schizoaffective disorder, bipolar disorder, and MDD, hypothesizing that molecular alterations mapping onto shared symptoms across disorders could effectively inform personalized medicine in psychiatry. We uncovered shared transcriptomic and epigenomic alterations in major psychiatric disorders, an endeavor not previously conducted at the single-cell level for a transdiagnostic phenotype, despite a bias towards schizophrenia in our cohort.

While reductions in the number of cortical glial cells and inhibitory neurons have been reported in MDD, bipolar disorder and schizophrenia in earlier research (Benes, McSparren, Bird, SanGiovanni, & Vincent, 1991; Cotter, Pariante, & Everall, 2001; Ongür, Drevets, & Price, 1998; Rajkowska et al., 1999), our study did not mirror these findings (Figure 3.13d-e). However, more recent single-cell sequencing and confocal microscopy studies did not observe such **differences in cell type proportions** either (Enwright et al., 2016; Ruzicka et al., 2022).

Our investigation of the **correlation between gene expression and chromatin accessibility** revealed an overall, though not universal, positive correlation. This was in line with the general understanding that open chromatin states in promoter regions facilitate transcription (Reske et al., 2020; Tsompana & Buck, 2014). While there was an overall trend of positive correlation at the cell type level, many genes did not have a peak indicative of open chromatin nearby (Figure 3.14), and the positive correlation within a cell type was often small when the cell type-specific signals were not present in the data (Figure 3.17). The observed low correlations within cell types could be due to distal and *trans*-regulatory elements, such as enhancers and silencers, that are not captured with our gene score-based approach, or other epigenetic modifications regulating gene expression, including histone acetylation and methylation (de la Torre-Ubieta et al., 2018; Natarajan et al., 2012). In addition, the absence of peaks in chromatin accessibility for many genes could be caused by data sparsity, which current technologies cannot sufficiently address (Baek & Lee, 2020).

Through the assessment of **differential expression between psychiatric cases and controls**, we identified differentially expressed genes in a variety of cell types (875 genes across 13 cell types), with a specifically high number in excitatory neurons which aligns with findings from previous single-cell transcriptomic studies of schizophrenia and MDD (Nagy et al., 2020; Ruzicka et al., 2022). However, it is crucial to acknowledge the differences in nuclei count and genes tested per cell type that drive the number of differentially expressed genes detected, as confirmed by the downsampling of nuclei (Figure 3.19). We observed cell type-specific alterations in genes previously implicated in psychiatric disorders, such as *SLIT2* and *KCNQ3* (Huang et al., 2020; Kaminsky et al., 2015). *SLIT2* has been shown to be associated with depression- and anxiety-like behavior (Huang et al., 2020) as well as the development of serotonergic and dopaminergic

circuits in the forebrain (Bagri et al., 2002). Further, its manipulation in oligodendrocytes is known to restrict the modulation of axon guidance by endocannabinoids (Alpár et al., 2014). We identified it as exclusively upregulated in excitatory neurons of layers 4-6 cluster 1. *KCNQ3*, a gene with reduced gene expression and altered DNA methylation in bipolar disorder (Kaminsky et al., 2015), and potential as a novel treatment target for depression and anhedonia (Costi et al., 2021), was exclusively downregulated in microglia. These findings underscore the added value of single-cell analyses over bulk studies, providing a more granular view of gene expression alterations.

Motivated by the significant role of environmental factors like stress and lifestyle in psychiatric disorders which can induce epigenetic modifications and thereby influence chromatin structure and gene expression (Cho et al., 2004; Keverne & Binder, 2020), we explored **differential chromatin accessibility**. We found only a small subset of genes to be both differentially expressed and accessible between cases and controls (5 out of 872 genes), with many more expression changes occurring without evident alterations in chromatin accessibility. When only examining genes identified as differentially expressed for differential accessibility, we pinpointed a small group where changes in gene expression paralleled changes in chromatin accessibility among psychiatric cases compared to controls (24 out of 872 genes). For example, *HES4* exhibited a consistent downregulation in both expression and accessibility within excitatory neurons of layers 4 to 6, cluster 1, and has been linked to atypical psychomotor behavior in schizophrenia (Yunqiao Zhang et al., 2020). Notably, previous studies have identified an association between epigenetic changes in *HES4* and processes involved in neuronal development and neurodegeneration (Bai et al., 2015). Similarly, *IGFBP5* was found to be upregulated in expression and accessibility in OPCs and has connections to depressive symptoms and cognitive impairment in aging (Capuano et al., 2019). Our findings indicate that transcriptomic changes in psychiatric disorders can occur without evident changes in chromatin accessibility and can be driven by various factors beyond chromatin accessibility near the gene body, as shown in many previous studies: Post-transcriptional mechanisms, such as the regulation of mRNA stability, splicing, and translation efficiency by micro RNAs, play a pivotal role in gene expression within the context of psychiatric disorders (Choi et al., 2015; Geaghan & Cairns, 2015), independently of chromatin accessibility. Epigenetic research has illuminated the role of DNA methylation and histone modifications in modulating gene expression related to psychiatric conditions (Gavin & Sharma, 2010; Grayson & Guidotti, 2013), possibly without directly altering chromatin states. Additional insights from psychiatric genomics suggest that gene expression modulation is not confined to the proximal promoter regions but can also be significantly influenced by distal enhancers or repressors (Klengel & Binder, 2015; Lynall et al., 2022; Penner-Goeke et al., 2023). However, it could be also the case that changes in chromatin accessibility are present, but too subtle to be capture by current technologies.

Building upon these results, we explored the **impact of genetic predispositions for psychiatric disorders on gene expression**. Our data revealed unique patterns of regulation linked to genetic risk across disorders and for bipolar disorder, MDD, and schizophrenia. These patterns showed minimal overlap with the ones linked to

psychiatric diagnoses. The observed discrepancies underscore the necessity to explore the influence of genetic risk on gene expression independently from diagnosis in psychiatric research. This independent study helps to isolate the genetic contributions to disease from environmental interactions and disease progression. Thereby, it aids in elucidating the complex interplay between genetic risk and environmental factors, forming a more detailed understanding of the etiology of psychiatric disorders.
Interestingly, while the number of differentially accessible genes between psychiatric cases and controls was minimal, there was a substantial increase in **differentially accessible genes related to genetic risk for psychiatric disorders**, with a count of 141 differentially expressed compared to 6,418 differentially accessible genes. The genes *INO80E* and *HCN2* stood out as being the only ones significant in both expression and accessibility analyses, specifically in excitatory neurons of layers 2/3 in the context of genetic risk for schizophrenia. *INO80E* has been implicated in GWAS, transcriptome-wide association studies, and copy number variation studies linked to schizophrenia (Gusev et al., 2018; Lago & Bahn, 2022; Liberzon et al., 2011; Marshall et al., 2017; Ripke et al., 2014), while *HCN2* has been shown to have altered methylation in the hippocampus and prefrontal cortex in schizophrenia (Alelú-Paz et al., 2016; Richetto & Meyer, 2021) and modulates antidepressant-like behaviors when knocked down in rodent models (Chung S. Kim, Chang, & Johnston, 2012; A. S. Lewis et al., 2011). These findings imply that alterations in chromatin accessibility may be related to the genetic architecture of psychiatric disorders more directly than gene expression changes.
To enhance our understanding of how different data modalities interact, particularly across various cell types, in the regulatory process of *INO80E* and *HCN2* in relation to genetic risk for psychiatric disorders, we applied an integrative correlation-based network analysis. This analysis showed primarily positive correlations within a data modality (e.g., gene expression, PRS) and mostly negative correlations across different data modalities, suggesting that genetic risk-related gene expression or accessibility variations may not have a monotonic relationship with polygenic risk scores. Overall, these polygenic risk scores show a closer association with chromatin accessibility than with gene expression. Further investigation into the regulatory elements of *INO80E*, using a transcription factor motif analysis, revealed a significant *KLF4* motif association. Although the *KLF4* gene is lowly expressed in excitatory neurons of layers 2/3, the respective protein could be still abundant and act as a transcription factor for *INO80E*. For *HCN2*, we identified a range of enriched motifs, suggesting complex, cell context-specific transcriptional regulation mechanisms.

Overall, the varied effects of genetic risk and clinical diagnosis on different **cell lineages**, specifically neurons and glial cells (Figure 4.2), are highlighted by the findings of this study. Excitatory neurons were highly influenced by both clinical diagnosis and genetic risk, aligning with the role of neuronal populations in the synaptic and circuit-level changes characteristic of psychiatric conditions (Citri & Malenka, 2008). Conversely, endothelial and glial cells, such as astrocytes, OPCs, and microglia, were more heavily influenced by genetic risk factors, with 76%-97% of altered genes (all DE/DA (risk) genes) being affected by genetic risk. This indicates that while glial cells are traditionally viewed as support cells, they may play a more proactive role in the genetic predisposition to psychiatric disorders (Yamamuro, Kimoto, Rosen, Kishimoto, &

Makinodan, 2015). In conclusion, the results of this study suggest that certain cell lineages may be genetically predisposed to psychiatric disorders, while others are more responsive to pathophysiological changes associated with diagnosis. Again, this underlines the significance of cell type-specific studies in advancing our understanding of psychiatric disorders at the molecular level.

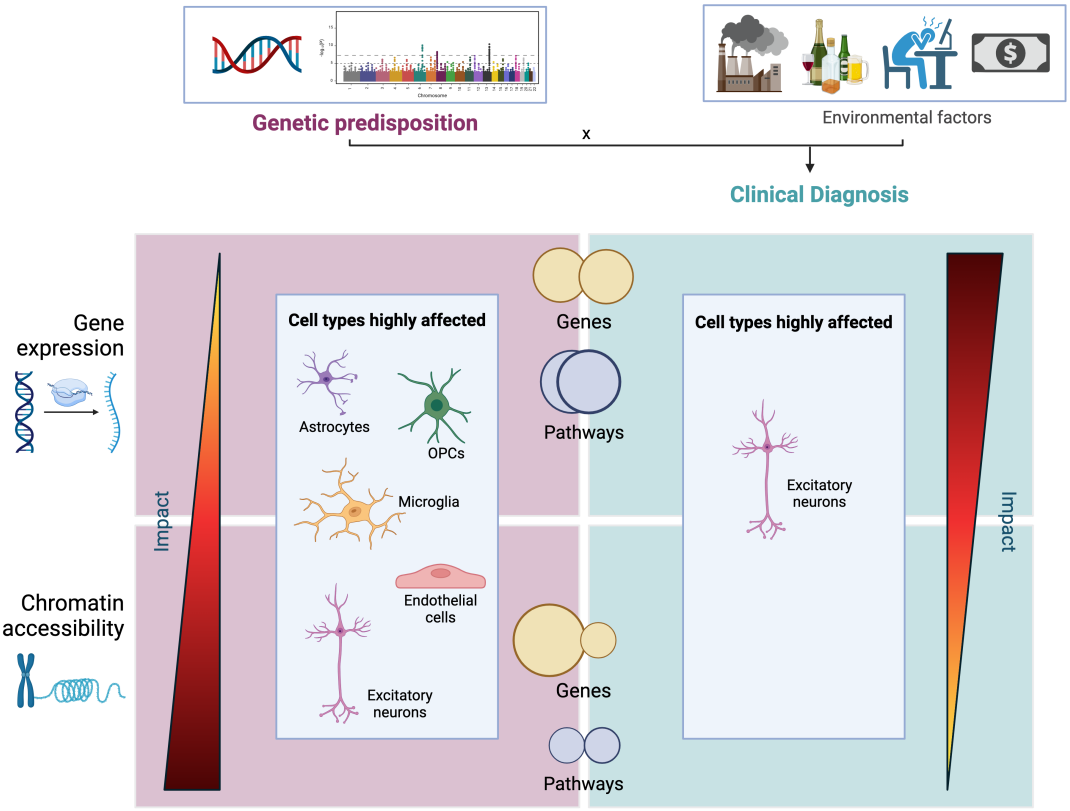


**Figure 4.2. Impact of clinical diagnosis and genetic predisposition on gene expression and chromatin accessibility.** The impact of genetic predisposition was observed to be higher on chromatin accessibility than gene expression, while it was the other way round for clinical diagnosis. Although differentially expressed genes hardly overlapped between genetic predisposition and clinical diagnosis, many common pathways were observed. Despite the very high number of differentially accessible genes for genetic predisposition, very few pathways were enriched. Endothelial cells and glia, such as astrocytes, OPCs and microglia, were highly affected by genetic predisposition, while excitatory neurons were affected by genetic predisposition and clinical diagnosis. Created with BioRender.com

An interesting aspect of our findings is the limited direct overlap in genes between diagnostic and genetic risk analyses, yet the impacted **pathways** frequently show parallels. This could be due to a functional convergence among the dysregulated genes or possibly due to insufficient power in our analysis to uncover additional overlapping genes. We noted a significant enrichment of ribosomal processes in upregulated genes within oligodendrocytes, OPCs, and endothelial cells. This aligns with previous studies that link ribosomal dysregulation to psychiatric disorders (Hori et al., 2018; Mekiten, Yitzhaky, Gould, Rosenblum, & Hertzberg, 2023), potentially impacting protein synthesis and synaptic function (Laguesse & Ron, 2020). Moreover, the enrichment of pathways related to neurodegenerative disorders and oxidative phosphorylation across

various cell types points to disruptions in protein synthesis and oxidative stress. Oxidative stress, often resulting from an imbalance in oxidative phosphorylation, can lead to excitation/inhibition imbalances, a condition implicated in schizophrenia (Cuenod et al., 2022; Mekiten et al., 2023). A distinct pattern of dysregulation in genes downregulated in microglia underscores their essential role in maintaining brain health (Q. Li & Barres, 2018), possibly related to increased inflammation and stress-induced brain changes, which have been associated with disorders such as schizophrenia (Calcia et al., 2016; Rodrigues-Neves, Ambrósio, & Gomes, 2022; Weickert et al., 2024).

When comparing the molecular response to glucocorticoid receptor activation in mice with alterations observed in postmortem brain tissue of psychiatric disorders, the overlap was small. Many of the cell type-specific differentially expressed genes in the human orbitofrontal cortex could not be tested in the mouse prefrontal cortex due to the absence of orthologs or because they were not expressed at sufficient levels (39.2%) – and vice versa (11.1%). For instance, *Abcd1* which emerged as significant in the mouse prefrontal cortex through differential network analysis and is known to be critical for synaptic signaling in microglia (Gong et al., 2017), could not be tested in human orbitofrontal cortex microglia due to its low expression levels. Various genes show differences in the direction of gene regulation, which has been also observed when comparing human blood and mouse brain responses to glucocorticoid activation and chronic stress (Arloth et al., 2015). While we assume a well-functioning stress response via the HPA axis in the mice treated with dexamethasone, the stress hormone system in psychiatric patients, including its negative feedback regulation, is possibly impaired (Binder, 2009; Gandal, Haney, et al., 2018; Pariante & Miller, 2001; Patrick F. Sullivan & Geschwind, 2019). The observed discordances in regulation direction might therefore be related to an impairment of the stress response system in psychiatric patients.

## 4.3 Limitations and Future Directions

The work detailed in my thesis represents an important step forward in translational psychiatric research, particularly in understanding the transcriptomic response to glucocorticoid stimulation in different brain regions and dissecting cell type-specific molecular signatures in psychiatric disorders in the orbitofrontal cortex. However, it also opens new doors for further exploration and improvement.

The use of transcriptome-wide analyses, while comprehensive, paves the way for future studies to explore the critical changes at the epigenetic or proteomic levels, which could provide an even more extensive understanding of molecular responses to glucocorticoid stimulation. Although the combined approach of differential expression and prior-knowledge-based differential network analysis proved to be powerful, it might still overlook relevant pathways or connections not covered by the prior network. Additionally, despite the well-conserved nature of the HPA axis across mammals, species-specific differences need to be recognized, as confirmed by the fact that for many of the altered genes related to psychiatric disorders identified in the postmortem study, no orthologs in mice could be identified.

The postmortem research presented in my thesis has yielded significant biological insights, offering opportunities for future extensions. While single-nuclei transcriptomes offer a reliable approximation of whole-cell transcriptomes (Trygve E. Bakken et al., 2018; Lake et al., 2017), there is a need to delve into more intricate processes such as mRNA splicing, which has been implicated in psychiatric disorders (Reble, Dineen, & Barr, 2018; Worf et al., 2022; C.-Y. Zhang, Xiao, Zhang, Hu, & Li, 2022). The prevalent droplet-based methods, also applied in this study, are highly scalable and optimal for high-throughput experiments with a relatively low cost per cell (Macosko et al., 2015). However, they are not suitable to capture full-length transcripts, as it is possible with plate-based methods (Picelli et al., 2014). Single-cell sequencing is further limited by issues of high sparsity and frequent dropouts due to low amounts of starting material in individual cells (Price et al., 2021). The glia-to-neuron ratio observed in this thesis and other droplet-based single-cell sequencing research (Lake et al., 2018; Nagy et al., 2020), which is notably lower than expected from histologically-based studies (see Introduction 1.5), indicates a potential limitation of these methodologies in capturing glial cells. Future advancements in technology may allow for the large-scale sequencing of full-length transcripts from intact cells. Additionally, I recognize the constraints of postmortem tissue studies in fully encompassing the variability related to clinical histories and disease progression stages.

The lack of a consistent correlation between gene expression and chromatin accessibility across all genes suggests the presence of other regulatory mechanisms, possibly *trans*-regulatory in nature, which were beyond the scope of our current study. This study, while notable for its large cohort in the field of psychiatric single-cell research, still necessitates additional research to fully capture the wide array of genetic and epigenetic variations present in the broader population. Moreover, the focus on participants of European ancestry in the cohort underscores a prevalent challenge in psychiatric research: the lack of diversity in biosample collections (A. R. Martin et al., 2022). It is essential for future efforts to focus on the collection of more comprehensive and inclusive samples to ensure that the research outcomes are representative and can be extended to diverse ethnic backgrounds (Danner et al., 2024).

While the focus on molecular profiling has revealed critical insights, I advocate for subsequent functional validations to solidify the biological significance of these findings. Future studies might focus on the inference of gene regulatory networks specific to each cell type, providing a more detailed perspective on the regulatory mechanisms driving the transcriptional and epigenomic variations observed. Building upon the molecular signatures that have been identified, I expect future research to develop personalized therapies and repurpose existing treatment options to target the specific molecular perturbations associated with psychiatric disorders.

# 5 Conclusion

The findings presented in my thesis underscore the multifaceted nature of gene regulation within the brain, particularly in the context of stress and psychiatric disorders. By examining the mouse brain in a region-specific manner and focusing on the shared and distinct transcriptomic changes elicited by glucocorticoid receptor activation – a central process in the body's response to stress – the utility of differential network analysis to gain more comprehensive insights into these responses became evident. This research affirms that genes function within complex networks and are accordingly also dysregulated upon stress within these networks, where their differential interactions are critical and shape the broader transcriptomic landscape.

Furthermore, cell type-specific dysregulations in the human orbitofrontal cortex revealed unique, often non-overlapping profiles among different cell types. This specificity suggests that genes implicated across severe psychiatric disorders may manifest in distinct cellular environments. A notable divergence between gene expression and chromatin accessibility suggests the presence of additional regulatory mechanisms not covered in this thesis. Moreover, the influence of genetic risk for psychiatric disorders on gene expression and chromatin accessibility seems to diverge from the alterations induced by the disease's progression. This distinction suggests that strategies aimed at enhancing resilience and preventing psychiatric disorders might need to target different molecular pathways than those addressed during active treatment of the manifest conditions.

The comprehensive investigation of glucocorticoid-induced transcriptomic responses across eight brain regions, including a detailed dissection of the hippocampus, alongside one of the largest single-cell datasets in psychiatric research to date encompassing both transcriptomic and epigenomic data from 92 donors (800,000 and 400,000 nuclei respectively), significantly contributes to our understanding of the molecular basis underlying stress response and psychiatric disorders in different regions and cell types of the brain. The datasets and the derived results, present important resources for future explorations and pave the way for the development of more targeted diagnostic and therapeutic strategies in personalized mental health care.

# Bibliography

Abbott, N. J., Patabendige, A. A. K., Dolman, D. E. M., Yusof, S. R., & Begley, D. J. (2010). Structure and function of the blood–brain barrier. *Neurobiology of Disease, 37*(1), 13-25. doi:10.1016/j.nbd.2009.07.030

Abi-Dargham, A., Rodenhiser, J., Printz, D., Zea-Ponce, Y., Gil, R., Kegeles, L. S., . . . Laruelle, M. (2000). Increased baseline occupancy of D2 receptors by dopamine in schizophrenia. *Proc Natl Acad Sci U S A, 97*(14), 8104-8109. doi:10.1073/pnas.97.14.8104

Akbarian, S., Liu, C., Knowles, J. A., Vaccarino, F. M., Farnham, P. J., Crawford, G. E., . . . Sestan, N. (2015). The PsychENCODE project. *Nature Neuroscience, 18*(12), 1707-1712. doi:10.1038/nn.4156

Alelú-Paz, R., Carmona, F. J., Sanchez-Mut, J. V., Cariaga-Martínez, A., González-Corpas, A., Ashour, N., . . . Ropero, S. (2016). Epigenetics in Schizophrenia: A Pilot Study of Global DNA Methylation in Different Brain Regions Associated with Higher Cognitive Functions. *Frontiers in Psychology, 7*.

Alpár, A., Tortoriello, G., Calvigioni, D., Niphakis, M. J., Milenkovic, I., Bakker, J., . . . Harkany, T. (2014). Endocannabinoids modulate cortical development by configuring Slit2/Robo1 signalling. *Nature Communications, 5*(1), 4421. doi:10.1038/ncomms5421

Andlauer, T. F. M., & Nöthen, M. M. (2020). Polygenic scores for psychiatric disease: from research tool to clinical application. *Medizinische Genetik, 32*(1), 39-45. doi:10.1515/medgen-2020-2006

Andrews Simon, K. F., Segonds-Pichon Anne, Biggins Laura, Krueger Christel, Montgomery Jo. (2019). fastQC.

Arias, D., Saxena, S., & Verguet, S. (2022). Quantifying the global burden of mental disorders and their economic value. *EClinicalMedicine, 54*, 101675. doi:10.1016/j.eclinm.2022.101675

Arloth, J., Bogdan, R., Weber, P., Frishman, G., Menke, A., Wagner, K. V., . . . PGC, M. D. D. W. G. o. t. P. G. C. (2015). Genetic Differences in the Immediate Transcriptome Response to Stress Predict Risk-Related Brain Function and Psychiatric Disorders. *Neuron, 86*(5), 1189-1202. doi:10.1016/j.neuron.2015.05.034

Arnsten, A. F. T. (2009). Stress signalling pathways that impair prefrontal cortex structure and function. *Nature Reviews. Neuroscience, 10*(6), 410-422. doi:10.1038/nrn2648

Ashburner, M., Ball, C. A., Blake, J. A., Botstein, D., Butler, H., Cherry, J. M., . . . Sherlock, G. (2000). Gene ontology: Tool for the unification of biology. *Nature Genetics, 25*(1), 25-29. doi:10.1038/75556

Atrooz, F., Liu, H., & Salim, S. (2019). Chapter Three - Stress, psychiatric disorders, molecular targets, and more. In S. Rahman (Ed.), *Progress in Molecular Biology and Translational Science* (Vol. 167, pp. 77-105): Academic Press.

Badowska, D. M., Brzózka, M. M., Kannaiyan, N., Thomas, C., Dibaj, P., Chowdhury, A., . . . Rossner, M. J. (2020). Modulation of cognition and neuronal plasticity in gain- and loss-of-function mouse models of the schizophrenia risk gene Tcf4. *Translational Psychiatry, 10*(1). doi:10.1038/s41398-020-01026-7

Baek, S., & Lee, I. (2020). Single-cell ATAC sequencing analysis: From data preprocessing to hypothesis generation. *Computational and Structural Biotechnology Journal, 18*, 1429-1439. doi:10.1016/j.csbj.2020.06.012

Bagot, Rosemary C. C., Cates, Hannah M. M., Purushothaman, I., Lorsch, Zachary S. S., Walker, Deena M. M., Wang, J., . . . Nestler, Eric J. J. (2016). Circuit-wide Transcriptional Profiling Reveals Brain Region-Specific Gene Networks

Regulating Depression Susceptibility. *Neuron, 90*(5), 969-983. doi:10.1016/j.neuron.2016.04.015

Bagri, A., Marín, O., Plump, A. S., Mak, J., Pleasure, S. J., Rubenstein, J. L. R., & Tessier-Lavigne, M. (2002). Slit Proteins Prevent Midline Crossing and Determine the Dorsoventral Position of Major Axonal Pathways in the Mammalian Forebrain. *Neuron, 33*(2), 233-248. doi:10.1016/S0896-6273(02)00561-5

Bai, G., Cheung, I., Shulha, H. P., Coelho, J. E., Li, P., Dong, X., . . . Chen, J.-F. (2015). Epigenetic dysregulation of hairy and enhancer of split 4 (HES4) is associated with striatal degeneration in postmortem Huntington brains. *Human Molecular Genetics, 24*(5), 1441-1456. doi:10.1093/hmg/ddu561

Bakken, T. E., Hodge, R. D., Miller, J. A., Yao, Z., Nguyen, T. N., Aevermann, B., . . . Tasic, B. (2018). Single-nucleus and single-cell transcriptomes compared in matched cortical cell types. *PLOS ONE, 13*(12), e0209648. doi:10.1371/journal.pone.0209648

Bakken, T. E., Jorstad, N. L., Hu, Q., Lake, B. B., Tian, W., Kalmbach, B. E., . . . Lein, E. S. (2021). Comparative cellular analysis of motor cortex in human, marmoset and mouse. *Nature, 598*(7879), 111-119. doi:10.1038/s41586-021-03465-8

Bem, J., Brożko, N., Chakraborty, C., Lipiec, M. A., Koziński, K., Nagalski, A., . . . Wiśniewska, M. B. (2019). Wnt/β-catenin signaling in brain development and mental disorders: keeping TCF7L2 in mind. *FEBS Letters, 593*(13), 1654-1674. doi:10.1002/1873-3468.13502

Benes, F. M., McSparren, J., Bird, E. D., SanGiovanni, J. P., & Vincent, S. L. (1991). Deficits in Small Interneurons in Prefrontal and Cingulate Cortices of Schizophrenic and Schizoaffective Patients. *Archives of General Psychiatry, 48*(11), 996-1001. doi:10.1001/archpsyc.1991.01810350036005

Benjamini, Y., & Hochberg, Y. (1995). *Controlling the False Discovery Rate: A Practical and Powerful Approach to Multiple Testing* (202211:21:05). Retrieved from

Bersanelli, M., Mosca, E., Remondini, D., Giampieri, E., Sala, C., Castellani, G., & Milanesi, L. (2016). Methods for the integration of multi-omics data: mathematical aspects. *BMC Bioinformatics, 17*(Suppl 2), 15. doi:10.1186/s12859-015-0857-9

Binder, E. B. (2009). The role of FKBP5, a co-chaperone of the glucocorticoid receptor in the pathogenesis and therapy of affective and anxiety disorders. *Psychoneuroendocrinology, 34*, S186-S195. doi:10.1016/j.psyneuen.2009.05.021

Blokland, G. A. M., Grove, J., Chen, C.-Y., Cotsapas, C., Tobet, S., Handa, R., . . . Goldstein, J. M. (2022). Sex-Dependent Shared and Nonshared Genetic Architecture Across Mood and Psychotic Disorders. *Biological Psychiatry, 91*(1), 102-117. doi:10.1016/j.biopsych.2021.02.972

Bowen, E. F. W., Burgess, J. L., Granger, R., Kleinman, J. E., & Rhodes, C. H. (2019). DLPFC transcriptome defines two molecular subtypes of schizophrenia. *Translational Psychiatry, 9*(1), 1-10. doi:10.1038/s41398-019-0472-z

Bristot, G., De Bastiani, M. A., Pfaffenseller, B., Kapczinski, F., & Kauer-Sant'Anna, M. (2020). Gene Regulatory Network of Dorsolateral Prefrontal Cortex: a Master Regulator Analysis of Major Psychiatric Disorders. *Molecular Neurobiology, 57*(3), 1305-1316. doi:10.1007/s12035-019-01815-2

Brodmann, K. (1909). *Vergleichende Lokalisationslehre der Grosshirnrinde in ihren Prinzipien dargestellt auf Grund des Zellenbaues*: Barth.

Brogan, M. D., Behrend, E. N., & Kemppainen, R. J. (2001). Regulation of Dexras1 Expression by Endogenous Steroids. *Neuroendocrinology, 74*(4), 244-250. doi:10.1159/000054691

Brückl, T. M., Spoormaker, V. I., Sämann, P. G., Brem, A.-K., Henco, L., Czamara, D., . . . Binder, E. B. (2020). The biological classification of mental disorders (BeCOME)

study: a protocol for an observational deep-phenotyping study for the identification of biological subtypes. *BMC Psychiatry, 20*, 213. doi:10.1186/s12888-020-02541-z

Bryois, J., Calini, D., Macnair, W., Foo, L., Urich, E., Ortmann, W., . . . Malhotra, D. (2022). Cell-type-specific cis-eQTLs in eight human brain cell types identify novel risk genes for psychiatric and neurological disorders. *Nature Neuroscience, 25*(8), 1104-1112. doi:10.1038/s41593-022-01128-z

Bryois, J., Garrett, M. E., Song, L., Safi, A., Giusti-Rodriguez, P., Johnson, G. D., . . . Crawford, G. E. (2018). Evaluation of chromatin accessibility in prefrontal cortex of individuals with schizophrenia. *Nature Communications, 9*(1), 3121. doi:10.1038/s41467-018-05379-y

Buenrostro, J. D., Giresi, P. G., Zaba, L. C., Chang, H. Y., & Greenleaf, W. J. (2013). Transposition of native chromatin for fast and sensitive epigenomic profiling of open chromatin, DNA-binding proteins and nucleosome position. *Nature Methods, 10*(12), 1213-1218. doi:10.1038/nmeth.2688

Buenrostro, J. D., Wu, B., Litzenburger, U. M., Ruff, D., Gonzales, M. L., Snyder, M. P., . . . Greenleaf, W. J. (2015). Single-cell chromatin accessibility reveals principles of regulatory variation. *Nature, 523*(7561), 486-490. doi:10.1038/nature14590

Buniello, A., Macarthur, J. A. L., Cerezo, M., Harris, L. W., Hayhurst, J., Malangone, C., . . . Parkinson, H. (2019). The NHGRI-EBI GWAS Catalog of published genome-wide association studies, targeted arrays and summary statistics 2019. *Nucleic Acids Research, 47*(D1), D1005-D1012. doi:10.1093/nar/gky1120

Bush, N., & Roubinov, D. S. (2021). 35Bringing a Neurobiological Perspective to Resilience. In *Multisystemic Resilience: Adaptation and Transformation in Contexts of Change* (pp. 0). doi:10.1093/oso/9780190095888.003.0003

Calcia, M. A., Bonsall, D. R., Bloomfield, P. S., Selvaraj, S., Barichello, T., & Howes, O. D. (2016). Stress and neuroinflammation: a systematic review of the effects of stress on microglia and the implications for mental illness. *Psychopharmacology, 233*, 1637-1650. doi:10.1007/s00213-016-4218-9

Campbell, P. D., Miller, A. M., & Woesner, M. E. (2017). Bright Light Therapy: Seasonal Affective Disorder and Beyond. *The Einstein journal of biology and medicine : EJBM, 32*, E13-E25.

Capuano, A. W., Wilson, R. S., Honer, W. G., Petyuk, V. A., Leurgans, S. E., Yu, L., . . . Arvanitakis, Z. (2019). Brain IGFBP-5 modifies the relation of depressive symptoms to decline in cognition in older persons. *J Affect Disord, 250*, 313-318. doi:10.1016/j.jad.2019.03.051

Carbon, S., Douglass, E., Good, B. M., Unni, D. R., Harris, N. L., Mungall, C. J., . . . Elser, J. (2021). The Gene Ontology resource: Enriching a GOld mine. *Nucleic Acids Research, 49*(D1), D325-D334. doi:10.1093/nar/gkaa1113

Cardno, A. G., & Owen, M. J. (2014). Genetic relationships between schizophrenia, bipolar disorder, and schizoaffective disorder. *Schizophrenia Bulletin, 40*(3), 504-515. doi:10.1093/schbul/sbu016

Carmeliet, P., & Jain, R. K. (2011). Molecular mechanisms and clinical applications of angiogenesis. *Nature, 473*(7347), 298-307. doi:10.1038/nature10144

Caspi, A., & Moffitt, T. E. (2006). Gene–environment interactions in psychiatry: joining forces with neuroscience. *Nature Reviews Neuroscience, 7*(7), 583-590. doi:10.1038/nrn1925

Cerami, E. G., Gross, B. E., Demir, E., Rodchenkov, I., Babur, Ö., Anwar, N., . . . Sander, C. (2010). Pathway Commons, a web resource for biological pathway data. *Nucleic Acids Research, 39*(suppl_1), D685-D690. doi:10.1093/nar/gkq1039

Chawla, A., Cakmakci, D., Zhang, W., Maitra, M., Rahimian, R., Mitsuhashi, H., . . . Turecki, G. (2023). Differential Chromatin Architecture and Risk Variants in

Deep Layer Excitatory Neurons and Grey Matter Microglia Contribute to Major Depressive Disorder. doi:10.1101/2023.10.02.560567

Cho, K. S., Elizondo, L. I., & Boerkoel, C. F. (2004). Advances in chromatin remodeling and human disease. *Current Opinion in Genetics & Development, 14*(3), 308-315. doi:10.1016/j.gde.2004.04.015

Choi, S.-Y., Pang, K., Kim, J. Y., Ryu, J. R., Kang, H., Liu, Z., . . . Han, K. (2015). Post-transcriptional regulation of SHANK3 expression by microRNAs related to multiple neuropsychiatric disorders. *Molecular Brain, 8*(1), 74. doi:10.1186/s13041-015-0165-3

Cholewa-Waclaw, J., Bird, A., Schimmelmann, M. v., Schaefer, A., Yu, H., Song, H., . . . Tsai, L.-H. (2016). The Role of Epigenetic Mechanisms in the Regulation of Gene Expression in the Nervous System. *Journal of Neuroscience, 36*(45), 11427-11434. doi:10.1523/JNEUROSCI.2492-16.2016

Citri, A., & Malenka, R. C. (2008). Synaptic Plasticity: Multiple Forms, Functions, and Mechanisms. *Neuropsychopharmacology, 33*(1), 18-41. doi:10.1038/sj.npp.1301559

Clark, S. Single cell RNA-seq: An introductory overview and tools for getting started. *10x Genomics*. Retrieved from https://www.10xgenomics.com/blog/single-cell-rna-seq-an-introductory-overview-and-tools-for-getting-started

Colonna, M., & Butovsky, O. (2017). Microglia Function in the Central Nervous System During Health and Neurodegeneration. *Annual Review of Immunology, 35*, 441-468. doi:10.1146/annurev-immunol-051116-052358

Conaway, R. C., & Conaway, J. W. (2009). The INO80 chromatin remodeling complex in transcription, replication and repair. *Trends in Biochemical Sciences, 34*(2), 71-77. doi:10.1016/j.tibs.2008.10.010

Consortium., C.-D. G. o. t. P. G. (2019). Genomic Relationships, Novel Loci, and Pleiotropic Mechanisms across Eight Psychiatric Disorders. *Cell, 179*(7), 1469-1482.e1411. doi:10.1016/j.cell.2019.11.020

Correll, C. U., Solmi, M., Veronese, N., Bortolato, B., Rosson, S., Santonastaso, P., . . . Stubbs, B. (2017). Prevalence, incidence and mortality from cardiovascular disease in patients with pooled and specific severe mental illness: a large-scale meta-analysis of 3,211,768 patients and 113,383,368 controls. *World Psychiatry, 16*(2), 163-180. doi:10.1002/wps.20420

Costi, S., Morris, L. S., Kirkwood, K. A., Hoch, M., Corniquel, M., Vo-Le, B., . . . Murrough, J. W. (2021). Impact of the KCNQ2/3 Channel Opener Ezogabine on Reward Circuit Activity and Clinical Symptoms in Depression: Results From a Randomized Controlled Trial. *American Journal of Psychiatry, 178*(5), 437-446. doi:10.1176/appi.ajp.2020.20050653

Cotter, D. R., Pariante, C. M., & Everall, I. P. (2001). Glial cell abnormalities in major psychiatric disorders: the evidence and implications. *Brain Res Bull, 55*(5), 585-595. doi:10.1016/s0361-9230(01)00527-5

Csardi, G. (2014). *The Igraph Software Package for Complex Network Research*. Retrieved from

Csárdi, G., Nepusz, T., Müller, K., Horvát, S., Traag, V., Zanini, F., & Noom, D. (2023). igraph for R: R interface of the igraph library for graph theory and network analysis (v1.5.1). *Zenodo*. doi:https://doi.org/10.5281/zenodo.8240644

Cuenod, M., Steullet, P., Cabungcal, J.-H., Dwir, D., Khadimallah, I., Klauser, P., . . . Do, K. Q. (2022). Caught in vicious circles: a perspective on dynamic feed-forward loops driving oxidative stress in schizophrenia. *Molecular Psychiatry, 27*(4), 1886-1897. doi:10.1038/s41380-021-01374-w

Dall'Aglio, L., Lewis, C. M., & Pain, O. (2021). Delineating the Genetic Component of Gene Expression in Major Depression. *Biological Psychiatry, 89*(6), 627-636. doi:10.1016/j.biopsych.2020.09.010

Danner, B., Gonzalez, A. D., Corbett, W. C., Alhneif, M., Etemadmoghadam, S., Parker-Garza, J., & Flanagan, M. E. (2024). Brain banking in the United States and Europe: Importance, challenges, and future trends. *Journal of Neuropathology & Experimental Neurology*, nlae014. doi:10.1093/jnen/nlae014

Daugherty, A. C., Yeo, R. W., Buenrostro, J. D., Greenleaf, W. J., Kundaje, A., & Brunet, A. (2017). Chromatin accessibility dynamics reveal novel functional enhancers in C. elegans. *Genome Research, 27*(12), 2096-2107. doi:10.1101/gr.226233.117

de Kloet, E. R., Joëls, M., & Holsboer, F. (2005). Stress and the brain: from adaptation to disease. *Nature Reviews. Neuroscience, 6*(6), 463-475. doi:10.1038/nrn1683

de la Fuente, A. (2010). From 'differential expression' to 'differential networking' - identification of dysfunctional regulatory networks in diseases. *Trends in Genetics, 26*(7), 326-333. doi:10.1016/j.tig.2010.05.001

de la Torre-Ubieta, L., Stein, J. L., Won, H., Opland, C. K., Liang, D., Lu, D., & Geschwind, D. H. (2018). The Dynamic Landscape of Open Chromatin during Human Cortical Neurogenesis. *Cell, 172*(1), 289-304.e218. doi:10.1016/j.cell.2017.12.014

Delaneau, O., Marchini, J., & Zagury, J. F. (2011). A linear complexity phasing method for thousands of genomes. *Nat Methods, 9*(2), 179-181. doi:10.1038/nmeth.1785

*Diagnostic and statistical manual of mental disorders: DSM-5™, 5th ed*. (2013). Arlington, VA, US: American Psychiatric Publishing, Inc.

Dickerson, F. B., & Lehman, A. F. (2011). Evidence-based psychotherapy for schizophrenia: 2011 update. *J Nerv Ment Dis, 199*(8), 520-526. doi:10.1097/NMD.0b013e318225ee78

Dickinson, R. E., Fegan, K. S., Ren, X., Hillier, S. G., & Duncan, W. C. (2011). Glucocorticoid Regulation of SLIT/ROBO Tumour Suppressor Genes in the Ovarian Surface Epithelium and Ovarian Cancer Cells. *PLOS ONE, 6*(11), e27792. doi:10.1371/journal.pone.0027792

Dijk, D. v., Sharma, R., Nainys, J., Yim, K., Kathail, P., Carr, A. J., . . . Pe'er, D. (2018). Recovering Gene Interactions from Single-Cell Data Using Data Diffusion. *Cell, 174*(3), 716-729.e727. doi:10.1016/j.cell.2018.05.061

Dobbyn, A., Huckins, L. M., Boocock, J., Sloofman, L. G., Glicksberg, B. S., Giambartolomei, C., . . . Sieberts, S. K. (2018). Landscape of Conditional eQTL in Dorsolateral Prefrontal Cortex and Co-localization with Schizophrenia GWAS. *Am J Hum Genet, 102*(6), 1169-1184. doi:10.1016/j.ajhg.2018.04.011

Dobin, A., Davis, C. A., Schlesinger, F., Drenkow, J., Zaleski, C., Jha, S., . . . Gingeras, T. R. (2013). STAR: Ultrafast universal RNA-seq aligner. *Bioinformatics, 29*(1), 15-21. doi:10.1093/bioinformatics/bts635

Docherty, A. R., Moscati, A. A., & Fanous, A. H. (2016). Cross-Disorder Psychiatric Genomics. *Current Behavioral Neuroscience Reports, 3*(3), 256-263. doi:10.1007/s40473-016-0084-3

Douglas, R. J., & Martin, K. A. C. (2004). Neuronal Circuits of the Neocortex. *Annual Review of Neuroscience, 27*(1), 419-451. doi:10.1146/annurev.neuro.27.070203.144152

Durinck, S., Moreau, Y., Kasprzyk, A., Davis, S., De Moor, B., Brazma, A., & Huber, W. (2005). BioMart and Bioconductor: a powerful link between biological databases and microarray data analysis. *Bioinformatics, 21*(16), 3439-3440. doi:10.1093/bioinformatics/bti525

Egervari, G. (2021). Chromatin accessibility in neuropsychiatric disorders. *Neurobiology of Learning and Memory, 181*, 107438. doi:10.1016/j.nlm.2021.107438

Engelhardt, B., & Ransohoff, R. M. (2005). The ins and outs of T-lymphocyte trafficking to the CNS: anatomical sites and molecular mechanisms. *Trends in Immunology, 26*(9), 485-495. doi:10.1016/j.it.2005.07.004

Engelhardt, C., Tang, F., Elkhateib, R., Bordes, J., Brix, L. M., van Doeselaar, L., . . . Schmidt, M. V. (2021). FKBP51 in the Oval Bed Nucleus of the Stria Terminalis Regulates Anxiety-Like Behavior. *eneuro, 8*(6). doi:10.1523/eneuro.0425-21.2021

Enwright, J. F., Sanapala, S., Foglio, A., Berry, R., Fish, K. N., & Lewis, D. A. (2016). Reduced Labeling of Parvalbumin Neurons and Perineuronal Nets in the Dorsolateral Prefrontal Cortex of Subjects with Schizophrenia. *Neuropsychopharmacology, 41*(9), 2206-2214. doi:10.1038/npp.2016.24

Ezra-Nevo, G., Prestori, F., Locatelli, F., Soda, T., Brinke, M. M. t., Engel, M., . . . Chen, A. (2018). Cerebellar Learning Properties Are Modulated by the CRF Receptor. *Journal of Neuroscience, 38*(30), 6751-6765. doi:10.1523/JNEUROSCI.3106-15.2018

Fang, L.-P., & Bai, X. (2023). Oligodendrocyte precursor cells: the multitaskers in the brain. *Pflügers Archiv - European Journal of Physiology, 475*(9), 1035-1044. doi:10.1007/s00424-023-02837-5

Fang, R., Xia, C., Close, J. L., Zhang, M., He, J., Huang, Z., . . . Zhuang, X. (2022). Conservation and divergence of cortical cell organization in human and mouse revealed by MERFISH. *Science, 377*(6601), 56-62. doi:doi:10.1126/science.abm1741

Fava, M., & Kendler, K. S. (2000). Major Depressive Disorder. *Neuron, 28*(2), 335-341. doi:10.1016/S0896-6273(00)00112-4

Fishell, G., & Kepecs, A. (2020). Interneuron Types as Attractors and Controllers. *Annual Review of Neuroscience, 43*(1), 1-30. doi:10.1146/annurev-neuro-070918-050421

Fornes, O., Castro-Mondragon, J. A., Khan, A., van der Lee, R., Zhang, X., Richmond, P. A., . . . Mathelier, A. (2020). JASPAR 2020: update of the open-access database of transcription factor binding profiles. *Nucleic Acids Research, 48*(D1), D87-D92. doi:10.1093/nar/gkz1001

Freeman, L. C. (1977). A Set of Measures of Centrality Based on Betweenness. *Sociometry, 40*(1), 35-41. doi:10.2307/3033543

Frisoni, G. B., Prestia, A., Adorni, A., Rasser, P. E., Cotelli, M., Soricelli, A., . . . Thompson, P. M. (2009). In vivo neuropathology of cortical changes in elderly persons with schizophrenia. *Biological Psychiatry, 66*(6), 578-585. doi:10.1016/j.biopsych.2009.02.011

Fritschy, J.-M., & Brünig, I. (2003). Formation and plasticity of GABAergic synapses: physiological mechanisms and pathophysiological implications. *Pharmacology & Therapeutics, 98*(3), 299-323. doi:10.1016/s0163-7258(03)00037-8

Fröhlich, A. S., Gerstner, N., Gagliardi, M., Ködel, M., Yusupov, N., Matosin, N., . . . Binder, E. B. Cell-type-specific aging effects in the human OFC and implications for psychiatric disease.

Fromer, M., Roussos, P., Sieberts, S. K., Johnson, J. S., Kavanagh, D. H., Perumal, T. M., . . . Sklar, P. (2016). Gene expression elucidates functional impact of polygenic risk for schizophrenia. *Nature Neuroscience, 19*(11), 1442-1453. doi:10.1038/nn.4399

Funahashi, S. (2001). Neuronal mechanisms of executive control by the prefrontal cortex. *Neuroscience Research, 39*(2), 147-165. doi:https://doi.org/10.1016/S0168-0102(00)00224-8

Fuster, J. M. (1988). Prefrontal Cortex. In L. N. Irwin (Ed.), *Comparative Neuroscience and Neurobiology* (pp. 107-109). Boston, MA: Birkhäuser Boston.

Gallagher, M., & Chiba, A. A. (1996). The amygdala and emotion. *Current Opinion in Neurobiology, 6*(2), 221-227. doi:https://doi.org/10.1016/S0959-4388(96)80076-6

Gandal, M. J., Haney, J. R., Parikshak, N. N., Leppa, V., Ramaswami, G., Hartl, C., . . . Geschwind, D. H. (2018). Shared molecular neuropathology across major psychiatric disorders parallels polygenic overlap. *Science, 359*(6376), 693-697. doi:10.1126/science.aad6469

Gandal, M. J., Zhang, P., Hadjimichael, E., Walker, R. L., Chen, C., Liu, S., . . . Geschwind, D. H. (2018). Transcriptome-wide isoform-level dysregulation in ASD, schizophrenia, and bipolar disorder. *Science, 362*(6420), eaat8127. doi:10.1126/science.aat8127

Gao, W.-J., Wang, H.-X., Snyder, M. A., Li, Y.-C., Gao, W.-J., Wang, H.-X., . . . Li, Y.-C. (2012). The Unique Properties of the Prefrontal Cortex and Mental Illness. In *When Things Go Wrong - Diseases and Disorders of the Human Brain*: IntechOpen.

Gavin, D. P., & Sharma, R. P. (2010). Histone modifications, DNA methylation, and Schizophrenia. *Neuroscience & Biobehavioral Reviews, 34*(6), 882-888. doi:10.1016/j.neubiorev.2009.10.010

Gayoso, A., Shor, J., Carr, A. J., Sharma, R., & Pe'er, D. (2020). DoubletDetection (Version v3.0). doi:http://doi.org/10.5281/zenodo.2678041

Ge, T., Chen, C.-Y., Ni, Y., Feng, Y.-C. A., & Smoller, J. W. (2019). Polygenic prediction via Bayesian regression and continuous shrinkage priors. *Nature Communications, 10*(1), 1776. doi:10.1038/s41467-019-09718-5

Geaghan, M., & Cairns, M. J. (2015). MicroRNA and Posttranscriptional Dysregulation in Psychiatry. *Biological Psychiatry, 78*(4), 231-239. doi:10.1016/j.biopsych.2014.12.009

Geng, R., Li, Z., Yu, S., Yuan, C., Hong, W., Wang, Z., . . . Fang, Y. (2020). Weighted gene co-expression network analysis identifies specific modules and hub genes related to subsyndromal symptomatic depression. *World Journal of Biological Psychiatry, 21*(2), 102-110. doi:10.1080/15622975.2018.1548782

Gerstner, N., Fröhlich, A. S., Matosin, N., Gagliardi, M., Cruceanu, C., Ködel, M., . . . Knauer-Arloth, J. Contrasting genetic predisposition and diagnosis in psychiatric disorders: a multi-omic single-nucleus analysis of the human orbitofrontal cortex.

Gerstner, N., Krontira, A. C., Cruceanu, C., Roeh, S., Pütz, B., Sauer, S., . . . Knauer-Arloth, J. (2022). DiffBrainNet: Differential analyses add new insights into the response to glucocorticoids at the level of genes, networks and brain regions. *Neurobiology of Stress, 21*, 100496. doi:https://doi.org/10.1016/j.ynstr.2022.100496

Geschwind, D. H., & Flint, J. (2015). Genetics and genomics of psychiatric disease. *Science, 349*(6255), 1489-1494. doi:10.1126/science.aaa8954

Giambartolomei, C., Vukcevic, D., Schadt, E. E., Franke, L., Hingorani, A. D., Wallace, C., & Plagnol, V. (2014). Bayesian Test for Colocalisation between Pairs of Genetic Association Studies Using Summary Statistics. *PLOS Genetics, 10*(5), e1004383. doi:10.1371/journal.pgen.1004383

Gong, Y., Sasidharan, N., Laheji, F., Frosch, M., Musolino, P., Tanzi, R., . . . Eichler, F. (2017). Microglial dysfunction as a key pathological change in adrenomyeloneuropathy. *Annals of Neurology, 82*(5), 813-827. doi:10.1002/ana.25085

Granja, J. M., Corces, M. R., Pierce, S. E., Bagdatli, S. T., Choudhry, H., Chang, H. Y., & Greenleaf, W. J. (2021). ArchR is a scalable software package for integrative single-cell chromatin accessibility analysis. *Nature Genetics, 53*(3), 403-411. doi:10.1038/s41588-021-00790-6

Grayson, D. R., & Guidotti, A. (2013). The dynamics of DNA methylation in schizophrenia and related psychiatric disorders. *Neuropsychopharmacology, 38*(1), 138-166. doi:10.1038/npp.2012.125

Greenwood, M. P., Greenwood, M., Mecawi, A. S., Antunes-Rodrigues, J., Paton, J. F. R., & Murphy, D. (2016). Rasd1, a small G protein with a big role in the hypothalamic response to neuronal activation. *Molecular Brain, 9*(1), 1. doi:10.1186/s13041-015-0182-2

Griffiths, B. B., & Hunter, R. G. (2014). Neuroepigenetics of stress. *Neuroscience, 275*, 420-435. doi:10.1016/j.neuroscience.2014.06.041

Grover, S., Sahoo, S., Rabha, A., & Koirala, R. (2019). ECT in schizophrenia: a review of the evidence. *Acta Neuropsychiatr, 31*(3), 115-127. doi:10.1017/neu.2018.32

Guillamón-Vivancos, T., Gómez-Pinedo, U., & Matías-Guiu, J. (2015). Astrocytes in neurodegenerative diseases (I): function and molecular description. *Neurología (English Edition), 30*(2), 119-129. doi:10.1016/j.nrleng.2014.12.005

Gusev, A., Mancuso, N., Won, H., Kousi, M., Finucane, H. K., Reshef, Y., . . . Price, A. L. (2018). Transcriptome-wide association study of schizophrenia and chromatin activity yields mechanistic disease insights. *Nature Genetics, 50*(4), 538-548. doi:10.1038/s41588-018-0092-1

Hafemeister, C., & Satija, R. (2019). Normalization and variance stabilization of single-cell RNA-seq data using regularized negative binomial regression. *Genome Biology, 20*(1), 296. doi:10.1186/s13059-019-1874-1

Hao, Y., Hao, S., Andersen-Nissen, E., Mauck, W. M., Zheng, S., Butler, A., . . . Satija, R. (2021). Integrated analysis of multimodal single-cell data. *Cell, 184*(13), 3573-3587.e3529. doi:10.1016/j.cell.2021.04.048

Harlé, G., Lalonde, R., Fonte, C., Ropars, A., Frippiat, J.-P., & Strazielle, C. (2017). Repeated corticosterone injections in adult mice alter stress hormonal receptor expression in the cerebellum and motor coordination without affecting spatial learning. *Behavioural Brain Research, 326*, 121-131. doi:10.1016/j.bbr.2017.02.035

Harrison, P. J. (2011). Using Our Brains: The Findings, Flaws, and Future of Postmortem Studies of Psychiatric Disorders. *Biological Psychiatry, 69*(2), 102-103. doi:10.1016/j.biopsych.2010.09.008

Hartmann, J., Wagner, K. V., Gaali, S., Kirschner, A., Kozany, C., Rühter, G., . . . Schmidt, M. V. (2015). Pharmacological Inhibition of the Psychiatric Risk Factor FKBP51 Has Anxiolytic Properties. *J Neurosci, 35*(24), 9007-9016. doi:10.1523/jneurosci.4024-14.2015

Hauberg, M. E., Creus-Muncunill, J., Bendl, J., Kozlenkov, A., Zeng, B., Corwin, C., . . . Roussos, P. (2020). Common schizophrenia risk variants are enriched in open chromatin regions of human glutamatergic neurons. *Nature Communications, 11*(1), 5581. doi:10.1038/s41467-020-19319-2

Häusl, A. S., Brix, L. M., Hartmann, J., Pöhlmann, M. L., Lopez, J.-P., Menegaz, D., . . . Schmidt, M. V. (2021). The co-chaperone Fkbp5 shapes the acute stress response in the paraventricular nucleus of the hypothalamus of male mice. *Molecular Psychiatry, 26*(7), 3060-3076. doi:10.1038/s41380-021-01044-x

Heim, C., & Binder, E. B. (2012). Current research trends in early life stress and depression: review of human studies on sensitive periods, gene-environment interactions, and epigenetics. *Experimental Neurology, 233*(1), 102-111. doi:10.1016/j.expneurol.2011.10.032

Herman, J. P., McKlveen, J. M., Ghosal, S., Kopp, B., Wulsin, A., Makinson, R., . . . Myers, B. (2016). Regulation of the Hypothalamic-Pituitary-Adrenocortical Stress Response. In *Comprehensive Physiology* (pp. 603-621): John Wiley & Sons, Ltd.

Hernandez, L. M., Kim, M., Hoftman, G. D., Haney, J. R., Torre-Ubieta, L. d. l., Pasaniuc, B., & Gandal, M. J. (2021). Transcriptomic Insight Into the Polygenic Mechanisms Underlying Psychiatric Disorders. *Biological Psychiatry, 89*(1), 54-64. doi:10.1016/j.biopsych.2020.06.005

Hill, M. N., & McEwen, B. S. (2010). Involvement of the endocannabinoid system in the neurobehavioural effects of stress and glucocorticoids. *Progress in Neuro-Psychopharmacology and Biological Psychiatry, 34*(5), 791-797. doi:10.1016/j.pnpbp.2009.11.001

Ho, D., Imai, K., King, G., & Stuart, E. A. (2011). MatchIt: Nonparametric Preprocessing for Parametric Causal Inference. *Journal of Statistical Software, 42*(8), 1 - 28. doi:10.18637/jss.v042.i08

Hoffman, G. E., Bendl, J., Voloudakis, G., Montgomery, K. S., Sloofman, L., Wang, Y.-C., . . . Roussos, P. (2019). CommonMind Consortium provides transcriptomic and epigenomic data for Schizophrenia and Bipolar Disorder. *Scientific Data, 6*(1), 180. doi:10.1038/s41597-019-0183-6

Hori, H., Nakamura, S., Yoshida, F., Teraishi, T., Sasayama, D., Ota, M., . . . Kunugi, H. (2018). Integrated profiling of phenotype and blood transcriptome for stress vulnerability and depression. *Journal of Psychiatric Research, 104*, 202-210. doi:10.1016/j.jpsychires.2018.08.010

Howard, D. M., Adams, M. J., Clarke, T.-K., Hafferty, J. D., Gibson, J., Shirali, M., . . . Major Depressive Disorder Working Group of the Psychiatric Genomics, C. (2019). Genome-wide meta-analysis of depression identifies 102 independent variants and highlights the importance of the prefrontal brain regions. *Nature Neuroscience, 22*(3), 343-352. doi:10.1038/s41593-018-0326-7

Huang, G., Wang, S., Yan, J., Li, C., Feng, J., Chen, Q., . . . Wang, L. (2020). Depression-/Anxiety-Like Behavior Alterations in Adult Slit2 Transgenic Mice. *Front Behav Neurosci, 14*, 622257. doi:10.3389/fnbeh.2020.622257

Huggett, S. B., & Stallings, M. C. (2020). Cocaine'omics: Genome-wide and transcriptome-wide analyses provide biological insight into cocaine use and dependence. *Addiction Biology, 25*(2), 1-10. doi:10.1111/adb.12719

*The ICD-10 classification of mental and behavioural disorders: clinical descriptions and diagnostic guidelines*. (1992).c(W. H. Organization Ed.). Geneva: World Health Organization.

Institute for Health Metrics and Evaluation, (IHME). (2020). *GBD Results.* Retrieved from: https://vizhub.healthdata.org/gbd-results/

Jackowski, A. P., Araújo Filho, G. M. d., Almeida, A. G. d., Araújo, C. M. d., Reis, M., Nery, F., . . . Lacerda, A. L. T. (2012). The involvement of the orbitofrontal cortex in psychiatric disorders: an update of neuroimaging findings. *Revista Brasileira De Psiquiatria (Sao Paulo, Brazil: 1999), 34*(2), 207-212. doi:10.1590/s1516-44462012000200014

Jassal, B., Matthews, L., Viteri, G., Gong, C., Lorente, P., Fabregat, A., . . . D'Eustachio, P. (2020). The reactome pathway knowledgebase. *Nucleic Acids Research, 48*(D1), D498-D503. doi:10.1093/nar/gkz1031

Joëls, M., Karst, H., & Sarabdjitsingh, R. A. (2018). The stressed brain of humans and rodents. *Acta Physiologica (Oxford, England), 223*(2), e13066. doi:10.1111/apha.13066

Joëls, M., Krugers, H., & Karst, H. (2007). Stress-induced changes in hippocampal function. In E. R. De Kloet, M. S. Oitzl, & E. Vermetten (Eds.), *Progress in Brain Research* (Vol. 167, pp. 3-15): Elsevier.

Joyce, J. B., Grant, C. W., Liu, D., MahmoudianDehkordi, S., Kaddurah-Daouk, R., Skime, M., . . . Athreya, A. P. (2021). Multi-omics driven predictions of response to acute phase combination antidepressant therapy: a machine learning approach with cross-trial replication. *Translational Psychiatry, 11*(1), 1-11. doi:10.1038/s41398-021-01632-z

Kaminsky, Z., Jones, I., Verma, R., Saleh, L., Trivedi, H., Guintivano, J., . . . Potash, J. B. (2015). DNA methylation and expression of KCNQ3 in bipolar disorder. *Bipolar Disord, 17*(2), 150-159. doi:10.1111/bdi.12230

Kanehisa, M. (2019). Toward understanding the origin and evolution of cellular organisms. *Protein Science, 28*(11), 1947-1951. doi:10.1002/pro.3715

Kanehisa, M., Furumichi, M., Sato, Y., Ishiguro-Watanabe, M., & Tanabe, M. (2021). KEGG: Integrating viruses and cellular organisms. *Nucleic Acids Research, 49*(D1), D545-D551. doi:10.1093/nar/gkaa970

Kanehisa, M., & Goto, S. (2000). KEGG: Kyoto Encyclopedia of Genes and Genomes. *Nucleic Acids Research, 28*(1), 27-30. doi:10.1093/nar/28.1.27

Kapoor, M., Wang, J. C., Farris, S. P., Liu, Y., McClintick, J., Gupta, I., . . . Goate, A. (2019). Analysis of whole genome-transcriptomic organization in brain to identify genes associated with alcoholism. *Translational Psychiatry, 9*(1). doi:10.1038/s41398-019-0384-y

Keverne, J., & Binder, E. B. (2020). A Review of epigenetics in psychiatry: focus on environmental risk factors. *Medizinische Genetik, 32*(1), 57-64. doi:10.1515/medgen-2020-2004

Kim, Chung S., Chang, Payne Y., & Johnston, D. (2012). Enhancement of Dorsal Hippocampal Activity by Knockdown of HCN1 Channels Leads to Anxiolytic- and Antidepressant-like Behaviors. *Neuron, 75*(3), 503-516. doi:10.1016/j.neuron.2012.05.027

Kim, J. J., & Diamond, D. M. (2002). The stressed hippocampus, synaptic plasticity and lost memories. *Nature Reviews Neuroscience, 3*(6), 453-462. doi:10.1038/nrn849

Kim Youngsoon, J. H., Yadu Gautam, Tesfaye B. Mersha, Mingon Kang. (2018). DiffGRN: differential gene regulatory network analysis. *International Journal of Data Mining and Bioinformatics, 20*(4), 362-362. doi:10.1504/ijdmb.2018.10016325

Kimelberg, H. K., & Nedergaard, M. (2010). Functions of Astrocytes and their Potential As Therapeutic Targets. *Neurotherapeutics, 7*(4), 338-353. doi:10.1016/j.nurt.2010.07.006

Kintner, C. (2002). Neurogenesis in embryos and in adult neural stem cells. *J Neurosci, 22*(3), 639-643. doi:10.1523/jneurosci.22-03-00639.2002

Kirov, G., Pocklington, A. J., Holmans, P., Ivanov, D., Ikeda, M., Ruderfer, D., . . . Owen, M. J. (2012). De novo CNV analysis implicates specific abnormalities of postsynaptic signalling complexes in the pathogenesis of schizophrenia. *Molecular Psychiatry, 17*(2), 142-153. doi:10.1038/mp.2011.154

Klengel, T., & Binder, Elisabeth B. (2015). Epigenetics of Stress-Related Psychiatric Disorders and Gene × Environment Interactions. *Neuron, 86*(6), 1343-1357. doi:https://doi.org/10.1016/j.neuron.2015.05.036

Krassner, M., Kauffman, J., Sowa, A., Cialowicz, K., Walsh, S., Farrell, K., . . . McKenzie, A. (2023). Postmortem changes in brain cell structure: a review. *Free Neuropathology, 4*, 10-10. doi:10.17879/freeneuropathology-2023-4790

Kulkarni, A., Anderson, A. G., Merullo, D. P., & Konopka, G. (2019). Beyond bulk: a review of single cell transcriptomics methodologies and applications. *Current Opinion in Biotechnology, 58*, 129-136. doi:10.1016/j.copbio.2019.03.001

Kwon, J., Kim, Y. J., Choi, K., Seol, S., & Kang, H. J. (2019). Identification of stress resilience module by weighted gene co-expression network analysis in Fkbp5-deficient mice. *Molecular Brain, 12*(1), 10-13. doi:10.1186/s13041-019-0521-9

Labonté, B., Engmann, O., Purushothaman, I., Menard, C., Wang, J., Tan, C., . . . Nestler, E. J. (2017). Sex-specific transcriptional signatures in human depression. *Nature Medicine, 23*(9), 1102-1111. doi:10.1038/nm.4386

Lachmann, A., Xu, H., Krishnan, J., Berger, S. I., Mazloom, A. R., & Ma'ayan, A. (2010). ChEA: transcription factor regulation inferred from integrating genome-wide ChIP-X experiments. *Bioinformatics, 26*(19), 2438-2444. doi:10.1093/bioinformatics/btq466

Lago, S. G., & Bahn, S. (2022). The druggable schizophrenia genome: from repurposing opportunities to unexplored drug targets. *NPJ Genom Med, 7*(1), 25. doi:10.1038/s41525-022-00290-4

Laguesse, S., & Ron, D. (2020). Protein Translation and Psychiatric Disorders. *The Neuroscientist : a review journal bringing neurobiology, neurology and psychiatry, 26*(1), 21-42. doi:10.1177/1073858419853236

Lake, B. B., Chen, S., Sos, B. C., Fan, J., Kaeser, G. E., Yung, Y. C., . . . Zhang, K. (2018). Integrative single-cell analysis of transcriptional and epigenetic states in the human adult brain. *Nature Biotechnology, 36*(1), 70-80. doi:10.1038/nbt.4038

Lake, B. B., Codeluppi, S., Yung, Y. C., Gao, D., Chun, J., Kharchenko, P. V., . . . Zhang, K. (2017). A comparative strategy for single-nucleus and single-cell transcriptomes confirms accuracy in predicted cell-type expression from nuclear RNA. *Scientific Reports, 7*(1), 6031. doi:10.1038/s41598-017-04426-w

Langfelder, P., & Horvath, S. (2008). WGCNA: An R package for weighted correlation network analysis. *BMC Bioinformatics, 9*. doi:10.1186/1471-2105-9-559

Lazarus, R. S., & Folkman, S. (1984). *Stress, appraisal, and coping*: Springer publishing company.

Leek, J. T. (2014). Svaseq: Removing batch effects and other unwanted noise from sequencing data. *Nucleic Acids Research, 42*(21), e161-e161. doi:10.1093/nar/gku864

Leung, C. M. C., Ho, M. K., Bharwani, A. A., Cogo-Moreira, H., Wang, Y., Chow, M. S. C., . . . Ni, M. Y. (2022). Mental disorders following COVID-19 and other epidemics: a systematic review and meta-analysis. *Translational Psychiatry, 12*(1), 1-12. doi:10.1038/s41398-022-01946-6

Levone, B. R., Cryan, J. F., & O'Leary, O. F. (2014). Role of adult hippocampal neurogenesis in stress resilience. *Neurobiology of Stress, 1*, 147-155. doi:10.1016/j.ynstr.2014.11.003

Lewis, A. S., Vaidya, S. P., Blaiss, C. A., Liu, Z., Stoub, T. R., Brager, D. H., . . . Chetkovich, D. M. (2011). Deletion of the Hyperpolarization-Activated Cyclic Nucleotide-Gated Channel Auxiliary Subunit TRIP8b Impairs Hippocampal Ih Localization and Function and Promotes Antidepressant Behavior in Mice. *Journal of Neuroscience, 31*(20), 7424-7440. doi:10.1523/JNEUROSCI.0936-11.2011

Lewis, C. M., & Vassos, E. (2020). Polygenic risk scores: from research tools to clinical instruments. *Genome Medicine, 12*(1), 44. doi:10.1186/s13073-020-00742-5

Lewis, D. A. (2002). The Human Brain Revisited: Opportunities and Challenges in Postmortem Studies of Psychiatric Disorders. *Neuropsychopharmacology, 26*(2), 143-154. doi:10.1016/S0893-133X(01)00393-1

Li, M., Santpere, G., Imamura Kawasawa, Y., Evgrafov, O. V., Gulden, F. O., Pochareddy, S., . . . Li, Z. (2018). Integrative functional genomic analysis of human brain development and neuropsychiatric risks. *Science, 362*(6420), eaat7615. doi:doi:10.1126/science.aat7615

Li, Q., & Barres, B. A. (2018). Microglia and macrophages in brain homeostasis and disease. *Nature Reviews Immunology, 18*(4), 225-242. doi:10.1038/nri.2017.125

Li, X., Zhang, Y., Wang, L., Lin, Y., Gao, Z., Zhan, X., . . . Wu, L. (2019). Integrated Analysis of Brain Transcriptome Reveals Convergent Molecular Pathways in Autism Spectrum Disorder. *Frontiers in Psychiatry, 10*(October), 1-8. doi:10.3389/fpsyt.2019.00706

Li, Y. E., Preissl, S., Miller, M., Johnson, N. D., Wang, Z., Jiao, H., . . . Ren, B. (2023). A comparative atlas of single-cell chromatin accessibility in the human brain. *Science, 382*(6667), eadf7044. doi:10.1126/science.adf7044

Li, Z., Chen, J., Yu, H., He, L., Xu, Y., Zhang, D., . . . Shi, Y. (2017). Genome-wide association analysis identifies 30 new susceptibility loci for schizophrenia. *Nature Genetics, 49*(11), 1576-1583. doi:10.1038/ng.3973

Liao, Y., Smyth, G. K., & Shi, W. (2014). FeatureCounts: An efficient general purpose program for assigning sequence reads to genomic features. *Bioinformatics, 30*(7), 923-930. doi:10.1093/bioinformatics/btt656

Liberzon, A., Subramanian, A., Pinchback, R., Thorvaldsdóttir, H., Tamayo, P., & Mesirov, J. P. (2011). Molecular signatures database (MSigDB) 3.0. *Bioinformatics, 27*(12), 1739-1740. doi:10.1093/bioinformatics/btr260

Lin, C.-Y., Sawa, A., & Jaaro-Peled, H. (2012). Better understanding of mechanisms of schizophrenia and bipolar disorder: From human gene expression profiles to mouse models. *Neurobiology of Disease, 45*(1), 48-56. doi:10.1016/j.nbd.2011.08.025

Linde, J., Schulze, S., Henkel, S. G., & Guthke, R. (2015). Data- and knowledge-based modeling of gene regulatory networks: an update. *Excli j, 14*, 346-378. doi:10.17179/excli2015-168

Liu, J., Jing, L., & Tu, X. (2016). Weighted gene co-expression network analysis identifies specific modules and hub genes related to coronary artery disease. *BMC Cardiovascular Disorders, 16*(1), 1-8. doi:10.1186/s12872-016-0217-3

Liu, Y., Sun, S., Bredy, T., Wood, M., Spitale, R. C., & Baldi, P. (2017). MotifMap-RNA: a genome-wide map of RBP binding sites. *Bioinformatics, 33*(13), 2029-2031. doi:10.1093/bioinformatics/btx087

Lonsdale, J., Thomas, J., Salvatore, M., Phillips, R., Lo, E., Shad, S., . . . Moore, H. F. (2013). The Genotype-Tissue Expression (GTEx) project. *Nature Genetics, 45*(6), 580-585. doi:10.1038/ng.2653

Lopez, J. P., Brivio, E., Santambrogio, A., De Donno, C., Kos, A., Peters, M., . . . Chen, A. (2021). Single-cell molecular profiling of all three components of the HPA axis reveals adrenal ABCB1 as a regulator of stress adaptation. *Science Advances, 7*(5), 1-18. doi:10.1126/sciadv.abe4497

Lotfollahi, M., Naghipourfar, M., Luecken, M. D., Khajavi, M., Büttner, M., Wagenstetter, M., . . . Theis, F. J. (2022). Mapping single-cell data to reference atlases by transfer learning. *Nature Biotechnology, 40*(1), 121-130. doi:10.1038/s41587-021-01001-7

Love, M. I., Huber, W., & Anders, S. (2014). Moderated estimation of fold change and dispersion for RNA-seq data with DESeq2. *Genome Biology, 15*(12), 550. doi:10.1186/s13059-014-0550-8

Lun, A. T. L., Riesenfeld, S., Andrews, T., Dao, T. P., Gomes, T., Marioni, J. C., & Jamboree, p. i. t. s. H. C. A. (2019). EmptyDrops: distinguishing cells from empty droplets in droplet-based single-cell RNA sequencing data. *Genome Biology, 20*(1), 63. doi:10.1186/s13059-019-1662-y

Luo, X., Rosenfeld, J. A., Yamamoto, S., Harel, T., Zuo, Z., Hall, M., . . . Wangler, M. F. (2017). Clinically severe CACNA1A alleles affect synaptic function and neurodegeneration differentially. *PLOS Genetics, 13*(7). doi:10.1371/journal.pgen.1006905

Lynall, M.-E., Soskic, B., Hayhurst, J., Schwartzentruber, J., Levey, D. F., Pathak, G. A., . . . Bullmore, E. (2022). Genetic variants associated with psychiatric disorders are enriched at epigenetically active sites in lymphoid cells. *Nature Communications, 13*(1), 6102. doi:10.1038/s41467-022-33885-7

Macosko, E. Z., Basu, A., Satija, R., Nemesh, J., Shekhar, K., Goldman, M., . . . McCarroll, S. A. (2015). Highly parallel genome-wide expression profiling of individual cells using nanoliter droplets. *Cell, 161*(5), 1202-1214. doi:10.1016/j.cell.2015.05.002

Majer, A. D., Paitz, R. T., Tricola, G. M., Geduldig, J. E., Litwa, H. P., Farmer, J. L., . . . Haussmann, M. F. (2023). The response to stressors in adulthood depends on the interaction between prenatal exposure to glucocorticoids and environmental context. *Scientific Reports, 13*(1), 6180. doi:10.1038/s41598-023-33447-x

Makwana, N. (2019). Disaster and its impact on mental health: A narrative review. *Journal of Family Medicine and Primary Care, 8*(10), 3090-3095. doi:10.4103/jfmpc.jfmpc_893_19

Malaspina, D., Owen, M. J., Heckers, S., Tandon, R., Bustillo, J., Schultz, S., . . . Carpenter, W. (2013). Schizoaffective Disorder in the DSM-5. *Schizophrenia Research, 150*(1), 21-25. doi:https://doi.org/10.1016/j.schres.2013.04.026

Malik, J. A., Yaseen, Z., Thotapalli, L., Ahmed, S., Shaikh, M. F., & Anwar, S. (2023). Understanding translational research in schizophrenia: A novel insight into animal models. *Molecular Biology Reports, 50*(4), 3767-3785. doi:10.1007/s11033-023-08241-7

Manolio, T. A., Collins, F. S., Cox, N. J., Goldstein, D. B., Hindorff, L. A., Hunter, D. J., . . . Visscher, P. M. (2009). Finding the missing heritability of complex diseases. *Nature, 461*(7265), 747-753. doi:10.1038/nature08494

Map., A. B. (2019). Human Multiple Cortical Areas SMART-seq - https://portal.brain-map.org/atlases-and-data/rnaseq/human-multiple-cortical-areas-smart-seq.

Marchini, J., Howie, B., Myers, S., McVean, G., & Donnelly, P. (2007). A new multipoint method for genome-wide association studies by imputation of genotypes. *Nat Genet, 39*(7), 906-913. doi:10.1038/ng2088

Markram, H., Toledo-Rodriguez, M., Wang, Y., Gupta, A., Silberberg, G., & Wu, C. (2004). Interneurons of the neocortical inhibitory system. *Nature Reviews Neuroscience, 5*(10), 793-807. doi:10.1038/nrn1519

Marshall, C. R., Howrigan, D. P., Merico, D., Thiruvahindrapuram, B., Wu, W., Greer, D. S., . . . Sebat, J. (2017). Contribution of copy number variants to schizophrenia from a genome-wide study of 41,321 subjects. *Nature Genetics, 49*(1), 27-35. doi:10.1038/ng.3725

Martin, A. R., Stroud, R. E., Abebe, T., Akena, D., Alemayehu, M., Atwoli, L., . . . Chibnik, L. B. (2022). Increasing diversity in genomics requires investment in equitable partnerships and capacity building. *Nature Genetics, 54*(6), 740-745. doi:10.1038/s41588-022-01095-y

Martin, M. *Cutadapt removes adapter sequences from high-throughput sequencing reads*. Retrieved from

Matevossian, A., & Akbarian, S. (2008). Neuronal nuclei isolation from human postmortem brain tissue. *Journal of Visualized Experiments: JoVE*(20), 914. doi:10.3791/914

Matosin, N., Arloth, J., Czamara, D., Edmond, K. Z., Maitra, M., Fröhlich, A. S., . . . Binder, E. B. (2023). Associations of psychiatric disease and ageing with FKBP5 expression converge on superficial layer neurons of the neocortex. *Acta Neuropathologica, 145*(4), 439-459. doi:10.1007/s00401-023-02541-9

McCarthy, T. L., & Centrella, M. (2010). Novel links among Wnt and TGF-βsignaling and Runx2. *Molecular Endocrinology, 24*(3), 587-597. doi:10.1210/me.2009-0379

McCutcheon, R. A., Reis Marques, T., & Howes, O. D. (2020). Schizophrenia—An Overview. *JAMA Psychiatry, 77*(2), 201-210. doi:10.1001/jamapsychiatry.2019.3360

McEwen, B. S., & Akil, H. (2020). Revisiting the Stress Concept: Implications for Affective Disorders. *Journal of Neuroscience, 40*(1), 12-21. doi:10.1523/JNEUROSCI.0733-19.2019

McEwen, B. S., Bowles, N. P., Gray, J. D., Hill, M. N., Hunter, R. G., Karatsoreos, I. N., & Nasca, C. (2015). Mechanisms of stress in the brain. *Nature Neuroscience, 18*(10), 1353-1363. doi:10.1038/nn.4086

McEwen, B. S., Nasca, C., & Gray, J. D. (2016). Stress Effects on Neuronal Structure: Hippocampus, Amygdala, and Prefrontal Cortex. *Neuropsychopharmacology, 41*(1), 3-23. doi:10.1038/npp.2015.171

McGrath, J. J., Lim, C. C. W., Plana-Ripoll, O., Holtz, Y., Agerbo, E., Momen, N. C., . . . de Jonge, P. (2020). Comorbidity within mental disorders: a comprehensive analysis based on 145 990 survey respondents from 27 countries. *Epidemiology and Psychiatric Sciences, 29*, e153. doi:10.1017/S2045796020000633

McIntyre, R. S., Berk, M., Brietzke, E., Goldstein, B. I., López-Jaramillo, C., Kessing, L. V., . . . Mansur, R. B. (2020). Bipolar disorders. *The Lancet, 396*(10265), 1841-1856. doi:10.1016/S0140-6736(20)31544-0

McKay, L. I., & Cidlowski, J. A. (1999). Molecular control of immune/inflammatory responses: interactions between nuclear factor-kappa B and steroid receptor-signaling pathways. *Endocrine Reviews, 20*(4), 435-459. doi:10.1210/edrv.20.4.0375

Mekiten, O., Yitzhaky, A., Gould, N., Rosenblum, K., & Hertzberg, L. (2023). Ribosome subunits are upregulated in brain samples of a subgroup of individuals with schizophrenia: A systematic gene expression meta-analysis. *Journal of Psychiatric Research, 164*, 372-381. doi:10.1016/j.jpsychires.2023.06.013

Merikangas, A. K., Shelly, M., Knighton, A., Kotler, N., Tanenbaum, N., & Almasy, L. (2022). What genes are differentially expressed in individuals with schizophrenia? A systematic review. *Molecular Psychiatry, 27*(3), 1373-1383. doi:10.1038/s41380-021-01420-7

Mesman, S., Bakker, R., & Smidt, M. P. (2020). Tcf4 is required for correct brain development during embryogenesis. *Molecular and Cellular Neuroscience, 106*(April), 103502-103502. doi:10.1016/j.mcn.2020.103502

Michalski, J.-P., & Kothary, R. (2015). Oligodendrocytes in a Nutshell. *Frontiers in Cellular Neuroscience, 9*.

Molyneaux, B. J., Arlotta, P., Menezes, J. R. L., & Macklis, J. D. (2007). Neuronal subtype specification in the cerebral cortex. *Nature Reviews Neuroscience, 8*(6), 427-437. doi:10.1038/nrn2151

Moreno-Rius, J. (2019). The cerebellum under stress. *Frontiers in Neuroendocrinology, 54*, 100774. doi:10.1016/j.yfrne.2019.100774

Müller, M. B., Keck, M. E., Binder, E. B., Kresse, A. E., Hagemeyer, T. P., Landgraf, R., . . . Uhr, M. (2003). ABCBI (MDRI)-Type P-Glycoproteins at the Blood-Brain Barrier Modulate the Activity of the Hypothalamic-Pituitary-Adrenocortical System: Implications for Affective Disorder. *Neuropsychopharmacology, 28*(11), 1991-1999. doi:10.1038/sj.npp.1300257

Müller-Oerlinghausen, B., Berghöfer, A., & Bauer, M. (2002). Bipolar disorder. *The Lancet, 359*(9302), 241-247. doi:https://doi.org/10.1016/S0140-6736(02)07450-0

Mullins, N., Forstner, A. J., O'Connell, K. S., Coombes, B., Coleman, J. R. I., Qiao, Z., . . . Andreassen, O. A. (2021). Genome-wide association study of more than 40,000 bipolar disorder cases provides new insights into the underlying biology. *Nat Genet, 53*(6), 817-829. doi:10.1038/s41588-021-00857-4

Nag, S. (2011). Morphology and Properties of Brain Endothelial Cells. In S. Nag (Ed.), *The Blood-Brain and Other Neural Barriers: Reviews and Protocols* (pp. 3-47). Totowa, NJ: Humana Press.

Nagai, T., Aruga, J., Takada, S., Günther, T., Spörle, R., Schughart, K., & Mikoshiba, K. (1997). The expression of the mouse Zic1, Zic2, and Zic3 gene suggests an essential role for Zic genes in body pattern formation. *Developmental Biology, 182*(2), 299-313. doi:10.1006/dbio.1996.8449

Nagy, C., Maitra, M., Tanti, A., Suderman, M., Théroux, J.-F., Davoli, M. A., . . . Turecki, G. (2020). Single-nucleus transcriptomics of the prefrontal cortex in major depressive disorder implicates oligodendrocyte precursor cells and excitatory neurons. *Nature Neuroscience, 23*(6), 771-781. doi:10.1038/s41593-020-0621-y

Natarajan, A., Yardımcı, G. G., Sheffield, N. C., Crawford, G. E., & Ohler, U. (2012). Predicting cell-type–specific gene expression from regions of open chromatin. *Genome Research, 22*(9), 1711-1722. doi:10.1101/gr.135129.111

Nayak, D., Roth, T. L., & McGavern, D. B. (2014). Microglia Development and Function. *Annual Review of Immunology, 32*(1), 367-402. doi:10.1146/annurev-immunol-032713-120240

Nestler, E. J., & Hyman, S. E. (2010). Animal Models of Neuropsychiatric Disorders. *Nature Neuroscience, 13*(10), 1161-1169. doi:10.1038/nn.2647

Newman, A. M., Liu, C. L., Green, M. R., Gentles, A. J., Feng, W., Xu, Y., . . . Alizadeh, A. A. (2015). Robust enumeration of cell subsets from tissue expression profiles. *Nature Methods, 12*(5), 453-457. doi:10.1038/nmeth.3337

Newson, J. J., Pastukh, V., & Thiagarajan, T. C. (2021). Poor Separation of Clinical Symptom Profiles by DSM-5 Disorder Criteria. *Frontiers in Psychiatry, 12*, 775762. doi:10.3389/fpsyt.2021.775762

Nieuwenhuys, R. (1994). The neocortex. *Anatomy and Embryology, 190*(4), 307-337. doi:10.1007/BF00187291

Nishiyama, A. (2007). Polydendrocytes: NG2 Cells with Many Roles in Development and Repair of the CNS. *The Neuroscientist, 13*(1), 62-76. doi:10.1177/1073858406295586

Ogris, C., Hu, Y., Arloth, J., & Müller, N. S. (2021). Versatile knowledge guided network inference method for prioritizing key regulatory factors in multi-omics data. *Scientific Reports, 11*(1), 1-12. doi:10.1038/s41598-021-85544-4

Ongür, D., Drevets, W. C., & Price, J. L. (1998). Glial reduction in the subgenual prefrontal cortex in mood disorders. *Proc Natl Acad Sci U S A, 95*(22), 13290-13295. doi:10.1073/pnas.95.22.13290

Opel, N., Goltermann, J., Hermesdorf, M., Berger, K., Baune, B. T., & Dannlowski, U. (2020). Cross-Disorder Analysis of Brain Structural Abnormalities in Six Major Psychiatric Disorders: A Secondary Analysis of Mega- and Meta-analytical Findings From the ENIGMA Consortium. *Biological Psychiatry, 88*(9), 678-686. doi:10.1016/j.biopsych.2020.04.027

Padoan, C. S., Garcia, L. F., Crespo, K. C., Longaray, V. K., Martini, M., Contessa, J. C., . . . VS Magalhães, P. (2022). A qualitative study exploring the process of postmortem brain tissue donation after suicide. *Scientific Reports, 12*(1), 4710. doi:10.1038/s41598-022-08729-5

Pariante, C. M., & Miller, A. H. (2001). Glucocorticoid receptors in major depression: relevance to pathophysiology and treatment. *Biological Psychiatry, 49*(5), 391-404. doi:10.1016/S0006-3223(00)01088-X

Parikshak, N. N., Gandal, M. J., & Geschwind, D. H. (2015). Systems biology and gene networks in neurodevelopmental and neurodegenerative disorders. *Nature Reviews Genetics, 16*(8), 441-458. doi:10.1038/nrg3934

Patel, K. R., Cherian, J., Gohil, K., & Atkinson, D. (2014). Schizophrenia: Overview and Treatment Options. *Pharmacy and Therapeutics, 39*(9), 638-645.

Paul, S. M., & Potter, W. Z. (2024). Finding new and better treatments for psychiatric disorders. *Neuropsychopharmacology, 49*(1), 3-9. doi:10.1038/s41386-023-01690-5

Paxinos, G., & Franklin, K. B. (2008). The mouse brain in stereotaxic coordinates. Third. In: Academic Press.

Penner-Goeke, S., Bothe, M., Rek, N., Kreitmaier, P., Pöhlchen, D., Kühnel, A., . . . Binder, E. B. (2023). High-throughput screening of glucocorticoid-induced enhancer activity reveals mechanisms of stress-related psychiatric disorders. *Proceedings of the National Academy of Sciences, 120*(49), e2305773120. doi:10.1073/pnas.2305773120

Perduca, V., Omichessan, H., Baglietto, L., & Severi, G. (2018). Mutational and epigenetic signatures in cancer tissue linked to environmental exposures and lifestyle. *Current Opinion in Oncology, 30*(1), 61-67. doi:10.1097/CCO.0000000000000418

Persson, E., Castresana-Aguirre, M., Buzzao, D., Guala, D., & Sonnhammer, E. L. L. (2021). FunCoup 5: Functional Association Networks in All Domains of Life, Supporting Directed Links and Tissue-Specificity. *Journal of Molecular Biology, 433*(11), 166835-166835. doi:10.1016/j.jmb.2021.166835

Perugi, G., Medda, P., Toni, C., Mariani, M. G., Socci, C., & Mauri, M. (2017). The Role of Electroconvulsive Therapy (ECT) in Bipolar Disorder: Effectiveness in 522 Patients with Bipolar Depression, Mixed-state, Mania and Catatonic Features. *Current Neuropharmacology, 15*(3), 359-371. doi:10.2174/1570159X14666161017233642

Petherick, K. J., Williams, A. C., Lane, J. D., Ordóñez-Morán, P., Huelsken, J., Collard, T. J., . . . Greenhough, A. (2013). Autolysosomal β-catenin degradation regulates Wnt-autophagy-p62 crosstalk. *EMBO Journal, 32*(13), 1903-1916. doi:10.1038/emboj.2013.123

Philips, T., & Rothstein, J. D. (2017). Oligodendroglia: metabolic supporters of neurons. *The Journal of Clinical Investigation, 127*(9), 3271-3280. doi:10.1172/JCI90610

Phuc Le, P., Friedman, J. R., Schug, J., Brestelli, J. E., Parker, J. B., Bochkis, I. M., & Kaestner, K. H. (2005). Glucocorticoid receptor-dependent gene regulatory networks. *PLOS Genetics, 1*(2), e16. doi:10.1371/journal.pgen.0010016

Picelli, S., Faridani, O. R., Björklund, Å. K., Winberg, G., Sagasser, S., & Sandberg, R. (2014). Full-length RNA-seq from single cells using Smart-seq2. *Nature Protocols, 9*(1), 171-181. doi:10.1038/nprot.2014.006

Pierson, E., Koller, D., Battle, A., & Mostafavi, S. (2015). Sharing and Specificity of Co-expression Networks across 35 Human Tissues. *PLoS Computational Biology, 11*(5), 1-19. doi:10.1371/journal.pcbi.1004220

Polderman, T. J. C., Benyamin, B., de Leeuw, C. A., Sullivan, P. F., van Bochoven, A., Visscher, P. M., & Posthuma, D. (2015). Meta-analysis of the heritability of human traits based on fifty years of twin studies. *Nature Genetics, 47*(7), 702-709. doi:10.1038/ng.3285

Porcu, E., Sadler, M. C., Lepik, K., Auwerx, C., Wood, A. R., Weihs, A., . . . Kutalik, Z. (2021). Differentially expressed genes reflect disease-induced rather than disease-causing changes in the transcriptome. *Nature Communications, 12*(1), 5647. doi:10.1038/s41467-021-25805-y

Price, A. J., Jaffe, A. E., & Weinberger, D. R. (2021). Cortical cellular diversity and development in schizophrenia. *Molecular Psychiatry, 26*(1), 203-217. doi:10.1038/s41380-020-0775-8

Purcell, S., Neale, B., Todd-Brown, K., Thomas, L., Ferreira, M. A., Bender, D., . . . Sham, P. C. (2007). PLINK: a tool set for whole-genome association and population-based linkage analyses. *Am J Hum Genet, 81*(3), 559-575. doi:10.1086/519795

Purcell, S. M., Wray, N. R., Stone, J. L., Visscher, P. M., O'Donovan, M. C., Sullivan, P. F., & Sklar, P. (2009). Common polygenic variation contributes to risk of schizophrenia and bipolar disorder. *Nature, 460*(7256), 748-752. doi:10.1038/nature08185

R: A language and environment for statistical computing. R Foundation for Statistical Computing, Vienna, Austria. (2021).

Rajkowska, G., Miguel-Hidalgo, J. J., Wei, J., Dilley, G., Pittman, S. D., Meltzer, H. Y., . . . Stockmeier, C. A. (1999). Morphometric evidence for neuronal and glial prefrontal cell pathology in major depression. *Biol Psychiatry, 45*(9), 1085-1098. doi:10.1016/s0006-3223(99)00041-4

Ramaker, R. C., Bowling, K. M., Lasseigne, B. N., Hagenauer, M. H., Hardigan, A. A., Davis, N. S., . . . Myers, R. M. (2017). Post-mortem molecular profiling of three psychiatric disorders. *Genome Medicine, 9*(1), 72. doi:10.1186/s13073-017-0458-5

Rasband, M. N. (2016). Glial Contributions to Neural Function and Disease. *Mol Cell Proteomics, 15*(2), 355-361. doi:10.1074/mcp.R115.053744

Reble, E., Dineen, A., & Barr, C. L. (2018). The contribution of alternative splicing to genetic risk for psychiatric disorders. *Genes, Brain, and Behavior, 17*(3), e12430. doi:10.1111/gbb.12430

Reske, J. J., Wilson, M. R., & Chandler, R. L. (2020). ATAC-seq normalization method can significantly affect differential accessibility analysis and interpretation. *Epigenetics & Chromatin, 13*(1), 22. doi:10.1186/s13072-020-00342-y

Ribeiro, P. F., Ventura-Antunes, L., Gabi, M., Mota, B., Grinberg, L. T., Farfel, J. M., . . . Herculano-Houzel, S. (2013). The human cerebral cortex is neither one nor many: neuronal distribution reveals two quantitatively different zones in the gray matter, three in the white matter, and explains local variations in cortical folding. *Front Neuroanat, 7*, 28. doi:10.3389/fnana.2013.00028

Richetto, J., & Meyer, U. (2021). Epigenetic Modifications in Schizophrenia and Related Disorders: Molecular Scars of Environmental Exposures and Source of Phenotypic Variability. *Biological Psychiatry, 89*(3), 215-226. doi:10.1016/j.biopsych.2020.03.008

Richtand, N. M., Harvey, B. H., & Hoffman, K. L. (2022). Editorial: Animal Models in Psychiatry: Translating Animal Behavior to an Improved Understanding and Treatment of Psychiatric Disorders. *Frontiers in Psychiatry, 13*.

The right treatment for each patient: unlocking the potential of personalized psychiatry. (2023). *Nature Mental Health, 1*(9), 607-608. doi:10.1038/s44220-023-00131-y

Ripke, S., Neale, B. M., Corvin, A., Walters, J. T. R., Farh, K.-H., Holmans, P. A., . . . Consortium, P. E. I. (2014). Biological insights from 108 schizophrenia-associated genetic loci. *Nature, 511*(7510), 421-427. doi:10.1038/nature13595

Ritchie, M. E., Phipson, B., Wu, D., Hu, Y., Law, C. W., Shi, W., & Smyth, G. K. (2015). limma powers differential expression analyses for RNA-sequencing and microarray studies. *Nucleic Acids Research, 43*(7), e47. doi:10.1093/nar/gkv007

Rodrigues-Neves, A. C., Ambrósio, A. F., & Gomes, C. A. (2022). Microglia sequelae: brain signature of innate immunity in schizophrenia. *Translational Psychiatry, 12*(1), 1-16. doi:10.1038/s41398-022-02197-1

Romeo, R. D. (2010). Stress and Brain Morphology. In G. F. Koob, M. L. Moal, & R. F. Thompson (Eds.), *Encyclopedia of Behavioral Neuroscience* (pp. 304-309). Oxford: Academic Press.

Romero, L. M. (2004). Physiological stress in ecology: lessons from biomedical research. *Trends in Ecology & Evolution, 19*(5), 249-255. doi:10.1016/j.tree.2004.03.008

Roshanaei-Moghaddam, B., & Katon, W. (2009). Premature mortality from general medical illnesses among persons with bipolar disorder: a review. *Psychiatric Services (Washington, D.C.), 60*(2), 147-156. doi:10.1176/ps.2009.60.2.147

Rossner, M. J., Hirrlinger, J., Wichert, S. P., Boehm, C., Newrzella, D., Hiemisch, H., . . . Nave, K.-A. (2006). Global Transcriptome Analysis of Genetically Identified Neurons in the Adult Cortex. *Journal of Neuroscience, 26*(39), 9956-9966. doi:10.1523/JNEUROSCI.0468-06.2006

Rouillard, A. D., Gundersen, G. W., Fernandez, N. F., Wang, Z., Monteiro, C. D., McDermott, M. G., & Ma'ayan, A. (2016). The harmonizome: a collection of processed datasets gathered to serve and mine knowledge about genes and proteins. *Database : the journal of biological databases and curation, 2016*, 1-16. doi:10.1093/database/baw100

Ruzicka, W. B., Mohammadi, S., Fullard, J. F., Davila-Velderrain, J., Subburaju, S., Tso, D. R., . . . Kellis, M. (2022). Single-cell multi-cohort dissection of the schizophrenia transcriptome. *medRxiv*, 2022.2008.2031.22279406. doi:10.1101/2022.08.31.22279406

Saint-Antoine, M. M., & Singh, A. (2020). Network inference in systems biology: recent developments, challenges, and applications. *Current Opinion in Biotechnology, 63*, 89-98. doi:10.1016/j.copbio.2019.12.002

Santoro, B., Liu, D. T., Yao, H., Bartsch, D., Kandel, E. R., Siegelbaum, S. A., & Tibbs, G. R. (1998). Identification of a Gene Encoding a Hyperpolarization-Activated Pacemaker Channel of Brain. *Cell, 93*(5), 717-729. doi:10.1016/S0092-8674(00)81434-8

Sapolsky, R. M., Romero, L. M., & Munck, A. U. (2000). How Do Glucocorticoids Influence Stress Responses? Integrating Permissive, Suppressive, Stimulatory, and Preparative Actions*. *Endocrine Reviews, 21*(1), 55-89. doi:10.1210/edrv.21.1.0389

Sathyanarayanan, A., Mueller, T. T., Ali Moni, M., Schueler, K., Baune, B. T., Lio, P., . . . Xicota, L. (2023). Multi-omics data integration methods and their applications in psychiatric disorders. *European Neuropsychopharmacology, 69*, 26-46. doi:10.1016/j.euroneuro.2023.01.001

Sato, K., Mano, T., Matsuda, H., Senda, M., Ihara, R., Suzuki, K., . . . Iwata, A. (2019). Visualizing modules of coordinated structural brain atrophy during the course of conversion to Alzheimer's disease by applying methodology from gene co-expression analysis. *NeuroImage: Clinical, 24*(July), 101957-101957. doi:10.1016/j.nicl.2019.101957

Satpathy, A. T., Granja, J. M., Yost, K. E., Qi, Y., Meschi, F., McDermott, G. P., . . . Chang, H. Y. (2019). Massively parallel single-cell chromatin landscapes of human immune cell development and intratumoral T cell exhaustion. *Nature Biotechnology, 37*(8), 925-936. doi:10.1038/s41587-019-0206-z

Saveanu, R. V., & Nemeroff, C. B. (2012). Etiology of Depression: Genetic and Environmental Factors. *Psychiatric Clinics of North America, 35*(1), 51-71. doi:10.1016/j.psc.2011.12.001

Sayols, S. (2023). rrvgo: a Bioconductor package for interpreting lists of Gene Ontology terms. *microPublication Biology*. doi:10.17912/micropub.biology.000811

Schmidt, M. V., Wang, X.-D., & Meijer, O. C. (2011). Early life stress paradigms in rodents: potential animal models of depression? *Psychopharmacology, 214*(1), 131-140. doi:10.1007/s00213-010-2096-0

Schneiderman, N., Ironson, G., & Siegel, S. D. (2005). STRESS AND HEALTH: Psychological, Behavioral, and Biological Determinants. *Annual review of clinical psychology, 1*, 607-628. doi:10.1146/annurev.clinpsy.1.102803.144141

Seifuddin, F., Pirooznia, M., Judy, J. T., Goes, F. S., Potash, J. B., & Zandi, P. P. (2013). Systematic review of genome-wide gene expression studies of bipolar disorder. *BMC Psychiatry, 13*(1), 213. doi:10.1186/1471-244X-13-213

Sey, N. Y. A., Hu, B., Mah, W., Fauni, H., McAfee, J. C., Rajarajan, P., . . . Won, H. (2020). A computational tool (H-MAGMA) for improved prediction of brain-disorder risk genes by incorporating brain chromatin interaction profiles. *Nat Neurosci, 23*(4), 583-593. doi:10.1038/s41593-020-0603-0

Shlyueva, D., Stampfel, G., & Stark, A. (2014). Transcriptional enhancers: from properties to genome-wide predictions. *Nature Reviews Genetics, 15*(4), 272-286. doi:10.1038/nrg3682

Sidoryk-Wegrzynowicz, M., Wegrzynowicz, M., Lee, E., Bowman, A. B., & Aschner, M. (2011). Role of Astrocytes in Brain Function and Disease. *Toxicologic Pathology, 39*(1), 115-123. doi:10.1177/0192623310385254

Siletti, K., Hodge, R., Mossi Albiach, A., Lee, K. W., Ding, S.-L., Hu, L., . . . Linnarsson, S. (2023). Transcriptomic diversity of cell types across the adult human brain. *Science, 382*(6667), eadd7046. doi:10.1126/science.add7046

Simons, M., & Nave, K.-A. (2016). Oligodendrocytes: Myelination and Axonal Support. *Cold Spring Harbor Perspectives in Biology, 8*(1), a020479. doi:10.1101/cshperspect.a020479

Sinclair, D., Fillman, S. G., Webster, M. J., & Weickert, C. S. (2013). Dysregulation of glucocorticoid receptor co-factors FKBP5, BAG1 and PTGES3 in prefrontal cortex in psychotic illness. *Scientific Reports, 3*(1), 3539. doi:10.1038/srep03539

Singh, B., Olds, T., Curtis, R., Dumuid, D., Virgara, R., Watson, A., . . . Maher, C. (2023). Effectiveness of physical activity interventions for improving depression, anxiety and distress: an overview of systematic reviews. *British Journal of Sports Medicine, 57*(18), 1203-1209. doi:10.1136/bjsports-2022-106195

Sirp, A., Roots, K., Nurm, K., Tuvikene, J., Sepp, M., & Timmusk, T. (2021). Functional consequences of TCF4 missense substitutions associated with Pitt-Hopkins syndrome , mild intellectual disability , and schizophrenia. *1*, 1-16. doi:10.1016/j.jbc.2021.101381

Sivakumaran, S., Agakov, F., Theodoratou, E., Prendergast, J. G., Zgaga, L., Manolio, T., . . . Campbell, H. (2011). Abundant pleiotropy in human complex diseases and traits. *American Journal of Human Genetics, 89*(5), 607-618. doi:10.1016/j.ajhg.2011.10.004

Slota, J. A., Sajesh, B. V., Frost, K. F., Medina, S. J., & Booth, S. A. (2022). Dysregulation of neuroprotective astrocytes, a spectrum of microglial activation states, and altered hippocampal neurogenesis are revealed by single-cell RNA sequencing in prion disease. *Acta Neuropathologica Communications, 10*(1), 161. doi:10.1186/s40478-022-01450-4

Smith, S. M., & Vale, W. W. (2006). The role of the hypothalamic-pituitary-adrenal axis in neuroendocrine responses to stress. *Dialogues in Clinical Neuroscience, 8*(4), 383-395.

Smith, T., Heger, A., & Sudbery, I. (2017). UMI-tools: Modeling sequencing errors in Unique Molecular Identifiers to improve quantification accuracy. *Genome Research, 27*(3), 491-499. doi:10.1101/gr.209601.116

Smoller, J. W., Andreassen, O. A., Edenberg, H. J., Faraone, S. V., Glatt, S. J., & Kendler, K. S. (2019). Psychiatric genetics and the structure of psychopathology. *Molecular Psychiatry, 24*(3), 409-420. doi:10.1038/s41380-017-0010-4

Soliman, M. A., Aboharb, F., Zeltner, N., & Studer, L. (2017). Pluripotent stem cells in neuropsychiatric disorders. *Molecular Psychiatry, 22*(9), 1241-1249. doi:10.1038/mp.2017.40

Sollis, E., Mosaku, A., Abid, A., Buniello, A., Cerezo, M., Gil, L., . . . Harris, Laura W. (2022). The NHGRI-EBI GWAS Catalog: knowledgebase and deposition resource. *Nucleic Acids Research, 51*(D1), D977-D985. doi:10.1093/nar/gkac1010

Sondka, Z., Bamford, S., Cole, C. G., Ward, S. A., Dunham, I., & Forbes, S. A. (2018). The COSMIC Cancer Gene Census: describing genetic dysfunction across all human cancers. *Nature Reviews Cancer, 18*(11), 696-705. doi:10.1038/s41568-018-0060-1

Spruston, N. (2008). Pyramidal neurons: dendritic structure and synaptic integration. *Nature Reviews Neuroscience, 9*(3), 206-221. doi:10.1038/nrn2286

Squair, J. W., Gautier, M., Kathe, C., Anderson, M. A., James, N. D., Hutson, T. H., . . . Courtine, G. (2021). Confronting false discoveries in single-cell differential expression. *Nature Communications, 12*(1), 5692. doi:10.1038/s41467-021-25960-2

Stan, A. D., Ghose, S., Gao, X.-M., Roberts, R. C., Lewis-Amezcua, K., Hatanpaa, K. J., & Tamminga, C. A. (2006). Human postmortem tissue: What quality markers matter? *Brain Research, 1123*(1), 1-11. doi:10.1016/j.brainres.2006.09.025

Starks, R. R., Biswas, A., Jain, A., & Tuteja, G. (2019). Combined analysis of dissimilar promoter accessibility and gene expression profiles identifies tissue-specific genes and actively repressed networks. *Epigenetics & Chromatin, 12*(1), 16. doi:10.1186/s13072-019-0260-2

Subramanian, A., Tamayo, P., Mootha, V. K., Mukherjee, S., Ebert, B. L., Gillette, M. A., . . . Mesirov, J. P. (2005). Gene set enrichment analysis: A knowledge-based approach for interpreting genome-wide expression profiles. *Proceedings of the National Academy of Sciences of the United States of America, 102*(43), 15545-15550. doi:10.1073/pnas.0506580102

Sullivan, P. F. (2010). The psychiatric GWAS consortium: big science comes to psychiatry. *Neuron, 68*(2), 182-186. doi:10.1016/j.neuron.2010.10.003

Sullivan, P. F., & Geschwind, D. H. (2019). Defining the Genetic, Genomic, Cellular, and Diagnostic Architectures of Psychiatric Disorders. *Cell, 177*(1), 162-183. doi:10.1016/j.cell.2019.01.015

Tasic, B., Yao, Z., Graybuck, L. T., Smith, K. A., Nguyen, T. N., Bertagnolli, D., . . . Zeng, H. (2018). Shared and distinct transcriptomic cell types across neocortical areas. *Nature, 563*(7729), 72-78. doi:10.1038/s41586-018-0654-5

Teixeira, J. R., Szeto, R. A., Carvalho, V. M. A., Muotri, A. R., & Papes, F. (2021). Transcription factor 4 and its association with psychiatric disorders. *Translational Psychiatry, 11*(1). doi:10.1038/s41398-020-01138-0

Torshizi, A. D., Armoskus, C., Zhang, H., Forrest, M. P., Zhang, S., Souaiaia, T., . . . Wang, K. (2019). Deconvolution of transcriptional networks identifies TCF4 as a master regulator in schizophrenia. *Science Advances, 5*(9). doi:10.1126/sciadv.aau4139

Traag, V. A., Waltman, L., & van Eck, N. J. (2019). From Louvain to Leiden: guaranteeing well-connected communities. *Scientific Reports, 9*(1), 5233. doi:10.1038/s41598-019-41695-z

Trubetskoy, V., Pardiñas, A. F., Qi, T., Panagiotaropoulou, G., Awasthi, S., Bigdeli, T. B., . . . Bertolino, A. (2022). Mapping genomic loci implicates genes and synaptic biology in schizophrenia. *Nature, 604*(7906), 502-508. doi:10.1038/s41586-022-04434-5

Tsompana, M., & Buck, M. J. (2014). Chromatin accessibility: a window into the genome. *Epigenetics & Chromatin, 7*(1), 33. doi:10.1186/1756-8935-7-33

Tyner, S., Briatte, F., & Hofmann, H. (2017). Network Visualization with ggplot2. *The R Journal, 9*(1), 27-59. doi:https://doi.org/10.32614/RJ-2017-023

Uher, R. (2014). Gene–Environment Interactions in Severe Mental Illness. *Frontiers in Psychiatry, 5*.

Uhr, M., Holsboer, F., & Müller, M. B. (2002). Penetration of endogenous steroid hormones corticosterone, cortisol, aldosterone and progesterone into the brain is enhanced in mice deficient for both mdr1a and mdr1b P-glycoproteins. *Journal of Neuroendocrinology, 14*(9), 753-759. doi:10.1046/j.1365-2826.2002.00836.x

Vancampfort, D., Correll, C. U., Galling, B., Probst, M., De Hert, M., Ward, P. B., . . . Stubbs, B. (2016). Diabetes mellitus in people with schizophrenia, bipolar disorder and major depressive disorder: a systematic review and large scale meta-analysis. *World psychiatry: official journal of the World Psychiatric Association (WPA), 15*(2), 166-174. doi:10.1002/wps.20309

Velmeshev, D., Schirmer, L., Jung, D., Haeussler, M., Perez, Y., Mayer, S., . . . Kriegstein, A. R. (2019). Single-cell genomics identifies cell type-specific molecular changes in autism. *Science, 364*(6441), 685-689. doi:10.1126/science.aav8130

Vieta, E., Berk, M., Schulze, T. G., Carvalho, A. F., Suppes, T., Calabrese, J. R., . . . Grande, I. (2018). Bipolar disorders. *Nature Reviews Disease Primers, 4*(1), 1-16. doi:10.1038/nrdp.2018.8

Vigo, D., Thornicroft, G., & Atun, R. (2016). Estimating the true global burden of mental illness. *The Lancet Psychiatry, 3*(2), 171-178. doi:10.1016/S2215-0366(15)00505-2

Vindegaard, N., & Benros, M. E. (2020). COVID-19 pandemic and mental health consequences: Systematic review of the current evidence. *Brain, Behavior, and Immunity, 89*, 531-542. doi:10.1016/j.bbi.2020.05.048

Volkmann, P., Stephan, M., Krackow, S., Jensen, N., & Rossner, M. J. (2021). PsyCoP – A Platform for Systematic Semi-Automated Behavioral and Cognitive Profiling Reveals Gene and Environment Dependent Impairments of Tcf4 Transgenic Mice Subjected to Social Defeat. *Frontiers in Behavioral Neuroscience, 14*(January), 1-15. doi:10.3389/fnbeh.2020.618180

von Bartheld, C. S., Bahney, J., & Herculano-Houzel, S. (2016). The search for true numbers of neurons and glial cells in the human brain: A review of 150 years of cell counting. *J Comp Neurol, 524*(18), 3865-3895. doi:10.1002/cne.24040

Vos, T., Lim, S. S., Abbafati, C., Abbas, K. M., Abbasi, M., Abbasifard, M., . . . Murray, C. J. L. (2020). Global burden of 369 diseases and injuries in 204 countries and territories, 1990–2019: a systematic analysis for the Global Burden of Disease Study 2019. *The Lancet, 396*(10258), 1204-1222. doi:10.1016/S0140-6736(20)30925-9

Võsa, U., Claringbould, A., Westra, H.-J., Bonder, M. J., Deelen, P., Zeng, B., . . . Franke, L. (2021). Large-scale cis- and trans-eQTL analyses identify thousands of genetic loci and polygenic scores that regulate blood gene expression. *Nature Genetics, 53*(9), 1300-1310. doi:10.1038/s41588-021-00913-z

Wagner, A., Regev, A., & Yosef, N. (2016). Revealing the vectors of cellular identity with single-cell genomics. *Nature Biotechnology, 34*(11), 1145-1160. doi:10.1038/nbt.3711

Waltman, L., & van Eck, N. J. (2013). A smart local moving algorithm for large-scale modularity-based community detection. *The European Physical Journal B, 86*(11), 471. doi:10.1140/epjb/e2013-40829-0

Wang, Z., Gerstein, M., & Snyder, M. (2009). RNA-Seq: a revolutionary tool for transcriptomics. *Nat Rev Genet, 10*(1), 57-63. doi:10.1038/nrg2484

Watanabe, K., Taskesen, E., Van Bochoven, A., & Posthuma, D. (2017). Functional mapping and annotation of genetic associations with FUMA. *Nature Communications, 8*(1). doi:10.1038/s41467-017-01261-5

Weaver, I. C. G., Cervoni, N., Champagne, F. A., D'Alessio, A. C., Sharma, S., Seckl, J. R., . . . Meaney, M. J. (2004). Epigenetic programming by maternal behavior. *Nature Neuroscience, 7*(8), 847-854. doi:10.1038/nn1276

Weaver, I. C. G., Meaney, M. J., & Szyf, M. (2006). Maternal care effects on the hippocampal transcriptome and anxiety-mediated behaviors in the offspring that are reversible in adulthood. *Proceedings of the National Academy of Sciences of the United States of America, 103*(9), 3480-3485. doi:10.1073/pnas.0507526103

Weickert, T. W., Jacomb, I., Lenroot, R., Lappin, J., Weinberg, D., Brooks, W. S., . . . Shannon Weickert, C. (2024). Adjunctive canakinumab reduces peripheral inflammation markers and improves positive symptoms in people with schizophrenia and inflammation: A randomized control trial. *Brain, Behavior, and Immunity, 115*, 191-200. doi:10.1016/j.bbi.2023.10.012

Weikum, E. R., Knuesel, M. T., Ortlund, E. A., & Yamamoto, K. R. (2017). Glucocorticoid receptor control of transcription : precision and plasticity via allostery. *Nature Reviews, 18*, 159-174. doi:10.1038/nrm.2016.152

Wilkinson, P. O., & Goodyer, I. M. (2011). Childhood adversity and allostatic overload of the hypothalamic-pituitary-adrenal axis: a vulnerability model for depressive disorders. *Development and Psychopathology, 23*(4), 1017-1037. doi:10.1017/S0954579411000472

Wingender, E., Dietze, P., Karas, H., & Knüppel, R. (1996). TRANSFAC: A Database on Transcription Factors and Their DNA Binding Sites. *Nucleic Acids Research, 24*(1), 238-241. doi:10.1093/nar/24.1.238

Wolf, F. A., Angerer, P., & Theis, F. J. (2018). SCANPY: large-scale single-cell gene expression data analysis. *Genome Biology, 19*(1), 15. doi:10.1186/s13059-017-1382-0

Wong, Y. Y., Harbison, J. E., Hope, C. M., Gundsambuu, B., Brown, K. A., Wong, S. W., . . . Barry, S. C. (2023). Parallel recovery of chromatin accessibility and gene expression dynamics from frozen human regulatory T cells. *Scientific Reports, 13*(1), 5506. doi:10.1038/s41598-023-32256-6

Worf, K., Matosin, N., Gerstner, N., Fröhlich, A. S., Koller, A. C., Degenhardt, F., . . . Mueller, N. S. (2022). Variant-risk-exon interplay impacts circadian rhythm and dopamine signaling pathway in severe psychiatric disorders. doi:10.1101/2022.08.09.22278128

Wu, T., Hu, E., Xu, S., Chen, M., Guo, P., Dai, Z., . . . Yu, G. (2021). clusterProfiler 4.0: A universal enrichment tool for interpreting omics data. *The Innovation, 2*(3). doi:10.1016/j.xinn.2021.100141

Xiao, Y., & Czopka, T. (2023). Myelination-independent functions of oligodendrocyte precursor cells in health and disease. *Nature Neuroscience, 26*(10), 1663-1669. doi:10.1038/s41593-023-01423-3

Xu, C., Lopez, R., Mehlman, E., Regier, J., Jordan, M. I., & Yosef, N. (2021). Probabilistic harmonization and annotation of single-cell transcriptomics data with deep generative models. *Molecular Systems Biology, 17*(1), e9620. doi:10.15252/msb.20209620

Yamamuro, K., Kimoto, S., Rosen, K. M., Kishimoto, T., & Makinodan, M. (2015). Potential primary roles of glial cells in the mechanisms of psychiatric disorders. *Frontiers in Cellular Neuroscience, 9*, 154. doi:10.3389/fncel.2015.00154

Yan, L., Ma, C., Wang, D., Hu, Q., Qin, M., Conroy, J. M., . . . Liu, S. (2012). OSAT: a tool for sample-to-batch allocations in genomics experiments. *BMC Genomics, 13*(1), 689. doi:10.1186/1471-2164-13-689

Yang, J., Zeng, J., Goddard, M. E., Wray, N. R., & Visscher, P. M. (2017). Concepts, estimation and interpretation of SNP-based heritability. *Nature Genetics, 49*(9), 1304-1310. doi:10.1038/ng.3941

Yengo, L., Vedantam, S., Marouli, E., Sidorenko, J., Bartell, E., Sakaue, S., . . . Bisgaard, H. (2022). A saturated map of common genetic variants associated with human height. *Nature, 610*(7933), 704-712. doi:10.1038/s41586-022-05275-y

Yu, G., Wang, L. G., Han, Y., & He, Q. Y. (2012). clusterProfiler: an R package for comparing biological themes among gene clusters. *Omics, 16*(5), 284-287. doi:10.1089/omi.2011.0118

Zhang, C.-Y., Xiao, X., Zhang, Z., Hu, Z., & Li, M. (2022). An alternative splicing hypothesis for neuropathology of schizophrenia: evidence from studies on historical candidate genes and multi-omics data. *Molecular Psychiatry, 27*(1), 95-112. doi:10.1038/s41380-021-01037-w

Zhang, Y., Liu, T., Meyer, C. A., Eeckhoute, J., Johnson, D. S., Bernstein, B. E., . . . Liu, X. S. (2008). Model-based Analysis of ChIP-Seq (MACS). *Genome Biology, 9*(9), R137. doi:10.1186/gb-2008-9-9-r137

Zhang, Y., You, X., Li, S., Long, Q., Zhu, Y., Teng, Z., & Zeng, Y. (2020). Peripheral Blood Leukocyte RNA-Seq Identifies a Set of Genes Related to Abnormal Psychomotor Behavior Characteristics in Patients with Schizophrenia. *Medical Science Monitor : International Medical Journal of Experimental and Clinical Research, 26*, e922426-922421-e922426-922431. doi:10.12659/MSM.922426

Zheng, G. X. Y., Terry, J. M., Belgrader, P., Ryvkin, P., Bent, Z. W., Wilson, R., . . . Bielas, J. H. (2017). Massively parallel digital transcriptional profiling of single cells. *Nature Communications, 8*(1), 14049. doi:10.1038/ncomms14049

Zhou, Y., Xiong, L., Chen, J., & Wang, Q. (2023). Integrative Analyses of scRNA-seq, Bulk mRNA-seq, and DNA Methylation Profiling in Depressed Suicide Brain Tissues. *International Journal of Neuropsychopharmacology*, pyad057. doi:10.1093/ijnp/pyad057

Zimmerman, K. D., Espeland, M. A., & Langefeld, C. D. (2021). A practical solution to pseudoreplication bias in single-cell studies. *Nature Communications, 12*(1), 738. doi:10.1038/s41467-021-21038-1

Zimmermann, C. A., Arloth, J., Santarelli, S., Löschner, A., Weber, P., Schmidt, M. V., . . . Binder, E. B. (2019). Stress dynamically regulates co-expression networks of glucocorticoid receptor-dependent MDD and SCZ risk genes. *Translational Psychiatry, 9*(1), 1-11. doi:10.1038/s41398-019-0373-1

Zlokovic, B. V. (2008). The Blood-Brain Barrier in Health and Chronic Neurodegenerative Disorders. *Neuron, 57*(2), 178-201. doi:10.1016/j.neuron.2008.01.003

# Appendix A Supplementary Material

## A.1 Supplementary Figures

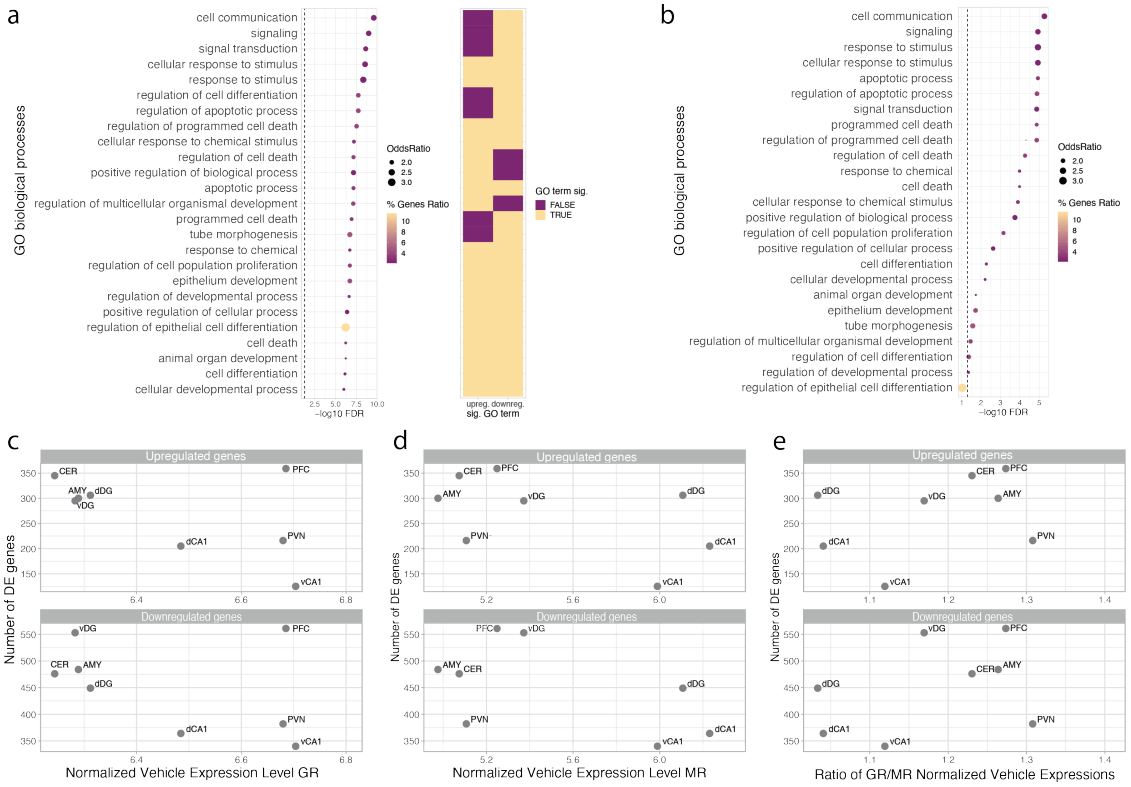


**Supplementary Figure 1. Enrichments for commonly dysregulated genes of all brain regions and patterns of GR and MR expression.** (a-b) Enrichment analysis of GO terms (biological processes) in the 172 shared DE genes (a) and 7 shared differential hub genes (b) across all eight brain regions. Color indicates gene ratio and dot size represents the respective odds ratio. The heatmap in (a) indicates if the respective term is also significant for up- or downregulated genes only. (c-d) Number of DE genes for each brain region plotted against the normalized expression level of GR (c) and MR (d) for up- and downregulated genes separately. (e) Number of DE genes for each brain region plotted against the ratio of the normalized expression levels of GR over MR.

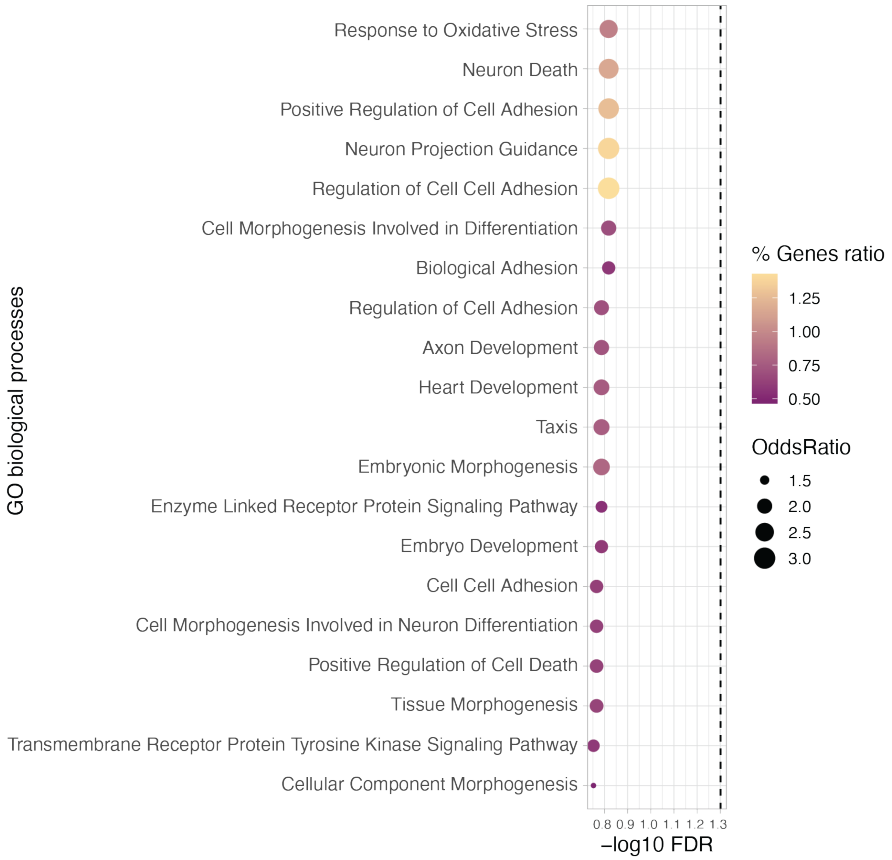


**Supplementary Figure 2. Enrichment analysis for unique DE genes in the vCA1.** Genes uniquely differentially expressed in vCA1 are not significantly enriched for any GO terms (biological processes). Color indicates gene ratio and dot size represents the respective odds ratio.

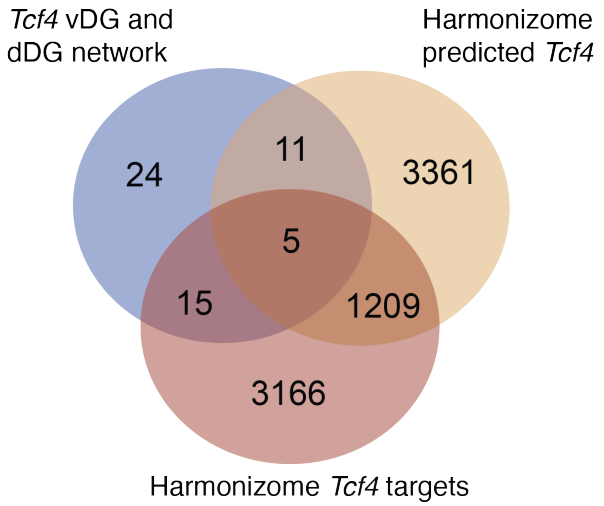


**Supplementary Figure 3. *Tcf4* cDG and dDG network members.** Overlap of genes that are members of the differential vDG and dDG *Tcf4* network with data from the CHEA (Lachmann et al., 2010), TRANSFAC (Wingender et al., 1996) and MotifMap (Y. Liu et al., 2017) transcription factor target databases and from the Pathway commons protein-protein interactions database (Cerami et al., 2010) collected from Harmonizome (Rouillard et al., 2016).

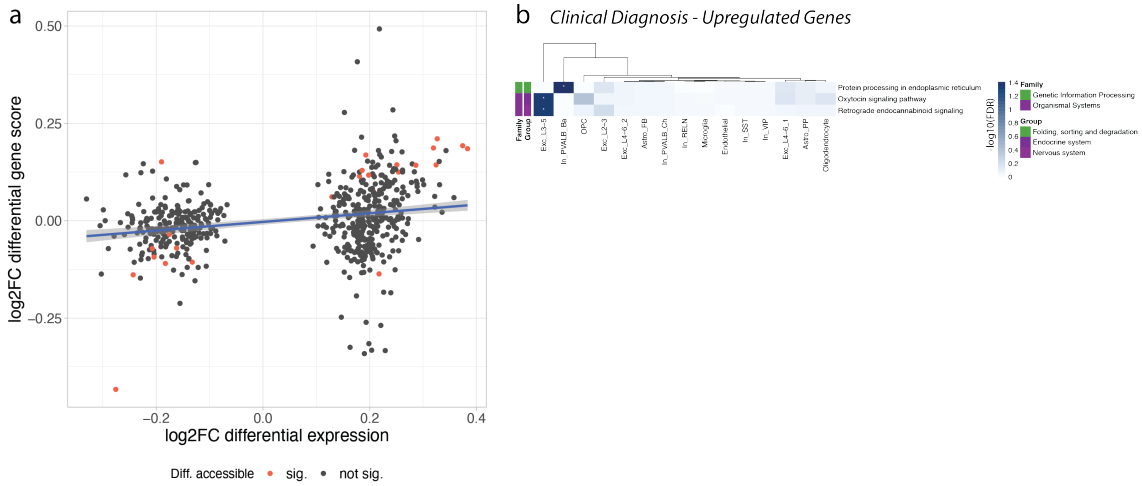


**Supplementary Figure 4. Epigenomic differences between psychiatric cases and controls.** (a) Dotplot showing $\log_2$-transformed fold changes in both differential expression and accessibility for all DE genes across cell types, with color highlighting significance within the same cell type. A blue line indicates the linear regression fit to the data. (b) Heatmap displaying the findings from KEGG pathway enrichment analysis conducted on the 250 most upregulated genes for each cell type. The heatmap displays all pathways that have shown significant enrichment in at least one cell type. The intensity of color correlates with the -$\log_{10}$-transformed FDR values, with asterisks indicating significance (FDR ≤ 0.05). Pathway classifications are color-coded on the left of each heatmap to indicate the specific pathway group and family. K-means clustering dendrograms are provided to show how cell types group together based on their pathway enrichment profiles. There was no significant enrichment of pathways among downregulated DA genes.

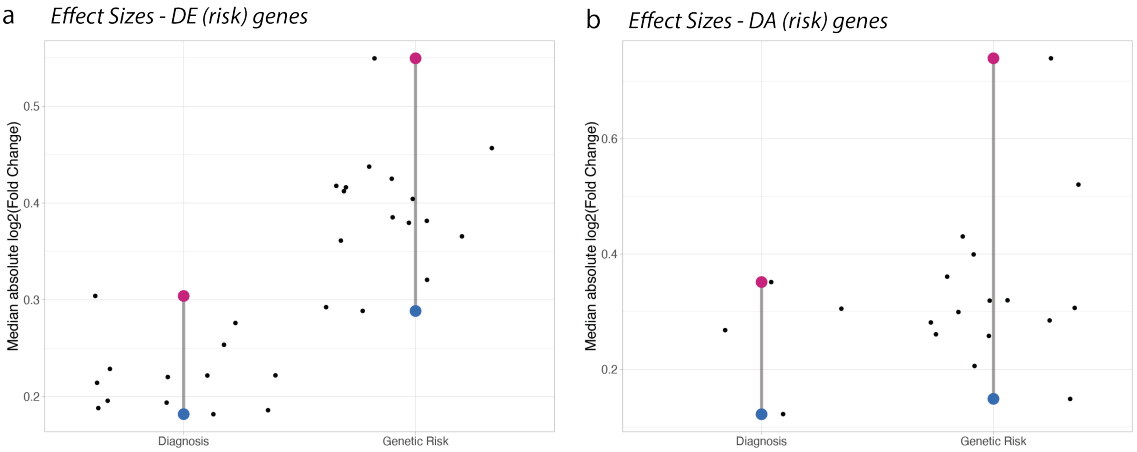


**Supplementary Figure 5. Variability of effect sizes associated with clinical diagnoses and genetic risk.** (a-b) Visualizations of the variability of absolute median $\log_2$-transformed fold changes for each cell type, for DE (risk) genes (a) and DA (risk) genes (b). The vertical lines denote the range of effect sizes observed across cell types,e with the colored dots representing the minimum and maximum effect size each. Smaller black dots indicate the median effect sizes corresponding to particular cell types.

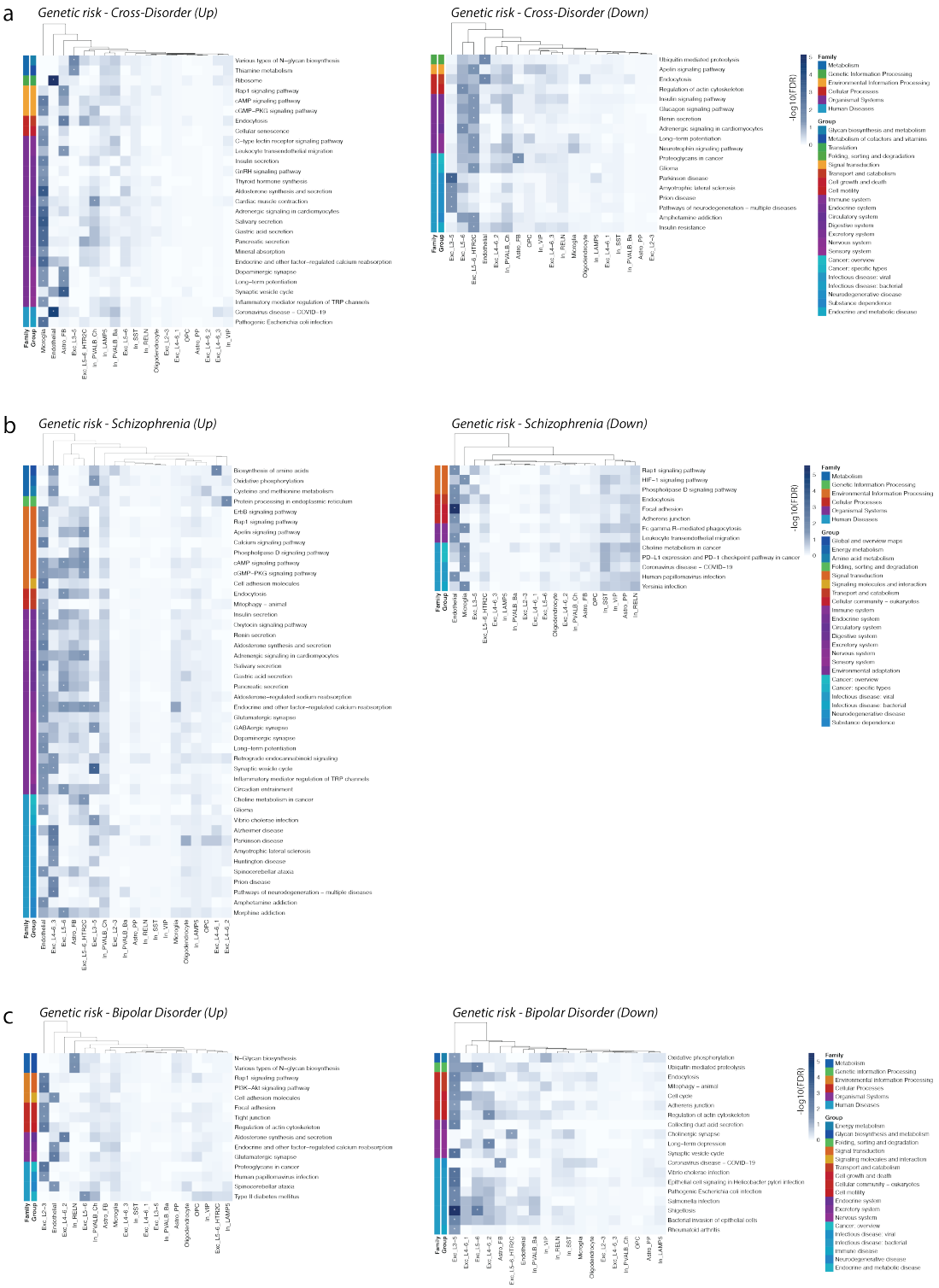
a
Genetic risk - Cross-Disorder (Up)
Various types of N−glycan biosynthesis
Thiamine metabolism
Ribosome
Rap1 signaling pathway
cAMP signaling pathway
cGMP−PKG signaling pathway
Endocytosis
Cellular senescence
C−type lectin receptor signaling pathway
Leukocyte transendothelial migration
Insulin secretion
GnRH signaling pathway
Thyroid hormone synthesis
Aldosterone synthesis and secretion
Cardiac muscle contraction
Adrenergic signaling in cardiomyocytes
Salivary secretion
Gastric acid secretion
Pancreatic secretion
Mineral absorption
Endocrine and other factor−regulated calcium reabsorption
Dopaminergic synapse
Long−term potentiation
Synaptic vesicle cycle
Inflammatory mediator regulation of TRP channels
Coronavirus disease − COVID−19
Pathogenic Escherichia coli infection
Genetic risk - Cross-Disorder (Down)
Ubiquitin mediated proteolysis
Apelin signaling pathway
Endocytosis
Regulation of actin cytoskeleton
Insulin signaling pathway
Glucagon signaling pathway
Renin secretion
Adrenergic signaling in cardiomyocytes
Long−term potentiation
Neurotrophin signaling pathway
Proteoglycans in cancer
Glioma
Parkinson disease
Amyotrophic lateral sclerosis
Prion disease
Pathways of neurodegeneration − multiple diseases
Amphetamine addiction
Insulin resistance
-log10(FDR)
Family
Metabolism
Genetic Information Processing
Environmental Information Processing
Cellular Processes
Organismal Systems
Human Diseases
Group
Glycan biosynthesis and metabolism
Metabolism of cofactors and vitamins
Translation
Folding, sorting and degradation
Signal transduction
Transport and catabolism
Cell growth and death
Cell motility
Immune system
Endocrine system
Circulatory system
Digestive system
Excretory system
Nervous system
Sensory system
Cancer: overview
Cancer: specific types
Infectious disease: viral
Infectious disease: bacterial
Neurodegenerative disease
Substance dependence
Endocrine and metabolic disease
b
Genetic risk - Schizophrenia (Up)
Biosynthesis of amino acids
Oxidative phosphorylation
Cysteine and methionine metabolism
Protein processing in endoplasmic reticulum
ErbB signaling pathway
Rap1 signaling pathway
Apelin signaling pathway
Calcium signaling pathway
Phospholipase D signaling pathway
cAMP signaling pathway
cGMP−PKG signaling pathway
Cell adhesion molecules
Endocytosis
Mitophagy − animal
Insulin secretion
Oxytocin signaling pathway
Renin secretion
Aldosterone synthesis and secretion
Adrenergic signaling in cardiomyocytes
Salivary secretion
Gastric acid secretion
Pancreatic secretion
Aldosterone−regulated sodium reabsorption
Endocrine and other factor−regulated calcium reabsorption
Glutamatergic synapse
GABAergic synapse
Dopaminergic synapse
Long−term potentiation
Retrograde endocannabinoid signaling
Synaptic vesicle cycle
Inflammatory mediator regulation of TRP channels
Circadian entrainment
Choline metabolism in cancer
Glioma
Vibrio cholerae infection
Alzheimer disease
Parkinson disease
Amyotrophic lateral sclerosis
Huntington disease
Spinocerebellar ataxia
Prion disease
Pathways of neurodegeneration − multiple diseases
Amphetamine addiction
Morphine addiction
Genetic risk - Schizophrenia (Down)
Rap1 signaling pathway
HIF−1 signaling pathway
Phospholipase D signaling pathway
Endocytosis
Focal adhesion
Adherens junction
Fc gamma R−mediated phagocytosis
Leukocyte transendothelial migration
Choline metabolism in cancer
PD−L1 expression and PD−1 checkpoint pathway in cancer
Coronavirus disease − COVID−19
Human papillomavirus infection
Yersinia infection
-log10(FDR)
Family
Metabolism
Genetic Information Processing
Environmental Information Processing
Cellular Processes
Organismal Systems
Human Diseases
Group
Global and overview maps
Energy metabolism
Amino acid metabolism
Folding, sorting and degradation
Signal transduction
Signaling molecules and interaction
Transport and catabolism
Cellular community − eukaryotes
Immune system
Endocrine system
Circulatory system
Digestive system
Excretory system
Nervous system
Sensory system
Environmental adaptation
Cancer: overview
Cancer: specific types
Infectious disease: viral
Infectious disease: bacterial
Neurodegenerative disease
Substance dependence
c
Genetic risk - Bipolar Disorder (Up)
N−Glycan biosynthesis
Various types of N−glycan biosynthesis
Rap1 signaling pathway
PI3K−Akt signaling pathway
Cell adhesion molecules
Focal adhesion
Tight junction
Regulation of actin cytoskeleton
Aldosterone synthesis and secretion
Endocrine and other factor−regulated calcium reabsorption
Glutamatergic synapse
Proteoglycans in cancer
Human papillomavirus infection
Spinocerebellar ataxia
Type II diabetes mellitus
Genetic risk - Bipolar Disorder (Down)
Oxidative phosphorylation
Ubiquitin mediated proteolysis
Endocytosis
Mitophagy − animal
Cell cycle
Adherens junction
Regulation of actin cytoskeleton
Collecting duct acid secretion
Cholinergic synapse
Long−term depression
Synaptic vesicle cycle
Coronavirus disease − COVID−19
Vibrio cholerae infection
Epithelial cell signaling in Helicobacter pylori infection
Pathogenic Escherichia coli infection
Salmonella infection
Shigellosis
Bacterial invasion of epithelial cells
Rheumatoid arthritis
-log10(FDR)
Family
Metabolism
Genetic Information Processing
Environmental Information Processing
Cellular Processes
Organismal Systems
Human Diseases
Group
Energy metabolism
Glycan biosynthesis and metabolism
Folding, sorting and degradation
Signal transduction
Signaling molecules and interaction
Transport and catabolism
Cell growth and death
Cellular community − eukaryotes
Cell motility
Endocrine system
Excretory system
Nervous system
Cancer: overview
Infectious disease: viral
Infectious disease: bacterial
Immune disease
Neurodegenerative disease
Endocrine and metabolic disease

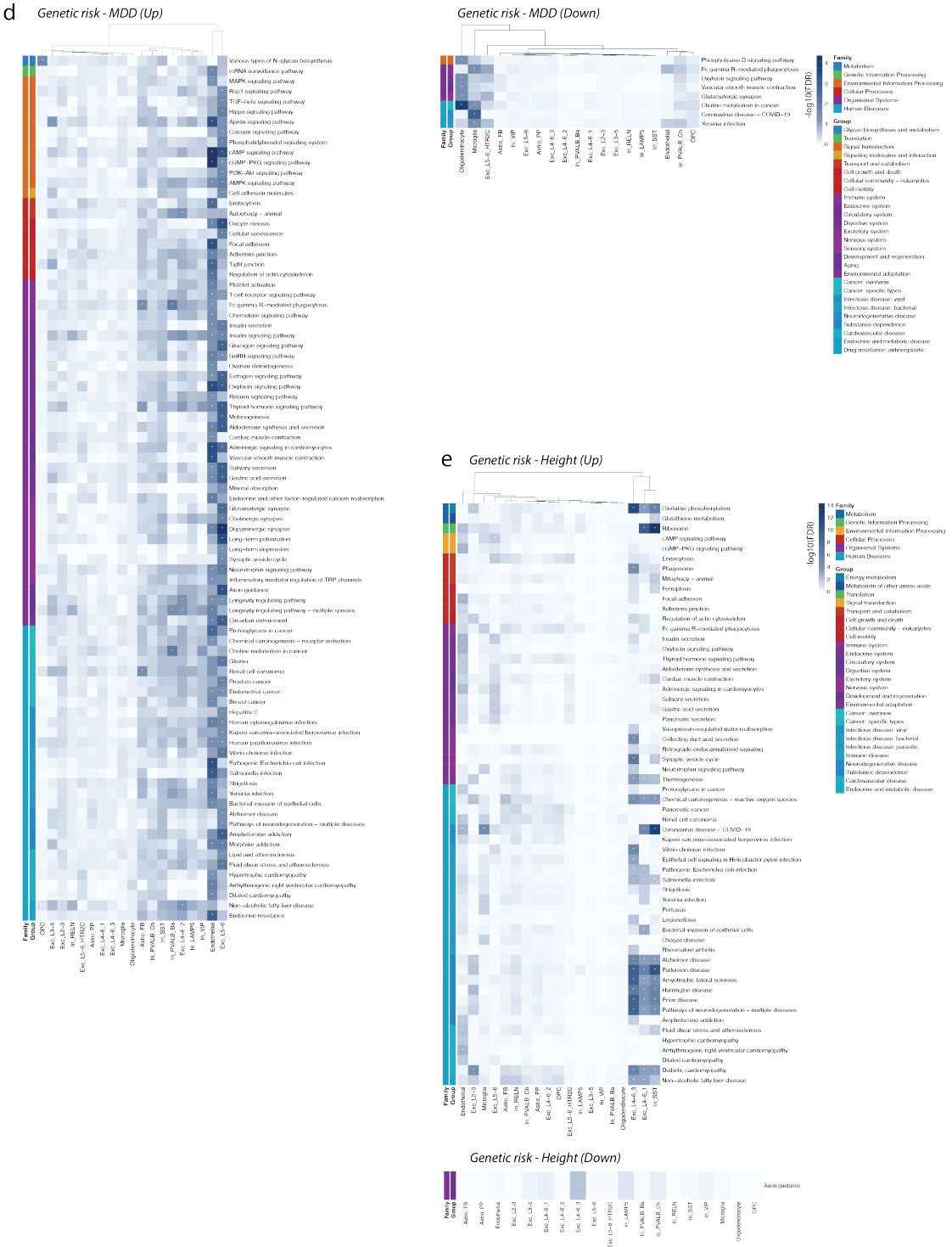


**Supplementary Figure 6. Pathways affected by differential expression between high and low genetic risk groups.** (a-e) Heatmap displaying the findings from KEGG pathway enrichment analysis conducted on the 250 most up- and downregulated genes for each cell type between high and low genetic risk groups for cross-disorder phenotype (a), schizophrenia (b), bipolar disorder (c), MDD (d), and height (e). Pathways enriched among upregulated genes are shown on the left of each panel, while pathways enriched among the downregulated genes are shown on the right of each panel. The heatmap displays all pathways that have shown significant enrichment in at least one cell type. The intensity of color correlates with the -$\log_{10}$-transformed FDR values, with asterisks indicating significance (FDR ≤ 0.05). Pathway classifications are color-coded on the left of each heatmap to indicate the specific pathway group and family. K-means clustering dendrograms are provided to show how cell types group together based on their pathway enrichment profiles.

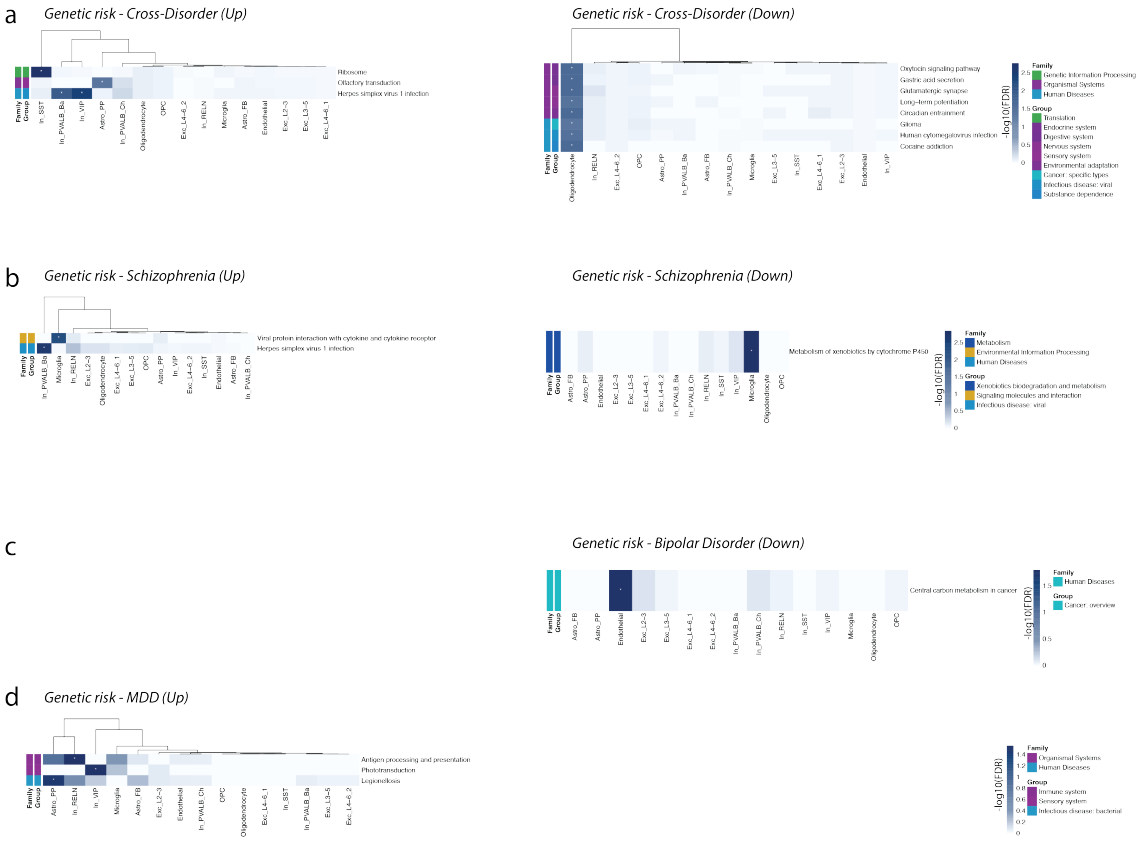


**Supplementary Figure 7. Pathways affected by differential chromatin accessibility between high and low genetic risk groups.** (a-d) Heatmap displaying the findings from KEGG pathway enrichment analysis conducted on the 250 most up- and downregulated genes for each cell type between high and low genetic risk groups for cross-disorder phenotype (a), schizophrenia (b), bipolar disorder (c), and MDD (d). Pathways enriched among upregulated genes are shown on the left of each panel, while pathways enriched among the downregulated genes are shown on the right of each panel. The heatmap displays all pathways that have shown significant enrichment in at least one cell type. The intensity of color correlates with the -$\log_{10}$-transformed FDR values, with asterisks indicating significance (FDR ≤ 0.05). Pathway classifications are color-coded on the left of each heatmap to indicate the specific pathway group and family. K-means clustering dendrograms are provided to show how cell types group together based on their pathway enrichment profiles. There was no significant enrichment of pathways among DA risk genes related to height.

## A.2 Supplementary Tables

**Supplementary Table 1. Number of genes tested and samples per brain region and treatment group in the mouse brain dataset.** Number of genes refers to the genes tested for differential expression after quality control. The number of samples per treatment group refers to the samples remaining after exclusion of samples during quality control and outlier removal.

| Brain region | Genes | Outliers Vehicle-Treated | Samples Vehicle-Treated | Outliers Dex-treated | Samples Dex-Treated | Significant surrogate variables |
|---|---|---|---|---|---|---|
| **AMY** | 12,937 | 0 | 15 | 0 | 15 | 9 |
| **CER** | 12,927 | 1 | 14 | 0 | 15 | 8 |
| **dCA1** | 12,924 | 1 | 14 | 0 | 13 | 7 |
| **dDG** | 12,941 | 0 | 15 | 0 | 15 | 8 |
| **PFC** | 12,928 | 0 | 15 | 1 | 13 | 7 |
| **PVN** | 12,924 | 0 | 14 | 0 | 15 | 8 |
| **vCA1** | 12,940 | 0 | 14 | 3 | 12 | 7 |
| **vDG** | 12,957 | 0 | 15 | 1 | 14 | 8 |

**Supplementary Table 2. Number of (unique) differentially expressed and hub genes per brain.** The numbers refer to differentially expressed (DE) genes exhibiting an FDR ≤ 0.1 according to differential testing with DESeq2 (Love et al., 2014) and hub genes with a normalized node-betweenness > 1. Unique genes are those identified as DE/hub genes in only one brain region.

| Brain region | DE Genes | Unique DE genes | Hub Genes | Unique Hub Genes |
|---|---|---|---|---|
| **AMY** | 784 | 105 | 293 | 29 |
| **CER** | 821 | 176 | 284 | 21 |
| **dCA1** | 569 | 74 | 302 | 22 |
| **dDG** | 755 | 141 | 313 | 22 |
| **PFC** | 920 | 245 | 293 | 29 |
| **PVN** | 598 | 77 | 307 | 26 |
| **vCA1** | 465 | 25 | 260 | 24 |
| **vDG** | 848 | 139 | 289 | 19 |

**Supplementary Table 3. Top 10 differentially expressed genes in the amygdala.** Full list of differentially expressed genes in response to glucocorticoid receptor stimulation in amygdala (n=784) available at https://doi.org/10.5281/zenodo.10864161, Online Table 2.

| gene_symbol | baseMean | log2FoldChange | lfcSE | *p* | FDR |
|---|---|---|---|---|---|
| **Cx3cr1** | 89.0654571 | -2.2149356 | 0.10550043 | 9.11E-100 | 1.18E-95 |
| **Cdkn1a** | 204.145839 | 3.45171765 | 0.18604411 | 1.24E-76 | 8.00E-73 |
| **Synm** | 86.6907622 | 1.8107745 | 0.10114147 | 6.76E-73 | 2.91E-69 |
| **Fkbp5** | 41.9730919 | 2.5443663 | 0.14691873 | 5.31E-68 | 1.72E-64 |
| **Mt2** | 467.641314 | 0.92309406 | 0.06161485 | 1.93E-51 | 5.00E-48 |
| **Phactr3** | 165.989417 | 1.24079198 | 0.08540937 | 4.11E-50 | 8.86E-47 |
| **Ccng1** | 53.7591584 | 1.75779552 | 0.12042269 | 2.48E-49 | 4.58E-46 |
| **Trim59** | 38.4214773 | -2.1923465 | 0.15878357 | 1.77E-45 | 2.86E-42 |
| **Mxd4** | 127.191593 | 1.11523069 | 0.07996072 | 2.80E-45 | 4.02E-42 |
| **Dio2** | 89.2624892 | 1.51774366 | 0.11086074 | 4.57E-44 | 5.91E-41 |

**Supplementary Table 4. Top 10 differentially expressed genes in the cerebellum.** Full list of differentially expressed genes in response to glucocorticoid receptor stimulation in cerebellum (n=821) available at https://doi.org/10.5281/zenodo.10864161, Online Table 3.

| gene_symbol | baseMean | log2FoldChange | lfcSE | *p* | FDR |
|---|---|---|---|---|---|
| **Synm** | 155.917 | 1.89100685 | 0.08688926 | 6.30E-107 | 8.14E-103 |
| **Phactr3** | 180.478122 | 1.68685903 | 0.08065733 | 7.21E-99 | 4.66E-95 |
| **Nt5c3** | 139.575818 | 1.63217634 | 0.0847939 | 1.05E-83 | 4.51E-80 |
| **Sgk3** | 64.9922474 | 2.33697765 | 0.1285318 | 2.88E-75 | 9.30E-72 |
| **Ccng1** | 80.357405 | 2.06915689 | 0.11858892 | 9.91E-70 | 2.56E-66 |
| **Cx3cr1** | 45.7958471 | -2.340605 | 0.13740997 | 1.16E-66 | 2.49E-63 |
| **Fkbp5** | 38.7224706 | 2.67600753 | 0.16711032 | 4.22E-59 | 7.80E-56 |
| **Cdkn1a** | 281.91692 | 3.12473503 | 0.20339631 | 1.00E-54 | 1.62E-51 |
| **Trim59** | 49.4480732 | -2.2827252 | 0.15428947 | 4.77E-51 | 6.86E-48 |
| **Mxd4** | 147.262714 | 1.11240658 | 0.07829108 | 9.72E-47 | 1.26E-43 |

**Supplementary Table 5. Top 10 differentially expressed genes in the dorsal *cornu ammonis* 1**. Full list of differentially expressed genes in response to glucocorticoid receptor stimulation in the dorsal *cornu ammonis* 1 (n=569) available at https://doi.org/10.5281/zenodo.10864161, Online Table 4.

| gene_symbol | baseMean | log2FoldChange | lfcSE | *p* | FDR |
|---|---|---|---|---|---|
| **Cx3cr1** | 71.5810893 | -1.8426352 | 0.12806666 | 9.32E-48 | 1.21E-43 |
| **Cdkn1a** | 134.113197 | 2.8705463 | 0.21251828 | 1.60E-42 | 1.03E-38 |
| **Mthfd2** | 30.9847353 | 2.6936094 | 0.20967862 | 3.15E-38 | 1.36E-34 |
| **Dio2** | 175.313369 | 1.0642026 | 0.08546181 | 5.96E-37 | 1.93E-33 |
| **Fkbp5** | 49.2283834 | 1.71831954 | 0.15051982 | 1.26E-31 | 3.26E-28 |
| **Nfkbia** | 170.318549 | 1.20156184 | 0.10718048 | 5.24E-31 | 1.13E-27 |
| **Sox9** | 182.538918 | -0.9080968 | 0.08452176 | 2.44E-28 | 4.51E-25 |
| **Slc2a1** | 94.2762862 | 1.22790506 | 0.12422674 | 7.00E-25 | 1.13E-21 |
| **Mt1** | 1180.28251 | 0.65311629 | 0.06939741 | 4.65E-23 | 6.67E-20 |
| **Mt2** | 710.519261 | 1.01418824 | 0.11019874 | 3.60E-22 | 4.65E-19 |

**Supplementary Table 6. Top 10 differentially expressed genes in the dorsal *dentate gyrus***. Full list of differentially expressed genes in response to glucocorticoid receptor stimulation in the dorsal *dentate gyrus* (n=755) available at https://doi.org/10.5281/zenodo.10864161, Online Table 5.

| gene_symbol | baseMean | log2FoldChange | lfcSE | *p* | FDR |
|---|---|---|---|---|---|
| **Cdkn1a** | 127.302652 | 3.00936287 | 0.18300767 | 1.05E-64 | 1.36E-60 |
| **Cx3cr1** | 58.5389349 | -2.0408996 | 0.13983053 | 9.94E-50 | 6.43E-46 |
| **Mthfd2** | 25.8910363 | 2.73982255 | 0.19807453 | 9.24E-45 | 3.99E-41 |
| **Tsc22d3** | 92.1374449 | 1.44983647 | 0.11155805 | 3.96E-40 | 1.28E-36 |
| **Nfkbia** | 174.207042 | 1.31289884 | 0.10432934 | 4.86E-38 | 1.26E-34 |
| **Slc2a1** | 92.8660118 | 1.11257185 | 0.09045336 | 1.29E-36 | 2.77E-33 |
| **Errfi1** | 35.7050562 | 1.79103464 | 0.14523494 | 4.60E-36 | 8.51E-33 |
| **Fkbp5** | 45.9621499 | 1.62278702 | 0.13909269 | 3.44E-32 | 5.56E-29 |
| **Ddit4** | 64.2629499 | 1.37113061 | 0.11838184 | 6.19E-32 | 8.90E-29 |
| **Mt2** | 560.676772 | 0.84878225 | 0.07733517 | 9.84E-30 | 1.27E-26 |

**Supplementary Table 7. Top 10 differentially expressed genes in the prefrontal cortex**. Full list of differentially expressed genes in response to glucocorticoid receptor stimulation in the prefrontal cortex (n=920) available at https://doi.org/10.5281/zenodo.10864161, Online Table 6.

| gene_symbol | baseMean | log2FoldChange | lfcSE | *p* | FDR |
|---|---|---|---|---|---|
| **Cdkn1a** | 144.9020448 | 1.936002026 | 0.088388692 | 4.20E-109 | 5.43E-105 |
| **Cx3cr1** | 77.69273276 | -2.042626247 | 0.105675594 | 1.07E-83 | 6.93E-80 |
| **Fkbp5** | 38.10974824 | 2.898776928 | 0.168575632 | 1.43E-68 | 6.16E-65 |

| | | | | | |
|---|---|---|---|---|---|
| **Sox9** | 176.8618563 | -1.097228016 | 0.068295387 | 3.98E-59 | 1.28E-55 |
| **Mthfd2** | 24.53018208 | 2.874590781 | 0.196841836 | 3.27E-49 | 8.47E-46 |
| **Wipf3** | 195.7570523 | 0.989430069 | 0.069827784 | 1.46E-46 | 3.15E-43 |
| **Tiparp** | 50.80106841 | 1.749342973 | 0.123969166 | 1.20E-45 | 2.21E-42 |
| **Irs2** | 105.5129903 | 1.054074937 | 0.075956183 | 4.08E-45 | 6.60E-42 |
| **Nfkbia** | 178.6596523 | 1.29689783 | 0.098600406 | 1.20E-40 | 1.73E-37 |
| **Id3** | 96.86971702 | -1.176929753 | 0.09064925 | 8.66E-40 | 1.12E-36 |

**Supplementary Table 8. Top 10 differentially expressed genes in the paraventricular nucleus of the hypothalamus**. Full list of differentially expressed genes in response to glucocorticoid receptor stimulation in the paraventricular nucleus of the hypothalamus (n=598) available at https://doi.org/10.5281/zenodo.10864161, Online Table 7.

| gene_symbol | baseMean | log2FoldChange | lfcSE | *p* | FDR |
|---|---|---|---|---|---|
| **Dio2** | 67.505075 | 2.49364385 | 0.12971355 | 1.14E-83 | 1.47E-79 |
| **Cdkn1a** | 207.741575 | 3.45062892 | 0.1944233 | 5.77E-71 | 3.73E-67 |
| **Fkbp5** | 41.9199776 | 2.61606961 | 0.15443434 | 3.43E-65 | 1.48E-61 |
| **Phactr3** | 140.122899 | 1.30992268 | 0.08563011 | 3.39E-54 | 1.09E-50 |
| **Mt2** | 592.407405 | 1.13695944 | 0.07549168 | 5.94E-54 | 1.53E-50 |
| **Cx3cr1** | 49.9728943 | -2.1774376 | 0.14561437 | 1.21E-51 | 2.60E-48 |
| **Nfkbia** | 161.697488 | 1.52168227 | 0.10685479 | 3.46E-48 | 6.39E-45 |
| **Mxd4** | 138.468049 | 1.12022122 | 0.08004466 | 1.03E-45 | 1.66E-42 |
| **Smim3** | 25.1944839 | 2.34785568 | 0.18756755 | 6.62E-37 | 9.50E-34 |
| **Zbtb16** | 30.2145981 | 2.20819826 | 0.18143306 | 3.52E-35 | 4.55E-32 |

**Supplementary Table 9. Top 10 differentially expressed genes in the ventral *cornu ammonis* 1**. Full list of differentially expressed genes in response to glucocorticoid receptor stimulation in the ventral *cornu ammonis* 1 (n=465) available at https://doi.org/10.5281/zenodo.10864161, Online Table 8.

| gene_symbol | baseMean | log2FoldChange | lfcSE | *p* | FDR |
|---|---|---|---|---|---|
| **Cdkn1a** | 138.373439 | 3.35495113 | 0.22394223 | 2.66E-53 | 3.44E-49 |
| **Cx3cr1** | 84.8880055 | -2.0033494 | 0.13940091 | 1.44E-47 | 9.31E-44 |
| **Dio2** | 194.435804 | 1.38229923 | 0.0980219 | 2.16E-46 | 9.33E-43 |
| **Fkbp5** | 47.8784655 | 2.51816728 | 0.18221116 | 4.61E-45 | 1.49E-41 |
| **Slc2a1** | 103.02543 | 1.33164613 | 0.10399143 | 1.21E-38 | 3.13E-35 |
| **Mt2** | 688.581684 | 0.94914244 | 0.07580518 | 9.62E-37 | 2.07E-33 |
| **Mthfd2** | 32.9101229 | 2.71436572 | 0.22067105 | 6.17E-36 | 1.14E-32 |
| **Sox9** | 207.102319 | -1.0054523 | 0.08669965 | 1.31E-32 | 2.12E-29 |
| **Mxd4** | 162.871616 | 0.92744365 | 0.08915185 | 4.95E-26 | 7.12E-23 |
| **Gadd45g** | 29.8711425 | 1.77837312 | 0.18809477 | 1.01E-22 | 1.31E-19 |

**Supplementary Table 10. Top 10 differentially expressed genes in the ventral dentate gyrus**. Full list of differentially expressed genes in response to glucocorticoid receptor stimulation in the ventral dentate gyrus (n=848) available at https://doi.org/10.5281/zenodo.10864161, Online Table 9.

| gene_symbol | baseMean | log2FoldChange | lfcSE | *p* | FDR |
|---|---|---|---|---|---|
| **Cx3cr1** | 63.880212 | -2.2370212 | 0.12274106 | 2.56E-75 | 3.31E-71 |
| **Nfkbia** | 193.024945 | 1.50499026 | 0.08757915 | 1.20E-67 | 7.80E-64 |
| **Fkbp5** | 57.7549998 | 2.37331813 | 0.14219277 | 1.13E-63 | 4.88E-60 |
| **Cdkn1a** | 152.924088 | 3.20866117 | 0.20612115 | 3.23E-57 | 1.05E-53 |
| **Mthfd2** | 35.7443156 | 2.80971841 | 0.18610411 | 1.09E-52 | 2.82E-49 |
| **Dio2** | 157.625803 | 1.45005428 | 0.09745452 | 1.44E-51 | 3.12E-48 |
| **Slc2a1** | 105.206294 | 1.32877368 | 0.09412672 | 8.44E-47 | 1.56E-43 |
| **Tsc22d3** | 138.174837 | 1.39992617 | 0.10091649 | 9.08E-46 | 1.47E-42 |
| **Errfi1** | 42.9399649 | 1.84278171 | 0.13076356 | 1.29E-45 | 1.86E-42 |
| **Ddit4** | 70.6919893 | 1.43810642 | 0.10972943 | 2.50E-40 | 3.24E-37 |

**Supplementary Table 11. Top 10 differential hub genes in the amygdala.** Full list of differential hub genes in response to glucocorticoid receptor stimulation in the amygdala (n=293) available at https://doi.org/10.5281/zenodo.10864161, Online Table 11.

| gene_symbol | nodebetweenness | nodebetweenness_prior | nodebetweenness_norm |
|---|---|---|---|
| **Ikbkg** | 92687.3978 | 10576.5141 | 8.76351104 |
| **Kif3a** | 61260.9573 | 16516.5492 | 3.70906517 |
| **Traf6** | 127109.34 | 41214.3559 | 3.08410352 |
| **Esrrb** | 54640.1599 | 20250.8657 | 2.69816416 |
| **Prkn** | 27778.4846 | 10834.5226 | 2.56388635 |
| **Kcnd3** | 58199.3427 | 29503.9499 | 1.97259495 |
| **Syt14** | 50008.5679 | 27970.7196 | 1.78788993 |
| **H2bc21** | 29293.3862 | 16559.6436 | 1.76896236 |
| **Cyb5rl** | 31358.7496 | 19026.5815 | 1.64815469 |
| **Nudt11** | 105282.913 | 64479.9007 | 1.63280203 |

**Supplementary Table 12. Top 10 differential hub genes in the cerebellum.** Full list of differential hub genes in response to glucocorticoid receptor stimulation in the cerebellum (n=284) available at https://doi.org/10.5281/zenodo.10864161, Online Table 12.

| gene_symbol | nodebetweenness | nodebetweenness_prior | nodebetweenness_norm |
|---|---|---|---|
| **Pla2g4a** | 73337.9323 | 13484.7109 | 5.43859879 |
| **Dmd** | 51216.4826 | 18737.001 | 2.73344077 |
| **Fbn1** | 56812.1287 | 22987.853 | 2.47139777 |
| **Pbx3** | 43042.3386 | 18902.1145 | 2.27711765 |
| **Tmem53** | 84180.7716 | 39286.8943 | 2.14271891 |
| **Tdp1** | 28192.1311 | 14059.2649 | 2.00523508 |
| **Arhgap35** | 17654.3587 | 10032.2927 | 1.75975314 |
| **Reep3** | 22578.1212 | 14869.8651 | 1.51838104 |
| **Otx2** | 35273.4165 | 24479.7751 | 1.44092077 |
| **Bgn** | 120390.733 | 86582.8525 | 1.39046855 |

**Supplementary Table 13. Top 10 differential hub genes in the dorsal *cornu ammonis* 1.** Full list of differential hub genes in response to glucocorticoid receptor stimulation in the dorsal *cornu ammonis* 1 (n=302) available at https://doi.org/10.5281/zenodo.10864161, Online Table 13.

| gene_symbol | nodebetweenness | nodebetweenness_prior | nodebetweenness_norm |
|---|---|---|---|
| **Map2k5** | 65327.7668 | 10460.1049 | 6.24542175 |
| **Slc43a3** | 59988.1894 | 13271.1897 | 4.52018176 |
| **Map1s** | 22406.5949 | 11893.5678 | 1.88392544 |
| **Sv2b** | 35078.1214 | 20466.5239 | 1.71392668 |
| **Irak1** | 41968.7662 | 25879.8891 | 1.62167489 |
| **Zfp24** | 17356.2601 | 11242.4499 | 1.54381476 |
| **Hipk3** | 31404.4678 | 20406.7419 | 1.5389261 |
| **Cdh8** | 64802.8076 | 43761.191 | 1.48082824 |
| **Gbp2** | 21331.4366 | 15378.8677 | 1.38706159 |
| **Jup** | 23668.9096 | 17693.6594 | 1.33770574 |

**Supplementary Table 14. Top 10 differential hub genes in the dorsal dentate gyrus.** Full list of differential hub genes in response to glucocorticoid receptor stimulation in the dorsal dentate gyrus (n=313) available at https://doi.org/10.5281/zenodo.10864161, Online Table 14.

| gene_symbol | nodebetweenness | nodebetweenness_prior | nodebetweenness_norm |
|---|---|---|---|
| **Parp16** | 101406.214 | 21360.8165 | 4.74730045 |
| **Tek** | 33931.6694 | 11439.5801 | 2.96616388 |
| **Pum3** | 17767.0185 | 10548.1674 | 1.68437016 |

| | | | |
|---|---|---|---|
| **Sema6d** | 41618.0452 | 26224.8943 | 1.58696713 |
| **Ctnnd1** | 57803.4899 | 37149.412 | 1.55597321 |
| **Sord** | 29571.0994 | 19152.935 | 1.5439461 |
| **Dync2h1** | 35114.2965 | 22926.0863 | 1.53163065 |
| **Dvl1** | 16778.7327 | 11098.0064 | 1.51186908 |
| **Fech** | 22059.4606 | 15086.1899 | 1.46222874 |
| **Tmem109** | 24844.8143 | 17237.6236 | 1.44131319 |

**Supplementary Table 15. Top 10 differential hub genes in the prefrontal cortex.** Full list of differential hub genes in response to glucocorticoid receptor stimulation in the prefrontal cortex (n=293) available at https://doi.org/10.5281/zenodo.10864161, Online Table 15.

| gene_symbol | nodebetweenness | nodebetweenness_prior | nodebetweenness_norm |
|---|---|---|---|
| **Abcd1** | 62281.8632 | 10684.718 | 5.829060091 |
| **Slc39a3** | 42127.932 | 10496.4137 | 4.013554854 |
| **Ror2** | 81086.6847 | 26778.6327 | 3.028036778 |
| **Myo7a** | 26651.4248 | 10044.9813 | 2.653207998 |
| **Slc8a1** | 52031.1229 | 21875.2656 | 2.378536737 |
| **Sulf1** | 39128.083 | 17721.985 | 2.207883763 |
| **Arntl** | 44832.9063 | 21714.0036 | 2.064700136 |
| **Tm7sf2** | 28589.656 | 13853.7012 | 2.0636836 |
| **Aldh18a1** | 50038.5522 | 25541.1117 | 1.959137599 |
| **Dab2ip** | 40797.4348 | 21685.6071 | 1.881313936 |

**Supplementary Table 16. Top 10 differential hub genes in the paraventricular nucleus of the hypothalamus.** Full list of differential hub genes in response to glucocorticoid receptor stimulation in the paraventricular nucleus of the hypothalamus (n=307) available at https://doi.org/10.5281/zenodo.10864161, Online Table 16.

| gene_symbol | nodebetweenness | nodebetweenness_prior | nodebetweenness_norm |
|---|---|---|---|
| **Itga1** | 85034.9231 | 10889.4243 | 7.80894572 |
| **Fcgr2b** | 62168.4431 | 10637.7956 | 5.84410955 |
| **Mitf** | 69172.0995 | 12964.464 | 5.33551557 |
| **Fas** | 70795.5052 | 37743.912 | 1.87568012 |
| **Ccdc8** | 65849.387 | 36734.4584 | 1.79257814 |
| **Sgce** | 66707.6331 | 39578.4807 | 1.68545209 |
| **Evc2** | 36712.4354 | 23084.3162 | 1.5903627 |
| **Kcnu1** | 25818.2285 | 18157.345 | 1.4219165 |
| **Arhgef6** | 49114.1117 | 34924.3985 | 1.406298 |
| **Samd8** | 24253.7529 | 17452.3192 | 1.38971517 |

**Supplementary Table 17. Top 10 differential hub genes in the ventral *cornu ammonis* 1.** Full list of differential hub genes in response to glucocorticoid receptor stimulation in the ventral *cornu ammonis* 1 (n=260) available at https://doi.org/10.5281/zenodo.10864161, Online Table 17.

| gene_symbol | nodebetweenness | nodebetweenness_prior | nodebetweenness_norm |
|---|---|---|---|
| **Slc4a8** | 37736.95562 | 12808.42081 | 2.946261383 |
| **Pex13** | 42516.55658 | 15369.69044 | 2.766259786 |
| **Pdlim4** | 83290.92368 | 34727.89363 | 2.398386858 |
| **Zfp235** | 43535.20672 | 18700.50365 | 2.32802322 |
| **Syt16** | 162904.908 | 78925.49487 | 2.064034039 |
| **Hbp1** | 32467.37703 | 18173.25717 | 1.786546942 |
| **Pcdh8** | 100955.9267 | 57784.29357 | 1.747117087 |
| **Pth1r** | 23426.23622 | 14094.84185 | 1.662043212 |
| **Hk2** | 16414.27236 | 10028.84675 | 1.636705871 |
| **Ntsr2** | 99093.03558 | 61109.97619 | 1.621552515 |

**Supplementary Table 18. Top 10 differential hub genes in the ventral dentate gyrus.** Full list of differential hub genes in response to glucocorticoid receptor stimulation in the ventral dentate gyrus (n=289) available at https://doi.org/10.5281/zenodo.10864161, Online Table 18.

| gene_symbol | nodebetweenness | nodebetweenness_prior | nodebetweenness_norm |
|---|---|---|---|
| **Gucy2e** | 31035.2829 | 10140.5326 | 3.06051802 |
| **Lin9** | 24842.9309 | 10013.8357 | 2.48086064 |
| **Zfp12** | 32804.0641 | 18919.1681 | 1.73390626 |
| **Rerg** | 16604.6167 | 10129.7909 | 1.63918652 |
| **Cd44** | 81825.1292 | 50486.5829 | 1.62073019 |
| **Kcnh8** | 19542.9439 | 12269.2924 | 1.59283382 |
| **Nkain3** | 26860.8918 | 20391.8625 | 1.31723583 |
| **Pxn** | 14820.5661 | 11604.3408 | 1.27715709 |
| **Irs1** | 82902.712 | 65355.2805 | 1.26849294 |
| **Nudt10** | 81539.1793 | 64452.2 | 1.26511088 |

**Supplementary Table 19. Nuclei counts and differences in cell type proportions between snRNA-seq and snATAC-seq data.** The difference in cell type proportions between snRNA-seq and snATAC-seq for each cell type was tested using a two-sided Wilcoxon signed-rank test.

| Cell Type | Number Nuclei RNA | Number Nuclei ATAC | *p* value | FDR |
|---|---|---|---|---|
| **Astro_FB** | 26,789 | 16,158 | 5.3613E-04 | 6.1862E-04 |
| **Astro_PP** | 86,351 | 31,902 | 3.9645E-11 | 1.1893E-10 |
| **Endothelial** | 14,353 | 5,996 | 3.9153E-02 | 3.9153E-02 |
| **Exc_L2-3** | 218,679 | 95,711 | 1.3736E-09 | 2.5756E-09 |
| **Exc_L3-5** | 12,152 | 5,041 | 8.2961E-05 | 1.1313E-04 |
| **Exc_L4-6_1** | 36,166 | 22,852 | 2.6669E-09 | 4.4449E-09 |
| **Exc_L4-6_2** | 35,090 | 4,950 | 1.0817E-14 | 4.0564E-14 |
| **Exc_L4-6_3** | 14,479 | NA | NA | NA |
| **Exc_L5-6** | 7,564 | NA | NA | NA |
| **Exc_L5-6_HTR2C** | 4,164 | NA | NA | NA |
| **In_LAMP5** | 15,116 | NA | NA | NA |
| **In_PVALB_Ba** | 31,504 | 14,396 | 2.3570E-04 | 2.9462E-04 |
| **In_PVALB_Ch** | 6,717 | 2,925 | 1.8237E-03 | 1.9539E-03 |
| **In_RELN** | 24,095 | 19,425 | 8.1309E-16 | 6.0982E-15 |
| **In_SST** | 34,069 | 22,410 | 8.8831E-11 | 2.2208E-10 |
| **In_VIP** | 42,154 | 17,492 | 1.7051E-10 | 3.6538E-10 |
| **Microglia** | 39,433 | 34,983 | 4.3114E-15 | 2.1557E-14 |
| **Oligodendrocyte** | 92,744 | 87,086 | 1.2677E-07 | 1.9015E-07 |
| **OPC** | 45,427 | 18,112 | 8.1309E-16 | 6.0982E-15 |

**Supplementary Table 20. Glia-to-neuron ratio in single-nucleus sequencing data.** Total number of nuclei in snRNA-seq and snATAC-seq data, along with the number of glia and neurons, and the glia-to-neuron ratio per data modality.

| | RNA | ATAC |
|---|---|---|
| **Total** | 787,046 | 399,439 |
| **Glia** | 224,522 | 188,241 |
| **Neurons** | 481,949 | 205,202 |
| **Glia:Neuron Ratio** | 0.47 | 0.92 |

**Supplementary Table 21. Differentially expressed genes for various cell types between psychiatric cases and controls.** Per cell type a maximum of 10 differentially expressed genes is shown here. Full list of differentially expressed genes for all cell types available at https://doi.org/10.5281/zenodo.10864161, Online Table 33.

| cell type | gene_symbol | baseMean | log2FoldChange | lfcSE | *p* | FDR |
|---|---|---|---|---|---|---|
| **Astro_FB** | CAB39L | 28.81014790 | 0.27243328 | 0.06884160 | 4.39E-05 | 9.95E-02 |
| **Astro_FB** | L3MBTL4 | 32.40612498 | 0.27968614 | 0.07372429 | 4.38E-05 | 9.95E-02 |
| **Endothelial** | MEG8 | 20.74041906 | 0.30400439 | 0.06992844 | 3.30E-05 | 8.73E-02 |
| **Exc_L2-3** | MIEN1 | 173.86975625 | 0.28891269 | 0.05481492 | 8.05E-08 | 7.21E-04 |
| **Exc_L2-3** | POU2F2 | 1,026.59249054 | -0.25262255 | 0.04617773 | 5.79E-08 | 7.21E-04 |
| **Exc_L2-3** | AC034268.2 | 9,121.33622633 | -0.30408274 | 0.06492070 | 3.74E-07 | 1.84E-03 |
| **Exc_L2-3** | AC005972.3 | 335.37440497 | -0.27137913 | 0.05524922 | 4.10E-07 | 1.84E-03 |
| **Exc_L2-3** | DGKD | 293.54470692 | 0.32182652 | 0.06856127 | 5.78E-07 | 2.07E-03 |
| **Exc_L2-3** | CALB1 | 253.95166858 | 0.37427501 | 0.07276923 | 1.13E-06 | 3.21E-03 |
| **Exc_L2-3** | KCNE2 | 22.32591926 | -0.33054163 | 0.07020575 | 1.25E-06 | 3.21E-03 |
| **Exc_L2-3** | AC105180.2 | 75.65001315 | -0.34702343 | 0.07306697 | 1.51E-06 | 3.27E-03 |
| **Exc_L2-3** | NFX1 | 1,606.83471202 | -0.13007411 | 0.02717061 | 1.65E-06 | 3.27E-03 |
| **Exc_L2-3** | STAB2 | 37.06856663 | 0.35789714 | 0.07340386 | 2.01E-06 | 3.27E-03 |
| **Exc_L3-5** | AC068282.1 | 23.16550766 | 0.20863521 | 0.05664445 | 5.87E-06 | 4.01E-02 |
| **Exc_L3-5** | RIT2 | 119.32522585 | 0.24874240 | 0.05576373 | 9.40E-06 | 4.01E-02 |
| **Exc_L4-6_1** | SLIT2 | 528.16894479 | 0.38332639 | 0.06182622 | 1.09E-10 | 1.38E-06 |
| **Exc_L4-6_1** | TIMP2 | 147.61594280 | 0.32208732 | 0.05647373 | 2.56E-09 | 1.61E-05 |
| **Exc_L4-6_1** | AC012404.1 | 87.19238118 | 0.29896487 | 0.06024576 | 9.83E-08 | 4.13E-04 |
| **Exc_L4-6_1** | PCP4L1 | 33.58207229 | 0.33093782 | 0.06641521 | 4.88E-07 | 1.35E-03 |
| **Exc_L4-6_1** | BTBD11 | 65.15141725 | 0.31950542 | 0.06735957 | 5.36E-07 | 1.35E-03 |
| **Exc_L4-6_1** | TRPC4 | 37.15815670 | 0.34300392 | 0.06667601 | 8.74E-07 | 1.83E-03 |
| **Exc_L4-6_1** | NFX1 | 255.73413526 | -0.15084974 | 0.03181411 | 1.93E-06 | 3.48E-03 |
| **Exc_L4-6_1** | KLHL5 | 313.70325378 | -0.18094030 | 0.03888953 | 2.28E-06 | 3.59E-03 |
| **Exc_L4-6_1** | LCN15 | 26.79836800 | -0.27889190 | 0.06529515 | 3.40E-06 | 4.76E-03 |
| **Exc_L4-6_1** | AC090578.1 | 787.57649550 | -0.21906726 | 0.04880094 | 4.31E-06 | 4.98E-03 |
| **Exc_L4-6_2** | COX5B | 95.74082887 | 0.23318186 | 0.04992042 | 5.35E-07 | 4.52E-03 |
| **Exc_L4-6_2** | AC012404.1 | 81.01612790 | 0.26140653 | 0.05985582 | 7.69E-07 | 4.52E-03 |
| **Exc_L4-6_2** | LINC00513 | 166.14217370 | 0.23728024 | 0.05826286 | 4.07E-06 | 1.20E-02 |
| **Exc_L4-6_2** | RAB11A | 228.40256652 | 0.17757332 | 0.03903647 | 4.02E-06 | 1.20E-02 |
| **Exc_L4-6_2** | IGSF11 | 274.56512613 | -0.20471159 | 0.04541945 | 8.68E-06 | 2.04E-02 |
| **Exc_L4-6_2** | ABHD14A | 77.20857420 | 0.17907253 | 0.04456717 | 1.98E-05 | 2.18E-02 |
| **Exc_L4-6_2** | MCTP1 | 472.03156077 | 0.22357017 | 0.05222439 | 1.82E-05 | 2.18E-02 |
| **Exc_L4-6_2** | MAK | 56.17350115 | 0.21897463 | 0.05364213 | 1.62E-05 | 2.18E-02 |
| **Exc_L4-6_2** | UBB | 119.90996118 | 0.22341695 | 0.05842757 | 2.04E-05 | 2.18E-02 |
| **Exc_L4-6_2** | RHBDL3 | 140.93836867 | 0.23960576 | 0.06234199 | 1.54E-05 | 2.18E-02 |
| **Exc_L4-6_3** | SNAP91 | 424.81719204 | -0.11016166 | 0.02252115 | 9.12E-07 | 7.56E-03 |
| **Exc_L4-6_3** | COL19A1 | 161.06127926 | -0.22608318 | 0.05057608 | 5.85E-06 | 1.62E-02 |
| **Exc_L4-6_3** | LINC00923 | 34.97198587 | -0.33258490 | 0.07172967 | 5.29E-06 | 1.62E-02 |
| **Exc_L4-6_3** | NTN4 | 41.99015877 | -0.29791632 | 0.06451338 | 9.91E-06 | 2.05E-02 |
| **Exc_L4-6_3** | LINC01202 | 46.31304885 | -0.28287352 | 0.06955769 | 3.69E-05 | 3.40E-02 |
| **Exc_L4-6_3** | PMPCB | 49.37211724 | 0.19443960 | 0.04990928 | 3.32E-05 | 3.40E-02 |
| **Exc_L4-6_3** | SCN2B | 46.76789447 | 0.24589974 | 0.06173362 | 3.37E-05 | 3.40E-02 |
| **Exc_L4-6_3** | ALDOC | 27.41642012 | 0.27127043 | 0.06609752 | 2.32E-05 | 3.40E-02 |
| **Exc_L4-6_3** | PCSK1N | 143.35810447 | 0.24612738 | 0.06339140 | 3.38E-05 | 3.40E-02 |
| **Exc_L4-6_3** | AC034268.2 | 766.17224436 | -0.26312537 | 0.07195336 | 4.63E-05 | 3.83E-02 |
| **Exc_L5-6** | GNB5 | 55.04442805 | -0.21893311 | 0.04925575 | 1.31E-05 | 6.14E-02 |
| **Exc_L5-6** | CCNT2-AS1 | 27.94981846 | -0.27539975 | 0.06417439 | 4.35E-05 | 6.76E-02 |
| **Exc_L5-6** | GALNTL6 | 182.74255279 | -0.22196000 | 0.06714698 | 5.79E-05 | 6.76E-02 |
| **Exc_L5-6** | CTBP2 | 31.90543248 | 0.25448668 | 0.06694304 | 7.19E-05 | 6.76E-02 |
| **Exc_L5-6** | GPC5 | 91.34310305 | 0.27400580 | 0.06835849 | 5.68E-05 | 6.76E-02 |
| **Exc_L5-6** | ARHGEF3 | 80.15178777 | 0.20723646 | 0.05156498 | 1.41E-04 | 9.47E-02 |
| **Exc_L5-6** | TANC2 | 397.06947776 | -0.13734910 | 0.03613396 | 1.31E-04 | 9.47E-02 |
| **In_LAMP5** | KLHL5 | 65.20306812 | -0.22347981 | 0.05057992 | 7.79E-06 | 7.38E-02 |
| **In_LAMP5** | AC012404.1 | 30.53607648 | 0.20480644 | 0.05565332 | 1.80E-05 | 8.54E-02 |
| **In_VIP** | TP53I11 | 117.06951258 | -0.20737439 | 0.04715767 | 1.77E-06 | 2.16E-02 |
| **In_VIP** | AC012404.1 | 47.92389704 | 0.18816550 | 0.05288196 | 9.37E-06 | 5.73E-02 |

| | | | | | | |
|---|---|---|---|---|---|---|
| **In_VIP** | CORO2B | 125.99490856 | -0.17556354 | 0.04092296 | 2.33E-05 | 9.51E-02 |
| **Microglia** | WDR70 | 127.28394944 | -0.19007806 | 0.04185745 | 7.35E-06 | 1.81E-02 |
| **Microglia** | KCNQ3 | 725.47094178 | -0.25327751 | 0.05861334 | 8.01E-06 | 1.81E-02 |
| **Oligodendrocyte** | ANKS1B | 1,094.31882649 | -0.16170514 | 0.03425079 | 2.42E-06 | 8.25E-03 |
| **Oligodendrocyte** | UBB | 108.37590048 | 0.24760225 | 0.05516280 | 1.21E-06 | 8.25E-03 |
| **Oligodendrocyte** | CDH8 | 125.93870049 | -0.30514296 | 0.06498672 | 4.28E-06 | 9.74E-03 |
| **Oligodendrocyte** | RPL5 | 65.64096890 | 0.20333004 | 0.05356452 | 6.30E-05 | 7.08E-02 |
| **Oligodendrocyte** | CRB1 | 84.58282042 | -0.21660119 | 0.05313032 | 5.60E-05 | 7.08E-02 |
| **Oligodendrocyte** | MAL | 267.53115499 | 0.18880388 | 0.05007365 | 1.05E-04 | 7.08E-02 |
| **Oligodendrocyte** | WDR70 | 196.54263131 | -0.12665983 | 0.03298209 | 1.13E-04 | 7.08E-02 |
| **Oligodendrocyte** | PLAAT3 | 268.28328829 | 0.18721997 | 0.04909912 | 1.14E-04 | 7.08E-02 |
| **Oligodendrocyte** | SARM1 | 26.84034871 | -0.24517115 | 0.06251949 | 1.10E-04 | 7.08E-02 |
| **Oligodendrocyte** | TTYH2 | 249.19568448 | 0.21405321 | 0.05524731 | 5.54E-05 | 7.08E-02 |
| **OPC** | SPARCL1 | 349.31341668 | 0.25041470 | 0.05373613 | 1.89E-06 | 1.76E-02 |
| **OPC** | IGFBP5 | 16.60954963 | 0.32656977 | 0.07243997 | 1.70E-05 | 6.48E-02 |
| **OPC** | RAMP1 | 143.53953302 | 0.24219085 | 0.06570503 | 4.16E-05 | 6.48E-02 |
| **OPC** | GRAMD1C | 113.15461920 | 0.28638900 | 0.07081784 | 3.75E-05 | 6.48E-02 |
| **OPC** | SORCS1 | 549.20497883 | -0.19382779 | 0.04697509 | 2.40E-05 | 6.48E-02 |
| **OPC** | ALDOC | 64.63193269 | 0.26069679 | 0.06593691 | 2.84E-05 | 6.48E-02 |
| **OPC** | HIST1H4C | 21.97725534 | 0.21506579 | 0.06985243 | 4.97E-05 | 6.63E-02 |
| **OPC** | KCNMA1 | 1,044.99299534 | -0.15948756 | 0.03973330 | 7.65E-05 | 8.94E-02 |
| **OPC** | FDFT1 | 37.92183451 | 0.27086732 | 0.06674194 | 1.00E-04 | 9.98E-02 |
| **OPC** | UNC13C | 26.07561909 | -0.25688809 | 0.07052918 | 1.07E-04 | 9.98E-02 |

**Supplementary Table 22. Differentially accessible genes for various cell types between psychiatric cases and controls.** Per cell type a maximum of 10 differentially accessible genes is shown here. Full list of differentially accessible genes for all cell types available at https://doi.org/10.5281/zenodo.10864161, Online Table 34.

| cell type | gene_symbol | log2FoldChange | stat | *p* | FDR |
|---|---|---|---|---|---|
| **Astro_PP** | PDCD6IP | -0.17510947 | 19.92906139 | 8.04E-06 | 3.34E-02 |
| **Astro_PP** | CCDC112 | -0.175290541 | 21.55747347 | 3.43E-06 | 2.86E-02 |
| **Exc_L2-3** | PEF1 | -0.131126715 | 16.51527133 | 4.83E-05 | 5.38E-02 |
| **Exc_L2-3** | TIE1 | -0.124018363 | 14.49210923 | 1.41E-04 | 7.66E-02 |
| **Exc_L2-3** | GPR37L1 | -0.103466593 | 17.31492285 | 3.17E-05 | 4.13E-02 |
| **Exc_L2-3** | DYRK3 | 0.1179966 | 14.40042598 | 1.48E-04 | 7.66E-02 |
| **Exc_L2-3** | VIT | -0.114143862 | 13.88138489 | 1.95E-04 | 9.07E-02 |
| **Exc_L2-3** | GALM | 0.075239978 | 14.84326911 | 1.17E-04 | 7.26E-02 |
| **Exc_L2-3** | MAP4K4 | 0.079174742 | 15.17998062 | 9.77E-05 | 7.08E-02 |
| **Exc_L2-3** | FBLN2 | -0.133475835 | 21.67419425 | 3.23E-06 | 1.05E-02 |
| **Exc_L2-3** | SEMA5B | -0.109595985 | 21.8189582 | 3.00E-06 | 1.05E-02 |
| **Exc_L2-3** | SLC12A8 | -0.09244186 | 18.19075816 | 2.00E-05 | 3.26E-02 |
| **Exc_L3-5** | RIPOR2 | 0.351549129 | 22.25912579 | 2.38E-06 | 1.78E-02 |
| **Exc_L3-5** | PPP1R3E | -0.293602744 | 17.99222452 | 2.22E-05 | 8.27E-02 |

**Supplementary Table 23. Transcription factor motif enrichments for *INO80E* and *HCN2*.** Table includes enrichment results (-log10 transformed *p* values) for *INO80E* and *HCN2* based on the JASPAR motif database (Fornes et al., 2020).

| *INO80E* | | *HCN2* | |
|---|---|---|---|
| **TF motif** | **-log10(padj)** | **TF motif** | **-log10(padj)** |
| **KLF4_587** | 2.080057 | **MAZ_410** | 11.09635749 |
| | | **ZNF148_548** | 10.26775749 |
| | | **ZNF740_525** | 7.689057491 |
| | | **EGR1_563** | 7.625157491 |
| | | **KLF15_401** | 6.955257491 |
| | | **KLF4_587** | 6.564757491 |
| | | **KLF11_400** | 6.380857491 |
| | | **ZBTB14_545** | 6.210657491 |
| | | **CTCFL_560** | 6.069157491 |
| | | **ZNF460_476** | 5.581957491 |
| | | **KLF5_57** | 5.420357491 |
| | | **TFAP2A.var.2_231** | 5.121057491 |
| | | **TFAP2C.var.2_627** | 4.942257491 |
| | | **SP9_449** | 4.781157491 |
| | | **KLF9_588** | 4.583957491 |
| | | **ASCL1.var.2_526** | 4.504257491 |
| | | **ZIC5_468** | 4.376557491 |
| | | **TFAP2B_232** | 4.280557491 |
| | | **KLF16_169** | 4.114957491 |
| | | **EGR3_162** | 3.987757491 |
| | | **TFAP2E_454** | 3.971057491 |
| | | **TFDP1_318** | 3.885657491 |
| | | **PLAG1_28** | 3.879457491 |
| | | **RREB1_11** | 3.325557491 |
| | | **TCF4_622** | 3.225157491 |
| | | **TFAP2A_626** | 3.141757491 |
| | | **E2F6_561** | 3.033657491 |
| | | **SP3_522** | 2.962257491 |
| | | **SP4_117** | 2.789457491 |
| | | **ZIC4_172** | 2.761557491 |
| | | **TFAP2C_235** | 2.694457491 |
| | | **SP8_170** | 2.654857491 |
| | | **EBF1_562** | 2.534657491 |
| | | **ZEB1_320** | 2.518957491 |
| | | **TCF12.var.2_543** | 2.449557491 |
| | | **EBF3_532** | 2.301857491 |
| | | **KLF14_168** | 2.116057491 |
| | | **KLF17_402** | 2.089657491 |
| | | **NRF1_40** | 1.995457491 |
| | | **ESR2_47** | 1.925057491 |
| | | **EGR4_163** | 1.888357491 |
| | | **EGR2_161** | 1.871657491 |
| | | **ZNF135_470** | 1.854157491 |
| | | **KLF10_399** | 1.799957491 |
| | | **SP2_521** | 1.795057491 |
| | | **SP1_520** | 1.604557491 |
| | | **ZNF263_632** | 1.553157491 |
| | | **ZBTB7B_128** | 1.542657491 |
| | | **ASCL1_482** | 1.536557491 |
| | | **TFAP2B.var.2_233** | 1.429457491 |
| | | **ZBTB7C_129** | 1.327757491 |
| | | **GLIS2_165** | 1.326757491 |
| | | **TCF3_621** | 1.324957491 |
| | | **TCFL5_523** | 1.315657491 |

**Supplementary Table 24. Common differentially expressed genes between mouse and human.** Table shows genes that are commonly differentially expressed in cell types of the human orbitofrontal cortex (OFC) related to psychiatric diagnoses and the mouse prefrontal cortex (PFC) in response to glucocorticoid stimulation. Gene column indicates the gene symbol of the respective human gene.

| Gene | Cell type human OFC | log2FC human OFC | FDR human OFC | Log2FC mouse PFC | FDR mouse PFC |
|---|---|---|---|---|---|
| **MFSD2A** | Exc_L2-3 | 0.2672 | 6.43E-02 | 0.7275 | 1.43E-08 |
| **CCN1** | Exc_L2-3 | 0.2603 | 7.85E-02 | 1.3067 | 2.81E-02 |
| **PRDX6** | Exc_L2-3 | 0.2037 | 5.71E-02 | -0.1923 | 1.06E-03 |
| **LYST** | Exc_L2-3 | -0.0846 | 9.10E-02 | 0.4273 | 2.80E-03 |
| **MAT2A** | Exc_L2-3 | 0.1364 | 8.51E-02 | 0.4335 | 1.36E-11 |
| **CTDSPL** | Exc_L2-3 | -0.0944 | 9.26E-02 | 0.2561 | 6.91E-02 |
| **TMEM44** | Exc_L2-3 | 0.1801 | 8.87E-02 | -0.2148 | 6.62E-02 |
| **NREP** | Exc_L2-3 | -0.1604 | 6.62E-02 | -0.3202 | 3.99E-03 |
| **EDN1** | Exc_L2-3 | -0.2286 | 6.17E-02 | 0.8200 | 3.46E-03 |
| **FKBP5** | Exc_L2-3 | 0.2267 | 6.46E-02 | 2.8988 | 6.16E-65 |
| **CD164** | Exc_L2-3 | 0.1308 | 5.11E-02 | 0.6505 | 1.39E-08 |
| **RPA3** | Exc_L2-3 | 0.2248 | 5.44E-03 | -0.5164 | 4.71E-02 |
| **FAM126A** | Exc_L2-3 | 0.2211 | 9.29E-02 | 0.6333 | 1.48E-04 |
| **FZD1** | Exc_L2-3 | 0.2716 | 4.41E-02 | 0.5162 | 2.10E-02 |
| **TCIM** | Exc_L2-3 | 0.2470 | 5.19E-02 | 2.6988 | 1.49E-13 |
| **CHCHD7** | Exc_L2-3 | 0.1778 | 3.12E-02 | -0.3187 | 9.62E-02 |
| **PTPN3** | Exc_L2-3 | -0.1498 | 6.98E-02 | 0.3322 | 9.29E-02 |
| **DDIT4** | Exc_L2-3 | 0.2539 | 8.57E-02 | 1.7206 | 9.15E-26 |
| **CPNE7** | Exc_L2-3 | 0.2456 | 6.06E-02 | 0.4080 | 5.43E-03 |
| **RASD1** | Exc_L2-3 | 0.2309 | 6.86E-02 | 1.2574 | 5.35E-04 |
| **POU2F2** | Exc_L2-3 | -0.2526 | 7.21E-04 | -0.5663 | 5.16E-04 |
| **MID1IP1** | Exc_L2-3 | 0.2062 | 8.65E-02 | -0.2610 | 4.63E-03 |
| **TSC22D3** | Exc_L2-3 | 0.1747 | 9.29E-02 | 1.2296 | 4.29E-13 |
| **POU2F1** | Exc_L4-6_1 | -0.0895 | 9.71E-02 | -0.4827 | 3.56E-04 |
| **MAT2A** | Exc_L4-6_1 | 0.1489 | 3.51E-02 | 0.4335 | 1.36E-11 |
| **LRRC58** | Exc_L4-6_1 | 0.1554 | 8.11E-02 | 0.5501 | 7.09E-16 |
| **BCL6** | Exc_L4-6_1 | 0.2263 | 7.36E-02 | 0.3576 | 1.10E-02 |
| **SLIT2** | Exc_L4-6_1 | 0.3833 | 1.38E-06 | -0.6548 | 2.62E-05 |
| **CDH9** | Exc_L4-6_1 | -0.2068 | 4.16E-02 | -0.7743 | 1.89E-03 |
| **NREP** | Exc_L4-6_1 | -0.1958 | 8.74E-03 | -0.3202 | 3.99E-03 |
| **MLIP** | Exc_L4-6_1 | -0.1811 | 4.84E-02 | -0.2869 | 4.13E-02 |
| **ST3GAL1** | Exc_L4-6_1 | -0.1847 | 5.66E-02 | -0.4335 | 4.09E-02 |
| **PTPN3** | Exc_L4-6_1 | -0.1789 | 3.91E-02 | 0.3322 | 9.29E-02 |
| **PPFIBP2** | Exc_L4-6_1 | 0.2188 | 7.41E-02 | 0.9575 | 8.26E-04 |
| **TRPC4** | Exc_L4-6_1 | 0.3430 | 1.83E-03 | 0.4773 | 1.16E-02 |
| **GALNT16** | Exc_L4-6_1 | 0.1858 | 5.30E-02 | 0.2729 | 5.15E-02 |
| **CLMN** | Exc_L4-6_1 | 0.2588 | 6.26E-03 | 0.3965 | 5.81E-08 |
| **IGDCC3** | Exc_L4-6_1 | 0.2172 | 7.27E-02 | 0.8148 | 1.38E-02 |
| **SPIRE1** | Exc_L4-6_1 | -0.0732 | 5.77E-02 | 0.3460 | 5.89E-05 |
| **RNF152** | Exc_L4-6_1 | 0.2837 | 2.64E-02 | -0.3505 | 1.84E-02 |
| **POU2F2** | Exc_L4-6_1 | -0.2021 | 3.56E-02 | -0.5663 | 5.16E-04 |
| **RCAN2** | Exc_L4-6_2 | -0.1626 | 5.71E-02 | 0.3014 | 1.28E-02 |
| **SYNE1** | Exc_L4-6_2 | -0.1047 | 8.75E-02 | 0.2546 | 8.63E-06 |
| **RASD1** | Exc_L4-6_2 | 0.2209 | 7.39E-02 | 1.2574 | 5.35E-04 |
| **RHBDL3** | Exc_L4-6_2 | 0.2396 | 2.18E-02 | 0.2857 | 6.87E-02 |
| **PTCHD1** | Exc_L4-6_2 | -0.2233 | 2.66E-02 | -0.5094 | 6.56E-04 |
| **POU2F1** | Exc_L4-6_3 | -0.1244 | 9.56E-02 | -0.4827 | 3.56E-04 |
| **C2orf72** | Exc_L4-6_3 | 0.2182 | 9.80E-02 | -2.035 | 3.86E-10 |
| **KIAA1958** | Exc_L4-6_3 | 0.1726 | 9.56E-02 | 0.3669 | 1.91E-02 |
| **ARHGEF3** | Exc_L5-6 | 0.2072 | 9.47E-02 | 0.3624 | 1.96E-02 |
| **MAL** | Oligodendrocyte | 0.1888 | 7.08E-02 | 0.4010 | 1.20E-02 |
| **ANKS1B** | Oligodendrocyte | -0.1617 | 8.25E-03 | 0.1068 | 6.34E-02 |
| **SORCS1** | OPC | -0.1938 | 6.48E-02 | 0.3024 | 4.55E-02 |

# List of Abbreviations

| | |
|---|---|
| **ACTH** | adrenocorticotrophic hormone |
| **AMY** | amygdala |
| **ASD** | autism spectrum disorder |
| **ATAC** | assay for transposase-accessible chromatin |
| **ATP** | adenosine triphosphate |
| **BBB** | blood-brain barrier |
| **BIP** | bipolar disorder |
| **bp** | base pairs |
| **CER** | cerebellum |
| **CNS** | central nervous system |
| **CNV** | copy number variation |
| **CRH** | corticotrophin releasing hormone |
| **D2** | dopamine receptor 2 |
| **DA** | differential accessibility/differentially accessible |
| **DALYs** | disability-adjusted life years |
| **dCA1** | dorsal hippocampal *cornu ammonis* 1 region |
| **dDG** | dorsal dentate gyrus |
| **DE** | differential expression/differentially expressed |
| **DN** | differential network |
| **DNA** | deoxyribonucleic acid |
| **DSM-5** | 5$^{th}$ edition of the diagnostic and statistical manual of mental disorders |
| **FC** | $log_2$-transformed fold change |
| **FDR** | false discovery rate |
| **GABA** | gamma-aminobutyric acid |
| **GEM** | gel bead in emulsion |
| **GO** | gene ontology |
| **GR** | glucocorticoid receptor |
| **GRE** | glucocorticoid response element |
| **GWAS** | genome-wide association study |
| **HPA** | hypothalamic-pituitary-adrenal |
| **ICD-10** | 10$^{th}$ revision of the international classification of diseases |
| **kb** | kilobases |
| **MDD** | major depressive disorder |
| **MR** | mineralocorticoid receptor |
| **OFC** | orbitofrontal cortex |
| **OPC** | oligodendrocyte precursor cell |
| **PC** | principal component |
| **PCA** | principal component analysis |
| **PFC** | prefrontal cortex |
| **PMI** | postmortem interval |
| **PRS** | polygenic risk scores |
| **PVN** | paraventricular nucleus of the hypothalamus |
| **RIN** | RNA integrity number |
| **RNA** | ribonucleic acid |
| **SCA** | schizoaffective disorder |

| | |
|---|---|
| **SCZ** | schizophrenia |
| **sn** | single-nucleus |
| **SNP** | single nucleotide polymorphism |
| **SV** | surrogate variable |
| **SVA** | surrogate variable analysis |
| **TF** | transcription factor |
| **TWAS** | transcriptome-wide association study |
| **UMAP** | uniform manifold approximation and projection |
| **vCA1** | ventral hippocampal *cornu ammonis* 1 region |
| **vDG** | ventral dentate gyrus |

# List of Figures

# List of Tables

# Data and Code Availability

*Data Availability*

The online tables supporting this thesis, as referenced in its chapters, are available at https://doi.org/10.5281/zenodo.10864161. This repository further provides files containing complete lists of differential expression and network results, which extend beyond the significant genes, from the analysis of the response to glucocorticoid receptor activation in 8 mouse brain regions. Additionally, it includes complete lists of differential expression and chromatin accessibility analyses of psychiatric disorders in the orbitofrontal cortex, based on the postmortem brain cohort. Interactive exploration of the mouse brain project results as well as tailored visualizations and downloads are facilitated at http://diffbrainnet.psych.mpg.de/.

Access to the raw and preprocessed RNA-seq data from the mouse brain project is available through the Gene Expression Omnibus (GEO) under the accession number GSE190712. The raw and preprocessed sequencing data from the postmortem brain study can also be accessed on GEO under the accession numbers GSE254569 (single-nucleus RNA-seq) and GSE256207 (single-nucleus ATAC-seq).

*Code Availability*

The data analysis scripts and the code used to generate the figures presented in this thesis are available on GitHub: https://github.molgen.mpg.de/mpip/DiffBrainNet. The source code of the R shiny app "DiffBrainNet" can be found at GitHub as well: https://github.molgen.mpg.de/mpip/DiffBrainNet_ShinyApp. Additionally, the app can be deployed locally using the Docker image that can be accessed on Docker Hub (https://hub.docker.com/r/ngerst/diffbrainnet).

Scripts for the single-nucleus analysis of the orbitofrontal cortex are likewise accessible on GitHub at https://github.molgen.mpg.de/mpip/SingleNuclei_Analysis_OFC.

# Acknowledgements

My journey through this PhD has been a path paved with support, guidance, and collaboration. I would like to sincerely thank everyone who made this journey both possible and meaningful.

I am deeply grateful to Dr. Janine Knauer-Arloth for accepting me as her first PhD student in her research group. Your consistent support, availability, and guidance have been crucial to the success of my research projects. Under your supervision and mentorship, I have grown both personally and professionally. Your passion for science has been truly inspirational.

Thank you to Prof. Dr. Dr. Elisabeth Binder for the opportunity to pursue my PhD at the Max Planck Institute of Psychiatry, and her guidance as a member of my thesis advisory committee. The dataset I was able to work with has been as exciting as it was challenging.

I would like to thank PD Dr. Mathias Schmidt and Prof. Dr. Korbinian Schneeberger. Your presence on my thesis advisory committee, together with your insightful feedback, have been invaluable to the refinement of my work. I would also like to express my gratitude to you for kindly accepting your roles as examiners – along with Prof. Dr. Laura Busse, Prof. Dr. John Parsch, PD Dr. Cordelia Bolle, and Prof. Dr. Simon Heilbronner.

A special thank you to my collaborators Dr. Anna Fröhlich and Dr. Anthi Krontira for the excellent teamwork and the mutual support we have provided to each other. I would like to acknowledge Monika Rex-Haffner, Maik Ködel, and Susann Sauer whose organizational support and work in the wet-lab has been essential to this research. For the great collaborations with Dr. Cristiana Cruceanu from the Karolinska Institute, and Dr. Natalie Matosin and Dominic Kaul from the University of Sydney, I am extremely grateful.

To Prof. Dr. Sara Mostafavi, thank you for the opportunity to visit your lab at the University of Washington and for the valuable advice on snATAC-seq data analysis and data integration that you and Xinming Tu provided. A warm thank you to Dr. Erin Wilson, Anna Spiro, and everyone else who made me feel so welcome in Seattle.

I am deeply appreciative of the Joachim Herz Foundation's Add-on Fellowship for Interdisciplinary Life Sciences, which facilitated my research stay in Seattle. The workshops and fellow meetings provided by the Joachim Herz Foundation have significantly broadened my horizons.

I want to acknowledge my colleagues from the Medical Genomics research group – Anastasiia Hryhorzhevska, Ghalia Rehawi, Jonas Hagenberg, and Tamim Ahsan – the Translational Genomics team – Dr. Darina Czamara, Dr. Linda Dieckmann, Alicia Schowe, and Vera Karlbauer – and Dr. Simone Röh, whose feedback has been invaluable, consistently enhancing the outcomes of my research. A special thanks to my office mate

Jonas Hagenberg, not only for his insightful contributions during numerous brainstorming sessions and statistical challenges but also for being a great friend and companion throughout these years. Thank you to Dr. Linda Dieckmann, Ghalia Rehawi, Dr. Natan Yusupov, Dr. Nico Rost, and all the other colleagues who have turned into good friends, thank you for being part of my life these past few years.

To Tatjana Ammer and Josef Duft, who have been with me since day one of our bioinformatics adventure. Besides being great study companions, you are wonderful friends who never failed to ensure a healthy balance between work and recreation. Thank you to all my friends who have been part of this journey, adding excitement and unforgettable moments to it.

To my family, your love and encouragement have been the foundation of everything I do. My parents, Dagmar and Kurt Gerstner, I am deeply grateful for the joyful childhood you gave me and your endless support, up until today. The weekends I spent at your home during these past few years have consistently recharged my energy. And to my siblings, Janina Gerstner, and Jonas Gerstner, along with Kati Pichler, your presence in my life is deeply cherished, and I am grateful for our close bond.

Mi Javi (*aka* Dr. Javier Cuesta), your love has been a source of spirit and happiness during these years. Not only have you constantly encouraged me, but you have also been an inspiration, being so passionate about the things you do. Thank you for believing in me, being by my side, in moments both demanding and delightful, and sharing the joy of life with me.

Thank you all for being a part of this chapter in my life!